Technische Universität München

WACKER-Lehrstuhl für Makromolekulare Chemie

Development of Novel Phosphine Sulphonate-Based Palladium Catalysts for Ethene Homo- and Co-Polymerisation Reactions with Polar-Functionalised Olefins

Timo Martin Jürgen Anselment

Vollständiger Abdruck der von der Fakultät für Chemie der Technischen Universität München zur Erlangung des akademischen Grades eines

Doktors der Naturwissenschaften

(Dr. rer. nat.)

genehmigten Dissertation.

Vorsitzender: Univ.-Prof. Dr.-Ing. Kai Olaf Hinrichsen

Prüfer der Dissertation: 1. Univ.-Prof. Dr. Dr. h.c. Bernhard Rieger

2. Priv.-Doz. Dr. Wolfgang Eisenreich

Die Dissertation wurde am 17.06.2011 bei der Technischen Universität München eingereicht und durch die Fakultät für Chemie am 02.08.2011 angenommen.

Danksagung:

An dieser Stelle möchte ich mich, allen voran, bei Herrn Prof. Dr. Dr. h.c. B. Rieger für die Möglichkeit dieses spannende, herausfordernde und äußerst aktuelle Promotionsthema zu bearbeiten bedanken. Zudem danke ich ihm für das große Vertrauen und die Freiheit die er mir während dieser Zeit gewährt hat, die weitreichenden Einblicke in unterschiedliche katalytische Polymerisationsreaktionen mit späten Übergangsmetallen sowie seine Anregungen und Vorschläge aus vielen fachlichen Diskussionen.

Herrn Dr. C. Troll möchte ich für die stets tatkräftige Unterstützung, sei es beim Basteln im Bunker oder mit fachlichen Ratschlägen, danken. Außerdem natürlich für all seinen Einsatz dafür, dass der Lehrstuhl stets am Laufen bleibt und eine tolle Atmosphäre besteht.

Herrn Prof. Dr. O. Nuyken und Frau Dr. H. Samarian danke ich für ihre fachliche sowie persönliche Unterstützung während meiner akademischen Arbeiten.

Danke auch an Dr. S. Vagin für seine exzellente fachliche Hilfe und die Unterstützung beim Schreiben von Publikationen, sowie all seinen Einsatz für den Lehrstuhl.

Special thanks go to Ms. Dr. C. Anderson for friendship and scientific support. Both were very important to fully mobilise the potential of my work, especially in writing well received publications. Oh, and of course, thank you for teaching me strange British dialects. I will always hide some very necessary letters like "z´s" for you.

Für Unterstützung bei Analytik und fachlichen Fragen danke ich Prof. P. Köhler, S. Kaviani und PD Dr. W. Eisenreich, dem analytischen Labor sowie unseren technischen Angestellten.

Den vielen Laborkollegen über die Jahre insbesondere D. Lanzinger, S. Weidle und T. Korfmann gilt natürlich ein großer Dank für die hervorragende Arbeitsatmosphäre in 56404. Auf Eure moralische Unterstützung bei fachlichen Tiefschlägen war immer Verlass. Hier bedanke ich mich natürlich auch für die exzellente Arbeit von Studenten und Praktikanten, allen voran S. Weidle, S. Walter, B. Schemmer und C. Wichmann.

Allen ehemaligen und aktuellen Makros danke ich für das tolle Arbeitsumfeld, bei welchem nie der entsprechende Ausgleich vergessen wurde. Skihütte, Wiesn-Skandale, Freiburg und Feierabendbier sind einfach essentiell. An dieser Stelle möchte ich vor allem S. Erhardt unserem Labor-Nomaden, U. Seemann, P. Zehetmaier und F. Schultz für geniale Skitage, T. Diesner dem Luftballonschlucker, der Latexgruppe C. Gantner, J. Müller und M. Schneider, M. Kellner, P. Heinz für den Fahrradfahrversuch nach der Weihnachtsfeier, S. Klaus mit seinen Eisbären sowie N. Hutter danken. A. Schöbel und M. Winkenstette danke ich für die gute Kooperation beim Schreiben und allen nicht namentlich erwähnten Makros gebührt natürlich genauso ein großer Dank für die tolle Atmosphäre und den Zusammenhalt der Arbeitsgruppe. Großer Dank auch an die ehemaligen Makros vor allem M. Bortenschlager, R. Luxenhofer, S. Jungermann und A. Junger für die vermittelte Freude an der Polymerchemie.

Meiner Familie sowie meiner Freundin S. Rach danke ich für all Eure Unterstützung und Motivation. Ohne Euch wäre diese Arbeit für mich nicht möglich gewesen.

Abbreviations:

Ar	**Ar**yl
Boc	*tert*-**b**ut**o**xy**c**arbonyl
Bu	**bu**tyl
COSY	**co**rrelated **s**pectroscop**y**
DCM	methylene chloride
DEPT	**d**istortionless **e**nhancement by **p**olarisation **t**ransfer
DFT	**d**ensity **f**unctional **t**heory
DMSO	**di**methyl **s**ulph**o**xide
DP	**d**egree of **p**olymerisation
DSC	**d**ifferential **s**canning **c**alorimetry
EA	**e**lemental **a**nalysis
ESI	**e**lectron **s**pray **i**onisation
EWG	**e**lectron **w**ithdrawing **g**roup
HSQC	**h**eteronuclear **s**ingle **q**uantum **c**oherence
HMBC	**h**eteronuclear **m**ultiple **b**ond **c**orrelation
GPC	**g**el **p**ermeation chromatography
gpc	**g**rowing **p**olymer **c**hain
LUMO	**l**owest **u**noccupied **m**olecular **o**rbital
m	*m*eta
Me	**me**thyl
M_n	**m**olecular weight, **n**umber average
MS	**m**ass **s**pectrometry
M_w	**m**olecular weight, **w**eight average
NMR	**n**uclear **m**agnetic **r**esonance
1D	**1 d**imensional
2D	**2 d**imensional

d	**d**oublet	
dd	**d**oublet of **d**oublets	
ddd	**d**oublet of **d**oublet of **d**oublets	
J	coupling constant	
m	**m**ultiplet	
ppm	chemical shift	
q	**q**uartet	
s	**s**inglet	
t	**t**riplet	

nOe   **n**uclear **O**verhouser **eff**ect

NOESY   **n**uclear **O**verhauser **eff**ect **s**pectroscop**y**

o   *ortho*

OMe   methoxy

p   *para*

PDI   **p**oly **d**ispersity **i**ndex; $PDI = \dfrac{M_n}{M_w}$

PE   **p**oly**e**thene

PP   **p**oly**p**ropene

SEC   **s**ize **e**xclusion **c**hromatography

SMe   thiomethyl

tmeda   *N,N,N',N'*-**t**etra**m**ethyl**e**thylene**dia**mine

THF   **t**etra**h**ydro**f**uran

TOCSY   **to**tal **c**orrelation **s**pectroscop**y**

TPP   **t**ri**p**henyl**p**hosphine

TPPMS   **t**ri**p**henyl**p**hosphine **m**ono**s**ulphonate

TPPDS   **t**ri**p**henyl**p**hosphine **d**i**s**ulphonate

TPPTS   **t**ri**p**henyl**p**hosphine **t**ri**s**ulphonate

Index

1. Introduction

Major advances have been made in polymerisation chemistry during the last century, both in scientific research and industrial application. Due to the numerous synthetic approaches to polymer synthesis a great variability of polymer classes with different structures and properties is accessible. This scope covers large volume polymer products from inexpensive monomers to polymers for highly specialised products. However, the polymer properties and their modification are the deciding factors which govern research in a field which is traditionally relatively close to industrial applications. Control of specific polymer properties can be relatively easily achieved by modification of characteristic features such as molecular weight, polymer architecture and copolymer composition. However thorough understanding of polymerisation processes is essential for explanation of experimental observations and rational material property oriented process modification.

Insertion polymerisation processes produce some of the most important bulk polymers, namely polyethene PE and polypropene PP. Progress in the corresponding homogeneous catalysed polymerisations can eloquently highlight the possibilities to express control on the polymer microstructure *via* catalyst design.[1] Stunning developments are for example tacticity control in propene polymerisation[2], synthesis of optically active, essentially chiral, copolymers from CO and propene[3], generation of biodegradable copolymers from propylene oxide and CO_2[4] or control of the polymer microstructure in ethene polymerisation[5]. Recent advances focus on thorough understanding of the basic mechanistic principles and development of advanced polymerisation processes. In this respect for example the concepts of multinuclear catalysts[6] and chain-shuttling mechanisms[1a, 7] can be highlighted. However introduction of functionalised comonomers to modify polymer properties is still an ongoing challenge[8], as catalysts for insertion polymerisation reactions are sensitive towards poisoning by coordination of donor functionalities[8a, 9] and alternative routes such as protection of functional groups[8a] or metathesis-based polymerisation reactions are cumbersome[10]. Even more desirable would be the prospect for introducing tacticity in the homopolymerisation of polar-functionalised olefins. This feature cannot be achieved by radical or group transfer polymerisations which are normally used for generation of these polymers.[11] Due to the relatively low Lewis acidity of late transition metal olefin polymerisation catalysts, neutral complexes, mostly based on Pd(II), are usually regarded as the most promising perspectives in homo- or co-polymerisation reactions of functionalised olefins.[5b, 8b, 9, 12]

1. Introduction

2. Sulphonated Phosphines in Homogeneous Catalysis

2.1. Introduction and general remarks concerning phosphine ligands

Phosphines in general are one of the most versatile and widely used ligand classes. The parent compound phosphine (PH_3) can be substituted with alkyl or aryl groups which significantly alters the electronic properties of the resulting alkyl or arylphosphines. In contrast to the homologous amines, the basicity of phosphines increases significantly by introduction of groups providing inductive effects and changes of the phosphorus hybridisation (PH_3 < PPh_3/PMe_3 < Pt-Bu_3). As phosphines are neutral ligands which bind to transition metals *via* their electron lone pair the basicity of the phosphine is directly proportional to its σ-donor strength. Parallel to the increase in basicity, the ability of the phosphorus centre to accept π-back donation decreases.[13] Due to this reason, coordination ability, bond strength and the properties of their resulting transition metal complexes are often directly connected to the substituents of the employed phosphines. In addition the phosphine structure can drastically influence the coordination behaviour *via* steric effects. Several models are available to rationalise these influences for interpretation of observed ligand effects in catalysis. A direct correlation of these effects on a catalytic system would greatly facilitate effective ligand design for catalyst optimisation. However due to the complex nature of catalytic processes the detailed understanding of all underlying effects is required. Furthermore the blending of electronic and steric effects complicate unambiguous interpretation of substitution effects, as detailed in the literature.[14] Classification of phosphines, based on their steric and electronic characteristics, usually follows the *Tolman* cone angle (Θ) concept for the interpretation of observed substitution effects.[15] This is defined as the angle of a cone described by the centre 2.28 Å from the phosphine as the vertex and the van der Waals radii of the outermost atoms of the phosphine, with alignments giving a minimised cone, at the perimeter (Figure 1). In non-symmetrically substituted phosphines Θ is determined by Equation 1.

Equation 1: $$\Theta = (2/3)\sum_{i=1}^{3}(\theta_i/2)$$ (compare Figure 1)

Although this definition is also valid for other ligands such as *N*-heterocyclic carbenes (NHC's) or bidentate ligands the cone angle principle is not ideal to describe these ligands.

3

2. Sulphonated Phosphines in Homogeneous Catalysis

Here the "percent buried volume" of a sphere around the metal centre which is occupied by the ligand is a valuable tool for comparison.[16] Additionally in bidentate ligands, for example with κ^2-(P,P) coordination, the "bite angle" concept is noteworthy which describes the LML angle upon coordination to a metal centre (M). Changes of this parameter can control electronic properties of metals by the control over metal hybridisation.[14]
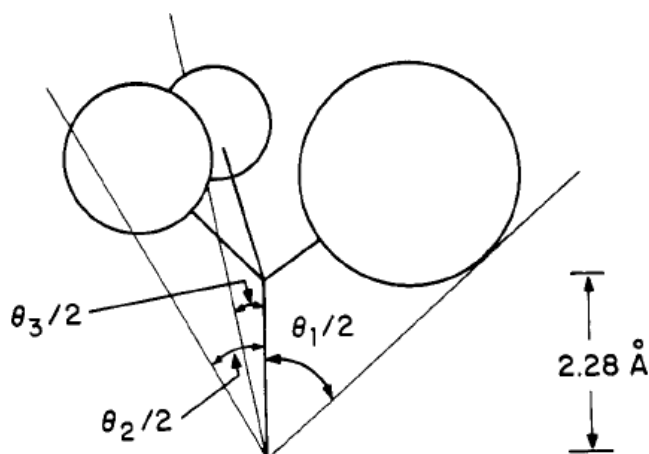
Figure 1: *Schematic definition of the Tolman cone angle Θ in a non-symmetrically substituted phosphine.*[15b]

However all attempts for the rationalisation of observed ligand influences on catalysis show a complex interaction of steric and electronic effects. Therefore purpose directed ligand design still requires empirical tests to assess the key influence factors for a chemical reaction. Specifically a detailed knowledge of the relevant mechanistic steps is important. Nevertheless it is clear that modification of the steric demand of the substituents in phosphines can drastically affect the reactivity of transition metal catalysts. For instance, steric protection or hindrance can increase or respectively decrease the ability for substrate coordination on the metal centre due to steric congestion or alteration of the phosphine hybridisation, leading to modification of the ligand basicity. Furthermore steric repulsion may also lead to stabilisation of highly reactive electronic configuration-states of the metal or modified ligand exchange behaviour.

Additionally the possibility to create asymmetric phosphines thereby introducing chirality in transition metal complexes is of huge importance in late transition metal-based catalysis.[17] This is highlighted by the Nobel Prize to *Knowles*, *Sharpless* and *Noyori* for their research in the area of asymmetric catalysis. Additional recent prominent examples for the relevance of

transition metal-based organometallic reactions in chemistry are the Nobel Prizes 2010 for C-C coupling reactions to *Heck*, *Negishi* and *Suzuki* as well as 2005 for metathesis reactions to *Chauvin*, *Grubbs* and *Schrock*.

For specific purposes chelating phosphine ligands, where at least one of the binding functionalities is a phosphine donor, can be employed. Numerous other hetero atoms, for example with O-, N- based donor functionalities, can be employed to modify steric and electronic properties of the corresponding chelated metal complexes. These heteroditopic chelating ligands based on two different coordinating functionalities are important in asymmetric catalysis, as the non-symmetric substitution pattern at the metal centre can induce a differentiation of additional relevant coordination sites, due to the varying *trans*-effects from the employed ligand.[18] As detailed later (Section 3.2), site selectivity for reactions can be introduced together with new reaction pathways *via* variation of the chelate donor atoms.

2.2. *Meta*-sulphonated arylphosphines

2.2.1.   Water soluble phosphines for aqueous or biphasic catalysis

Besides activity and stability of a catalyst, facile methods for separation from the reaction products are important for industrial catalytic processes. Specifically for expensive noble metals or toxic heavy metals used in catalytic reactions this aspect can be the deciding factor for the application of catalytic processes. Furthermore, alternatives to often hazardous and expensive organic solvents are attractive for industrial processes. Besides several drawbacks, water is an attractive solvent for chemical reactions if conditions and reaction components are carefully chosen.[19]

The concept of two-phase catalysis represents an interesting and economically convenient method for a facile catalyst separation from the reaction products. Hereby the solubility difference of the created product, catalyst and reactants ensures preferential solubility in two different phases, for example water/organic or ionic liquid/organic, which allows facile product recovery by phase separation or precipitation and filtration of the reaction products. Amongst the most prominent examples for this concept are the hydroformylation of olefins with water soluble rhodium based catalysts[20] as well as the ethene oligomerisation in the Shell higher olefin process (SHOP)[21]. In the former process, *meta*-sulphonated triphenylphosphines are employed, which are structurally related to the phosphines described

later in this work. The latter process is based on a polar solvent for example 1,4-butandiole or sulpholane in which the generated ethene oligomers are insoluble. Due to the high polarity of the employed catalyst, leaching into the organic product phase is reduced. Reaction products can be easily separated by decanting and purification by reextraction to remove minor amounts of catalysts, followed by the required product isolation steps.[20-21]

2.2.2. Synthesis, purification and phase mediation reactions for sulphonated phosphines

Synthesis and application of catalysts based on hydrophilic ligands is covered in a number of excellent review papers.[19-20] Conceptually these ligands can be divided in anionic, cationic or neutral hydrophilic structures. Amongst these, the majority of ligand structures are sulphonated phosphines, due to the possibility for facile introduction of sulphonate functionalities into the aryl substituents at phosphorus by electrophilic aromatic substitution. Parent structures are the *meta*-sulphonated triphenylphosphine derivatives triphenylphosphine *mono*-sulphonate (TPPMS), *di*-sulphonate (TPPDS) and *tri*-sulphonate (TPPTS) (Figure 2).

m-TPPMS   *m,m*-TPPDS   *m,m,m*-TPPTS
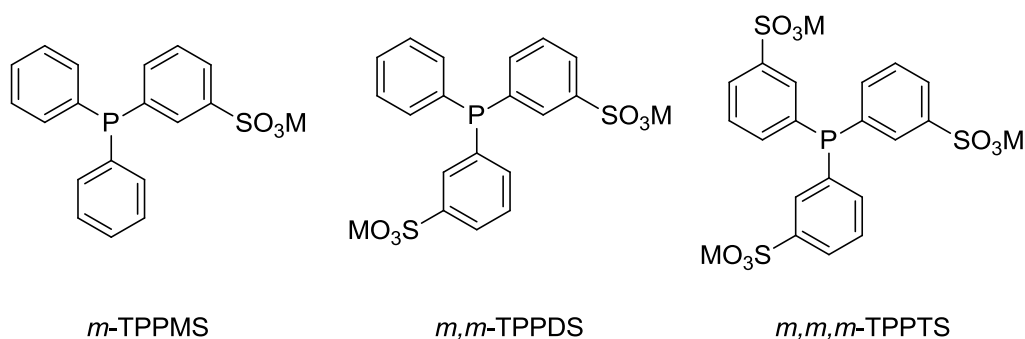
Figure 2: *Structure of the common hydrophilic phosphine ligands* m-*TPPMS,* m,m-*TPPDS and* m,m,m-*TPPTS.*

Unfortunately these ligands, their related complexes and the desired target reactions have several inherent problems. Specifically purification of the ligands as well as of their derived metal complexes is challenging. However, the interesting properties of these ligands led to detailed investigations for the optimisation and development of novel synthetic procedures within this field. Thus a large selection of monodentate, chelating or chiral hydrophilic ligand structures and their application is described in the literature.[19] The following sub sections

2. Sulphonated Phosphines in Homogeneous Catalysis

address important key problems in the synthesis of sulphonated phosphines which cover the theoretical background required for the sulphonation reactions described in this work

i) Synthesis and purification of meta-*sulphonated triphenylphosphines*

Sulphonation of triphenylphosphine **1** (TPP) in fuming sulphuric acid leads to the formation of *m,m,m*-TPPTS **2** together with several by-products. Depending on the reaction parameters *meta*-sulphonated TPP derivatives, with a varying degree of substitution (*m*-TPPMS, *m,m*-TPPDS, *m,m,m*-TPPTS, Figure 2), as well as the respective phosphine oxides (such as *m,m,m*-TPPTSO) are obtained.[22] Optimisation of the reaction conditions leads to an increased selectivity for *m,m,m*-TPPTS generation accompanied by a reduced oxide content. Due to the very similar solubility of sulphonated phosphines and phosphine oxides separation of *m,m,m*-TPPTS is laborious. Several improvements for the purification of these compounds have been developed, based on the original process which involves repeated recrystallisation steps to remove phosphine oxides and inorganic salts (Scheme 1). These optimised protocols allow isolation of the desired reaction products in relatively high purities with the prospect of reaction scale up.[22a, 23] For example, based on a process reported for the isolation of water soluble sulphonated aryl compounds from slightly diluted aqueous sulphuric acid solutions[24], the purification of sulphonated phosphines could be significantly improved.[25] Here the sulphonation mixture is first hydrolysed with water followed by addition of a water insoluble alkylamine or alkylphosphine oxide, such as *tri-n*-octylamine or terabutylphosphine oxide. By vigorous stirring the sulphonated phosphine is transferred to the organic phase which can then be easily separated. However, emulsion formation has to be prevented by the correct choice of the phase transfer agent. The pure sulphonated phosphine salt is obtained after extraction of the organic phase with an appropriate water soluble base which also regenerates the water immiscible alkyl amine.[25]

2. Sulphonated Phosphines in Homogeneous Catalysis
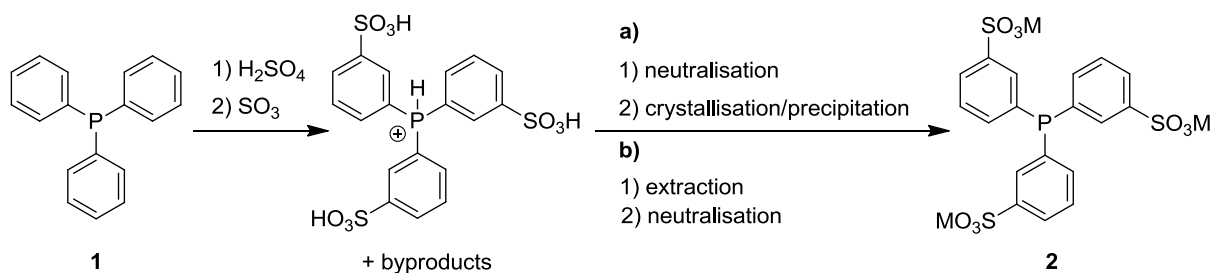
Scheme 1: *Sulphonation of TPP **1** and purification of m,m,m-TPPTS **2** either by: a) neutralisation and consecutive crystallisation/precipitation steps or b) reactive extraction followed by neutralisation; M = suitable alkali metal ions for example Na$^+$, K$^+$; anions for the protonated phosphine intermediate omitted.*

Further improvements include separation of **2** from other sulphonation products such as phosphine oxides by size exclusion chromatography (SEC) on Sephadex columns[26] or by a laborious multistep procedure. This involves complete oxidation of **1** followed by subsequent esterification, reduction of the phosphine oxide with trichlorosilane and ester hydrolysis to the phosphine **2**.[27] However development of a process based on an elegant protection of phosphorus(III) during the sulphonation in the presence of boric acid facilitated the synthesis of pure sulphonated phosphines[28], and is conveniently employed in the controlled sulphonation of valuable chiral phosphines.[19]

ii)   Selectivity and reaction control of the TPP sulphonation

A large number of publications concern the reaction control in the sulphonation of **1** and similar phosphines. The key problem addressed by these reports is the selectivity and possible ways to influence this during the sulphonation reaction. It has been established that the two major influences controlling the reaction selectivity are the phosphine structure as well as the reaction conditions.

As the phosphorus is protonated during sulphonation by the acidic reaction medium, a deactivating influence for the electrophilic aromatic substitution is introduced (Figure 3), which leads to harsh required reaction conditions and thus promoted phosphine oxidation. However, it has to be noted that protonation of phosphorus is also an effective protection group against oxidation in the aggressive SO$_3$ containing reaction medium. Furthermore the sulphonation is exclusively directed to the *meta*-position respective to phosphorus, and desired *ortho*- or *para*-sulphonated aromatic rings have to be introduced by other reaction pathways.[29] By introduction of activating functionalities which compliment the directing

effect of the protonated phosphorus, the reaction can be facilitated and controlled.[30] For example methoxy or methyl groups in the *ortho*-position selectively direct the sulphonation to the opposed *meta*-position (respective to the phosphorus) due to steric and mainly electronic reasons. This activating effect also results in shorter reaction times with milder reaction conditions which therefore limit phosphorus oxidation. In phosphines with mixed substitution patterns (*e.g.* Ph and *o*-OMe-Ph, Figure 3) only the aromatic substituents bearing activating functionalities react at these relatively mild reaction conditions with a low SO_3 content of ca. 20 % (w/w). An excellent overview of structural control in phosphine sulphonation and reported phosphines can be found in literature.[19]
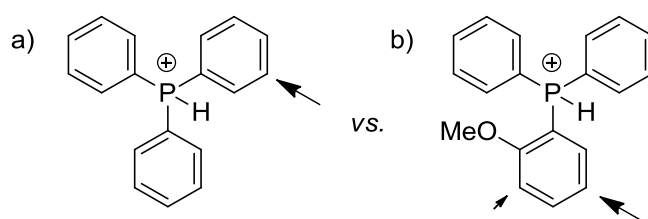
Figure 3: *Directing effects in a) protonated TPP, b) protonated partially activated TPP, only* meta-*sulphonation in trans-position to the OMe group observed due to steric reasons; Anions omitted for clarity.*

Exclusive selectivity in the sulphonation of non-activated phosphines, such as TPP, towards only one reaction product is relatively hard to achieve. For example *m*-TPPMS can be obtained by incomplete monosulphonation and recycling of the unreacted TPP.[31] Unfortunately this process is rather inefficient. A more elegant way is reported for the selective formation of TPPDS. Here TPP is sulphonated in a super acidic solution of fuming sulphuric acid with *ortho*-boric acid (Scheme 2) and reaction at 58 °C for three days which leads to a selective formation of TPPDS. Temperature increase only favours oxidation but not trisulphonation of TPP. Only if an excess of SO_3 (30% (w/w)) is applied in this system TPPTS is obtained in three days at room temperature. This super acidic medium seems to be more efficient in the protonation of the phosphorus atom as only negligible amounts of oxides were observed.[28]

$$B(OH)_3 + 5\ H_2SO_4 \rightleftharpoons [H_3SO_4]^+ + [B(OSO_3H)_4]^- + 3\ H_2O$$

$$3\ H_2O + 3\ SO_3 \rightleftharpoons 3\ H_2SO_4$$
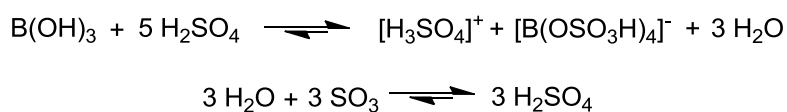
Scheme 2: *Proposed formation of the sulphonating species in the super acidic boric acid/fuming sulphuric acid medium.*

2. Sulphonated Phosphines in Homogeneous Catalysis

iii) Phase transfer and mediation in biphasic catalysis

The described sulphonated phosphines are ideal for reactions in the aqueous phase or in biphasic systems, if the reactants show sufficient water-solubility to overcome mass transfer limitations. For the hydroformylation of higher olefins which show low water solubility, the addition of phase mediators such as quaternary ammonium salts can significantly increase catalyst productivities. The resulting phosphine-ammonium salts can be either created *in situ* or by preformation to prevent possible negative influences of the reaction additives.[32] Likewise the importance of the counterion could also be observed, for example in C-C coupling reactions with a rhodium/*m,m,m*-TPPTS-based catalyst system. Upon change of the reaction medium from a mixture water/methanol to pure water a drastic drop of the conversion could be observed with Na^+ as counterion. Introduction of tetraalkylammonium salts (NMe_4^+, Net_4^+ and NBu_4^+) improves the conversion in water and can fully restore catalytic activity whilst maintaining catalyst recyclability.[33] Other examples describe the usage of surfactants, polymeric supports or catalysis in micelles.[19]

3. Copolymerisation of Olefins with Polar-Functionalised Olefin Comonomers

3.1. Late transition metal-based olefin polymerisation catalysts

Two prominent examples of systems in late transition metal catalysed ethene homopolymerisation are palladium based κ^2-(N,N)-α-diimine[5b, 34] and κ^2-(P,O)-phosphine sulphonate-based catalysts[9] (Figure 4).

3   4
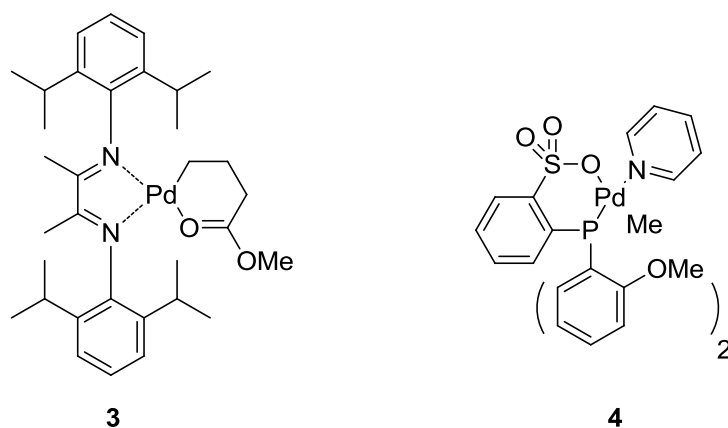
Figure 4: *Structure of the most prominent and widely used examples for palladium based α-diimine 3 and phosphine sulphonate 4 catalysts.*

Despite the fact that these systems employ the same catalytically active metal, the different catalyst structures involve different reaction pathways, which lead to drastically varying polymer architectures and hence, polymer properties. The α-diimine system **3** on the one hand normally produces branched to highly branched PE[5b], whilst the phosphine sulphonate-based catalysts related to **4** produce highly linear PE (see below).[9, 35] This difference can be attributed to the underlying reaction mechanisms. A prominent feature observed for the α-diimine catalyst system is chain walking, where the metal can move along the polymer chain by a series of fast *β*-hydride eliminations, reorientation and reinsertion steps which leads to the branched PE structures. The equilibrium between chain walking and chain propagation is dependent on the catalyst structure as well as the reaction conditions (Scheme 3).Therefore the polymer branching can be directly controlled.[5, 36] The high activity and stability of these complexes (Type **3**) as well as the obtained high molecular weights of

11

3. Copolymerisation with Polar-Functionalised Olefins

resulting PE can be attributed to a blocking of the axial positions by substituents on the ligand, which protects the growing polymer chain towards chain termination by associative ligand exchange.[37]
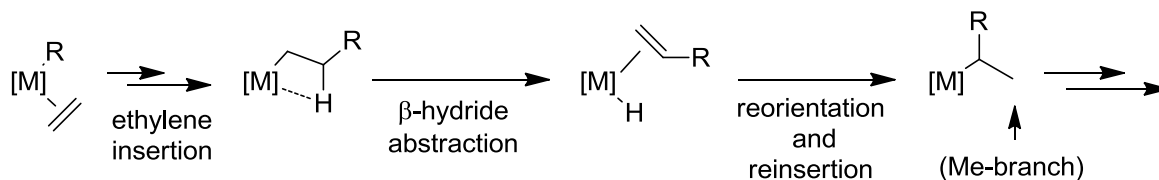
Scheme 3: *Description of the chain walking mechanism responsible for branch formation in α-diimine based late transition metal catalysed polymerisation reactions; ligand omitted for clarity; [M] = metal* e.g. *Ni, Pd.*

In comparison to the homotopic α-diimine-based system the phosphine sulphonate palladium catalyst system **4** employs a heteroditopic chelating ligand. This leads to major differences in reactivity (*vide infra*). Despite the partially open catalyst structure with minor steric bulk in proximity of the sulphonate coordination site these complexes are remarkably stable and active. The reason for this observation is based on induced site selectivity and site differentiation from the heteroditopic ligand coordination which stabilises alkyl groups only *cis* to phosphorus. Thus the growing polymer chain is effectively protected by the steric bulk of the phosphine substituents and ethene polymerisation produces highly linear PE as detailed below (Section 3.2.2, Figure 5).[35]
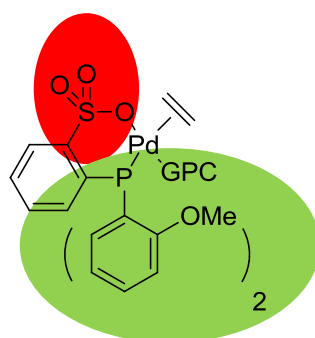
Figure 5: *Schematic visualisation of the non-symmetric distribution of steric bulk in a heteroditopic [{κ²-(P,O)-phosphine sulphonate}Pd(II)]-based catalysts; GPC: growing polymer chain protected by the aryl substituents of the phosphorus atom.*

12

3. Copolymerisation with Polar-Functionalised Olefins

3.2. Polymerisation reactions with [κ^2-(P,O)-phosphine sulphonate] Pd(II)-based catalysts

3.2.1. General information on polymerisation reactions with κ^2-(P,O)-chelated late transition metal catalysts

Heteroditopic chelating ligands based on different donor atoms ,such as phosphorus and oxygen, are widely employed in late transition metal-based polymerisation catalysis.[5b, 34] One prominent example is the "Shell Higher Olefin Process" (SHOP) based on κ^2-(P,O)-chelated nickel catalysts (Scheme 4).[21]
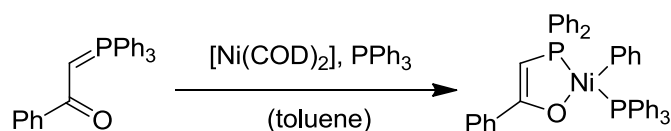
Scheme 4: *Structure and formation of a SHOP-type nickel catalyst.*

Phosphine sulphonate ligands were developed in the search for alternatives to SHOP-type catalysts for ethene oligomerisation.[38] *In situ* prepared nickel-based catalysts with phosphine sulphonate ligands in polar solvents such as sulpholane or ethanol are described in the patent literature as catalysts for ethene oligomerisation after activation. Successive patents, concerning palladium-based phosphine sulphonate complexes, show their activity *i)* in ethene/CO copolymerisation reactions as well as *ii)* in terpolymerisation reactions with propene or *iii)* in the copolymerisation of ethene with polar-functionalised norbornenes.[39] Subsequent reports on the first successful non-alternating copolymerisation of ethene and CO as well as the formation of linear ethene/methyl acrylate (MA) copolymers attracted considerable interest of the scientific community.[40] In the following the section ethene homopolymerisation is discussed to explain the important characteristics of this catalyst system in copolymerisation reactions of ethene with polar functionalised olefins.

3. Copolymerisation with Polar-Functionalised Olefins
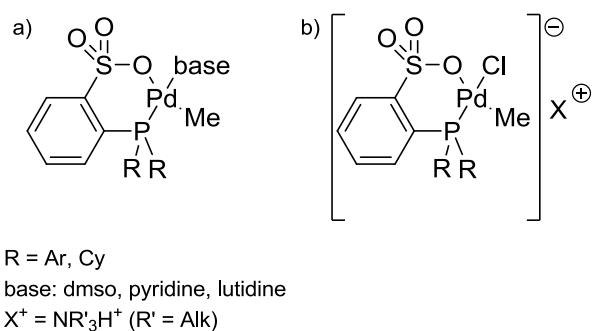
Scheme 5: *General structure of [κ^2-(P,O)-phosphine sulphonate]Pd(II) complexes a) neutral active catalysts, b) anionic chloro coordinated pre-catalysts.*

Scheme 5 shows the general structure of [κ^2-(P,O)phosphine sulphonate]palladium(II)-based polymerisation catalysts. Detailed investigation of the ethene polymerisation has been first reported by *Jordan et al.*[41] for pyridine coordinated [{κ^2-(P,O)-phosphine sulphonato}PdR(pyridine)] complexes (R = Me). Pyridine as an unusual, strongly coordinating base was shown to efficiently stabilise a mononuclear configuration of the catalysts. Its abstraction *via* Lewis acids leads to the formation of sulphonate-bridged dimers. These can be cleaved again by addition of coordinating solvents acting as Lewis bases. Direct comparison of ethene polymerisation experiments with catalysts bearing 2-methoxyphenyl or 2-ethylphenyl substituents on phosphorus show similar catalyst activity and microstructure of the resulting PE homopolymer, respective to each other. The obtained highly linear PE has molecular weights M_n between 5,000 and 70,000 g·mol^{-1}, dependant on the reaction conditions. NMR spectroscopy of these polymers, as well as theoretical investigations, confirm a significantly higher barrier for β-hydride elimination compared to α-diimine-based Pd(II) catalysts described above.[42] Terminal olefinic end groups and internal olefins from chain termination can be observed, indicating a β-hydride elimination which also leads to chain walking. This conclusion is also supported by product analysis of polymerisation attempts with 6-chloro-1-hexene where the catalyst decomposes by β-chloro elimination after chain walking. Unlike in polymerisation of ethene by α-diimine complexes **3** this chain walking seems to be slow for the phosphine sulphonate system and mainly 2- and 3-olefins could be observed next to terminal olefinic end groups. Insertion of the formed secondary alkyl species seems to be hindered, which results in a highly linear structure of the PE with melting points between 130 and 138 °C. [41]

14

3. Copolymerisation with Polar-Functionalised Olefins

Combination of experimental and theoretical investigations of discrete [{κ^2-(P,O)-phosphine sulphonate}Pd(alkyl)(lutidine)] complexes in 1-hexene isomerisation also show both, the presence of β-hydrogen elimination, as well as chain walking.[35] This report indicates a dynamic equilibrium between lutidine and an alkyl species with a proposed agostic H-Pd interaction at low ethene pressure, as observed by NMR spectroscopic investigations. These experiments also show a significant reduction of activity and molecular weight (R = Ph, M_n 6,000 g·mol^{-1}; R = *o*-OMePh, M_n 63,000 g·mol^{-1}; compare Scheme 5) in the direct comparison of lutidine coordinated catalysts. Density functional theory (DFT) calculations were employed to identify and compare the relevant intermediates in the polymerisation reactions for a simplified system (R = Me) which were also compared to the non-simplified actual active catalyst (R = Ph) and were focused on chain propagation, β-hydrogen elimination and the reinsertion in combination with a possible formation of branches.[35]

3.2.2. Mechanism of the ethene homopolymerisation reaction with phosphine sulphonate-based Pd(II) catalysts

i) Chain propagation and catalyst configuration

A site preference, originating from the heteroditopic character of the κ^2-(P,O)-chelate, is generated in the square planar coordination environment of the palladium centre. DFT calculations confirmed the experimental observation that alkyl groups are *cis*-located with respect to phosphorus in the stable catalyst resting state, due to the strong *trans*-effect of the phosphine donor (Scheme 6).
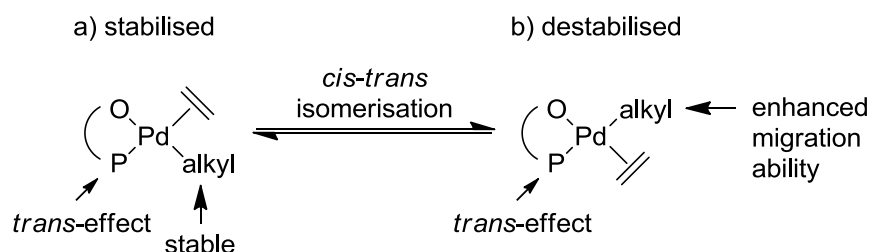
Scheme 6: *Comparison of the a) stable* cis- *and b) destabilised* trans-*position of the alkyl group in phosphine sulphonate-based palladium catalysts.* Cis-trans *isomerisation leads to an enhanced migration ability of the alkyl group.*

3. Copolymerisation with Polar-Functionalised Olefins

Destabilisation of the *trans*-position to phosphorus, and the resulting site preference in these complexes requires a *cis-trans*-isomerisation for chain growth *via* a *Cossee-Arlman* mechanism, as proposed in the literature.[43] Here the insertion of the olefin takes place *via* a four-membered intermediate. This was first noted during investigation of this system by DFT calculation by *Ziegler et al.*[42b] and later *Nozaki et al.*[35] After a *cis-trans* isomerisation the alkyl group, or growing polymer chain, possesses enhanced migration ability, as migratory insertion reforms the stable catalyst resting state with the generated new alkyl species in *cis*-position relative to phosphorus.
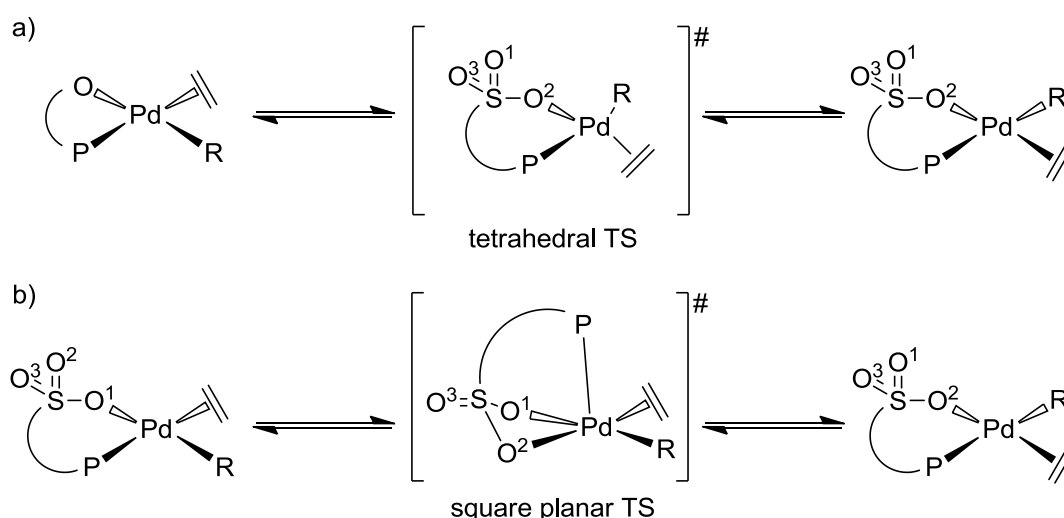
Scheme 7: *Comparison of the two possibilities proposed as* cis-trans-*isomerisation pathways during polymerisation with phosphine sulphonate-based Pd(II) catalysts; a) rotation* via *a tetrahedral transition state, b) associative* cis-trans *isomerisation leading to an exchange of coordinated oxygen atoms.*

Cis/trans-isomerisation can either take place *via* dissociative, associative or rotational configuration changes. Dissociative isomerisation by breaking of an agostic Pd-H interaction or the dissociation of the Pd-sulphonate bond is appraised as being unlikely from theoretical calculations.[35] Rotation *via* a tetrahedral transition state into the isomerised quadratic planar structure is possible (Path a), Scheme 7), but with a higher energy transition state compared to an associative isomerisation mechanism (Path b), Scheme 7). Here, the isomerisation takes place *via* a five-coordinated intermediate by association of a new ligand and subsequent dissociation to form the isomerised structure. It was found, that in the phosphine sulphonate system a second sulphonate oxygen can assist the isomerisation by formation of a five-

3. Copolymerisation with Polar-Functionalised Olefins

coordinated near square pyramidal transition state with phosphorus in the apical position. Upon exchange of the coordinated oxygen atoms the position of the two other ligands on the palladium is reversed.[35] A similar behaviour was observed in related [{κ^2-(P,O)-phosphine phosphonate}Pd]-based complexes. Variable temperature ^{31}P NMR spectroscopy indicated the involvement of a second oxygen atom in the Pd-O coordination (Figure 6).[44]

5
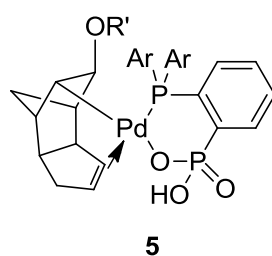
Figure 6: *General structure of reported phosphine phosphonate complexes 5 (R' = Me, Et; Ar = 2-R''-Ph, R'' = H, Me, OMe).*

Chain propagation follows a *Cossee-Arlman* mechanism by ethene insertion from the higher energy intermediate state with the alkyl group being located *trans* to phosphorus, facilitating the reaction. The reduced energy of the resulting four-membered transition state clearly favours chain propagation, as expected due to the restoration of the stable *cis*-configuration.[35]

ii) β-Hydride elimination, reinsertion and branch formation

To verify the origin of the internal olefins observed in ethene homopolymerisation reactions the possibility of β-hydride elimination was investigated for this system. As for chain propagation *cis-trans* isomerisation is required for hydride transfer from an alkyl species with an agostic Pd-H interaction, leading to a metal hydride and a coordinated olefin, due to the *trans*-effect as explained above. However, the reported data are not totally conclusive about the exact reaction path due to the high energies required for the formation of Pd-H species. This high energy barrier is in complete accordance with the findings reported by *Ziegler et al.* and experimental observations.[35, 41, 42b] Branch formation occurs by reinsertion of the generated olefin species after β-hydride elimination and rotation (Scheme 3). The transition state energies required for branch formation seem to be slightly increased, which is assumed to be the reason for the low observed branching degree.[35]

3. Copolymerisation with Polar-Functionalised Olefins

iii) Chain termination

Termination of the polymer chain has not been conclusively modelled by DFT calculations up to now. However a direct H-transfer to coordinated ethene was ruled out from the theoretically possible reaction pathways. Associative and dissociative olefin exchange reactions leading to chain termination are both possible, but an exact nature could not be specified. Not covered in the theoretical calculations is an associative replacement of coordinated olefin species with pyridine as chain termination reaction. Due to the strong coordinating nature of the base and its observed influence on catalyst stability, this possibility should not be disregarded, especially as a recent report notes a high concentration of pyridine coordinated species under reaction conditions.[45]

iv) Influences from the catalyst structure on the polymerisation reaction

In addition to these fundamental experimental and theoretical investigations, reports based on catalyst design were dedicated to the evaluation of the ligand structure influence on ethene polymerisation. For reasons of comparison, only pyridine-containing neutral catalysts are discussed here. Phenyl substituents on phosphorus lead to the formation of low molecular weight polymers with relatively low activity.[35] Introduction of OMe- or ethyl substituents in the *ortho*-position of the phenyl groups increases the PE molecular weights and catalyst activity.[41] High activity and molecular weights were reported for an extremely sterically encumbered phosphine sulphonate based catalyst **6**, where the axial positions are protected by the steric bulk of the ligand (Figure 7).[46]

3. Copolymerisation with Polar-Functionalised Olefins
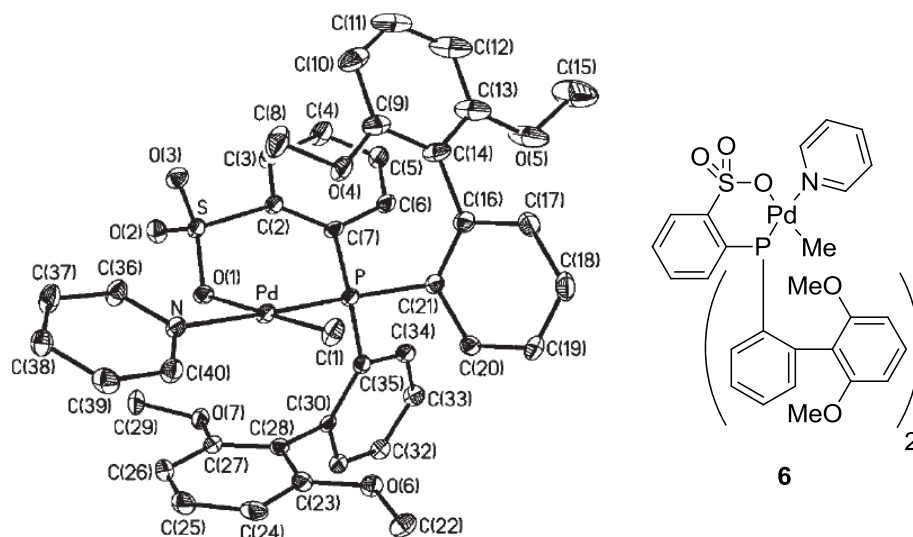
Figure 7: *Phosphine sulphonate catalyst **6** with the molecular structure; displacement ellipsoids are at the 30% probability level.[46] Steric bulk from the phosphorus substituents leads to protection of the axial positions at the palladium complex centre.*

However, very recently the dependence of the polymerisation activity on basicity and steric bulk of the employed ligand was examined by *Claverie et al.*[47] through direct comparison of phenyl, naphthyl, phenantryl and anthracenyl-substituted phosphine sulphonate Pd(II) catalysts. In contrast to the expected increase of molecular weight and activity these substitution patterns reduce both, for reasons which are currently not clearly understood.

In contrast to the substitution pattern, the influence of the employed base is well known, as for example shown by *Mecking et al.* [48] with introduction of dimethylsulphoxide (dmso) into a phosphine sulphonate catalyst instead of pyridine related bases, which results in an increase of the catalyst activity. Nevertheless, the stabilisation is sufficient to prevent dimerisation and fast catalyst decomposition under polymerisation conditions. Variations including the usage of water soluble bases can also be found in the literature.[49] In general the labile character of the stabilising base makes exchange relatively easy. However, its abstraction with Lewis acids leads to the formation of dimeric species with low solubility from which suitable Lewis bases can be introduced by cleavage of bridging sulphonate-Pd(II) interactions.[41] Alternatively the replacement of TMEDA in a κ-(N,N)-bridged dinuclear complex is possible.[50] The influence of the ligand structure on the catalyst activity is discussed in detail in Section 6.7.

3.3. Concept and challenges for (co-)polymerisation reactions in the presence of polar functionalised olefins

3.3.1. Early transition metals - Inhibition by σ-coordination

Transition metal-based polymerisation catalysts always show a significant competition between the desired η^2-π-coordination of functionalised olefins, which can lead to desired migratory insertion, and the direct coordination of the polar group causing a blocking of coordination sites. In most cases the highly Lewis acidic early transition metals undergo fast deactivation by σ-coordination to the active site of the metal after addition of polar functionalised olefins. One possibility to overcome this problem is the usage of protection groups for the hetero atoms.[8a] Relatively few publications exist concerning the coordination behaviour of polar comonomers to early transition metal catalysts. Amongst these a NMR spectroscopic study, which employed different α-ω-unsaturated alkyl ethers with $Cp_2ZrMe_2/B(C_6F_5)_3$ as the catalyst system, clearly shows, that the ability of η^2-coordination versus a direct coordination of the functional group is dependent on the electronic and steric effect of the protection group (Figure 8).[51]

R = Me, SiMe₃, Bz, SiPh₃, CPh₃,
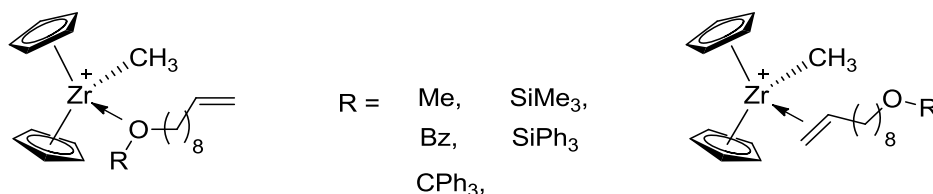
Figure 8: *σ-and π-coordination modes of various unsaturated ethers to a cationic zirconocene complex, R = protecting group.*

Increasing steric encumbrance leads to weaker coordination of the ether oxygen to the cationic zirconium centre. In addition silylethers are less Lewis basic because silicon is known to efficiently delocalise the π-electrons of the oxygen atom and hence coordination *via* the oxygen atom is reduced.

3. Copolymerisation with Polar-Functionalised Olefins

3.3.2. Late transition metals - coordination and insertion of olefins

Numerous reports on less Lewis acidic late transition metal-based catalysts concern the coordination and polymerisation behaviour of olefins in presence of functionalised olefin comonomers or polar solvents. Upon introduction of polar-functionalised olefins into a polymerisation reaction three important effects have to be taken into account. Firstly, the coordination of the olefin to the metal centre has to be assessed. Here the binding strengths of the employed monomers have to be considered, along with the resulting equilibrium between coordinated ethene and the functionalised olefin. The following step, after coordination of olefins, is the insertion into the metal-alkyl bond of the catalyst. The nature of a functional group can have a profound influence on the insertion rate, as well as on the orientation of the monomer during the migratory insertion. This can lead to a control of the insertion regioselectivity. Finally the ability of polar-functionalised olefins to form σ-bonds *via* the respective polar functionalities instead of π-bonds *via* the olefin has an influence on the reactivity and can lead to unfortunate restrictions in the olefin pool.

3.3.3. Influence of the olefin coordination equilibrium

A key requirement for insertion polymerisation of olefins is their ability to undergo π-coordination to metal complexes. In electron deficient late transition metal complexes the coordination of electron rich olefin monomers such as ethene is stronger than for olefins with electron withdrawing functional groups (EWG), as shown by DFT calculation. The coordination strength is proportionally linked to the energy level of the olefin HOMO (highest occupied molecular orbital), which is normally represented by the π(C=C) orbital. The origin is the strong electron donation from this π(C=C) orbital to a vacant d_σ orbital of the metal. This dominates the back donation from the d_π orbital to the π*(C=C) (LUMO, lowest unoccupied molecular orbital) orbital of the olefin. Introduction of an EWG group into olefins lowers the energy of the HOMO and thus the overall strength of the coordination. An overview concerning calculated HOMO/LUMO energies and coordination energies for some late transition metal complexes can be found in the literature.[9, 52] Additionally DFT calculations showed a strong influence of the ethene coordination strength on the overall charge of the metal complex. In all reports the binding strength to the electron rich monomer decreases in the order cationic > neutral > anionic metal complex.[53]

3. Copolymerisation with Polar-Functionalised Olefins

Brookhart et al.[5b] showed that the incorporation ratio of olefins in copolymerisation experiments with cationic α-diimine-based Pd(II) complexes is in first approximation dependant on the equilibrium of the employed olefin monomers. The insertion rate into the metal carbon bond, as well as the formation of stable resting states by coordination of functional groups to the metal centre after insertion is neglected for now. Furthermore it could be shown that this equilibrium is a result of the employed monomers, their concentration and the reaction conditions.[5b]

i)   Insertion of olefins into alkyl-metal bonds

Experimental observations as well as theoretical calculations show that the insertion rate of polar functionalised olefins and ethene are usually comparable. Some electron poor functionalised olefins have reduced insertion barriers compared to ethene, resulting in faster reaction.[54]

In non-symmetrically substituted olefins the regioselectivity of the insertion reaction is a critical point which has to be considered. Again theoretical calculations as well as experimental observations agree on a predominant 2,1-insertion mechanism for late transition metal catalysed copolymerisation reactions (Scheme 8).
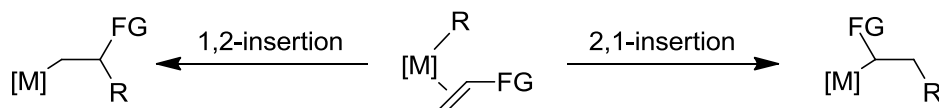
Scheme 8: *Modes for insertion regioselectivity for functionalised olefins:*

The insertion regioselectivity is assumed to be a cooperative result of steric and electronic effects which can be explained as following:

-   In EWG-functionalised olefins the LUMOs are relatively stable and possess similar coefficients for the sp^2-carbon orbitals ($2p_z$). Furthermore the calculations show no remarkable charge separation within the olefin molecule. Therefore it can be assumed that steric reasons lead to the favoured 2,1-insertion.
-   Conversely, electron rich olefins (*e.g.* propylene with no predominant insertion regioselectivity) display a different insertion behaviour. Here the substituted olefins show a considerable charge separation where the positive charge is mainly located on the substituted carbon atom. This results in a negation of the steric preferences for

some olefins such as propene. However with high steric hindrance the 1,2-insertion is again disfavoured and 2,1-insertion predominantly occurs.[54]

ii) Competing σ-coordination of polar olefin comonomers

Despite the fact that late transition metal catalysts, in comparison to early transition metal catalysts, are exceptionally stable towards polar functionalities and polar solvents several points have to be considered upon addition of functional groups to a reaction mixture. As in early transition metal-catalysed copolymerisation reactions functionalised olefins can undergo either σ- or π-coordination to late transition metal complexes, an effect which was studied in detail for α-diimine-based Pd(II) complexes (Scheme 9). σ-Coordination can prevent or retard desired π-coordination of olefins and thus lowers the overall copolymerisation rate. Reduction of the reaction rate was found to be directly proportional to the σ-coordination strength. Application of a large excess of the non-polar olefin (mostly ethene) can reduce this negative influence of σ-coordination by increasing the concentration of competing olefin which promotes ligand exchange.[55]

π-coordination   σ-coordination
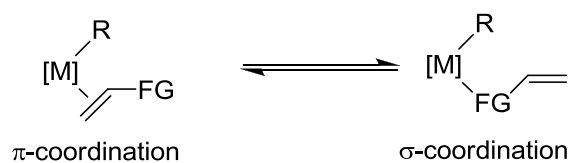
Scheme 9: *Competing σ- and π-coordination of functional olefins.*

In certain copolymerisation experiments with polar comonomers (*e.g.* carbon monoxide or methyl acrylate) formation of stable catalyst resting states can be observed. This is the so-called "backbiting" mechanism where the growing polymer chain bends back and the metal is stabilised by a chelating coordination (usually a 5 or 6 membered ring) of a functional group on the polymer chain (Figure 9).[5b, 56]

3. Copolymerisation with Polar-Functionalised Olefins
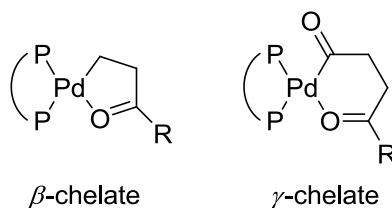
β-chelate   γ-chelate

Figure 9: *Structure of stable chelate intermediates from chain backbiting observed in the ethene/CO copolymerisation; R = alkyl or growing polymer chain.*

Due to these stable catalyst resting states further monomer coordination and insertion is retarded which again results in an overall decrease of the polymerisation rate. Depending on the nature of the coordinating functional group the polymerisation is either slowed or completely halted. *Brookhart et al.*[5b] showed this for α-diimine catalysts where a significant rate reduction could be observed for oxygen-containing functional comonomers and the copolymerisation was usually halted in presence of nitrogen-containing functional groups. Other examples for the drastic influence of chelate structures on the polymerisation mechanism can be found in olefin/CO copolymerisation reactions.[56]

3.4. Copolymerisation reactions with [{κ^2-(P,O)-phosphine sulphonate} Pd(II)]-based catalysts

3.4.1. Ethene/methyl acrylate copolymerisation

Brookhart et al.[5b, 57] established palladium based catalysts for the copolymerisation of ethene and methyl acrylate (MA). With the employed α-diimine catalysts highly branched polyolefins are formed in which the acrylate units are predominantly situated at the end of alkyl branches and form a block like polymer architecture (Example a), Scheme 10).[55] This was followed by the report of *Drent et al.*[40b] on the synthesis of highly linear ethene/MA copolymers with acrylate units incorporated in the main chain (Example b), Scheme 10). The employed system based on an *in situ* generated catalyst with 2-[Bis(2-methoxyphenyl)phosphine]benzenesulphonic acid [*o*-TPPMS(OMe)] **7** and Pd(OAc)$_2$ is ill defined, as shown later by *Rieger et al.*[58] (Section 3.4.4). However it could be established, that low molecular weight ethene/MA copolymers are accessible by late transition metal catalysed insertion polymerisation. The M$_n$ of these polymers ranges between $5 \cdot 10^3$ and

3. Copolymerisation with Polar-Functionalised Olefins

$1 \cdot 10^4$ g·mol^{-1} with MA incorporation between 7 and 17 mol%. Due to the high content of the polar comonomers in the reaction mixture of up to 80% (v/v), the activities are relatively low. At constant ethene pressure the obtained M_n is decreased by increasing MA content, as the increased MA concentration shifts the present coordination equilibrium towards coordination of the polar functionalised olefin.
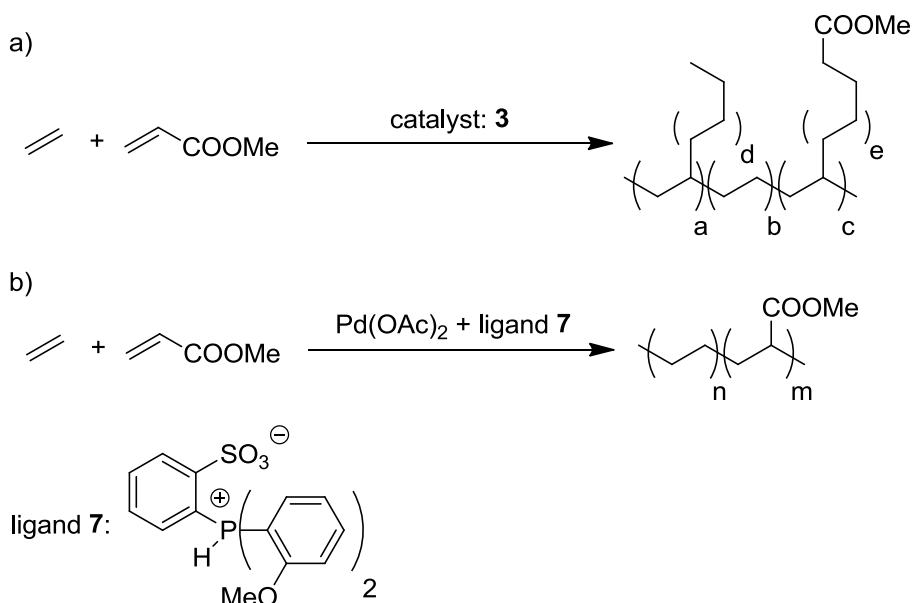
Scheme 10: *Comparison of the ethene/methyl acrylate copolymerisation with the a)* Brookhart *system (branched copolymer) and the b)* Drent *system (linear copolymer).*

Parallel to work from *Rieger et al.*,[59] anionic phosphine sulphonate-based pre-catalysts were developed by *Nozaki et al.*[60] (Type b), Scheme 5). Both systems are suitable for ethene/MA copolymerisation reactions and the MA incorporation ratio is limited to a maximum of 20%. Development of neutral base-coordinated [{(κ^2-P,O)-phosphine sulphonate}PdMe(base)] catalysts led to observations which significantly improved the understanding of the reaction mechanism, including possibilities and limitations imposed by the catalyst system. An increase of steric bulk, which led to higher catalyst activity (Section 3.2.2) was shown to reduce MA incorporation, attributed to a by hampered MA coordination through steric hindrance.[46] The important influence of the auxiliary base on catalyst stability was already established in ethene homopolymerisation. Exchange of pyridine-related bases to the weaker coordinating dmso base led to the breakthrough regarding the ethene/MA copolymerisation. Significantly increased catalyst activities were observed at similar polymer architectures. Additionally the dmso-coordinated complex shows activity at high MA

25

concentrations in combination with a low ethene pressure, conditions which significantly improve the MA insertion ratio. Copolymers with up to 52 mol% MA and even the formation of MA oligomers, in absence of ethene, with a degree of polymerisation (DP) of *ca.* 5 could be achieved. To prevent free radical polymerisation of MA at high reaction temperature and MA concentration, 3,5-di-*tert*-butyl-4-hydroxytoluene (BHT) was employed as a radical trap. Detailed investigation of coordination dynamics showed only a low competition of dmso with ethene coordination in this system. Furthermore, in contrast to the assumption that the formation of four membered chelates *via* the carboxylate oxygen slows the reaction, the insertion of olefins into the α-carbonyl substituted alkyl species has been identified as the rate determining step of the polymerisation reaction. Close examination of the MA oligomerisation by experimental and theoretic techniques showed the insertion-type character of the oligomerisation. Stable dimeric insertion products coordinated to the corresponding catalyst species could be analysed by X-ray diffraction.[61] The robust nature of the catalyst system could also be shown in the direct copolymerisation of acrylic acid (AA) with ethene providing copolymers with AA contents up to *ca.* 10 mol%. Acid stability of the catalyst has been proven by ethene homopolymerisation reference experiments in presence of propionic acid.[62] Again for prevention of radical polymerisation at high reaction temperatures BHT was added as stabilising agent. Although the role of radical inhibitors can be problematic[63], radical copolymerisation was prevented.

3.4.2.   Functional olefin copolymerisation reactions with low incorporation ratios

In addition to the now fairly well understood and relatively efficient (co-)polymerisation of acrylates numerous other functionalised olefins could be copolymerised with ethene by phosphine sulphonate-based Pd(II) catalysts. Although only very low incorporation rations in the range of 0.5-10 mol% were observed, comonomers which previously could not be incorporated by insertion polymerisation are amongst this selection. Copolymerisation activities are usually very low and the resulting molecular masses are greatly reduced in comparison to the related ethene homopolymers.

Scheme 11 shows an overview of the various suitable functionalised vinylic and allylic comonomers for copolymerisation with ethene, which proves the extremely high and unusual functional group tolerance of this catalyst system. One missing prominent example for functionalised vinyl olefins, methyl methacrylate (MMA), was recently reported as being

3. Copolymerisation with Polar-Functionalised Olefins

problematic in copolymerisation reactions, due to a weak coordination of this monomer to the phosphine sulphonate complexes. Insertion of MMA could be studied with base free complexes and shows a mixture of 1,2- and 2,1-insertion. However the reactions products from 2,1-insertion rearrange upon β-hydride elimination. Large concentrations of MMA hamper the activity of ethene polymerisation but do not lead to MMA insertion.[64]

To date, the following functional vinylic olefins could be copolymerised, acrylates[40b, 46, 48, 60-61], acrylic acid (AA)[62], vinylfluoride[65], acrylonitrile (AN)[66], vinyl ethers[67], vinyl acetate (VA)[68], vinyl sulphones[69], *N*-vinyl-2-pyrrolidone (NVP)[70], *N*-isopropylacrylamide (NIPAM)[70], functionalised norbornenes[71], vinyl methyl ketone[72], styrene and functionalised variants[72] in addition to the allylic-functionalised olefins[73] allyl acetate, allyl alcohol, allyl amine, N-Boc protected allyl amine, allyl chloride, allyl bromide. Additionally copolymers of ethene and propene, 1-hexene and vinylcyclohexane could be obtained.[72]

This large selection of suitable olefin comonomers shows the high robustness of the phosphine sulphonate-based Pd(II) catalyst system. Nevertheless only a very narrow selection of catalyst structures within the general complex class is reported to be active in thesereactions. Most often catalyst **4** is employed, either with dmso or pyridine-related bases. Recent reports mention the dicyclohexylphosphine analogue with slightly higher activities in copolymerisation reactions.[68] In general it has to be stated, that only MA could be oligomerised and copolymerised with insertion ratios greater than 50%. This indicates that insertion of olefins into alkenes with EWG-functionalised olefins is slow and disfavoured especially for functionalised olefins.

3. Copolymerisation with Polar-Functionalised Olefins
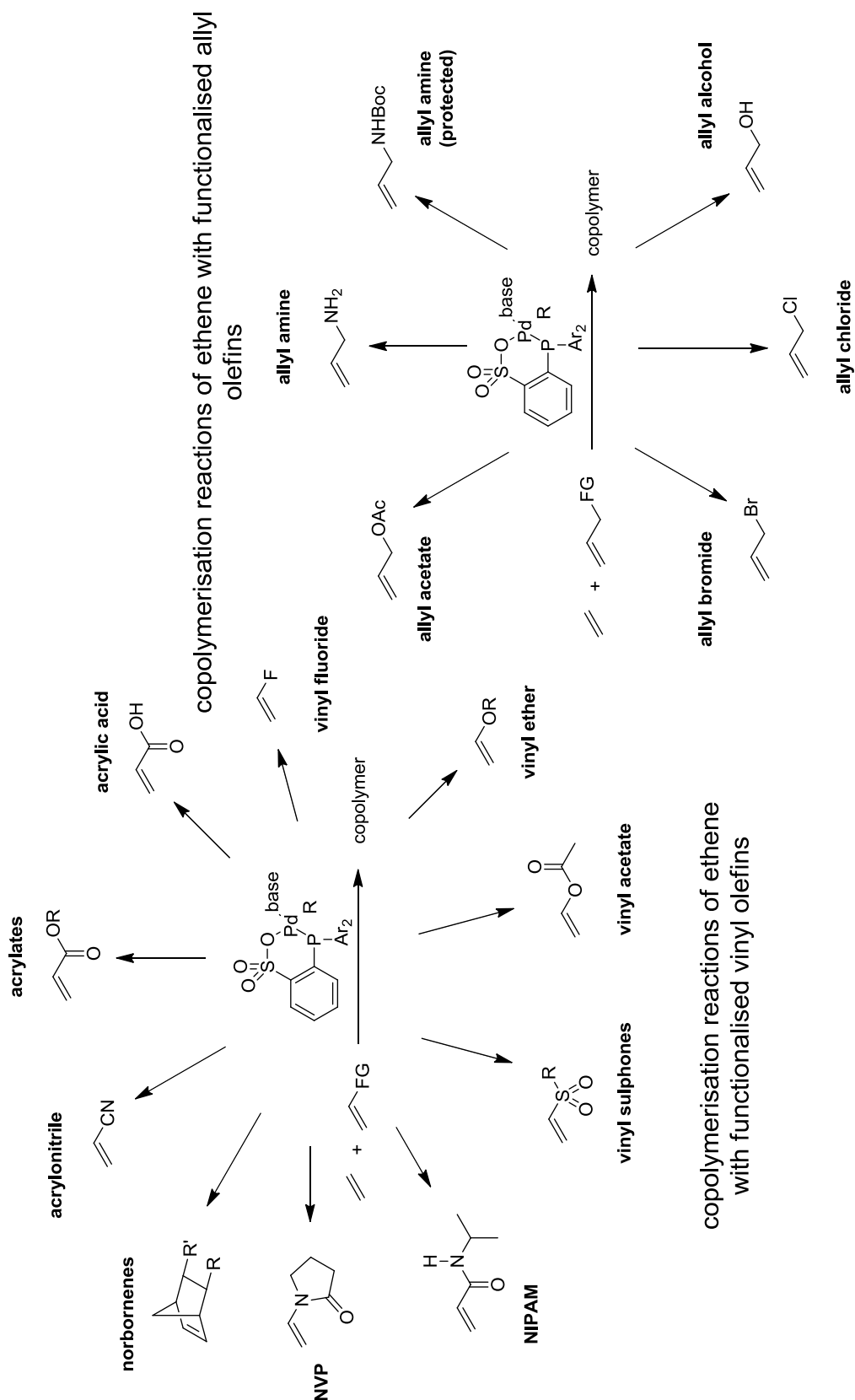
Scheme 11: *Overview of selected phosphine sulphonate Pd(II)-catalysed copolymerisation reactions of ethene with functionalised olefins. Examples for suitable catalyst substituents: Ar = o-OMe-Ph, R = Me, base = pyridine*

3. Copolymerisation with Polar-Functionalised Olefins

3.4.3.   Acrylonitrile insertion as an example for problems with insertion reactions of functionalised olefins

The challenging nature for insertion polymerisation of the monomers listed above (Scheme 11) can be explained with ACN as an ideal example. Not only the highly Lewis acidic early transition metal-based polymerisation catalysts do suffer from poisoning by coordination of functional groups. Even the functional group tolerant late transition metal-based catalysts show pronounced inhibition of polymerisation activity by σ-coordination of functional groups at higher functionalised olefin concentrations. *Ziegler et al.*[74] demonstrated by DFT calculation, that the coordination behaviour of ACN has a dependence on the formal charge of the metal centre of the catalyst. This means that in cationic α-diimine complexes the ACN favours σ-coordination, whereas in neutral salicylaldiminato ligand based Pd(II) or Ni(II) complexes the probability of σ- and π-coordination is equal. Concerning the insertion regioselectivity a 2,1-insertion has been proposed.

Wu et al.[75] investigated the insertion reaction of ACN in symmetric k^2-(N,N)-chelating ligands. It was shown that the first insertion of an ACN unit into the Pd-Me bond takes place easily but no second insertion occurs, due to aggregation of complex molecules. The ACN is not able to break the relatively strong bridging unit in the resulting Pd-CHEtCN----Pd aggregates (similar to the aggregates depicted in Figure 10). Likewise these aggregation complexes cannot react with ethene at room temperature. However their cleavage is possible by addition of a Lewis acid such as for example with B[C$_6$F$_5$]$_3$. The electron withdrawing character of the formed CN-B(C$_6$F$_5$)$_3$ substituent in α-position on the alkyl group inhibits the migratory insertion reaction of this nitrile functionalised alkyl-Lewis acid adduct. By these experiments it could be shown that ACN coordination is in principle able to compete with ethene coordination, despite its weaker π-coordination and insertion rate. A second report concerning neutral and anionic κ^2-(P,P) chelating ligands also showed the initial ACN insertion product (2,1-insertion) but no further reaction with ethene or CO.[76]

Comparison of neutral and anionic salicylaldiminato complexes allows the investigation of their behaviour in the reaction with ACN.[77] Here it could be shown that these complexes can co-oligomerise ACN with ethene.[77] Furthermore the oligomerisation rate could be slightly enhanced by the introduction of a negatively charged substituent which results in an overall anionic Pd complex. Unfortunately these complexes have a high tendency to

agglomerate. The resulting aggregate structures inhibit polymerisation and oligomerisation of ACN (Figure 10).
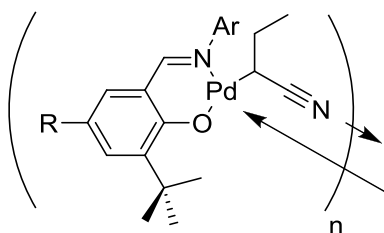
Figure 10: *Structure of aggregation products observed during the oligomerisation of ACN; R = alkyl, BF₃[K(18-crown-6)]*.[77]

To date the only example of a successful ACN copolymerisation reaction with ethene by an insertion mechanism was reported by *Nozaki et al.*[78] with a neutral phosphine sulphonate-based Pd(II) catalyst. This system is capable for ACN insertion up to 10 mol% in linear copolymers with ethene (Scheme 12). The resulting polymers posses nitrile-containing alkyl and olefinic end groups, which indicate 2,1-insertion, as well as nitrile groups in the polymer chain. The ratio of the nitrile group distribution on the PE backbone is approximately 1:1:2 (start:end:internal nitrile functionalities). The PE backbone structure of these small copolymers is highly linear and therefore a radical copolymerisation process was excluded as radically polymerised copolymers would show internal branching and usually prepared at extremely high reaction temperatures and ethene pressures.
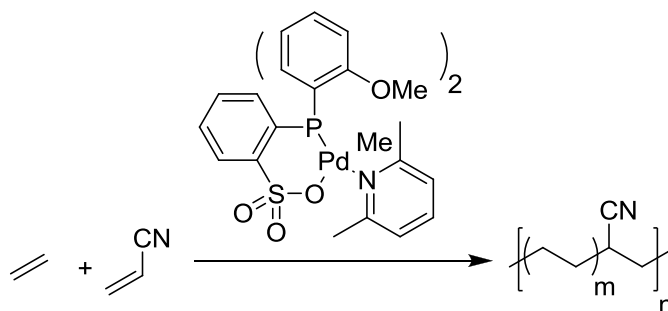
Scheme 12: *Copolymerisation of ACN with ethene by catalyst 4 (lutidine coordinated).*

Recent theoretic investigation by DFT calculations concern the origin for the observed differences between neutral salicylaldiminato, cationic chelating phosphine and neutral phosphine sulphonate catalysts.[66a] One finding is that for neutral phosphine sulphonate

catalysts, in presence of with strongly coordinating pyridine-related bases, the σ-coordination of ACN is slightly less favourable than coordination of the base. This indicates that it is possible to overcome the energy barrier by an excess of ACN, and that nitrogen bases can replace the undesired σ-coordinated functional groups. Calculations showed the relative similarity of the transition states for ACN and ethene insertion with the latter being slightly favoured in the phosphine sulphonate system. As for ethene polymerisation (*vide supra*) the insertion requires a *cis-trans* isomerisation to the less stable configuration with the alkyl group *trans* to phosphorus. The neutral salicylaldiminato system should be theoretically capable for ethene/ACN copolymerisation but seems to favour decomposition of the catalyst due to facile β-hydride elimination of the alkyl group, subsequent release of free ligand by reductive elimination leads to catalyst decomposition and formation of palladium black. In contrast to these two neutral catalyst systems, the cationic chelating bis-phosphine system is not capable for ACN incorporation.

In consequence, the unique behaviour of the phosphine sulphonate catalyst systems seems to be a reduced tendency for β-hydride elimination which prevents catalyst decomposition reactions and allows the incorporation of comonomers which are difficult to copolymerise by other catalyst systems, following an insertion type mechanism. The neutral character of this system seems to be sufficient to ensure π-coordination of functional monomers, from where insertion is only a matter of the insertion rate and the olefin coordination equilibrium. Continuation of the polymerisation reaction seems to be more problematic due to the slow insertion rate into α-EWG-functionalised alkyl groups, which can easily lead to decomposition or chain termination after β-hydride elimination.

3.4.4. The non-alternating ethene/CO copolymerisation

Copolymerisation of ethene and CO usually leads to the formation of a strictly alternating copolymer.[56] As a result of the high content of keto-functionalities in a regular and defined constitution, the resulting copolymers are highly crystalline, with melting points only slightly below the decomposition temperature and insolubility in common organic solvents. To facilitate processing and to control the polymer properties, terpolymerisation reactions of ethene/propene/CO were developed which show reduced crystallinity due to the introduced side chains. As propene shows a lower incorporation rate compared to ethene, the "pulse feed polymerisation process" was developed to achieve a constant polymer composition. Here the

3. Copolymerisation with Polar-Functionalised Olefins

regular injection of ethene into a propene/CO polymerisation at defined intervals leads to thermoplastic elastomers.[79]

Polyketones were also commercially available under the brand names Carillon™ (Shell) and Ketonex™ (BP), which indicates the highly effective polymerisation process based on readily available low cost monomers. The employed catalysts are homotopic cationic palladium complexes with bis-chelating phosphines of the $[\kappa^2\text{-(P,P)Pd}]$-type. The unique properties of the copolymerisation mechanism include the formation of intramolecular chelates by "backbiting" of the keto-functionalities and results in a strictly alternating copolymer structure. Double insertion of CO was found to be thermodynamically unfavourable and double ethene incorporation is prevented by the formation of β-chelate intermediates which can only be opened by the strongly coordinating CO (Scheme 13).[56]
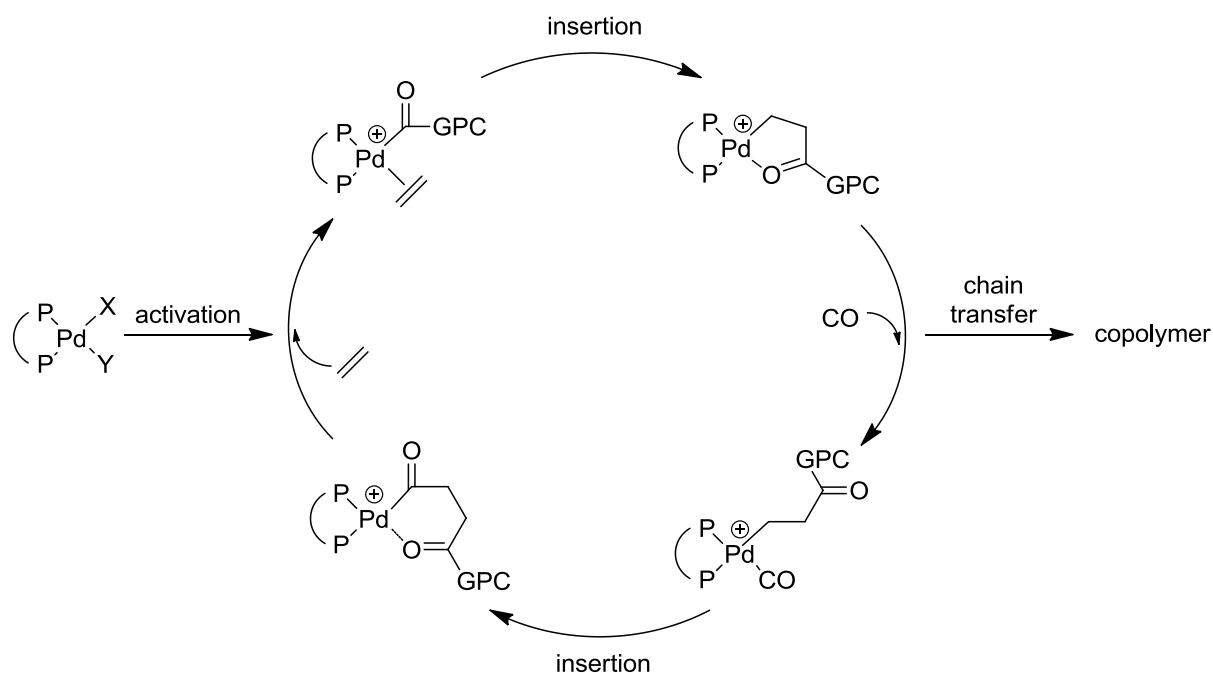
Scheme 13: *Mechanism of the strictly alternating ethene/CO copolymerisation reaction.*

Originating from work[39a] on the alternating copolymerisation of ethene and CO in 2002, *Drent et al.*[40a] reported the first example of a non-alternating copolymerisation with phosphine sulphonate-based Pd(II) catalysts. Here up to *ca.* 20 mol% ethene units were incorporated in a non-alternating fashion. However the employed *in situ* generated catalyst system based on Pd(OAc)$_2$ and **7** is problematic. *Rieger et al.*[58] proved that under the

3. Copolymerisation with Polar-Functionalised Olefins

employed conditions the formation of neutral bis-chelated complexes such as $[\{\kappa^2\text{-(P,O)-}$ phosphine sulphonate$\}_2\text{Pd}]$ is possible which are incapable for the formation of non-alternating copolymers. The reason for this is assumed to be a cleavage of the weaker Pd-O bonds causing the catalyst to act as a non-chelated cationic Pd-phosphine catalyst, which produces strictly alternating copolymers at low activity (Scheme 14).
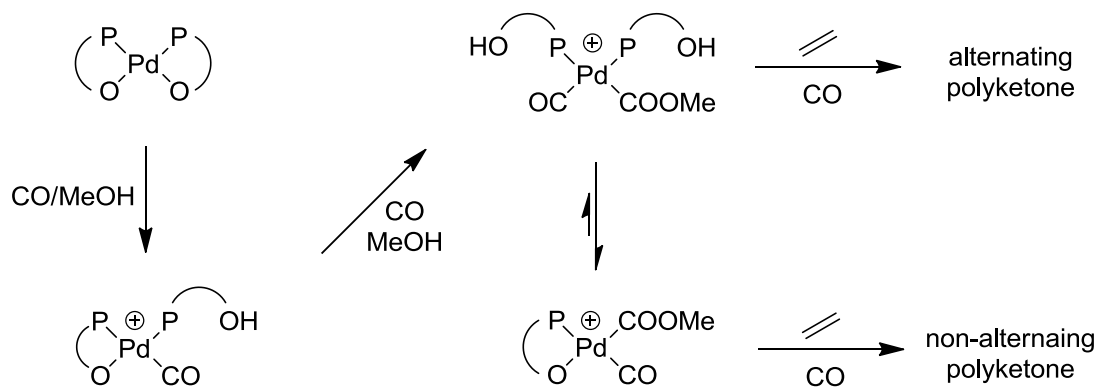
Scheme 14: *Proposed mechanism leading to predominantly alternating copolymerisation with neutral phosphine sulphonate [κ^2-(P,O)]$_2$Pd complexes.*

This problem can be prevented by selective pre-formation of a directly active single component catalyst which possesses both a metal-alkyl and a metal-olefin bond, in addition to the coordinated phosphine sulphonate. By this modification up to 30 mol% additional insertion of ethene could be achieved by control of the reaction conditions (Scheme 15).[58]
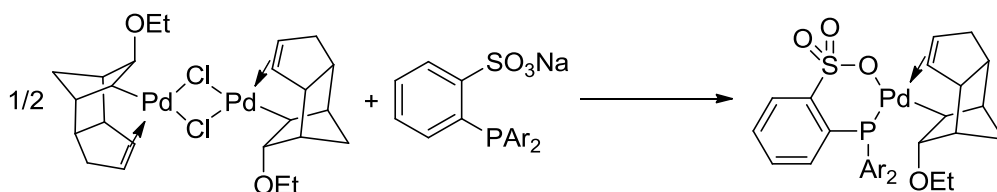
Scheme 15: *Synthesis of active single component catalysts developed by Rieger et al., Ar = 2-OMe-C$_6$H$_4$, Ph.*[58]

These observations concerning the non-alternating copolymerisation of ethene and CO were followed by DFT calculations to investigate the differences between classic κ^2-(P,P) bis-

3. Copolymerisation with Polar-Functionalised Olefins

phosphine- and κ^2-(P,O) phosphine sulphonate-based Pd(II) catalysts. It could be shown that the heteroditopic ligand, as well as the neutral character of the resulting phosphine sulphonate catalyst, are responsible for the non-alternating copolymerisation. The ligand structure was investigated to evaluate its direct effect on the copolymerisation reaction. As explained above for ethene homo- and co-polymerisation reactions a *cis-trans*-isomerisation is required for chain propagation (Section 3.2.2). Either introduction of steric bulk or the presence of electron rich substituents was found to facilitate this isomerisation.[42c] Noteworthy is also a weak binding of CO to the neutral Pd centre and the strong dependence of the alternation ratio on the reaction temperature as well as the monomer partial pressures. Additionally in this system a decarbonylation pathway is opened as palladium-oxygen chelate bonded intermediates are either not formed or are labile. This could be proven by exchange experiments with ^{13}C labelled and unlabeled CO by *Sen*[80] and *Bianchini*[81] who investigated the incorporation of ethene and CO by *in situ* NMR spectroscopic experiments at low temperatures. These reports generally confirm the mechanism proposed by *Ziegler* (Figure 11) and propose formation of weak β-chelate intermediates. Unlike for the alternating copolymerisation these chelates can be opened by ethene. Kinetic investigations with catalyst **4** allowed the experimental determination of the rate constants and thermodynamic parameters. As critical features decarbonylation, formation of weak chelates, necessity of *cis-trans* isomerisation and a strong dependence on reaction conditions, namely temperature and relative partial pressure of CO could be confirmed. Essential is also a weak CO binding for this neutral catalyst system resulting in a coordination equilibrium of 50/1 (ethene/CO respectively).[80, 82] The proposed mechanism from *Ziegler et al.*[42c] is depicted in Figure 11 for comparison.

3. Copolymerisation with Polar-Functionalised Olefins
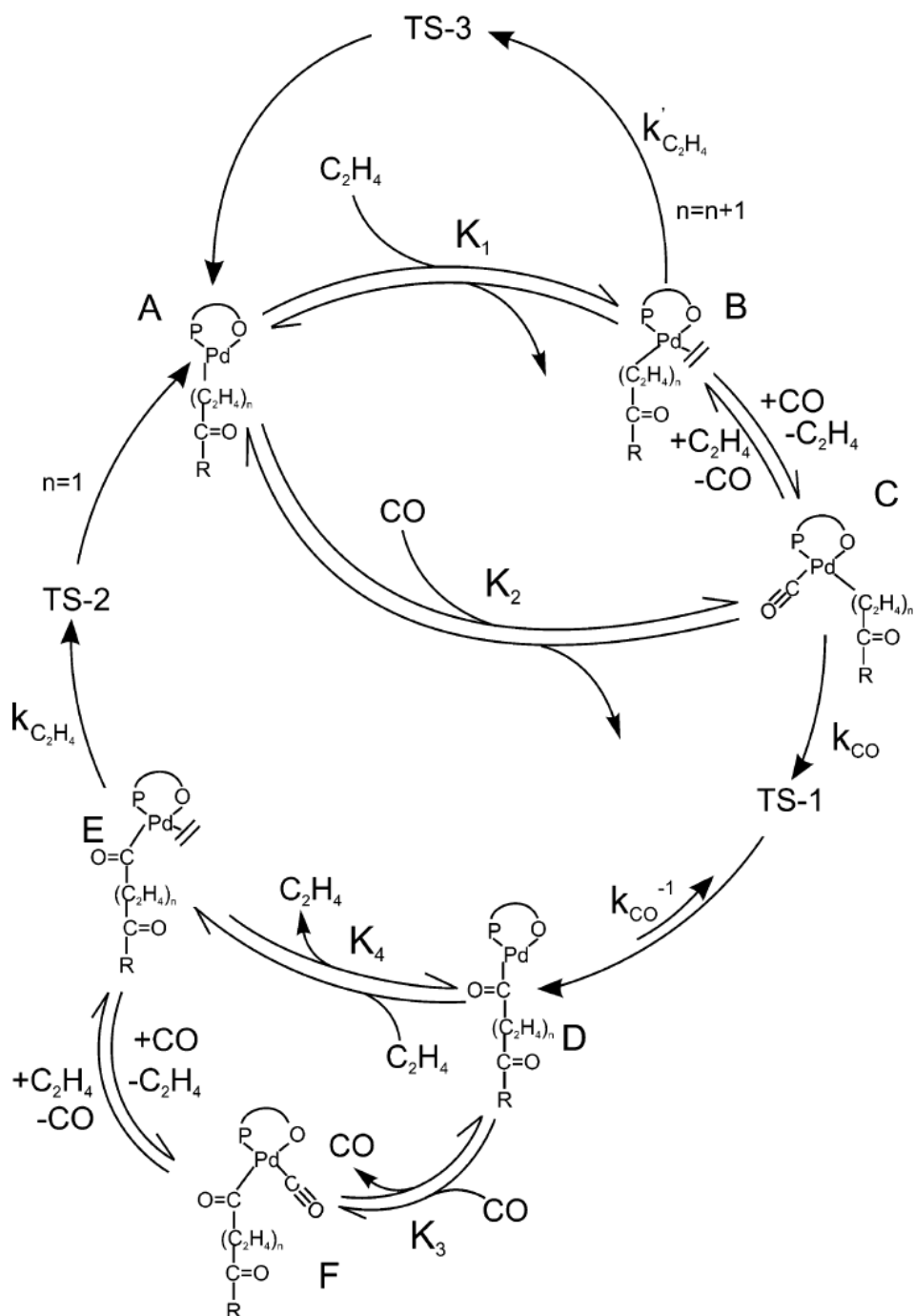
Figure 11: *Overview of the mechanism of the non-alternating copolymerisation of CO and ethene as proposed by* Ziegler *et al.[42c]; top cycle: non-alternating ethene incorporation; main cycle: alternating copolymerisation; bottom cycle: reversible formation of acyl-carbonyl complexes, no double incorporation of CO observed.*

3. Copolymerisation with Polar-Functionalised Olefins

4. Concept of this Work

Phosphine sulphonate-based Pd(II) complexes have shown their enormous potential in the copolymerisation of ethene and polar-functionalised olefins. These catalysts allow the incorporation of numerous functionalised olefin comonomers into linear PE *via* a controlled coordination-insertion mechanism. The scope for the introduced functional groups and the highly linear polymer architecture obtained from these polymerisation reactions are without precedent amongst transition metal-based polymerisation catalysts. Especially for the controlled synthesis of functionalised speciality polymers this catalyst system is of considerable interest to academic research. However a drawback is the relatively low polymerisation activity of the catalysts in presence of functional olefins with the costly palladium as the active metal.

The concept of this work focuses on possibilities for the improvement of phosphine sulphonate-based palladium catalysts by ligand and complex design. Critical questions which are addressed in this respect are both, the incorporation ratio of functionalised olefins as well as the investigation of methods which could lead to a potential increase of the catalyst activity in the parent ethene polymerisation as reference reaction.
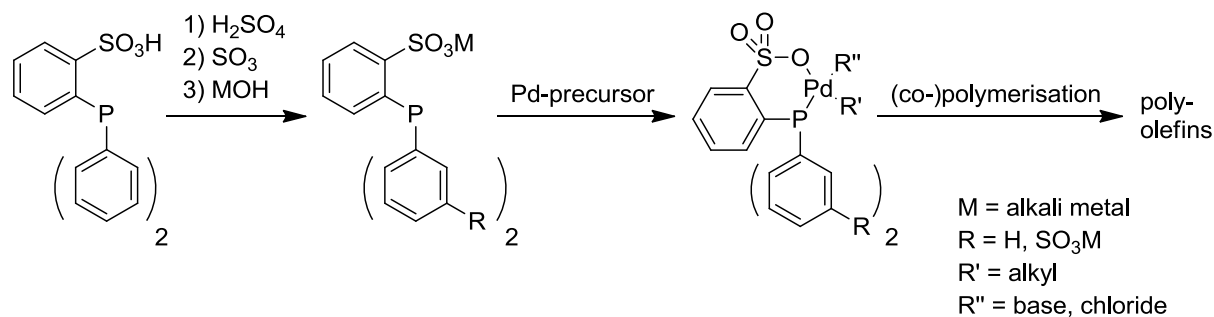
Scheme 16: *Modification concept for the introduction of anionic functionalities (R = SO₃M) by sulphonation for the synthesis of novel anionic [κ²-(P,O)-phosphine sulphonate]Pd(II)-based complexes. These complexes are potentially active olefin (co-)polymerisation catalysts.*

Several experimental and theoretical investigations concerning late transition metal-based polymerisation catalysts propose the introduction of anionic functionalities as a concept to increase the incorporation ratio for polar-functionalised olefins in copolymerisation reactions with ethene. Likewise the phosphine sulphonate system is examined for application of this concept (Scheme 16). An ideally suitable tool for the introduction of anionic functionalities is

4. Concept of this Work

the sulphonation of phosphines. This could lead to non-symmetrically sulphonated phosphines with chelating potential. With ligands of this type the subsequent synthesis of anionic phosphine sulphonate catalysts is examined, with respect to coordination chemistry and investigation of the homo- and copolymerisation behaviour with ethene and polar-functionalised olefins.
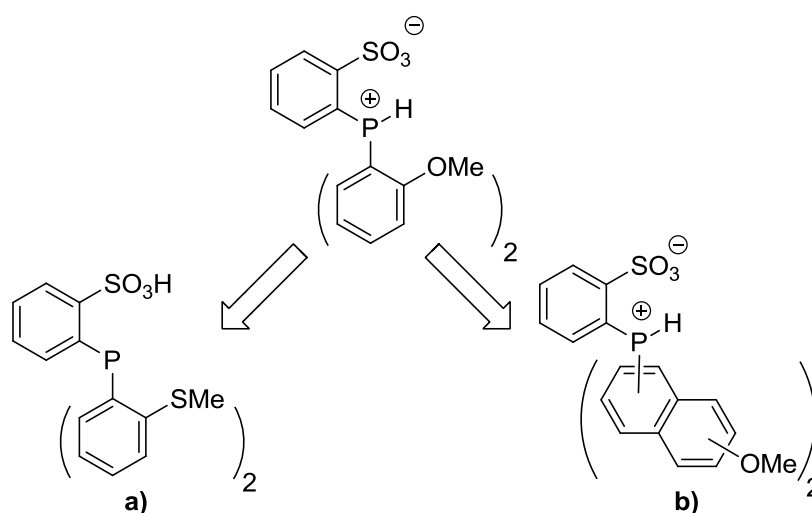
Figure 12: *Overview of examined phosphine sulphonate ligand modification concepts for investigation* ortho-*OMe influence on the corresponding Pd(II) catalysts; a) functional group exchange, b) alteration of the OMe location on a functionalised naphthalene substituent.*

Another approach for a possible improvement of the phosphine sulphonate catalyst system is the investigation of the structure/reactivity relationship of these catalysts. Here the identification of influences on the catalyst activity is important which could allow the specific modification of the system with respect to desired properties of the catalyst and resulting olefin (co-)polymers. Analysis of literature data, concerning the development of this research field during the course of this work, stimulated the investigation of possible ligand-metal interactions as a potential factor which influences the catalyst activity. Focus of this part is the investigation concerning the role of the methoxy functionality in *ortho*-position to phosphorus on the well known reference system (Figure 12). Therefore the exchange of this functionality as well as its position on the ligand backbone is examined, with respect to the metal centre of the corresponding complexes. Ethene homopolymerisation is performed as test reaction for determination of substitution effects.

5. Synthesis of Non-Symmetrically Sulphonated Triaryl-phosphine Ligands

5.1. Prospects for the sulphonation of *o*-TPPMS

In comparison to the known *meta*-sulphonated triphenylphosphines (Section 2.2) and the *ortho*-sulphonated arylphosphines (Section 3.2) described above, a combination of the attractive features from both systems could lead to a new class of phosphine ligands. The derived heteroditopic κ^2-(P,O)-chelating mode of hydrophobic phosphines could potentially result in attractive properties of corresponding transition metal-based complexes. A generic structure for these ligands is depicted in Figure 13.

M = Li, Na, K   n = 0-1
R$_1$ = H, OMe   m = 1-2
                   n+m = 2
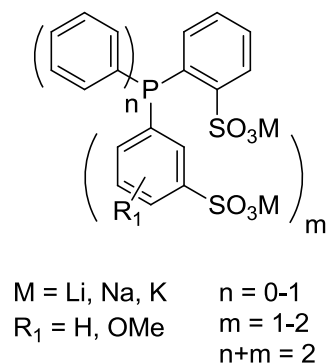
Figure 13: *General structure of the alkali metal salts of non-symmetrically substituted arylphosphines.*

As neutral or *mono*-anionic Pd(II)-based phosphine sulphonate complexes (Scheme 5) represent the most versatile catalyst system for the copolymerisation of ethene and polar olefins[9], the introduction of charge density in the coordination sphere of the complex is desired. This was proposed as a possible concept that could lead to improved copolymerisation behaviour by facilitating π-coordination of polar-functionalised olefins (detailed in Section 3.4.3).[77, 83] Introduction of sulphonate moieties by electrophilic aromatic substitution is a simple method for the functionalisation of aromatic substituents with anionic groups, perfectly suitable for the modification of phosphines (Section 2.2).[19] Sulphonation is carried out in a highly acidic reaction medium with large excess of oxidising SO$_3$, in which the phosphine is relatively well protected against oxidation by protonation at phosphorus.

5. Non-Symmetrically Sulphonated Phosphine Ligands

This results in a deactivating influence from the phosphonium centre on the electrophilic aromatic substitution which directs the sulphonation into the *meta*-position respective to phosphorus (Figure 3). Thus the *ortho*-sulphonate functionality has to be introduced prior to sulphonation of the phosphine. The retrosynthetic approach for the synthesis of non-symmetrically sulphonated aryl phosphines is depicted in Scheme 17. Introduction of two *ortho*-sulphonate functionalities was disregarded due to the anticipated competitive binding of two equivalent sulphonate groups on the polymerisation reaction and monomer coordination. This leads, as recently reported in literature, to aggregation of complex molecules and ethene oligomerisation at conditions which cause the decomposition of aggregates.[65b, 84]

M = Li, Na, K   n = 0-1
                 m = 1-2
                 n+m = 2
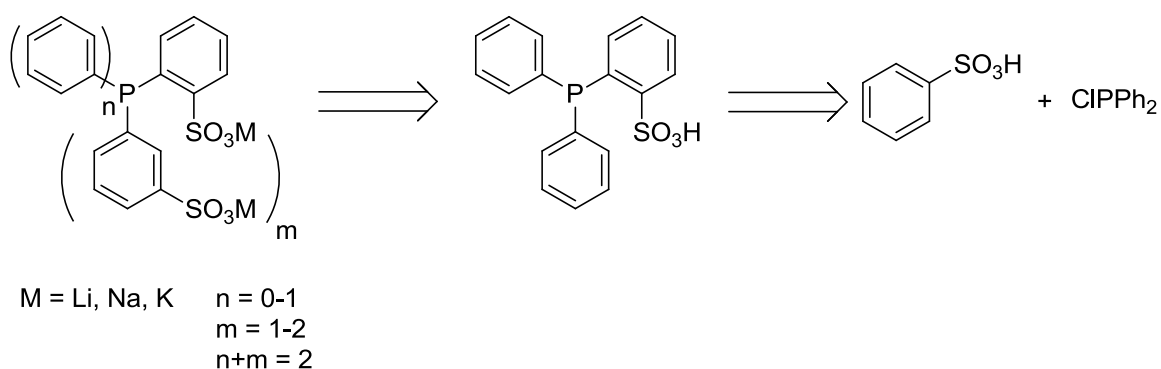
Scheme 17: *Retrosynthetic analysis of non-symmetrically sulphonated triphenylphosphine ligands with one* ortho-*sulphonate moiety*.

5.2. General description of the sulphonation of *o*-TPPMS

Sulphonation of *o*-TPPMS (or appropriate derivatives, Section 5.4) was carried out analogous to the sulphonation of TPP. The designated phosphine reactant, here *o*-TPPMS **8**, was dissolved in concentrated sulphuric acid or fuming sulphuric acid with a SO_3 concentration of up to 20% (w/w), to prevent immediate oxidation which is observed at higher SO_3 contents. In this acidic reaction medium phosphorus(III) is efficiently protonated as previously mentioned which provides protection towards oxidation to P(V) under the aggressive reaction conditions. To further reduce or prevent oxidation at this stage, the phosphine was added to the solvent at reduced temperature (0 °C) in small aliquots to facilitate the heat dissipation of the exothermic acid-base reaction (compare Section 5.3.2 for the influence of elevated temperature on phosphine oxidation).

5. Non-Symmetrically Sulphonated Phosphine Ligands
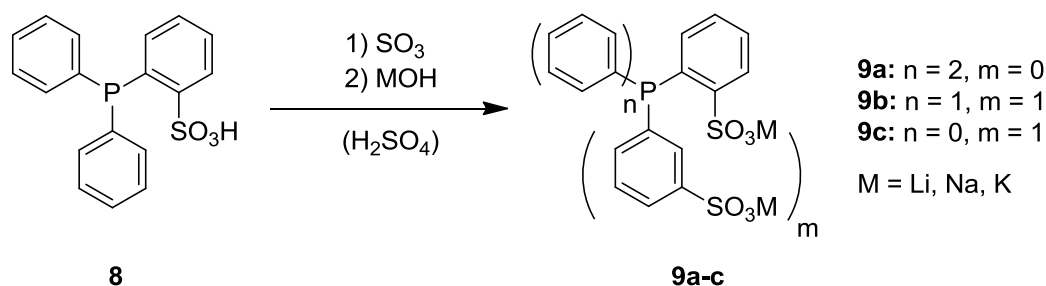
Scheme 18: *Schematic description for the sulphonation of 8 in fuming sulphuric acid.*

The sulphonation reaction commences upon slow addition of fuming sulphuric acid to the cooled phosphine solution. During addition the temperature was not allowed to rise above 30 °C to minimise oxidation and the reaction parameters were used to control the reaction. Namely SO_3 content, the SO_3 to phosphine ratio and the dilution, which is adjusted by addition of sulphuric acid, are the variables which govern the reaction rate and formation of different observed reaction products. Furthermore, in combination to these factors, reaction time and temperature additionally influence selectivity and rate of the sulphonation.

Due to the sensitivity of the ^{31}P nucleus towards NMR spectroscopy, reaction progress was followed by the use of ^{31}P NMR spectra.[85] Small aliquots were taken from the reaction mixture at defined time intervals and the reaction was halted by addition of a suitable alkali metal solution in deuterium oxide. Interpretation of the obtained spectra was found to be possible by comparison to reference compounds, despite the dependence of the chemical shift for phosphines on the pH and the ionic strength of the solution.[86]

Termination of the reaction was carried out by careful addition of degassed water to the cooled reaction mixture. Afterwards the reaction was diluted 2-5 fold with water, neutralised with an aqueous alkali metal hydroxide solution, such as NaOH or KOH, and the majority of the water was removed *in vacuo*. The desired products were obtained after extraction with refluxing methanol, filtration of the hot solution, followed by crystallisation or fractional precipitation upon addition of diethyl ether or ethanol. Choice of the employed cation was found to be a useful tool to control the solubility of the products and the inorganic salts formed as by-products (5.3.5).

5.3. Optimisation of reaction conditions for the sulphonation of *o*-TPPMS

Initial test reactions, performed as described above, indicated the formation of non-symmetrically substituted triphenylphosphines *via* direct sulphonation of **8**. Thus for optimisation of the reaction and determination of important influences a screening was carried out at different reaction conditions. Due to the similarity to the sulphonation of TPP, the optimal reaction conditions for the synthesis of *m,m,m*-TPPTS were taken as reference. Also the known influence factors controlling the sulphonation reaction were tested for the reaction of **8** with SO_3.[87] These factors are *i)* the concentration of the sulphonating species (SO_3), *ii)* the ratio n(SO_3):n(phosphine), *iii)* the dilution of the reaction adjusted by addition of H_2SO_4, *iv)* as well as the reaction time and *v)* reaction temperature.

Screening of the sulphonation at 20%, 30% and 50% SO_3 (w/w) content and different temperatures showed strong dependence of reaction rate, as well as product selectivity, on the SO_3 concentration. As expected, increased oxidation was observed at higher SO_3 concentration and significant influence was also found for the reaction time and temperature. The latter has been found to be a critical factor, as the temperature window for a fast reaction to the desired products is relatively narrow. For instance at higher SO_3 concentrations (*ca.* 50% (w/w)), slight heating to 30 °C was necessary to reduce viscosity of the solution. Optimal reaction conditions were found at 30 °C, whereas higher temperatures increased the rate of oxidation as described in the literature.[19, 87]

5.3.1. Observed reaction products in the sulphonation of *o*-TPPMS
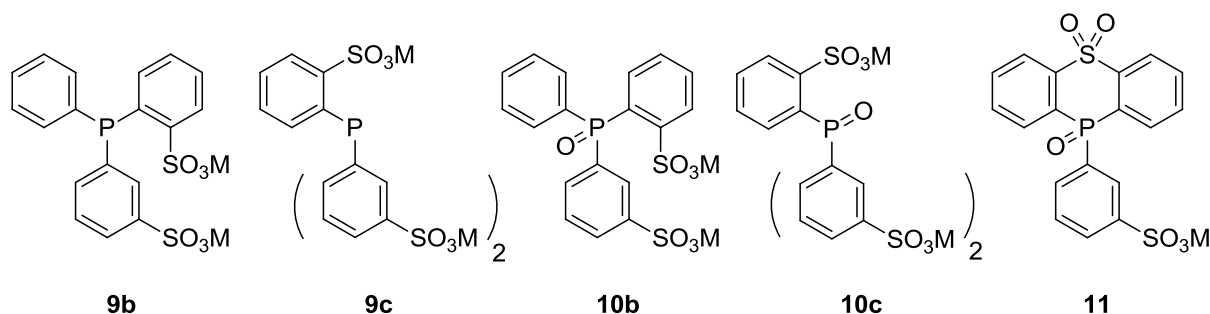
Figure 14*: Overview of the observed reaction products for the sulphonation of 8, namely:* rac-o,m-*TPPDS* ***(9b)****,* o,m,m-*TPPTS* ***(9c)****,* rac-o,m-*TPPDSO* ***(10b)****,* o,m,m-*TPPTSO* ***(10c)****, sulphone* ***(11)****; M = alkali metal.*

5. Non-Symmetrically Sulphonated Phosphine Ligands

The observed reaction products (Figure 14) are similar to the *meta*-sulphonated TPP analogues (Section 2.2.2). Hence, *rac-o,m*-TPPDS (**9b**) and *o,m,m*-TPPTS (**9c**) can be easily distinguished from their respective oxides by ^{31}P NMR spectroscopy due to the characteristic chemical shift associated with phosphine oxidation of approximately + 40-50 ppm. However as known from the literature the degree of *meta*-sulphonation has a minor influence on chemical shifts in ^{31}P NMR spectra.[29c] The combination of high resolution ESI-MS spectrometry complements NMR spectroscopy and allows unambiguous identification and full characterisation by independent analytical methods. Table 1 lists the reference NMR chemical shifts, together with the corresponding high resolution ESI MS data for all identified phosphorus-containing species. These values can be used to quantify and identify components of crude product mixtures of sulphonation reactions *via* spectra integration.

Table 1: *Reference shifts of identified reaction products from the sulphonation of* o-*TPPMS combined with the corresponding high resolution ESI-MS data. Values obtained after isolation of the respective Na*$^+$ *or K*$^+$ *salts.*

	rac-o,m- TPPDS **9b**	*m,m,m-* TPPTS **9c**	*rac-o,m-* TPPDSO **10b**	*m,m,m-* TPPTSO **10c**	Sulphone **11**
^{31}P NMR shift[1]; δ_P =	-10.5	-10.3	38.7	38.0	8.9
M$^-$ found[2]; m/z =	458.9561	544.9198	474.9476	560.9167	418.9831
M$^-$ calculated; m/z =	458.9528	544.9176	474.9477	560.9126	418.9813
counterion	K	Na	K	Na	Na

[1]Chemical shift observed by ^{31}P NMR spectroscopy, 121 MHz, D$_2$O; [2]obtained by high resolution ESI-MS spectrometry.

In detail, the sulphonation of **8** shows some differences compared to the reaction with TPP. Most obvious is the formation of 10-(3-sulphonatophenyl)-10*H*-9-thia-10-phosphaanthracene-9,9,10-trioxide, the sulphone species **11**, as detailed later (Section 5.3.4). This side reaction is not reported in the literature for the TPP system, although sulphone generation is a known side reaction in the electrophilic aromatic sulphonation.[88]

5. Non-Symmetrically Sulphonated Phosphine Ligands

5.3.2.   Interpretation of the obtained *o*-TPPMS sulphonation reaction data

Sulphonation reactions with **8**, carried out at different reaction conditions, were analysed in detail to evaluate formation of the identified reaction products. The screening parameters used for the reaction set, summarised in Table 2, are the SO_3 content, the ratio $n(SO_3)/n(phosphine)$ as well as the reaction time and temperature. Figure 15 gives an overview of the product distribution observed in the different experiments (entry numbers), after neutralisation and isolation of the crude product mixture as either Na^+ or K^+ salts. The effects of the reaction parameters are directly compared and investigated in the following paragraphs. Conditions used for the reactions represented by Entries 1-6 in Figure 15 are compared in Table 2. The exact composition of the product mixture is listed in Table 3.
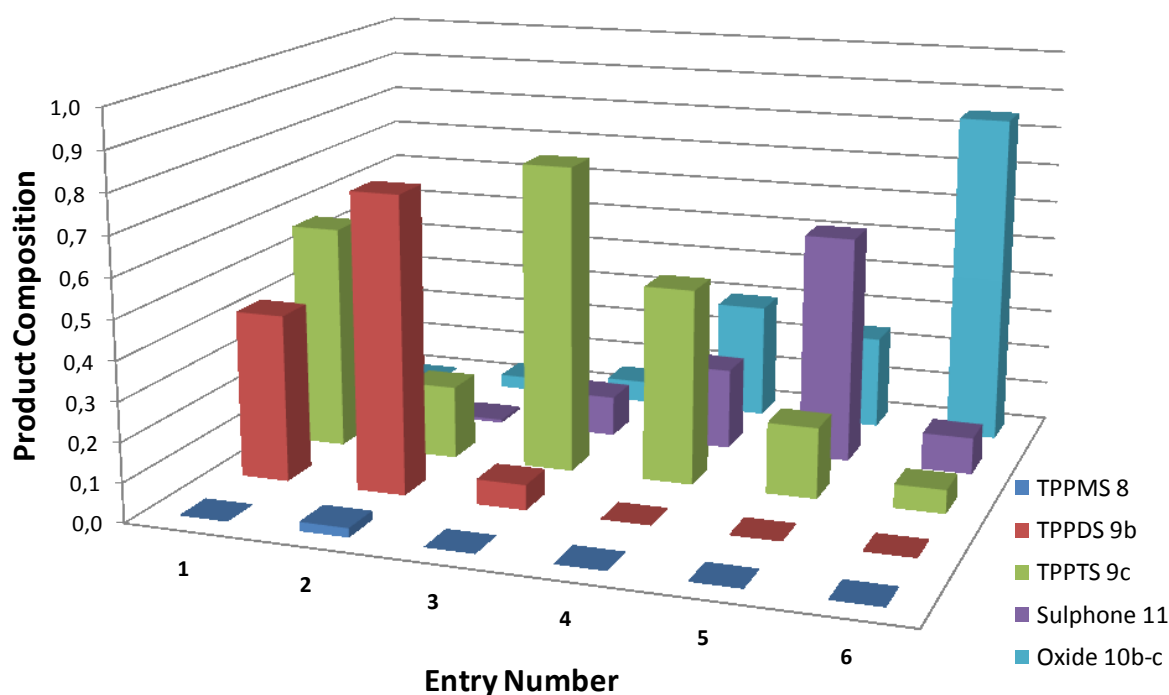
Figure 15: *Overview of the observed product composition for the sulphonation of* o-*TPPMS **8*** *at different reaction conditions (compare* Table 2 *and* Table 3*).*

5. Non-Symmetrically Sulphonated Phosphine Ligands

Table 2: *Reaction conditions employed in the screening of the sulphonation of 8.*[1]

Entry	Time	T (°C)	n(SO_3):n(Phosphine)	SO_3 (% w/w)	H_2SO_4 (% w/w)
1	20	RT	10	19	74
2	20	30	6	28	55
3	20	30	12	30	61
4	20	30	35	49	45
5	40	30	35	49	45
6	24	50	16	19	76

[1] Control of the SO_3 content and other parameters by combination of H_2SO_4 with fuming sulphuric acid (65 or 20% w/w).

Table 3: *Composition of the product mixtures observed in the sulphonation reactions of 8.*[1]

Entry	*o*-TPPMS **8**	*rac-o,m*-TPPDS **9b**	*o,m,m*-TPPTS **9c**	Sulphone **11**	Oxides **10b-c**
1	0.0	42.5	57.5	0.0	0.0
2	2.2	75.3	18.5	0.6	3.3
3	0.0	6.3	78.1	10.2	5.5
4	0.0	0.0	49.7	20.7	29.6
5	0.0	0.0	18.0	58.1	23.8
6	0.0	0.0	5.9	9.3	84.7

[1] Product mixture composition given in mol% of the total phosphorus content determined by ^{31}P NMR spectroscopy; graphical comparison in Figure 15.

i)   *Influence of the sulphonation reaction on the SO_3 concentration:*

In the experiments as detailed by Entries 1, 3 and 4, in Table 2 and Table 3, the SO_3 content of the reaction mixture is increased from 19% to 30% and 49% respectively. These reactions were carried out at room temperature (Entry 1) and 30 °C (Entries 3,4) for 20 hours. The slightly increased temperature is required at higher SO_3 contents to reduce the viscosity of the reaction mixture. The obtained results from crude product analysis by ^{31}P NMR spectroscopy, after neutralisation with an aqueous alkali metal hydroxide solution clearly show increasing formation of *o,m,m*-TPPTS **9c** combined with significantly higher sulphone **11** and oxide **10c** concentrations with increasing SO_3 content. In accordance to literature studies reduced oxidation was observed with constant agitation of the reaction mixture.[87a] Due to the high content of **9c** shown in Entry 3 (78.1%) these specific reaction conditions

were applied for isolation of this compound as detailed in the experimental part (Section 9.2.5). Continued reaction at a high SO_3 content, as shown by Entry 5 in Table 2 and Table 3 increases the ratio of **11** relative to formation of **9c** and the corresponding oxide **10c**. The conditions of this experiment proved to be suitable for the isolation of **11** as described in the experimental part (Section 9.2.6).

ii) Dependence of the sulphonation on the reaction temperature

Reaction temperatures below 40 °C have been described as ideal for the sulphonation of TPP as higher temperatures lead to increased oxide formation.[87a] Based on this report the effect of higher temperatures in the sulphonation reaction of **8** was investigated. The reactions represented by Entries 1 and 6 in Table 2 and Table 3 are compared, despite a slightly longer reaction time (24 instead of 20 h) for Entry 6, to evaluate the effect caused by a temperature increase from room temperature to 50 °C. Entry 1 clearly shows slow reaction at room temperature with a similar content of **9b** and **9c** and no observable oxide formation. In clear contrast, the reaction at 50 °C shows an extremely high oxide content of 84.7% accompanied with a relatively low formation of **11**.

iii) Effect of the $n(SO_3):n(phosphine)$ ratio on the selectivity of the sulphonation

In addition to the observations detailed above, a decisive influence of the molar ratio SO_3 to phosphine could be shown. Starting from the optimised reaction conditions for synthesis and isolation of **9c** (Entry 3, Table 2 and Table 3) the $n(SO_3):n(phosphine)$ ratio was reduced, as shown in Entry 2, from 12:1 to 6:1 at an almost constant SO_3 content (SO_3: 30% and 28% (w/w), respectively) and similar dilution (H_2SO_4: 61% and 55% (w/w), respectively). Remarkably, the product distribution shifted from favoured formation of **9c** to the formation of the disulphonated *rac-o,m*-TPPDS **9b**. Due to the high content of **9b** the respective conditions were suitable for its isolation as the potassium salt, detailed in the experimental part (Section 9.2.4).

5.3.3.   Kinetic investigation of the sulphonation reaction of *o*-TPPMS

Based on the information obtained from the screening of reaction conditions (Section 5.3.2), more detailed kinetic investigations were performed to gain further insight into the exact reaction mechanism leading to the formation of **9b-c**, the desired reaction products. As

previously stated integration of corresponding peaks observed in the ^{31}P NMR spectra was used to determine the content of the assigned components in the reaction mixture.[85] The reaction conditions used for the isolation of **9b-c** were employed in this kinetic investigation and the obtained relative compositions for identified phosphorus-containing species are compared in Figure 16 and Figure 17. Reactions, at both high and low $n(SO_3):n(phosphine)$ ratio, show a rapid decline of the concentration of **8** and formation of **9b**. Variation of the SO_3:phosphine ratio has a significant influence on the reaction rate, especially in the second sulphonation step from **9b** to **9c**. Formation of **9c** steadily increases with longer reaction time and, as expected, a higher ratio of SO_3 to phosphine leads to a faster formation of *o,m,m*-TPPTS. The slow increase of the oxide and sulphone content with the reaction time is clearly observed. Comparison and analysis of these trends confirm the expected two-step reaction from **8** *via* **9b** to **9c** with a clearly observable peak of **9b** concentration as the intermediate product. The shape of the graphs indicate that the second sulphonation step is slower compared to the first step as shown in the literature.[87a]
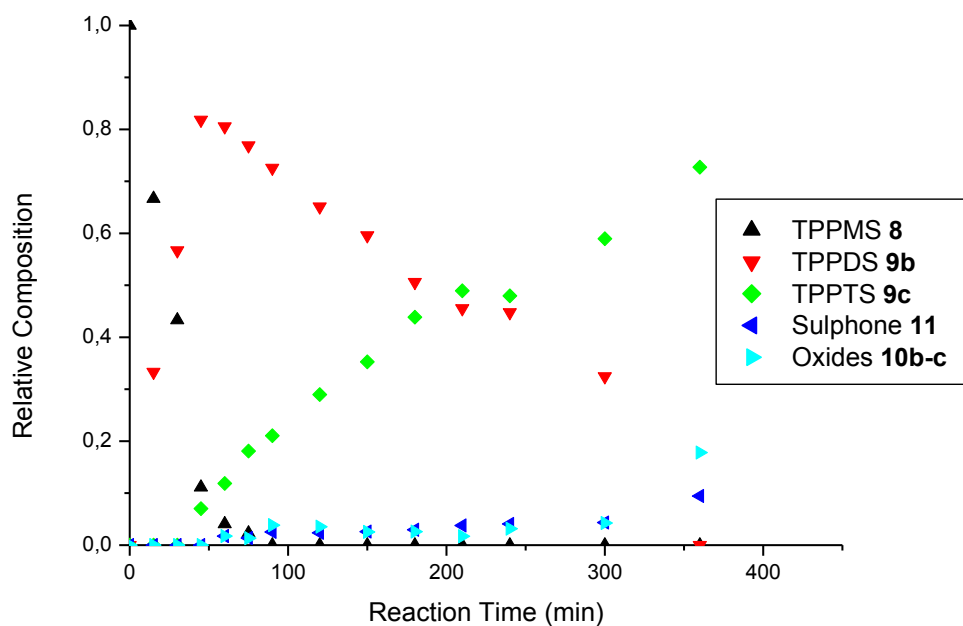
Figure 16: *^{31}P NMR spectroscopic kinetic investigation for the sulphonation of 8. Reaction conditions: 30% (w/w) SO₃, n(SO₃):n(phosphine) = 12, 61% (w/w) H₂SO₄, sample workup by reaction with 5 M NaOH in deuterium oxide.*
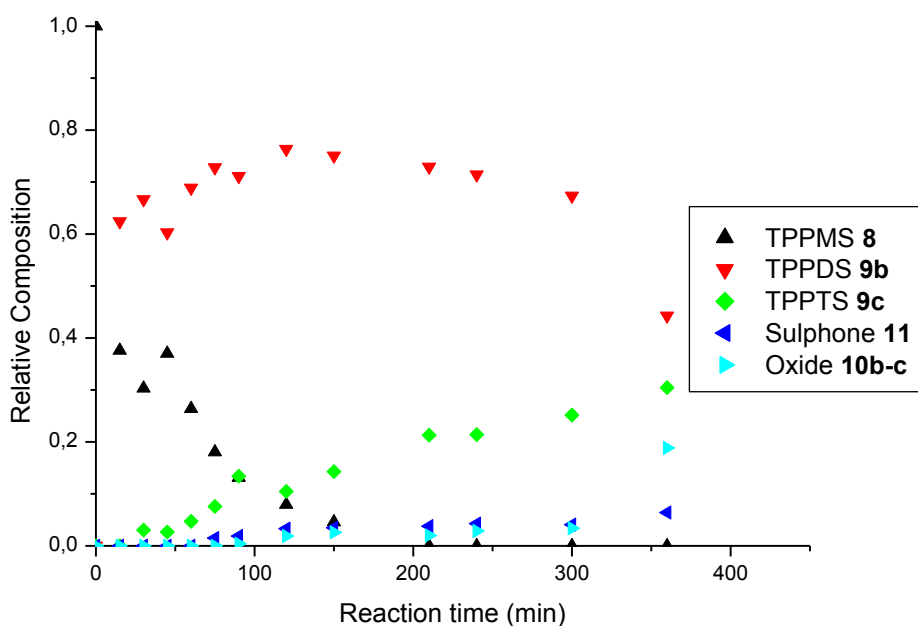
Figure 17: *^{31}P NMR spectroscopic kinetic investigation for the sulphonation of **8**. Reaction conditions: 31% (w/w) SO$_3$, n(SO$_3$):n(phosphine) = 7, 54% (w/w) H$_2$SO$_4$, sample workup by reaction with 5 M NaOH in deuterium oxide.*

5.3.4. Sulphone Formation and conclusions concerning the overall reaction mechanism in the sulphonation of *o*-TPPMS

All observations detailed above indicate a fast first sulphonation of *o*-TPPMS **8** to the disulphonate *rac-o,m*-TPPDS **9b**. As shown from the kinetic investigation (Section 5.3.3), the complete reaction sequence to **9c**, is a two step reaction. The formation of by-products (**10b-c** and **11**) is relatively slow and their concentration increases significantly at longer reaction times. As reversibility of sulphonation is disregarded under the present reaction conditions the proposed description of the reaction mechanism is depicted in Scheme 19. The main reaction pathway follows the sequence from **8** *via* protonation to **8**-H$^+$, fast first sulphonation to **9b**-H$^+$ and slower second sulphonation to **9c**-H$^+$. Oxidation is relatively slow and can occur either from **9b**-H$^+$ or **9c**-H$^+$. However the disulphonated oxide **10b** could only be identified in incomplete sulphonation reactions. This indicates a fast subsequent sulphonation to **10c**, or minor oxidation of formed **9b** during the hydrolysation and neutralisation step.

5. Non-Symmetrically Sulphonated Phosphine Ligands
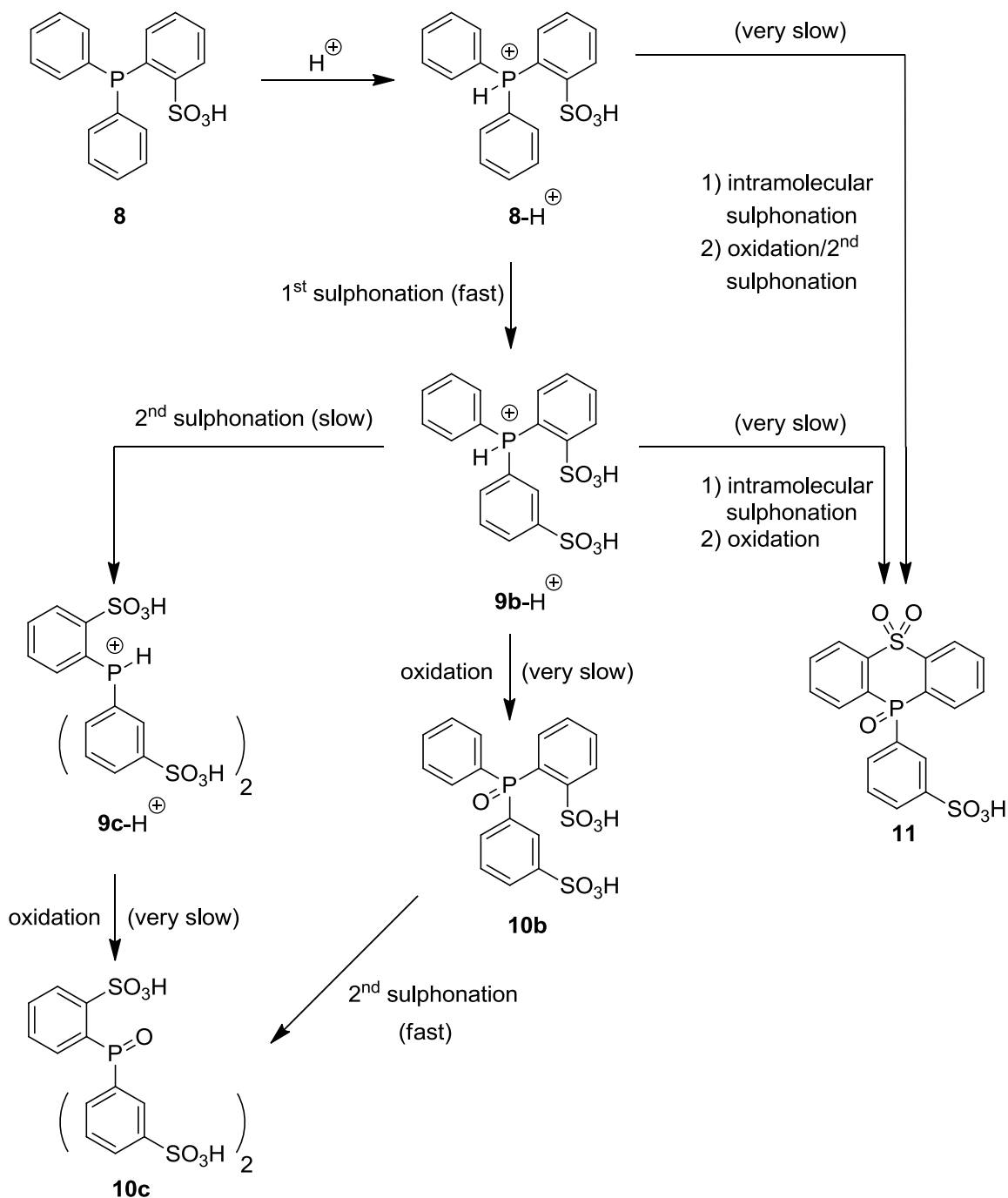
Scheme 19: *Proposed reaction mechanism, including side reactions, observed for the sulphonation of 8. Intramolecular sulphonation to 11 detailed in Scheme 20.*

Unexpected was the formation of **11**, the product of an intramolecular sulphone formation. The structure of this compound could be unambiguously identified by multinuclear NMR spectroscopy and high resolution ESI MS spectrometry. Sulphone formation occurs by transformation of a sulphonic acid group into an active electrophile (Scheme 20). High content of **11** under the reaction conditions, represented by Entries 4 and 5 in Table 2 and

5. Non-Symmetrically Sulphonated Phosphine Ligands

Table 3, indicate that high concentration of dehydrating SO_3 and low concentration of phosphine favour formation of **11**. Oxidation to **10c** and formation of **11** are competing reactions, as observed from Entries 5 and 6 in Table 2 and Table 3. High temperature exclusively favours oxidation whereas sulphone formation requires a high SO_3 content. Comparison with literature data available for TPP, indicate an overall faster sulphonation reaction, especially due to the fact that formation of **9c** compared to the synthesis of *m,m,m*-TPPTS from TPP requires only one sulphonation step instead of two, respectively.[87a]
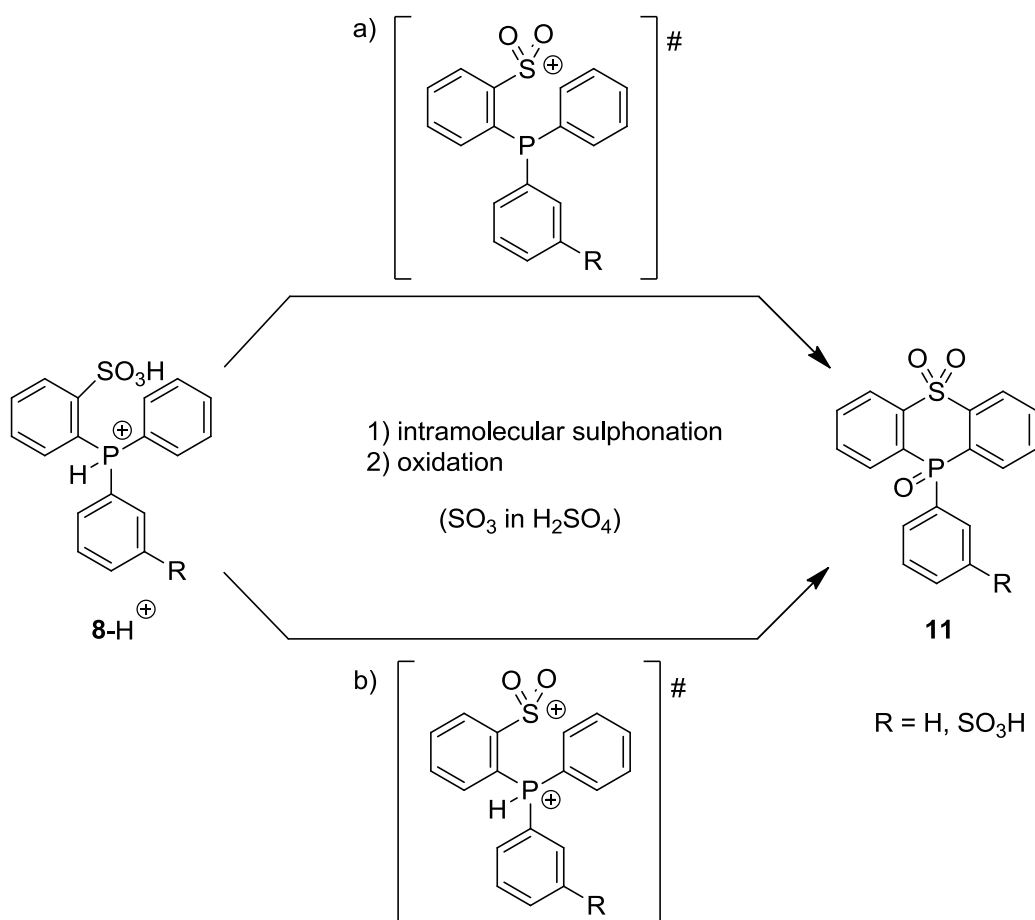
Scheme 20: *Intramolecular sulphonation of 8 to the sulphone 11 via a) a phosphine intermediate or b) a dicationic phosphonium intermediate in the formation of the electrophile with involvement of the acidic reaction medium. Anions generated by reaction with H_2SO_4 omitted for clarity.*

The proposed mechanism for the sulphone formation is depicted in Scheme 20. Dehydration, promoted by SO_3, generates the active electrophilic $R\text{-}SO_2^+$ species from the *ortho*-sulphonate functionality which is capable of an intramolecular cyclisation with a

second, non-sulphonated aryl substituent at phosphorus. The limited available data on this previously unprecedented reaction indicate the involvement of activated *ortho*-directing intermediates and a strongly favoured oxide formation. Protonation and dehydration of the sulphonate functionality most likely lead to a phosphine intermediate (Path a), Scheme 20) which is favoured over the alternative phosphonium analogue, due to the close contact of positive charges (Path b), Scheme 20). Additionally, Path a) is supported by the sulphonation in *ortho*-position which is disfavoured in deactivated aromatic systems. Subsequent oxidation of the unprotected phosphorus (III) centre leads to complete conversion to the corresponding P(V) compound **11**, while the corresponding phosphine could not be observed in this study. The deactivating influence of the sulphonate functionalities prevents double sulphonation on one aryl substituent.

5.3.5. Detailed discussion of the product isolation

Isolation and purification of sulphonated triphenylphosphine derivatives is usually a challenging procedure as explained above (2.2.2).[19] Desired reaction products are often obtained as hydrated salts or product mixtures with residual phosphine oxides. Exploitation of counter ion effects was found to be a useful tool to facilitate product separation, as the solubility of the obtained reaction component depends on the alkali metal cation. Suitable solvents for these ligands are for example water, methanol or in some cases ethanol. In these solvents the solubility of **9b-c** decreases in the order Li > Na > K. Similarly the solubility of K_2SO_4 in methanol with residual water is considerably reduced compared to Na_2SO_4.

Exploitation of this effect led to successful isolation of **9b** as the potassium salt (90,0% of total phosphorus content determined by ^{31}P NMR spectroscopy) from hot solutions in methanol. First the less soluble potassium salt of **9c** was removed by filtration. Fractionisation of the subsequent crystallisation upon cooling to -25 °C could further increase the purity of the obtained product. Residual impurities of the potassium salt of **9a** or possible Li-salt impurities introduced *via* the reactant **8** remain in solution.

Similarly **9c** was isolated as the sodium salt. First impurities of **11** were removed from the hot methanolic solution of the crude product by crystallisation upon cooling to 5 °C. Subsequent fractionised precipitation by addition of ethanol and cooling to -25 °C provides the desired phosphine (84,0% of total phosphorus content determined by ^{31}P NMR spectroscopy). All obtained components are received as hydrates.

5.4. Non-symmetric sulphonation of activated TPP derivatives

As detailed above (2.2), fast sulphonation and regioselectivity are observed with activated triphenylphosphine derivatives and this concept could be successfully transferred to the non-symmetric sulphonation of **7** (Scheme 21). Introduction of OMe-functionalities allowed a reduction of the required SO_3 content to ca. 20% (w/w), leading to full conversion over the course of 3 h. No oxidation was observed which could be the effect of higher basicity of the phosphine, which therefore remains protonated over a wide pH range. As proposed in literature this prevents oxidation during hydrolysis and neutralisation which are critical steps in the work up procedure.[19]
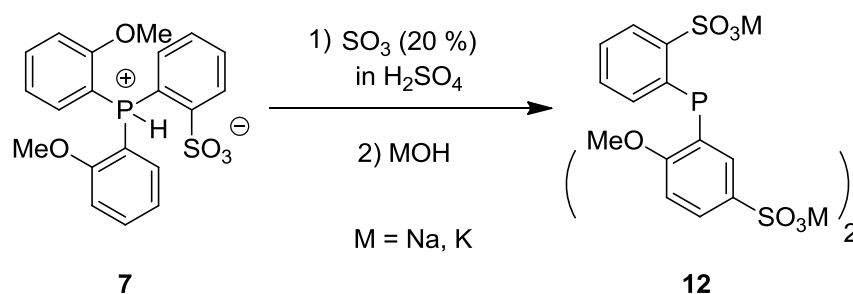
Scheme 21: *Non-symmetric sulphonation of the activated phosphine 7.*

Sulphonation of **7** was carried out by step wise addition of the phosphine to fuming sulphuric acid (20% (w/w) SO_3) at 0 °C. The solution was stirred for 3 h and terminated by the addition of degassed water at 0 °C. Dilution with water, neutralisation with KOH and successive removal of water *in vacuo* provided a brownish crude product mixture after extraction with hot methanol and complete removal of volatiles. The pure potassium salt of **12** could be obtained by crystallisation from hot dry methanol upon cooling to -25 °C as a pale brownish powder. A second crystal crop was obtained by reducing the volume of the mother solution and subsequent second crystallisation at -25 °C. **12** as the sodium salt could be obtained by a similar procedure but, due to the increased solubility, purification was carried out by fractionised precipitation with ethanol.

5.5. Phase transfer reactions with non-symmetrically sulphonated TPP derivatives and complex formation concept with Pd(II) compounds

5.5.1. General concept for phase transfer and ligand coordination in Pd(II) complexes

An active species of polymerisation catalysts for coordination insertion polymerisation requires an alkyl functionality as well as a position for olefin coordination. Furthermore, the migratory insertion reaction depends on a mutual *cis*-configuration of this group and position. In square planar palladium complexes this *cis*-arrangement is achieved by the employment of chelating ligands. These stabilise the complex in the desired configuration.[89]

Introduction of an alkyl group can either be carried out *in situ* by reaction of a pre-catalyst with alkylating agents or by complex formation with already alkylated organometallic precursors. The latter method is generally favoured in late transition metal-based polymerisation catalysts as the corresponding alkyl complexes are relatively stable. Likewise the position for the coordination of olefins can be generated either by precoordination of neutral bases, for subsequent replacement reactions, or by *in situ* activation through abstraction of ligands in presence of olefins.[9, 89]

Literature reports on $[\kappa^2$-(P,O)-Phosphine sulphonate]Pd(II)-based complexes prepared from (COD)PdMeCl[60] (COD: 1,5-cyclooctadiene) show the formation of monoanionic Pd(II) complexes **13a-b** which are stabilised by alkyl ammonium cations (Figure 18).[60] In contrast to the corresponding alkalimetal salts[64] the ammonium salt provides sufficient solubility in polar non-coordinating solvents. Formation of anionic Pd(II) complex species is unusual and seems to be facilitated by the *ortho*-sulphonate functionality. Its proximity to the palladium centre allows formation of a stable six membered κ^2-(P,O) chelate.[60] Analysis of the molecular structure of **13a** (Figure 18) shows the square planar coordination environment for the Pd(II) centre with κ^2-(P,O) coordination of the phosphine sulphonate. The methyl group is situated *cis* respective to phosphorus due to the *trans*-effect of the phosphine donor. Probably due to molecular packing in the solid state or electronic interactions the ammonium cation is situated relatively close to the functional groups with high electron density, namely the chloro ligand and the coordinated sulphonate. However, it is also evident that the Pd-O as well as the Pd-P bond are intact in the solid state, showing the quadratic planar coordination of this unusual electronic situation at the Pd centre.

5. Non-Symmetrically Sulphonated Phosphine Ligands
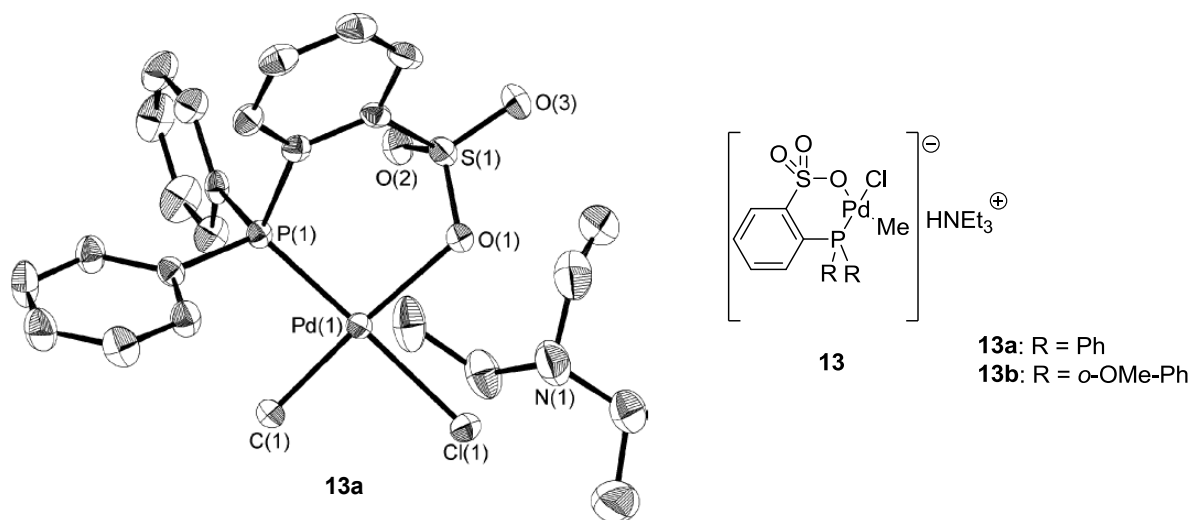
Figure 18: *Drawing of the phosphine sulphonate complexes **13a-b** together with the reported molecular structure for **13a**.*[60]

Ethene/methyl acrylate (MA) test copolymerisation reactions showed the suitability of these anionic [κ^2-(P,O)-phosphine sulphonate]Pd(II)-based complexes as catalyst precursors. These can be directly activated *via* chloride abstraction with silver salts in presence of olefins. Alternatively neutral single component catalysts are obtained by exchange of the chloro ligand with a suitable neutral base such as pyridine or lutidine.[66b] A more elegant way to bypass this multistep procedure based on (tmeda)PdMe$_2$ is detailed in chapter 6.[50]

The present hydrophilic sulphonated phosphine ligands are problematic for the synthesis of organometallic complexes. Ligand solubility would require water or short chain alcohol for coordination and subsequent polymerisation reactions. Generally these protic solvents are not ideal for the stability of metal-alkyl bonds or the reactivity of Lewis acidic metal complexes. Therefore phase transfer reactions similar to literature-known procedures (Section 2.2.2, iii)) were investigated for formation of phosphine sulphonate-based Pd(II) complexes suitable as polymerisation catalysts in polar non protic solvents. Reaction of the ligands with (COD)PdMeCl was assessed as a suitable concept for synthesis of derived anionic palladium complexes. Due to the high degree of anionic functionalities *in situ* activation reactions were ruled out, as alkylating agents are anticipated to lead to esterification of the sulphonate moieties and a disruption of the required Pd-O bond.

5. Non-Symmetrically Sulphonated Phosphine Ligands

5.5.2.   Phase Transfer by Ion Exchange

Exchange of alkali metal ions in sulphonated phosphines is mentioned in several publications. For example *Patin et al.*[33] reported on the possibility for controlled ion exchange reactions in the *m,m,m*-TPPTS system. Starting from the free acid of *m,m,m*-TPPTS, obtained by Na^+/H^+-exchange with an ion exchange resin, quaternary ammonium ions were introduced by reaction with alkyl ammonium hydroxides. By this procedure the synthesis of *m,m,m*-TPPTS ammonium salts $[NR_4]^+$ with R = Me, Et, Bu is described. These are also structurally related to the $[HNEt_3]^+$-coordinated ligands employed for the preparation of anionic phosphine sulphonate complexes shown above (Section 5.5.1).[60]

9b: n = 1, m = 1, R = H
9c: n = 0, m = 2, R = H
12: n = 0, m = 2, R = OMe

M = Li, Na, K

14b: n = 1, m = 1, R = H
14c: n = 0, m = 2, R = H
15: n = 0, m = 2, R = OMe

M = Li, Na, K
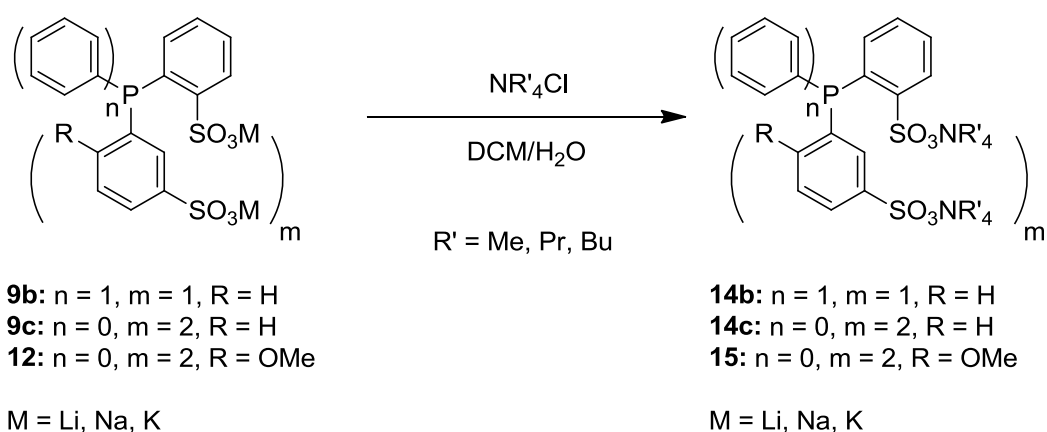
Scheme 22: *Overview of performed phase transfer reaction with alkali metal salts of 9b-c and 12 as well as the general structure of resulting ammonium salts 14b-c and the OMe-functionalised activated phosphine 15.*

Combination of alkali metal ion exchange with ammonium ions, was expected to provide solubility for modified sulphonated ligands and derived complex salts in non-coordinating polar organic solvents. Thus this concept was considered ideal for synthesis of novel phosphine sulphonate complexes with palladium. Phase transfer reactions of the non-symmetrically sulphonated phosphine salts **9b-c** and **12** were performed by exchange of Na^+ or K^+ ions with tetraalkylammonium salts NR_4Cl (R = Me, Pr, Bu) in aqueous solution (Scheme 22), by extraction with methylene chloride. However, phase transfer could only be achieved for the tetrabutylammonium salts. Shorter alkyl chains seem to be incapable of providing sufficient solubility in the organic solvent for the extremely hydrophilic phosphines. Removal of volatiles after separation of the organic phase provides the tetrabutylammonium salts $[NBu_4]_2[$*rac-o,m*-TPPDS$]$ **14b**, $[NBu_4]_3[$*o,m,m*-TPPTS$]$ **14c** and

5. Non-Symmetrically Sulphonated Phosphine Ligands

[NBu$_4$]$_3$[o,m,m-TPPTS(OMe)] **15**. Unexpected was the observation that during synthesis of **15** an excess of tetrabutylammonium halides (NBu$_4$X; X= Cl, Br) was also transferred into the organic solution. This could be validated by elemental analysis and ^{1}H NMR spectroscopy. As the comparative experiments towards **14b-c** lead to a correct stoichiometry of the ammonium ions to the phosphine salt, as shown by ^{1}H NMR spectroscopy, this observation can be most likely attributed to the presence of the polar methoxy functionalities. The assumed interaction with the alkylammonium halides seems to cause residual NBu$_4$X to stay in the organic solution, which is problematic as **15**, as well as **14b-c**, could not be purified by crystallisation. Also it has to be noted that **15** shows fast oxidation in solution, a feature which was found to be characteristic for electron rich donor substituted phosphine sulphonate salts.

5.5.3.   Phase Transfer by alkali metal complexation

i)   Concept for the crown ether complexation of alkali metal ions

Phase transfer by ion exchange, as explained above with ammonium salts, has several potential drawbacks. For example alkylammonium salts are temperature sensitive and the contact of bulky cations to anionic functionalities of the catalyst could produce steric or electronic hindrance in polymerisation reactions. An elegant way to complex alkali metal ions is the reaction with crown ethers or cryptands, a concept often applied in phase transfer catalysis. This possibility could be an alternative to the ion exchange reactions detailed above (Section 5.5.2).

The ideal crown ether-based chelator for potassium ion complexation is 18-crown-6 which typically demonstrates a D$_{3d}$-conformation in the coordinated state (Figure 19) and can complex the potassium ion in the molecular cavity by stabilisation *via* its oxygen donor atoms. Due to the near planar structure of the [K(18-crown-6)]$^+$ complex, charge compensation through the oxygen atoms occurs only in the molecular plane. Polarisation leads to the development of a solvent sphere as described for the hydration of [K(18-crown-6)]$^+$. Coordination to anions or polar molecules is strongly preferred at the axial positions which can also lead to a slight displacement of the potassium ion from the centre of the coordination complex.[90]

5. Non-Symmetrically Sulphonated Phosphine Ligands
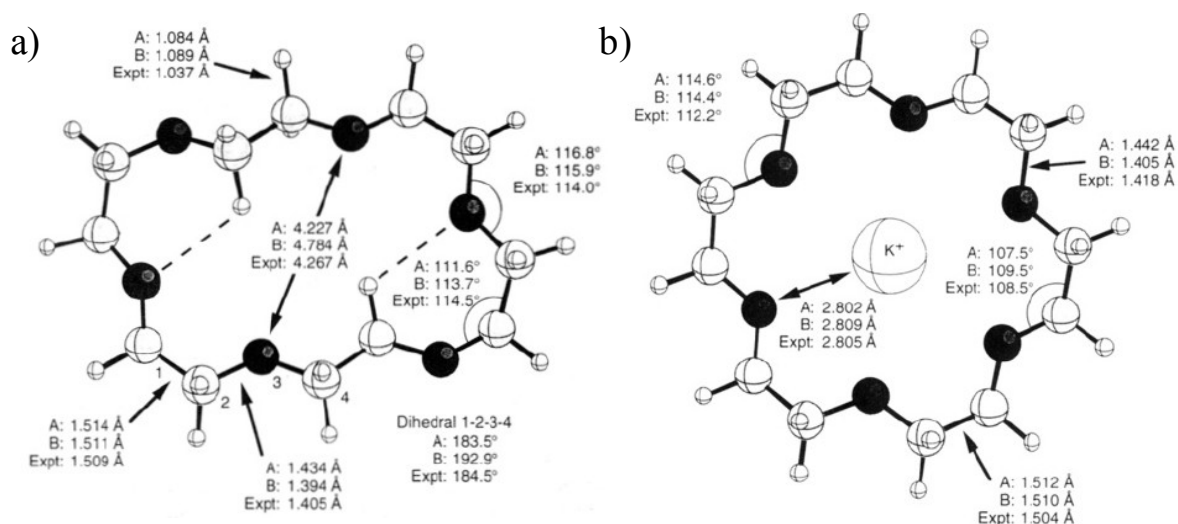
Figure 19: *Observed structure of a) free (most stable C_i conformation shown) and b) K^+ coordinated 18-crown-6 (D_{3d} configuration). Selected calculated and experimentally determined structural parameters listed.*[90b]

Due to the fixed location of the potassium ion in the chelate cage, dissolution of the corresponding salts could potentially lead to a separation of the ion pair. Thus reduced charge compensation for the anionic ligand and the resulting complexes in solution might lead to an increased negative charge density in the coordination sphere of the Pd(II) metal centre, a feature which would be desired for investigations on the coordination-insertion polymerisation of polar-functionalised olefins (Section 3.3).[83] Additionally the [K(18-crown-6)]$^+$ complexes are relatively symmetric cations which show a constrained structure compared to the bulky ammonium salts with dynamic and flexible butyl chains. Thus the corresponding complexes are expected to show improved crystallisation behaviour, despite frequent distortion of crown ether units in the molecular structure.

ii) Synthesis of crown ether coordinated sulphonated phosphine salts

For investigation of the alkali metal complexation in phase transfer reactions with non-symmetrically sulphonated phosphines the potassium salts of **9b** and **12**, as well as of the reference compound **9a**, were reacted with 18-crown-6 (Scheme 23). A suspension of the reactants in methylene chloride was stirred over night, leading to slow dissolution. After filtration over a glass microfiber filter (1.0 μm pore size) to remove minor residual salt impurities, removal of volatiles *in vacuo* provided the [K(18-crown-6)]$^+$ salts of the phosphine sulphonates **16a-b** and **17**.

5. Non-Symmetrically Sulphonated Phosphine Ligands

9a: m = 0, n = 2, R = H
9b: m = 1, n = 1, R = H
12: m = 2, n = 0, R = OMe

16a: m = 0, n = 2, R = H
16b: m = 1, n = 1, R = H
17: m = 2, n = 0, R = OMe
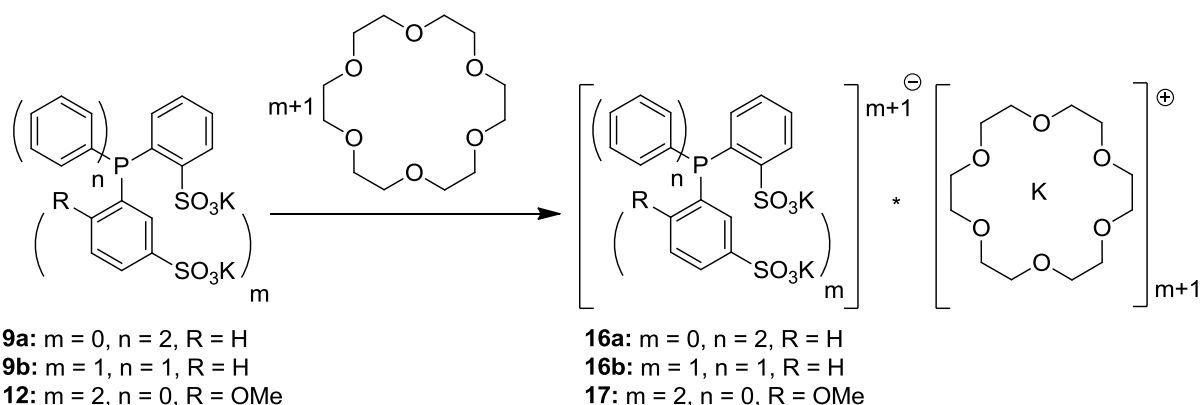
Scheme 23: *Alkali metal complexation by 18-crown-6 in the synthesis of [K(18-crown-6)]$_2$[rac-o,m-TPPDS].*

Upon analysis of the [K(18-crown-6)]$^+$-salts by ^{1}H NMR spectroscopy showed in several cases that excess 18-crown-6 was present, compared to the phosphine salt. This degree of impurity ranges from 0.4 to 0.75 additional equivalents 18-crown-6 for **16b** and **17**, respectively. A specific origin for this observation is unclear but could stem from deviations of the exact phosphine-crown ether ratio, due to the hydrate character of **9b** and **12**. Presence of coordination complexes with potassium-containing inorganic impurities from the reactants can also not be excluded. Unfortunately crystallisation was not adequate to purify the obtained compounds.

As observed for the NBu$_4$$^+$-coordinated analogue **15** described above, the ^{31}P NMR spectrum obtained for **17** confirms fast oxidation of the phosphine. Despite usage of degassed, dry solvents during the phase transfer reaction, partial oxidation in solution occurs over short time periods (hours) (9 h, 30.7% of total phosphorus content, as observed by ^{31}P NMR spectroscopy). The oxidation is slow in the solid state, but complete oxidation of **17** in a sealed flask stored under argon atmosphere was confirmed after several months. In contrast **16b** is stable in methylene chloride solution at room temperature for at least 14 days without observable oxidation. Difference of the observed behaviour for **16b** and **17** originates most likely in the electronic situation of phosphorus. Significant differences of the electronic environment for both compounds are indicated from the phosphorus shift in the ^{31}P NMR spectra (**16b**: δ_P = -9.3 ppm, **17**: δ_P = -21.5 ppm, respectively).

In general the non-activated sulphonated phosphines presented in this work show a relatively similar chemical shift of the phosphorus atom (δ_P = -10.7, -10.5, -10.3 ppm; **9a**, **9b**

and **9c**, respectively) which is practically independent from the alkali metal counterion. This similarity indicates only a weak influence of the introduced sulphonate functionalities in the *meta*-positions. By clear contrast stands the introduction of activating functionalities, as in the case of the methoxy group, which causes a drastic upfield shift (from δ_P = -10.2 to -29.5 ppm, **9c** and **12**, respectively). This indicates a distinct increase of electron density at phosphorus , which is also assumed to be the reason for the observed differences concerning oxidation of the phosphine. Exact comparison of the phosphine basicity *via* the corresponding $^1J\,(^{77}Se\text{-}^{31}P)$ coupling constants could not be performed.[91] Selenation of the phosphine salts with elemental selenium in refluxing methanol gave solely the phosphine oxides due to oxidation.

Starting from the alkali metal salts **9b-c** and **12**, which are oxygen and water stable for extended periods of time in the solid state, tendency towards oxidation is clearly increased by complexation of the alkali metal or exchange of the counterion for activated phosphines. The high stability of the parent alkali metal salts is attributed to an interaction of the cation with phosphorus, similar to several *ortho*-sulphonated phosphine sulphonic acids, for example **7** which exists in a zwitterionic state. This stabilisation of the P(III) centre by the alkali metal ion could be sterically disturbed by complexation or cation exchange resulting in facilitated oxidation of electron rich phosphines (Scheme 24). Oxidation originates most likely from trace amounts of oxygen or water, as phosphine sulphinates, which would be the product of an intramolecular oxidation, could not be detected by multinuclear NMR spectroscopy or mass spectrometry.

Ar = Ph, 2-OMe-Ph
 [Z][3-SO₃Ph], [Z][2-OMe-5-SO₃Ph]
Z = NBu₄, [K(18-crown-6)]
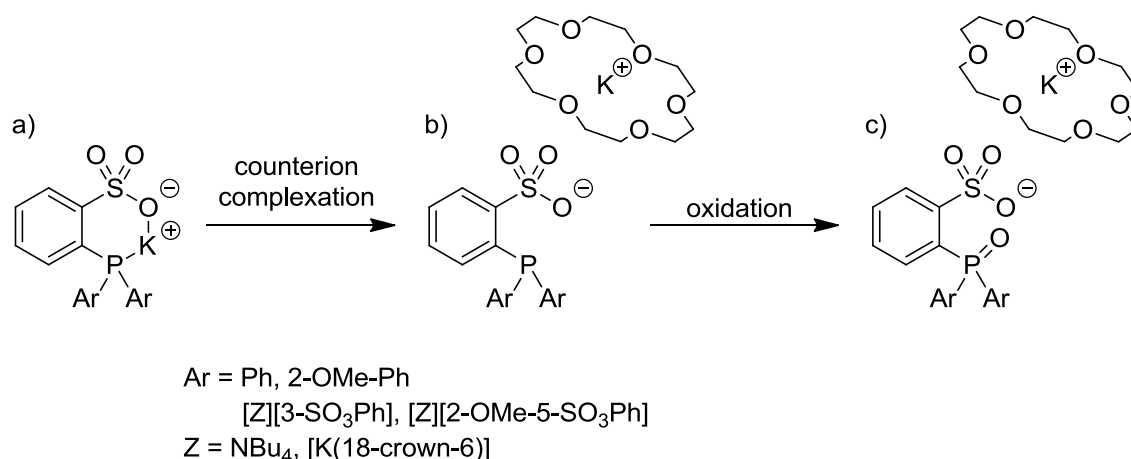
Scheme 24: *Schematic description of the proposed phosphine oxidation; a) stabilised species, b) counterion complexation and c) oxidation.*

5. Non-Symmetrically Sulphonated Phosphine Ligands

For reference purposes and test reactions the syntheses of [K(18-crown-6)][*o*-TPPMS] **16a**, [K(18-crown-6)][*o*-TPPMS(OMe)] **18** and [Na(15-crown-5)]₃[*o,m,m*-TPPTS] **16c** were performed as explained above. Only the complexation with 15-crown-5 was performed with an excess of crown ether by phase transfer in a mixture of methylene chloride and water, as described above for cation exchange reactions (Section 5.5.2). Besides **16a** which could be isolated, other reactions led either to oxide formation (**18**) or large excess of the chelating ligand (**16c**). Additionally modification of the solubility was attempted by introduction of dibenzo-18-crown-6 in the reaction with **9b**. However, reaction in methylene chloride or toluene did not lead to dissolution of the reaction products. Problems originating from solubility differences or steric hindrance most likely prevent complexation of the potassium ion. Unfortunately all obtained sulphonated phosphine-crown ether complexes cannot be purified by crystallisation to remove excess crown ether ligand or to separate phosphines from their corresponding oxides. In several cases the subsequently formed coordination complexes with palladium can be purified by crystallisation. This allows the usage of these ligand-crown ether complexes as received, after determination of their purity by ¹H NMR spectroscopy.

5.6. Synthesis of phosphine sulphonate-Pd(II) based (pre-)catalysts

As described above (Section 5.5.1) complex formation of obtained modified phosphine sulphonate ligands was performed by ligand exchange with (COD)PdMeCl. For the general reaction procedure the reactants were dissolved in methylene chloride and reacted in the absence of light. The volatiles of the obtained pale yellow solution were removed and the residue was purified by repeated precipitation from methylene chloride solution with pentane. In several cases (**19**, **20**) crystallisation from methylene chloride:pentane mixtures was successful to remove residual impurities which gives suitable polymerisation pre-catalysts. The other cases show residual impurities, for example phosphine oxides and phase transfer agent. Therefore complete characterisation and unambiguous determination of the complex structures are not possible which precludes their usage as catalysts for polymerisation reactions. An overview of attempted and performed synthesis of anionic phosphine sulphonate-Pd(II) complexes is depicted in Figure 20. Synthesis of neutral single component catalysts with phosphine sulphonates in presence of a chloride-abstracting reagent as shown by *Rieger et al.*[58, 92] (Scheme 15) was not carried out to facilitate characterisation.

5. Non-Symmetrically Sulphonated Phosphine Ligands

a) Anionic Pd(II) complexes with [K(18-crown-6)]+ counterions

19

21

20 rac

22
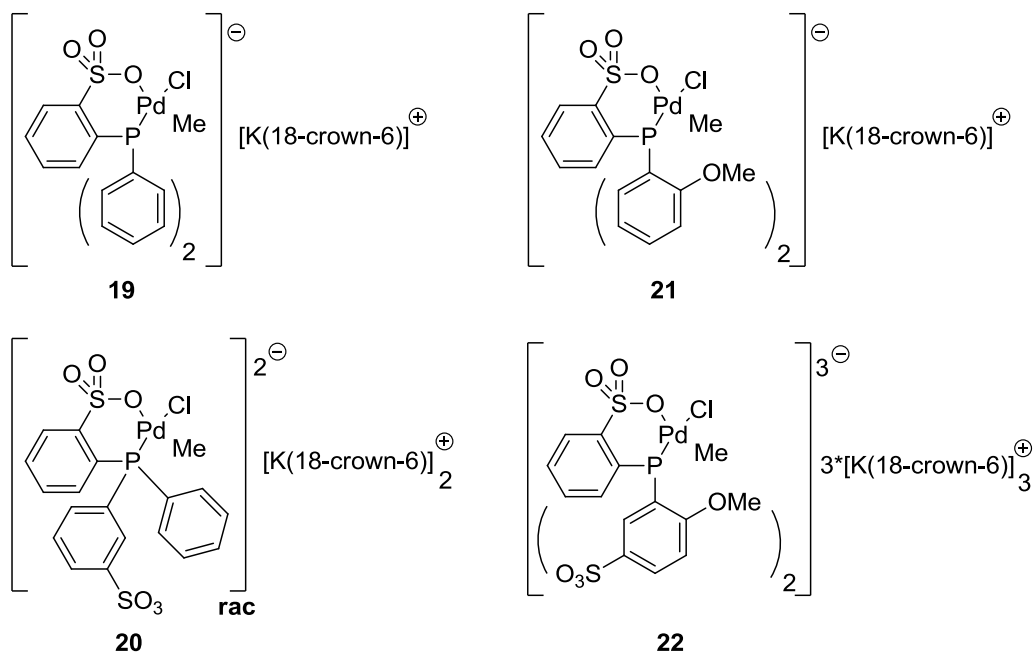
b) Anionic Pd(II) complexes with NBu4+ counterions

23 rac

24

25
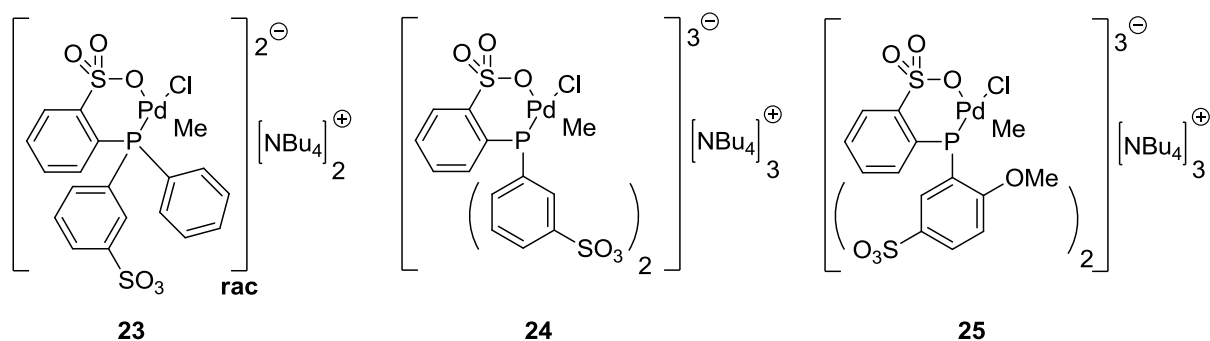
Figure 20: *Overview of the synthesised anionic phosphine sulphonate based Pd(II) complexes; a) **19-22** as [K(18-crown-6)]+-salts, b) **13-25** as NBu4+-salts.*

i) *Synthesis of anionic phosphine sulphonate based Pd(II) complexes as their respecitve [K(18-crown-6)]+-salts*

Synthesis of [K(18-crown-6)][{κ^2-(P,O)-*o*-TPPMS}PdMeCl] **19** and [K(18-crown-6)]$_2$[{κ^2-(P,O)-*rac-o,m*-TPPDS}PdMeCl] **20** could be performed, as described above, including purification by crystallisation from methylene chloride solutions in high yields (73.0 and 80.0%, respectively). Analysis by multinuclear NMR spectroscopy shows clean formation of the compounds without excess of crown ether molecules or other phosphorus-containing impurities. κ^2-(P,O)-Chelating coordination of the phosphine sulphonate by formation of a

61

5. Non-Symmetrically Sulphonated Phosphine Ligands

6-membered ring is indicated by the ^{1}H NMR signal of the methyl group on the palladium centre. The doublet with ^3J (H-P) coupling constants of 3.3 (**19**) and 3.2 Hz (**20**), respectively, is characteristic for a *cis*-situated methyl group with respect to phosphorus.[41] As explained above a *trans*-configuration is disfavoured by the strong *trans*-effect of phosphorus (Section 3.2). Complete coordination is also verified by the ^{31}P NMR spectra which show only a single peak with a characteristic downfield shift of approximately 40 ppm upon coordination of the phosphine ligand to Pd(II) (**16b**: d = -9.3 ppm, **20**: d = +27.4 ppm). Single crystals of **20** suitable for single crystal X-ray diffraction could be grown from methylene chloride:pentane mixtures (3:1). In the molecular structure of **20** (Figure 21) the racemate character of this compound could be directly observed.

The molecular structure of **20** (Figure 21) shows κ^2-(P,O)-chelated near square planar coordination of the ligand to the palladium centre. In addition to a well-resolved complex backbone strongly disordered cations are observed. Both [K(18-crown-6)]$^+$ ions of the dianionic complex **20** are located at the *meta*-sulphonate functionality, most likely due to molecular packing in the solid state, and show expected coordination *via* the axial position. Selected bond lengths of the complex backbone are listed in the caption of Figure 21. The problematic characterisation of sulphonated complex salts by single crystal X-ray diffraction results in a very limited selection of reported structural data for comparison with related compounds. All other obtained analytical data fully support the observed molecular structure of **20**.

5. Non-Symmetrically Sulphonated Phosphine Ligands
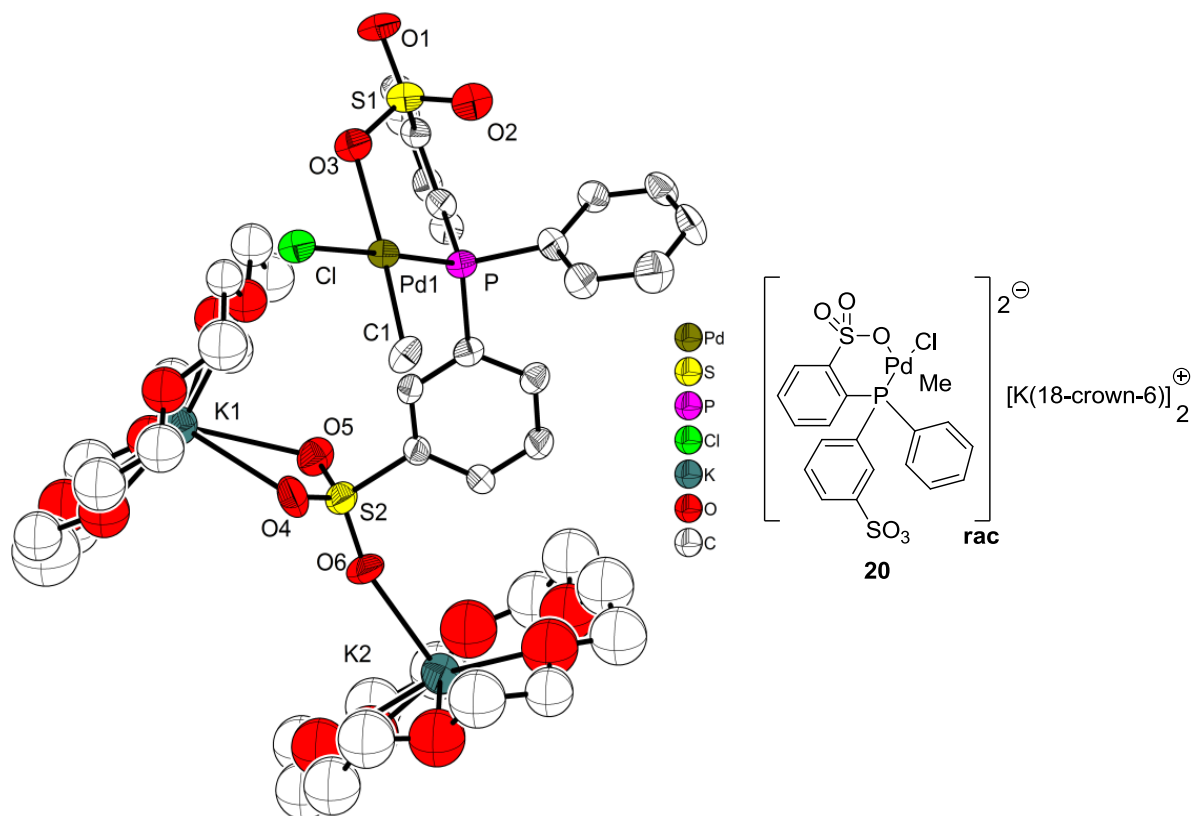
Figure 21: *ORTEP plot of compound **20**, hydrogen atoms and the atoms of the second orientation for the disordered crown ether molecule have been omitted for clarity, no labels for the crown ether atoms and the carbon atoms beside C(1) are displayed. Displacement ellipsoids are drawn at the 50% probability level. Both crown ether units were refined isotropically and the two conformations for the $[K(2)(18\text{-}crown\text{-}6)]^+$-crown ether refined with a ratio of 0.769(6):0.231(6). Selected bond lengths [Å] and angles [°]: Pd(1)-C(1) 2.0193(4), Pd(1)-Cl 2.387(3), Pd(1)-O(1) 2.184(5), Pd(1)-P 2.220(2), Pd(1)···O(2) 3.371(6), K(1)···O(4) 2.874(6), K(1)···O(5) 2.820(7), K(2)···O(6) 2.597(7), average K-O(crown ether) distance 2.83; C(1)-Pd(1)-P 88.74(5), C(1)-Pd(1)-O(3) 175.9(2), C(1)-Pd(1)-Cl 90.25(5), P-Pd(1)-O(3) 95.2(2), P-Pd(1)-Cl 177.68(7).*

Despite their relatively common application in homogeneous catalysis, reported molecular structures of complexes with di- and tri-sulphonated phosphines are rare in the literature, as formation of long range order for crystallisation is dependent on the nature of cations and possible packing. One known approach to crystallise respective complexes is the complexation of cations. Otherwise strong cation-sulphonate interactions can lead to formation of complex bridged networks between molecules. In addition to the five known

5. Non-Symmetrically Sulphonated Phosphine Ligands

structures *m,m,m*-TPPTS-based complexes only a tetrameric *o,o*-TPPDS-based aggregate and the present complex **20** exist for triphenylphosphine complexes with a higher degree of sulphonation (>1) (also note the molecular structure of **30,** Section 5.8).[84, 93]

In contrast to the successful isolation of **19** and **20**, syntheses of **21** and **22** show residual crown ether and oxide impurities. Crystallisation of these complexes was not successful. Analysis by multinuclear NMR spectroscopy shows a combination of excess crown ether molecules, residual phosphine oxide and the desired complex. However, the coordination can be monitored by ^{31}P NMR spectroscopy. In detail analysis of **21** shows 75.0 mol% purity of the complex ($\delta_{P,complex}$ = +22.2 ppm) with 25.0 mol% oxides ($\delta_{P,oxide}$ = +37.1 ppm), observed by ^{31}P NMR spectroscopy. No significant excess of crown ether molecules is present, however overlapping peaks for the crown ether and the phosphine methoxy group in the ^{1}H NMR spectrum prevent unambiguous assignment. **22** is obtained with 3.75 total equivalents of crown ether compared to the complex and phosphine oxide (0.75 excess crown ether). The ^{31}P NMR spectrum shows 63.7 mol% complex ($\delta_{P,phosphine}$ = +21.3 ppm), 36.3 mol% phosphine oxide ($\delta_{P,oxide}$ = +34.9 ppm) together with a [3]J (H-P) = 3.7 Hz coupling constant determined from the corresponding ^{1}H NMR spectrum.

ii) Synthesis of anionic phosphine sulphonate-based Pd(II) complexes as their respecitve

   NBu$_4$+-salts

Formation of **23-25** with tetrabutyl ammonium ions shows similar behaviour compared to the analogous [K(18-crown-6)]+ coordinated compounds. However, none of these complexes could be purified by crystallisation. Analogous to **21** and **22** the shifts upon coordination of the phosphines to Pd(II) indicate complete complexation in a κ^2-(P,O)-chelated environment as observed by [3]J (H-P) coupling constants. Analysis of **23** shows impurities from COD which could not be removed in this case, [3]J (H-P) = 3.4 Hz and $\delta_{complex}$ = +26.7 Hz observed by ^{1}H and ^{31}P NMR spectroscopy. In comparison the NMR spectra of **24** and **25** both show two similar coordination species with significant intensity differences. Detailed interpretation of the obtained ^{1}H and ^{31}P NMR spectra for **24** indicates full coordination of the phosphine. However the mentioned similar species can be recognised by two signals in the ^{31}P NMR spectrum ($\delta_{P, complex}$ = +27.1 ppm (major) and +26.7 ppm (minor)), as well as by two doublet signals of Pd-methyl coordinated species (0.54 ppm (79.3%) and 0.48 ppm (20.6%)) observed in the ^{1}H NMR spectrum. *Cis-trans* isomerisation is unlikely due to the [3]J (H-P) coupling

constants of 3.4 and 3.3 Hz, respectively. Again these values are characteristic for a configuration *cis* to phosphorus in the square planar environment of the κ^2(P,O)-chelated complexes. Instead, the matching phosphorus shifts of **23** with the minor component in **24** could indicate a desulphonation reaction. This is also indicated by the elemental analysis of **24** which shows a clear sulphur deficiency (found: 5.74%, calculated: 6.95%). A similar behaviour could also be observed for **25**. Two similar species could also be observed by NMR spectroscopy, characterised by $\delta_{P, complex}$ = +18.7 ppm (88.5%) and +17.3 ppm (11.5%) for the phosphorus as well as δ_P = 0.31 ppm, doublet ^3J (H-P) = 3.4 Hz and 0.37 ppm, not resolved for the proton, respectively. Again, elemental analysis shows an unexpected low sulphur content (found: 5.39%, calculated: 6.66%) for **25**. Additionally in this compound one equivalent of tetrabutylammonium halide (chloride and bromide) impurities is present which originates from the phosphine reactant. These impurities are highly problematic in polymerisation reactions, as it could be shown that alkyl halogen species can be created upon reaction with ammonium- or phosphonium halides.[63] An alternative explanation would be an origin of the two methyl signals from μ-Cl-bridged dimeric structures. However, this would require an opened Pd-O bond and thus no κ^2-(P,O) chelation.

iii) Synthesis of pyridine coordinated phosphine sulphonate Pd(II) complexes

The synthesis of pyridine coordinated anionic phosphine sulphonate Pd(II) complexes was attempted for comparative reasons and to enhance the stability of resulting polymerisation catalysts against decomposition. These compounds would facilitate direct comparison to the well known neutral phosphine sulphonate catalysts in order to evaluate the effect of the introduced negatively charged functionality. At first the "one pot synthesis" *via* the anionic complex, chloride abstraction with a silver salt and subsequent replacement with pyridine was attempted by stepwise addition of reactants (Scheme 25).

5. Non-Symmetrically Sulphonated Phosphine Ligands
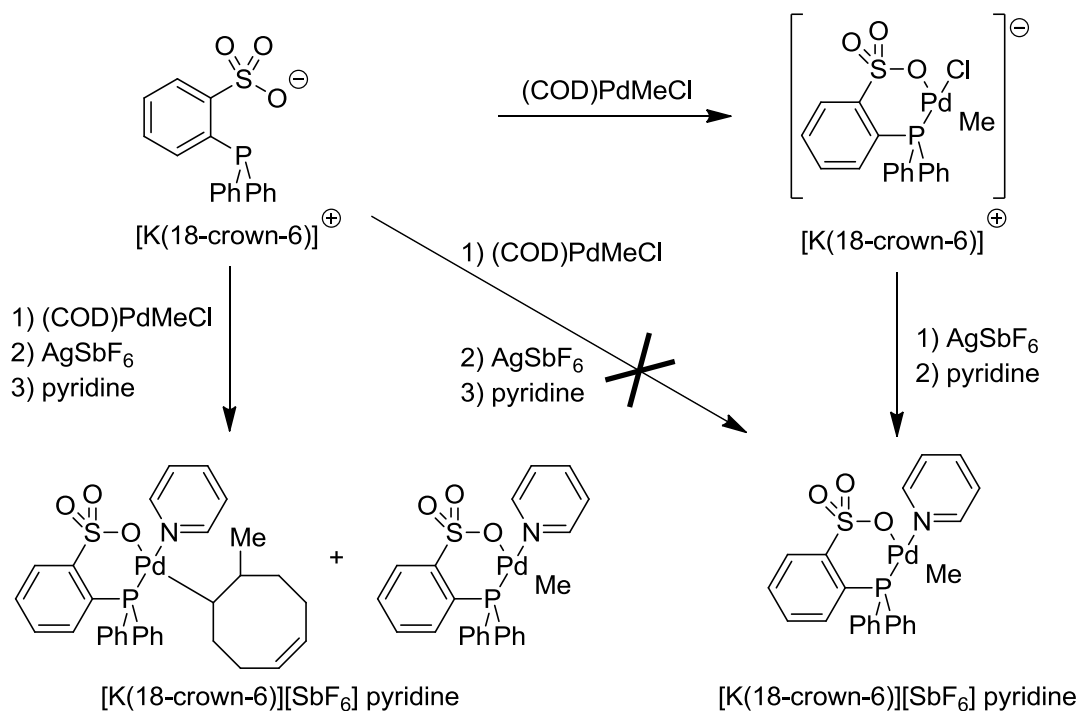
Scheme 25: *Schematic overview of the performed syntheses towards neutral phosphine sulphonate catalysts based on [K(18-crown-6]$^+$ salts.*

Unfortunately in this reaction the present COD acts as an olefin base after abstraction of the chloride. This leads to partial COD insertion in the Pd-methyl bond and formation of pyridine-alkyl coordinated complex mixtures. The reaction could be confirmed by halide abstraction without pyridine addition under different reaction conditions (Scheme 26). Slightly increased reaction temperature (30 °C) and addition of small quantities of diethyl ether favour formation of the insertion product **26** next to the COD adduct **27**. Two dimensional NMR spectroscopy directly confirmed the insertion by the relevant cross peaks in the corresponding COSY NMR spectrum (Figure 22 and Figure 23). The methyl group of **26** shows a ^1J (H-H) = 7.0 Hz coupling constant and the phosphorus is shifted upfield ($\delta_{P, \textbf{26}}$ = +14.5 ppm) in the respective ^{31}P NMR spectrum compared to the related anionic complex **19** ($\delta_{P, \textbf{19}}$ = +26.6 ppm). In contrast **27** shows a broad ^{31}P NMR peak indicating a dynamic equilibrium existing on the NMR timescale.

5. Non-Symmetrically Sulphonated Phosphine Ligands

Scheme 26: *Synthesis of 26 and 27 by partial insertion of COD and assignment for interpretation of 2D COSY NMR spectrum, compare* Figure 22 *and* Figure 23.

Figure 22: *COSY NMR spectrum of the partial COD insertion, peak assignement detailed in* Scheme 26 *and* Figure 22.
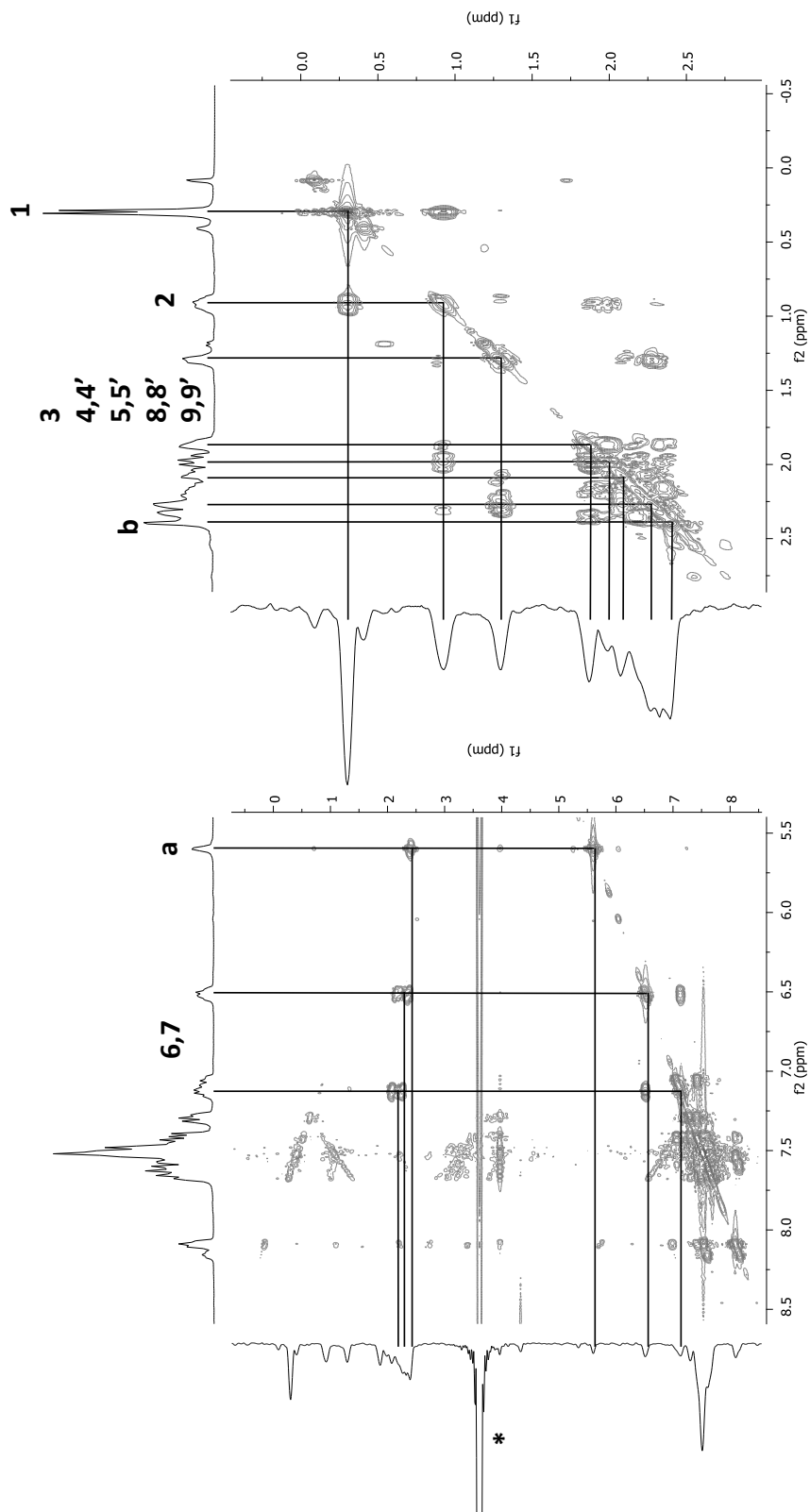
Figure 23: *Excerpts and interpretation of the COSY 2D NMR spectra for the partial COD insertion displayed in* Scheme 26. *Relevant cross peaks labelled and assigned to the corresponding structural motives.*

5. Non-Symmetrically Sulphonated Phosphine Ligands
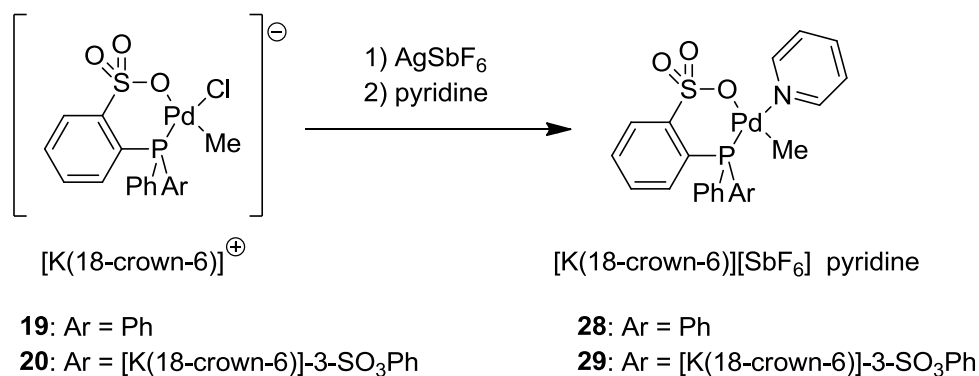
Scheme 27: *Formation of pyridine adducts 28 and 29 by chloride abstraction from 19 and 20, respectively.*

Formation of pyridine adducts **28** and **29** (Scheme 27) was achieved upon chloride abstraction with AgSbF$_6$ from **19** and **20**, respectively´, and subsequent addition of excess pyridine in methylene chloride solution under exclusion of light. Removal of volatiles gives **28** and **29** accompanied with residual [K(18-crown-6][SbF$_6$] and coordinated pyridine. The latter could not be removed by selective crystallisation of the complexes or this inorganic crown ether salt. Detailed analysis shows a ^3J (H-P) = 2.5 Hz coupling constant, 1 equivalent crown ether (attributed to [K(18-crown-6)][SbF$_6$]) and 1.5 equivalents coordinated pyridine in addition to $\delta_{P,\ 28}$ = +28.8 ppm by ^{1}H and ^{31}P NMR spectroscopy for **28**, respectively. Similar observations for **29** give ^3J (H-P) = 2.7 Hz, 2.5 equivalents of present pyridine, 2 equivalents of crown ether and $\delta_{P,\ 29}$ = +29.4 ppm determined from ^{1}H and ^{31}P NMR spectroscopy, respectively.

In general these experiments show the accessibility of pyridine coordinated complexes based on the non-symmetrically sulphonated **9b** as well as the reference compound **9a**. However, purification was not achieved and the obtained mixture with inorganic salts and non-stoichiometric amounts of coordinated pyridine is not suitable for polymerisation reactions of olefins.

5.7. Olefin polymerisation reactions with anionic phosphine sulphonate based Pd(II) complexes

The anionic [κ^2-(P,O)-phosphine sulphonate]Pd-based complexes described above (Section 5.6) were tested for their suitability in homo- and co-polymerisation reactions with a selection of olefins. Ethene homopolymerisation, as an initial test reaction for compounds **19** and **20**, was employed to investigate suitable polymerisation conditions and the general reaction behaviour in comparison to related literature reports. All other complexes (namely **21-29**) show high levels of impurities and were therefore disregarded for polymerisation.

According to literature reports, the catalyst activation was carried out *in situ* by chloride abstraction with AgSbF$_6$ in presence of olefins (Scheme 28).[60, 89] Suitability of this procedure was tested in advance by quantitative chloride abstraction reactions during the synthesis of the pyridine-stabilised neutral and anionic catalysts **28-29** (Section 5.6, *iii)*). Stainless steel reactors (100 or 200 mL) were chosen for batch (co-)polymerisation reactions with ethene (and suitable comonomers) as shown in Table 4. Subsequent tests with **20** concerned the catalyst behaviour in copolymerisation reactions with polar-functionalised olefins Table 5.

FG = C(O)OMe, CN, OC(O)Me

19: Ar = Ph
20: Ar = [K(18-crown-6)]-3-SO$_3$Ph
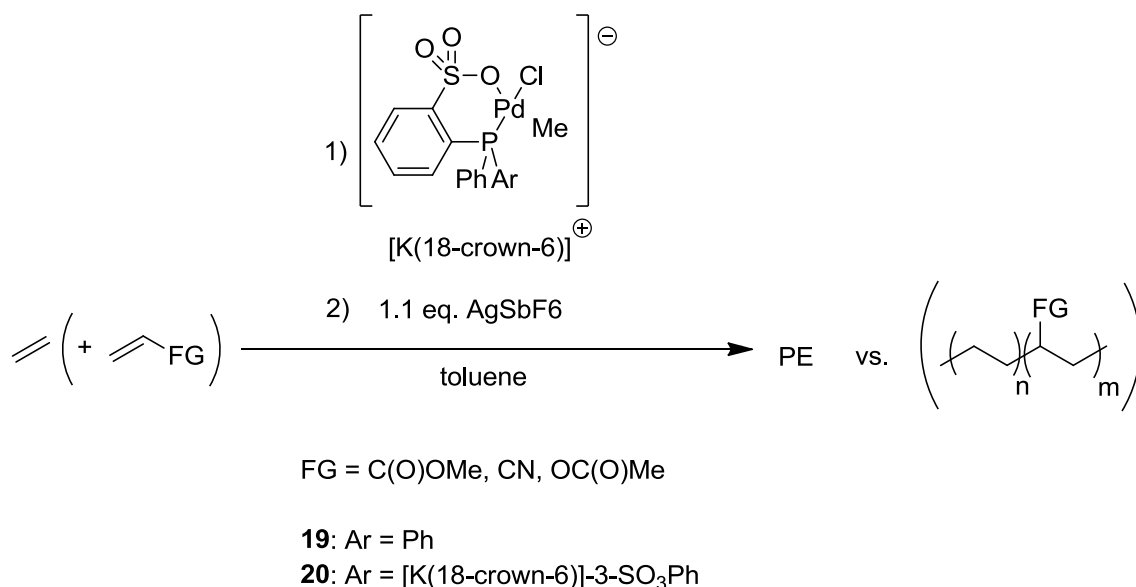
Scheme 28: *General scheme of the ethene (co-)polymerisation reaction with the pre-catalysts 19 and 20. Employed comonomers for ethene copolymerisation were methyl acrylate, vinyl acetate and acrylonitrile.*

5. Non-Symmetrically Sulphonated Phosphine Ligands

Table 4: *Polymerisation data for the ethene homopolymerisation with complexes **19** and **20**[1]*

Entry	Cat.	T (°C)	p (bar)	t (h)	Yield (g)	Activity[3]	M_w (high)[4]	M_w (low)[5]	PDI (high)[6]	PDI (low)[6]	T_m (°C)[7]
1	**20**	50	20	20	0.58	1.4	0.6 (M)	n.d.	7.1 (M)	n.d.	119
2	**20**	80	20	20	2.44	5.7	0.5 (R)	2.6 (R)	8.9 (R)	2.0 (R)	129
							0.4 (M)	3.0 (M)	7.1 (M)	1.4 (M)	126
3	**20**	100	20	20	2.86	6.7	0.4 (R)	3.0 (R)	5.7 (R)	4.6 (R)	
							0.3 (M)	2.4 (M)	6.0 (M)	2.3 (M)	125
							0.3 (R)	2.7 (R)	5.1 (R)	2.4 (R)	
4	**20**	80	10	20	1.27	6.0	0.3 (M)	3.0 (M)	6.4 (M)	1.6 (M)	125
							0.3 (R)	3.0 (R)	5.7 (R)	2.7 (R)	
5[2]	**20**	100	20	20	0.25	0.6	n.o.	3.4 (M)	n.o.	3.1 (M)	123
								4.0 (R)		3.9 (R)	
6	**19**	100	20	20	4.60	10.8	n.o.	5.0 (M)	n.o.	3.7 (M)	119
								5.4 (R)		4.9 (R)	
7	**19**	100	20	2	0.95	22.2	n.o.	4.8 (M)	n.o.	5.3 (M)	122
								5.5 (R)		5.8 (R)	

[1]200 mL stainless steel reactor, 10 μmol catalyst, 1.1 equivalents AgSbF$_6$, 30 mL toluene; [2]Additive 1-ethyl-3-methyl-imidazolium tetrafluoroborate (2 mL), 100 mL autoclave, 10 mL toluene; [3]Activity $g_{polymer} \cdot g_{palladium}^{-1} \cdot bar_{ethene}^{-1} \cdot h^{-1}$; [4]$10^6$ g/mol (high molecular weight fraction), [5]10^6 g/mol (low molecular weight fraction); PDI = M_w/M_n; [6]determined by DSC; n.d. = not determined, n.o. = not observed; (M) = multi detection (RI, viscometer, light scattering), (R) = RI detection.

5. Non-Symmetrically Sulphonated Phosphine Ligands

The obtained polymerisation data show significantly reduced activity of the dianionic non- symmetrically sulphonated catalyst precursor **20** compared to the monoanionic reference catalyst **19**. Catalyst activities for both complexes are also several orders of magnitude lower than the most active neutral phosphine sulphonate-based palladium catalysts stabilised with dmso (Section 6.1).[48]

Comparison of the data obtained in test reactions with the pre-catalyst **20** shows, as expected, decreasing molecular weight (Table 4, Entries 1-3) with increasing polymerisation temperature due to facilitated β-hydride elimination. An effect of a varying ethene concentration on the molecular weight is less pronounced (Table 4, Entries 2 and 4) but also leads to increased chain termination and lower M_w at lower ethene pressures. However, increasing ethene pressure clearly has a positive influence on the catalyst activity. Detailed analysis of the obtained PE by GPC and DSC was performed to investigate the effect of the catalyst structure on the polymer properties. Due to the partial formation of linear high molecular weight PE (detailed below) with low solubility at 120 °C in $C_2D_2Cl_4$ characterisation by NMR spectroscopy was not performed. Evaluation of the GPC plots for the PE obtained with **20** shows the presence of broad bimodal molecular weight distributions (Table 4, Entries 1-4). These bimodal traces indicate aggregation of the complex in solution which leads to formation of non-equally active catalyst sites. This behaviour has been previously described in literature reports and is dependent on the catalyst system and the solvent polarity.[84, 94] Here toluene, as a relatively non-polar solvent, is apparently not sufficient to stabilise the complex **20** in a mononuclear dissociated form. Steric effects from aggregation are expected to lead to differentiation of the active catalyst centres. These differences explain the observed broad bimolecular weight distribution, which is not possible by a single site mechanism in coordination-insertion polymerisation. Chain termination is reduced, which is confirmed by the obtained high molecular weights, attributed to the protection of the growing polymer chain towards associative olefin exchange through increased steric hindrance. Peak separation in GPC elugramms could be enhanced by viscometer and light scattering detectors, which are more sensitive towards high molecular weight fractions and compared to the RI detection traces, the bimodal character was more pronounced. To verify aggregation as the origin of the described catalyst behaviour a comparative test reaction with addition of the highly polar ionic liquid 1-ethyl-3-methyl-imidazolium tetrafluoroborate was performed (Table 4, Entry 5). This experiment clearly shows disappearance of the high M_w fraction and constant molecular weights for the low M_w

fraction. Therefore the polar co-solvent apparently provides sufficient stabilisation to break the catalyst aggregates. Furthermore the high content of polar ionic molecules also leads to a significant reduction of catalyst activity. Analysis of the thermal behaviour by DSC proves the linear character of the obtained PE for all samples.

Ethene homopolymerisation with the reference catalyst precursor **19** (Table 4, Entries 12 and 13) exclusively leads to formation of low molecular weight PE with a slightly increased catalyst activity. As expected no bimodal character of the obtained PE could be observed in the corresponding GPC elugrams due to the absence of ionic substituents which could allow for catalyst aggregation. This further supports the assumption that the low molecular weight polymer is formed at catalyst sites with minor influence of aggregation. Due to the aggregation and different reaction behaviour of **19** and **20** no speculation about possible influences from the introduced sulphonate functionality is possible. The observed reduced catalyst activity could also originate from mass transfer limitations or steric hindrance due to catalyst aggregation.

To determine the effect of introduced sulphonate functionalities on copolymerisation reactions with polar-functionalised olefins, namely methyl acrylate (MA), acrylonitrile (AN) and vinyl acetate (VA), were carried out. Pertinent questions which are addressed in these copolymerisation reactions are catalyst aggregation behaviour, stability and effectivity for incorporation of polar-functionalised comonomers. In this series MA is the first choice due to the relatively facile migratory insertion reaction into metal alkyl groups and consecutive polymerisation after MA insertion. The latter factor is important as the electron withdrawing α-substituent after 2,1-insertion of MA hinders a following olefin insertion.[48] AN and VA are attractive functional monomers which could give access to new polymeric materials either by copolymerisation reactions with ethene at higher incorporation rations (larger than 10 mol%) in linear PE or in homopolymerisation reactions by insertion polymerisation. Also an unprecedented homopolymerisation reaction *via* a coordination-insertion mechanism of these monomers could lead to the possibility of introducing stereocontrol with chiral catalysts.

Table 5 compares the obtained results for the performed copolymerisation reactions with the catalyst precursor **20**. The respective comonomer insertion ratios were determined by high temperature ^{1}H NMR spectroscopy by comparison with published literature data (references are given below for the specific cases). Furthermore the obtained polymers were characterised by DSC and GPC.

5. Non-Symmetrically Sulphonated Phosphine Ligands

Table 5: *Copolymerisation reactions of ethene and polar-functionalised monomers with compound **20**.*[1]

Entry[3]	T(°C)	p_{Ethen}	X, c_x (M/L)[5]	Yield (mg)	% x_{Pol}[6]	M_w[7]	PDI[7]	M_p[8]
1[2]	80	20	MA, 1.5	390	5.8	560 (M_{high})	3.3 (M_{high})	135[9]
						7.0 (M_{low})	3.9 (M_{low})	
2[2]	80	10	MA, 1.5	108	8.0	320 (M_{high})	5.5 (M_{high})	132[9]
						3.9 (M_{low})	2.3 (M_{low})	
3[2]	95	10	MA, 1.0	817	11.0	200 (R_{high})	2.5 (R_{high})	130
						4.1 (R_{low})	2.9 (R_{low})	
4[2]	95	10	MA, 2.5	3180[9]	100[9]	370 (M)	1.6 (M)	n.d.
						250 (R)	2.3 (R)	
5[3]	100	30	AN, 7.5	225	4.5	1.1(M)	1.7(M)	109[10]
6[4]	80	20	VA, 1.1	90	-	310 (M_{high})	5.3 (M_{high})	131[9]
						4.0 (M_{low})	2.5 (M_{low})	
7[4]	80	20	VA, 2.7	105	-	380 (M_{high})	7.4 (M_{high})	n.d.
						3.1 (M_{low})	3.2 (M_{low})	

[1]100 mL stainless steel reactor, 10 μmol catalyst, 1.1 equivalents $AgSbF_6$; [2]15 mL total solution of toluene and MA, 20 h; [3]200 mL stainless steel autoclave, 5 mL AN, 5 mL toluene, 120 h; [4]20 mL total solution of VA and toluene, 20 h; [5]comonomer with concentration; [6]from HT ^{1}H NMR spectroscopy at 110-120 °C; [7]$\cdot 10^3$ g·mol^{-1} GPC at 160 °C, bimodal molecular weight distributions observed as for PE homopolymers, only multi detection displayed, Entry 16 monomodal distribution, [8]determined by DSC, [9]T_m of linear PE dominates the DSC plots,[10]broadened towards lower temperatures, n.d. = not determined, [9]radical homopolymerisation of MA.

The obtained data clearly shows a reduced catalyst activity in the presence of MA (Table 5, Entries 1-3). Detailed analysis of the polymers resulting from ethene/MA copolymerisation indicates a non-uniform polymerisation mechanism. For instance, data obtained by GPC analyses show bimodal molecular weight distributions of obtained copolymers, similar to ethene homopolymerisation reactions with **20** described above. This is supported by the low solubility of fractions within the polymer samples in $C_2D_2Cl_4$ at 120 °C for high temperature NMR spectroscopy, as well as by the high melting points observed in DSC. The latter shows the distinct melting point of linear PE which clearly dominates the DSC plots in combination to broader melting areas. Therefore it can be assumed that the employed reaction conditions are not suitable to prevent catalyst aggregation, despite the relatively high concentration of the

polar solvent additive MA. Differentiation of active catalyst sites causes formation of polymer blends with a non-uniform MA incorporation. In addition to this observation, the investigation of the MA incorporation ratio by high temperature ^{1}H NMR spectroscopy shows reduced values compared to literature reports.[48, 60] Unfortunately at higher reaction temperatures and increasing MA concentration. These conditions could favour higher MA incorporation ratios but instead a radical homopolymerisation was observed, confirmed by comparison o to literature references (Table 5, Entry 4).[48] Therefore low catalyst stability and the possibility of homolytic bond cleavage during decomposition are indicated at more aggressive reaction conditions, leading to the initiation of a radical MA homopolymerisation.

In contrast to the example above, the copolymerisation of ethene with AN at high temperature and a high AN content of 7.5 mol/L led to the formation of a true ethene/AN copolymer with low AN incorporation (Entry 5, Table 5). GPC analysis of this polymer shows a monomodal distribution with low molecular weight. This is in accordance with high temperature ^{1}H NMR spectroscopic data in $C_2D_2Cl_4$ which confirm the low molecular weight character as well as the copolymerisation reaction. Detailed assignment of the observed signals gives an AN incorporation of 4.5 mol%. Compared to literature data (up to 7 mol% in a comparable experiment[66b]) this value is significantly decreased. The assignment of signals is shown in Figure 24 by an excerpt of the ^{1}H NMR spectrum. An overview of characteristic functionalities in the copolymer is displayed in Scheme 29. Reference data of model compounds which are reported in the literature were employed for this correlation.[66b] Hereby the direct incorporation of AN into the linear PE chain is confirmed by presence of AN units incorporated in the polymer chain, in addition to units as end groups from chain start and termination, with an overall ratio 1:1:1 (start/internal/terminal). The 2,1-insertion regioselectivity of AN was shown from the absence of terminal nitrile-substituted alkyl groups. Instead the 2,1-migratory insertion of AN into Pd-H bonds leads to 2-nitrile substituted polymer chains. Chain termination occurs by β-hydride elimination which generates these Pd-H species. This termination mechanism is also confirmed by the olefinic end groups observed by NMR spectroscopy. Presence of terminal nitrile substituted olefins in both E- and Z-conformations can be shown which originate from termination after 2,1-insertion of AN. non-functionalised olefinic end groups are also observed as terminal and internal olefin species. The occurrence of a partial internalisation was previously not precendented and indicates an overall reduced polymerisation rate due to a facilitated chain walking with the catalyst **20**. The increased content of non-functionalised olefinic end groups,

in comparison to the nitrile substituted ones, can be interpreted by an effectively reduced AN coordination to the catalyst centre. Also due to the uniform polymer structure AN, at the employed concentrations, seems to be efficiently suppressing aggregation of the catalyst. In contrast to MA the AN provides sufficient coordination strength to stabilise the catalyst in solution. Therefore AN homopolymerisation products originating from radical polymerisation could not be observed. A test reaction for AN homopolymerisation at 110 °C with 50% (v/v) AN (stabilised) in toluene solely led to formation of palladium black without any noticed polymerisation or oligomerisation.
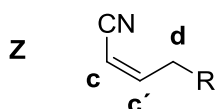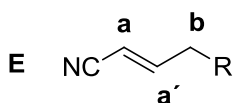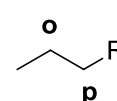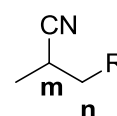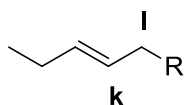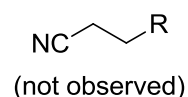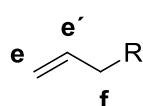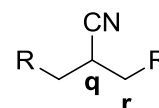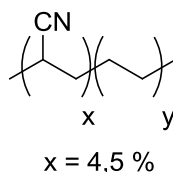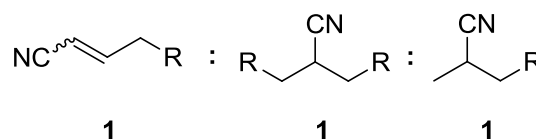
Scheme 29: *Labelling of characteristic H-atoms for the assignment of ^1H NMR spectra of AN/ethene copolymers, compare* Figure 24.
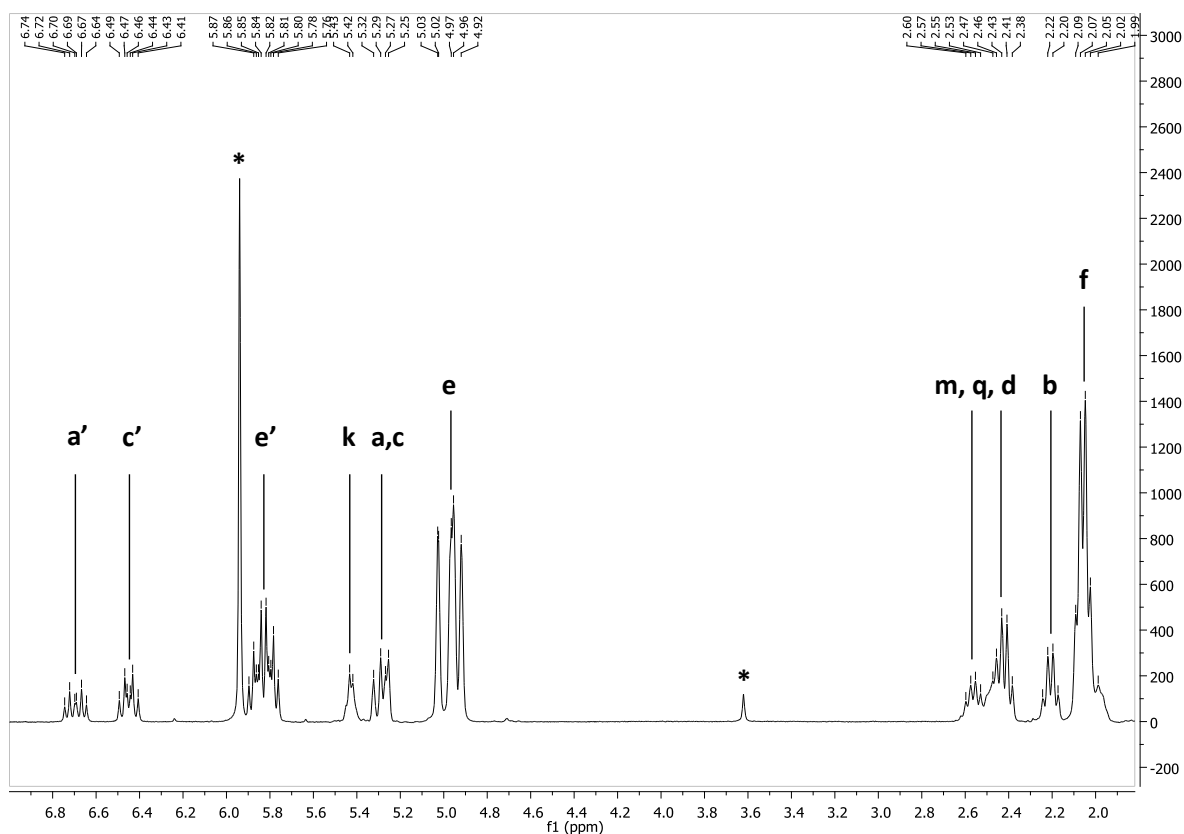
Figure 24: *Excerpt of the ^{1}H NMR spectrum (300 MHz, C$_2$D$_2$Cl$_4$, 110 °C) of an AN/ethene copolymer (Entry 5,* Table 5*). Assigned structural motives labelled for comparison with* Scheme 29.

In contrast to the successful AN/ethene copolymerisation the ^{1}H NMR spectroscopic analysis of attempted VA/ethene copolymerisation reactions (Table 5, Entries 6-7) do not show incorporation of VA into the PE chain. None of the relevant signals for methine groups or acetate groups are visible. However PE homopolymerisation occurred with greatly reduced catalytic activity. This indicates a weak π-coordination of VA as the limiting factor for the polymerisation.

5.8. Synthesis of dimeric *bis*-chelated neutral [{κ^2-(P,O)}$_2$Pd] complexes

To further study the coordination behaviour of the synthesised non-symmetrically sulphonated ligand salts **9b-c** and **12** the synthesis of *bis*-chelated complexes of type [{κ^2-(P,O)-phosphine sulphonate}$_2$Pd] was attempted in an analogous manner to previous literature studies.[58-59, 95] Similar to these reports Pd(OAc)$_2$ was reacted with the ligand salts. The

solvent of choice with the present ligands **9b-c** and **12** is either MeOH or water due to the hydrophilic character of these ligands. However the reactions carried out in water indicate oxidation of the phosphine parallel to formation of a coordination compound, observed in ESI-MS spectra. This species contains a single palladium atom in addition to one phosphine ligand as recognised by the molar mass and the characteristic isotope pattern of palladium. Furthermore other ligands or solvent adducts are present but unambiguous interpretation of the obtained mass spectra was not achieved. The analogous reactions in anhydrous methanol show partial phosphine oxidation observed from ^{31}P NMR spectroscopy and mass spectrometry, attributed to residual water introduced to the reaction with the phosphines which are present as hydrates.

Only in the reaction of two equivalents of **12** with Pd(OAc)$_2$ formation of a yellow to brownish solution was observed (Scheme 30). Removal of minor amounts of Pd(0) by filtration through Celite and subsequent crystallisation from methanol by slow evaporation of solvent provided small amounts of yellow crystals, suitable for determination of the molecular structure by X-ray diffraction. Refinement of the data showed that the obtained compound is a cocrystallate of the sodium-lithium salt **30** in a 1:1 mixture. Crystallisation of complex salts with sulphonated phosphines strongly depends on crystal packing and the cations which, in this case, apparently can form a defined long range order at this counterion ratio. The presence of lithium in the crystal mother solution could be validated by qualitative AES spectroscopy. ESI-MS spectrometry also indicates mixtures of the complex with different counterions, namely H$^+$, Li$^+$ and Na$^+$. However, heavily overlapping isotope patterns prevents the unambiguous assignment of individual species.
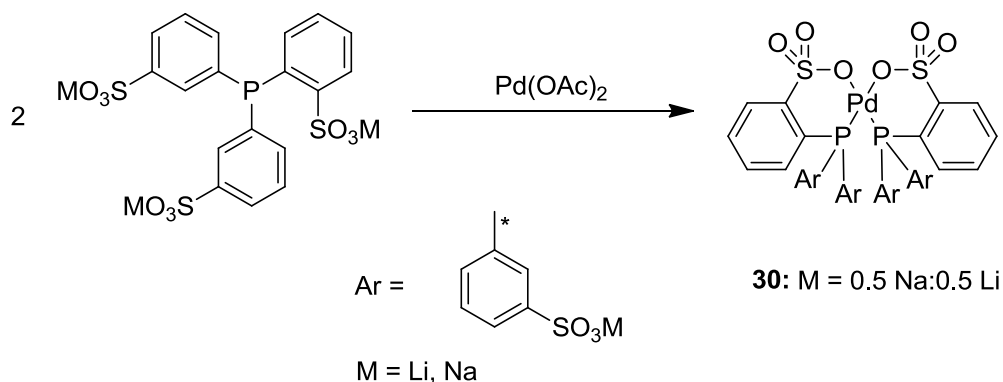
Scheme 30: *Synthesis of **30** as the 1:1 Na-Li co-crystallate starting from **12** as the sodium salt with Li impurities.*

5. Non-Symmetrically Sulphonated Phosphine Ligands
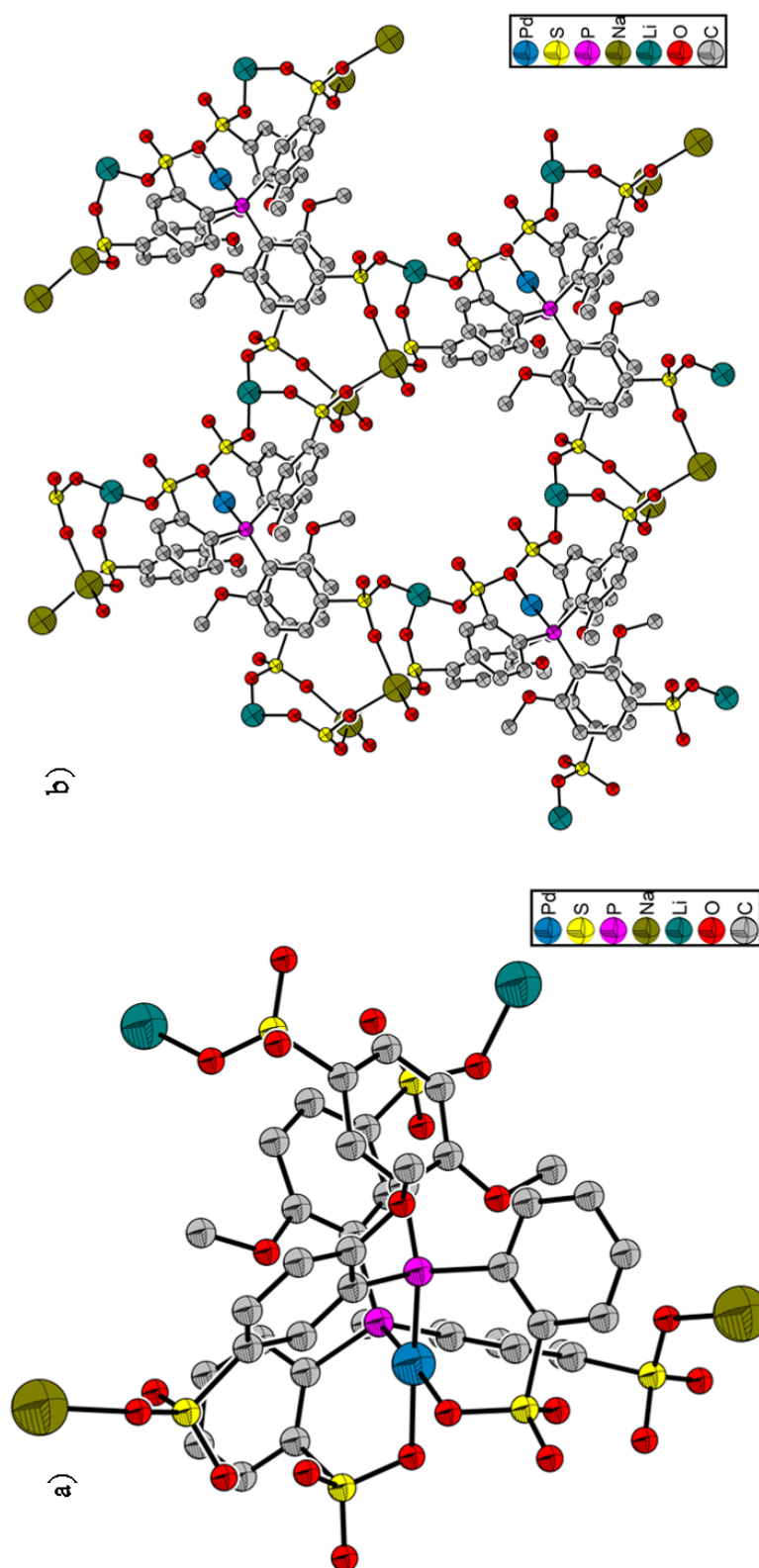
Figure 25: *a) Preliminary molecular structure of 30 and b) network formation via sulphonate alkali metal bridges. Displacement ellipsoids are drawn at the 50% probability level, hydrogen atoms and water molecules in the cavities emitted for clarity. Atom labels for the asymmetric unit displayed.*

5. Non-Symmetrically Sulphonated Phosphine Ligands

The observed lithium ions originate from contaminations of **7**, either as residual LiCl or the Li salt **7**. Subsequent sulphonation to **12** followed by neutralisation can lead to an enriched Li content upon fractionised precipitation due to the increased solubility of Li salts in MeOH. Varying content of these Li impurities in different charges of **12** are assumed to be the reason for the encountered difficulties in the reproduction of the crystallisation of **30**.

The preliminary molecular structure of **30** is depicted in Figure 25 which also shows the present network formed *via* sulphonate-alkali metal bridges. A *bis*-chelating coordination of the ligands to the Pd(II) centre can be clearly observed. Analysis of the molecular structure shows a distorted square planar configuration which is widened at the P(1)-Pd(1)-P(1') angle due to steric hindrance induced by the ligands. Similar to other molecular structures of phosphine sulphonate Pd(II) complexes with present OMe-functionalities these functionalities show two different alignments with distances greater than 3.5 Å to the palladium centre (compare to Section 6).

Reduction of Pd(II) to Pd(0), mentioned above, has been previously reported for similar reactions of Pd(OAc)$_2$ with sulphonated phosphines in aqueous solution (Scheme 31) and is described in the literature. For example during the reaction of *m,m,m*-TPPTS with Pd(OAc)$_2$ to Pd(*m,m,m*-TPPTS)$_3$ **31** oxidation of one phosphine equivalent occurs in addition to a decreasing pH.[96] Investigations concerning this oxidation showed the presence of (*m,m,m*-TPPTS)$_2$Pd(OAc)$_2$ intermediates and water as oxygen source. [97] Controlled synthesis of numerous hydrophilic metal complexes is described in the literature.[98]

a)

$$H_2O + Pd(OAc)_2 + 4\ TPPTS \longrightarrow Pd(TPPTS)_3 + OTPPTS + 2\ HOAc$$

31

b)

$$PdCl_2 + TPPTS \xrightarrow{H_2O} \left[\begin{array}{c} TPPTS \diagdown \quad \diagup Cl \\ Pd \\ TPPTS \diagup \quad \diagdown TPPTS \end{array} \right]^{\oplus}$$

32

$$\xrightarrow[slow]{H_2O} Pd(TPPTS)_3 + OTPPTS + 2\ HCl$$

31

$$\xrightarrow[H_2O,\ CO]{fast} Pd(TPPTS)_3 + CO_2 + 2\ HCl$$

31

TPPTS = [Na]$_3$[*m,m,m*-TPPTS]
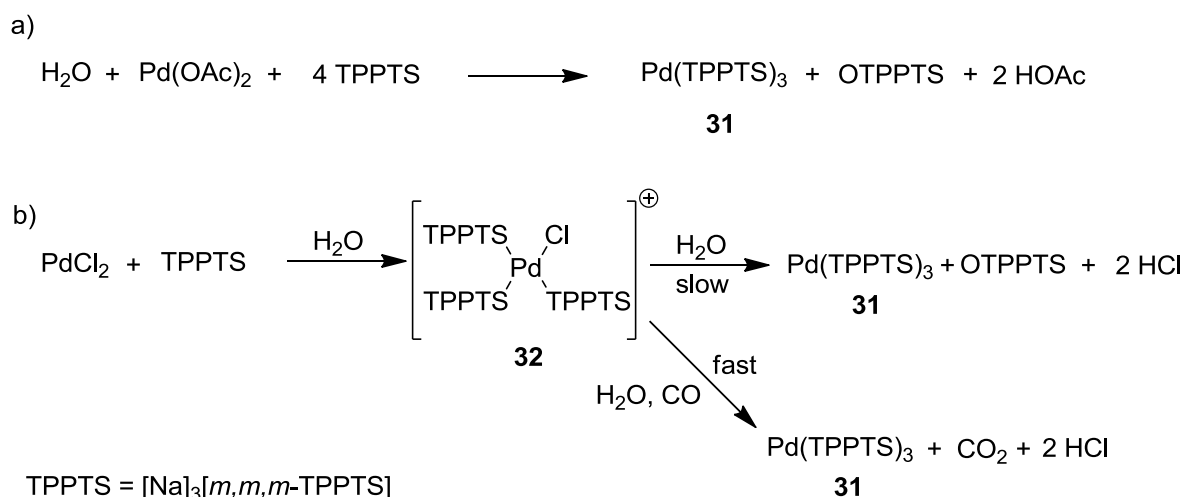
Scheme 31: *Possibilities for the synthesis of Pd(m,m,m-TPPTS)₃ a)* in situ *or b) via **32** an isoelectonic analogue to the hydrophobic Wilkinson catalyst, Cl⁻ anion of **32** omitted.*

6. Structural Modification of Neutral [{κ²-(P,O)-Phosphine Sulphonate}PdMe(Pyridine)] Catalysts for Investigation of Substitution Effects

6.1. General catalyst synthesis and modification concept

Despite numerous approaches to modify phosphine sulphonate-based Pd(II) catalysts in order to optimise their activity and the incorporation ratio of polar-functionalised comonomers, of the structure/activity relationship for this class of catalysts is still not clear. Thus identification and correlation of effects observed during polymerisation reactions to the employed catalyst structure is required. Only with a clear understanding of these aspects a directed and efficient catalyst development is possible. In general the modification of homogeneous polymerisation catalysts can either be achieved by change of the coordination environment, for example by exchange of the coordinating ligand type, or by alteration of steric and electronic effects by modification of a given ligand type. Furthermore addition or change of co-catalysts or activating agents can also have large influence on the catalyst efficiency. A change of the catalytically active metal is also an option. However, this has a drastic influence on the coordination chemistry and can result in significant changes of the catalyst reactivity.
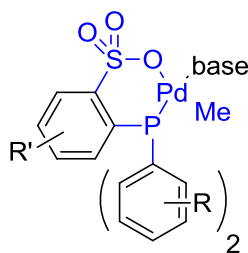
Figure 26: *General structure of a base-stabilised neutral phosphine sulphonate-based Pd(II) catalyst and possibilities for substitution (R, R'). Blue: required structural motives, no modification possible.*

For the modification of directly active neutral phosphine sulphonate-based Pd(II) single component catalysts the available positions as well as the required structural motives are shown in Figure 26. The κ²-(P,O)-phosphine sulphonate chelate as well as the Pd-Me group

(in general Pd-alkyl) cannot be exchanged without alteration of the catalyst type or the single component character of the catalyst system, respectively. However the aryl functionalities and the neutral Lewis base are ideal structural motives for the investigation of ligand substitution effects. Nevertheless synthetic limitations have to be considered as well.

In this respect some progress concerning the identification of structural effects in phosphine sulphonate-based Pd(II) catalysts could already be achieved and is reported in the literature. These successful reports mainly focus on to the role of the coordinated stabilising base which is now relatively clearly understood.[48-49] For example it could be shown, that in catalysts based on ligand **7** (for structure compare Scheme 10, Section 3.4.1) these Lewis bases are required to prevent dimerisation of two catalyst molecules *via* bridging through coordination of the sulphonate oxygen atoms to the palladium centres (Figure 27).[41, 81] These dimeric structures show only low solubility in weakly coordinating solvents, but can be transformed into monomeric stable neutral catalysts by addition of strongly coordinating solvents or Lewis bases. The back reaction to the dimeric form is possible by the removal of the respective Lewis bases with Lewis acids, for example $B(C_6F_5)_3$.
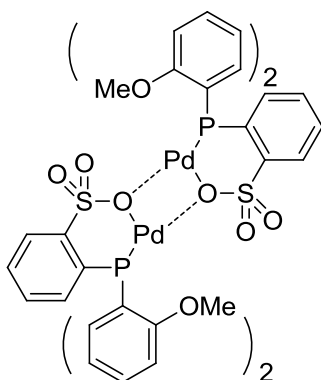
Figure 27: *Structure of base free dimerisation products based on the phosphine sulphonate ligand 7.*

Interestingly, the most common neutral phosphine sulphonate-based catalysts employ the strongly coordinating pyridine as Lewis base. Thus the relatively high observed catalyst activities are surprising in comparison to other transition metal-based polymerisation catalysts.[5b] This shows that ethene and other comonomers can effectively compete with pyridine coordination to the metal centre under reaction conditions. In fact presence of pyridine was reported to stabilise the catalyst and prevent decomposition during polymerisation (Section 3.2). Recent reports show that coordination of pyridine to the metal centre is a dynamic process *via* an associative replacement mechanism.[45] This is also the

6. Substitution Effects in Phosphine Sulphonate Catalysts

case for pyridine replacement by olefins such as acrylates. However the corresponding activation enthalpies were found to be low due to the associative nature of the process. Therefore it can be reasoned that replacement of pyridine by olefins has to be considered as the limiting factor which, however, allows polymerisation with relatively high catalyst activities. This could be validated by *Mecking et al.*[48] who exchanged pyridine for the weaker coordinating dmso ligand. Thus a catalyst with significantly increased polymerisation activity compared to the pyridine coordinated parent system was obtained which shows activity at low ethene pressures indicating little competition of dmso with ethene.

In contrast to this now relatively well understood influence of the Lewis base, a defined impact of the ligand structure cannot be deducted from available literature data. Nevertheless several important structural aspects for the modification of phosphine sulphonate ligand **7** (R' = OMe, Figure 28) as the parent structural motive have been reported. Modifications, such as the introduction of a *para*-methyl group (respective to the sulphonate) or alteration of the aryl substituents at phosphorus, for example by exchange of the functionalities in *ortho*-position by the introduction of *ortho*-Me or *ortho*-Et groups instead of *ortho*-OMe groups, only have a minor impact on the PE formation. Molecular weights are in the range of $20 \cdot 10^3$ g·mol^{-1} with moderate polymerisation activities.[35, 41] Most reported cases of copolymerisation reactions with functionalised olefins are also based on this phosphine sulphonate ligand **7**. In comparison the phenyl substituted system based on **8** (*o*-TPPMS, R = H, Figure 28) shows significantly reduced activities and low insertion ratios of polar-functionalised olefin comonomers.[35] Thus the question arises if the substituent effect on the polymerisation reaction is of steric and/or electronic nature and if mechanistic implications can be deducted.
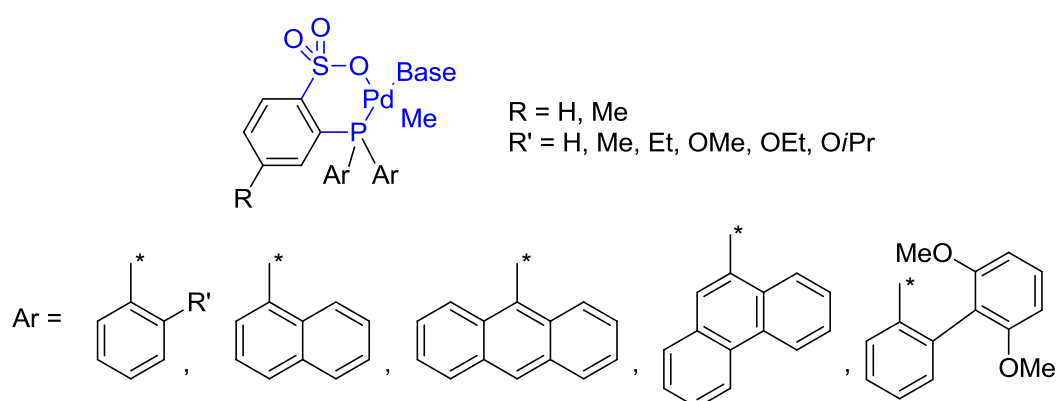
Figure 28: *Overview of selected ligand modifications for phosphine sulphonate-based Pd(II) catalysts, the non-modified complex centre highlighted in blue.*

6. Substitution Effects in Phosphine Sulphonate Catalysts

Consequently this problem was addressed by several reports. First by the introduction of extremely bulky *bis*-2,6-methoxyphenyl substituents, in *ortho*-position respective to phosphorus (Figure 28), which led to a significantly increased catalyst activity and formation of high molecular weight PE.[46] The enhanced steric bulk protects the coordination sites at palladium by shielding of the axial positions. Accessibility of these sites is required for chain termination by an associative mechanism. Unfortunately this substitution pattern resulted in a decreased incorporation of MA, most likely as a consequence of the described steric shielding of the palladium centre.[46] Based on these observations, the investigation of substitution effects was extended in a series of phenyl-, naphthyl-, anthracenyl-, and phenanthryl-based phosphine sulphonate Pd(II) catalysts (Figure 28). In this sequence, basicity and steric demand of the ligands systematically increase. This concept was anticipated to further elucidate the structure/activity relationship of respective catalysts. However, only a reduction of the corresponding catalyst activities and molecular weights of obtained polymers could be observed. Unfortunately, besides the complex with phenyl substituents, the molecular structures of related catalysts with more sterically demanding ligands are not available for a detailed comparison of the coordination behaviour and the alignment of substituents.[47] The authors propose a hindered ethene coordination which would favour termination by β-hydride elimination over chain growth as a result of this substitution pattern. However due to the missing molecular structures and comparison of these complexes to the related catalyst with *bis*-2,6-methoxyphenyl substituents, which shows high activity and major steric hindrance in the coordination environment, this has to be considered as speculative. In contrast, some very recent developments for the copolymerisation of ethene and polar-functionalised olefins by *Nozaki et al.* focus on the cyclohexyl-substituted phosphine sulphonate-based catalysts, for which slightly increased activities could be observed.[68] However the effect seems to be relatively minor.

From these reports it is evident that the investigated substitution patterns do not lead to clear distinguishable trends for the structure/activity relationship. Therefore after 10 years of intense scientific research control of the polymerisation reaction *via* the phosphine sulphonate-based catalyst structure is still problematic. Standard comparative models for the classification of phosphines and interpretation of observed ligand effects in catalysis, namely the basicity of the phosphine, the Tolman cone angle or the ligand bite angle (Section 2.1) are apparently not suitable for the interpretation of effects in the phosphine sulphonate-based catalyst system. Specifically the role of methoxy functionalities is an open question, as most

6. Substitution Effects in Phosphine Sulphonate Catalysts

of the highly active catalysts show presence of OMe-groups which increase ligand basicity and can align in orientations with relatively close proximity to the metal coordination centre.

Some reports already address this question and in the case of the non-alternating copolymerisation of carbon monoxide and ethene by *Ziegler* and *Rieger* (Section 3.4.4) experimental investigations on this system are supported by DFT calculations.[42c, 58] Direct comparison of several ligands show that the unusual increase of ethene incorporation is clearly dependant on the functional groups in *ortho*-position of the aryl substituents, respective to phosphorus. Steric bulk in this position facilitates a decarbonylation reaction, which permits increased ethene incorporation. However the exact nature of this interaction, being of electronic or steric nature could not be ascertained. Nevertheless, electronic repulsion with *o*-OMe substituents was proposed to support the isomerisation mechanism of the reaction. As already stated the molecular structures of phosphine sulphonate complexes with alkoxy substituents possess one OAlk-functionality directed to the metal centre *via* oxygen. Due to the relatively long Pd-O distance (~ 3-4 Å) speculations concerning possible interactions with palladium are problematic (Figure 29) as no direct means for their observation are available.
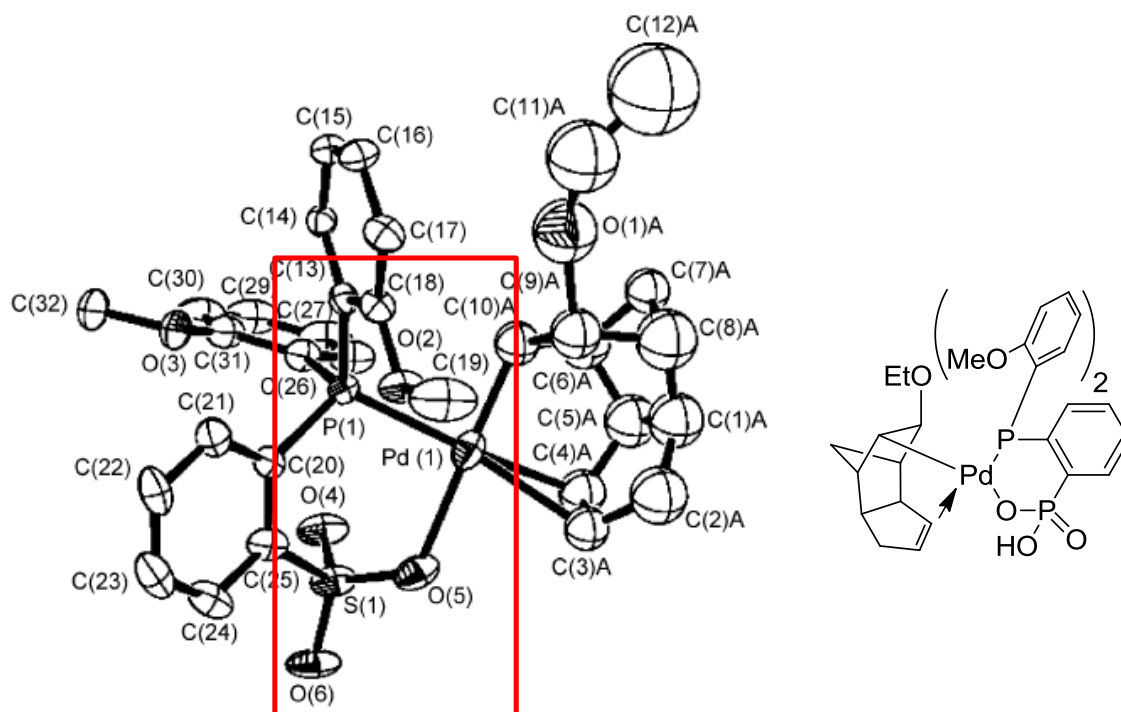
Figure 29: *Molecular and schematic structure of a phosphine phosphinate-based Pd(II) catalyst. One OMe-functionality [O(2)] aligned towards the palladium centre, close contact of O4 to the palladium centre.*[58]

6. Substitution Effects in Phosphine Sulphonate Catalysts

Unusual activating effects of arylphosphine ligands with *o*-OMe functionalities on other Pd-catalysed polymerisation reactions have been reported, for example in the alternating ethene/CO copolymerisation. Molecular structures of the employed *o*-OMe-dppp (1,3-*bis*{di (*o*-OMe)phenyl}phosphinopropane) also show a similar behaviour of the methoxy functionalities. To elucidate effects of this alignment *Bianchini et al.*[99] investigated this system in the solid state, in solution and under polymerisation conditions. A ROESY NMR spectroscopic experiment confirmed the similarity of the complex conformation in the solid state and in solution. A strong spatial interaction between the methyl group on the palladium centre and one *ortho*-hydrogen atom of the aryl functionalities, respective to phosphorus, is observed. Concerning the reactivity of this catalyst a significant activating effect on ethene/CO copolymerisation is observed in comparison to the non *o*-OMe-functionalised dppp-based (1,3-bis[diphenylphosphine]propane) catalysts. Also a facilitated opening of β-chelated resting states has been observed for the methoxylated catalysts. Although no direct evidence for metal-hydrogen or metal-oxygen interactions could be observed, it was shown that the aryl functionalities align in a way which would clearly favour possible interactions.

With respect to the described observations, both for the phosphine sulphonate palladium-based as well as for similar phosphine-based systems, a direct influence of substituents on the polymerisation reaction has to be considered. For instance, it could be very likely that minor steric or electronic changes, as well as possible ligand-metal interactions, might lead to small energetic contributions for relevant transition states. Given the proposed mechanism for the required *cis-trans* isomerisation *via* a Berry pseudorotation (Section 3.2.2), interactions from functional groups could favour, or disfavour, critical steps in the polymerisation mechanism. However difficulties are anticipated in the unambiguous determination of minor mechanistic changes if no direct analytical methods for their observation are available, even if experimental investigations are supported by DFT calculations. Therefore a synthetic concept was developed to address several key issues and questions concerning possible metal-substituent interactions by indirect means. Here the direct comparison of modified systems, in terms of catalyst activity and resulting polymer microstructure, is combined with the investigation of catalyst structure in solution. Detailed synthesis of novel ligands and the corresponding neutral single component catalysts is presented in the following sections, together with observed effects in polymerisation reactions.

6.2. Synthesis of phosphine sulphonate ligands and derived palladium complexes for the investigation of substitution effects

To clarify and evaluate the direct influence of the *o*-OMe-functionality on the polymerisation reaction two key questions have to be addressed. Firstly, the specific nature of the functionality, as well as secondly, the exact location of these substituents respective to the metal centre are of importance.

Dependence of effects on the nature of a substituent can be tested by a functional group exchange for suitable alternative functionalities. For example in the present case a replacement of the *ortho*-ether functionalities with respect to phosphorus by thioethers functionalities would be ideally suitable to expand the understanding of substituents in this position. The larger and softer sulphur donor could increase possible interactions with the metal centre (Section 6.4). Therefore in this work the introduction and effect of a SMe group on phosphine sulphonate-based Pd(II) catalysts and the corresponding polymerisation reactions is described.

To address the second question, the exact position of the OMe group in relation to the palladium centre can be altered *via* suitable ligand modifications. This is of importance to determine possible steric effects for example on the monomer coordination. Furthermore, the exact location of OMe groups on the aromatic moieties has a significant influence on the electronic environment and the basicity of the phosphine. Naphthalene-based phosphine sulphonate ligands with methoxy functionalities are ideal candidates for the investigation of this question.

The employed synthetic route for the synthesis of novel phosphine sulphonate ligands and corresponding catalysts is based on the available patent literature.[50] Following this protocol, formation of the relevant intermediate aryldichlorophosphine species is carried out without isolation and purification, which leads to a "one pot procedure" for the ligand synthesis. Compared to the multi step procedure with low overall yields reported previously[40a] this significantly facilitates ligand synthesis and modification for catalyst development. As shown in Scheme 32 benzene- or toluene-sulphonic acid is lithiated with *n*-BuLi and reacted with diluted PCl_3. Slow transfer of the aryllithium component is critical to reduce its local concentration during the reaction in order to ensure mono-substitution of PCl_3. Based on this intermediary formed reactive species, introduction of desired aryl substituents at phosphorus is straightforward *via* their respective organo-lithium salts. Finally termination, acidification with aqueous HCl and isolation of the phosphine sulphonate either gives the

6. Substitution Effects in Phosphine Sulphonate Catalysts

ligand as the free phosphine sulphonic acid or the corresponding zwitterionic form. This is dependent on the basicity of the phosphine sulphonate. The pure compounds are ideally purified by crystallisation, preferentially from chloroform.

R = H, Me
R' = Cy or Ar
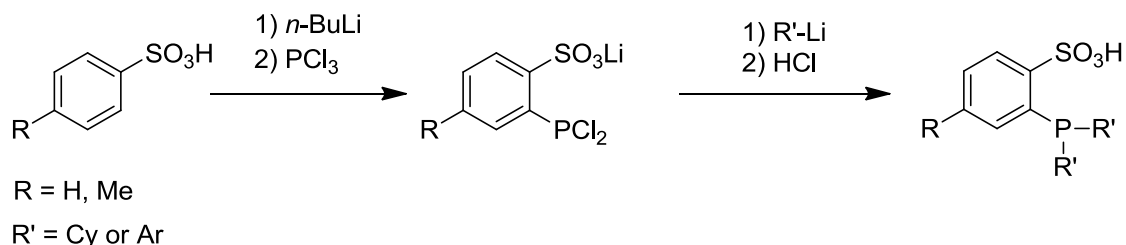
Scheme 32: *General synthesis of phosphine sulphonate ligands* via *the* in situ *generation of reactive aryldichlorphosphine intermediates*.

Based on this ligand class the laborious synthesis of pyridine-stabilised neutral phosphine sulphonate catalysts *via* an anionic Pd(II) species bearing alkyl ammonium counterions (Section 5.5.1) with subsequent chloride abstraction and pyridine coordination was also significantly improved.[50] With this protocol the problematic separation of alkyl ammonium salts from the desired catalysts is avoided by reaction of the phosphine sulphonate ligands with (tmeda)PdMe$_2$ (Scheme 33). Driving forces in this reaction are both the formation of methane and dimeric tmeda bridged complexes (κ-(N,N')-[{κ^2-(P,O)-phosphine sulphonato}PdMe]$_2$tmeda) with a relatively low solubility in weakly coordinating solvents. This facilitates purification and the subsequent addition of a stabilising base, for example pyridine, soluble neutral phosphine sulphonate catalysts [{κ^2-(P,O)-phosphine sulphonato}PdMe(pyridine)] are obtained in high purity.[48, 50]
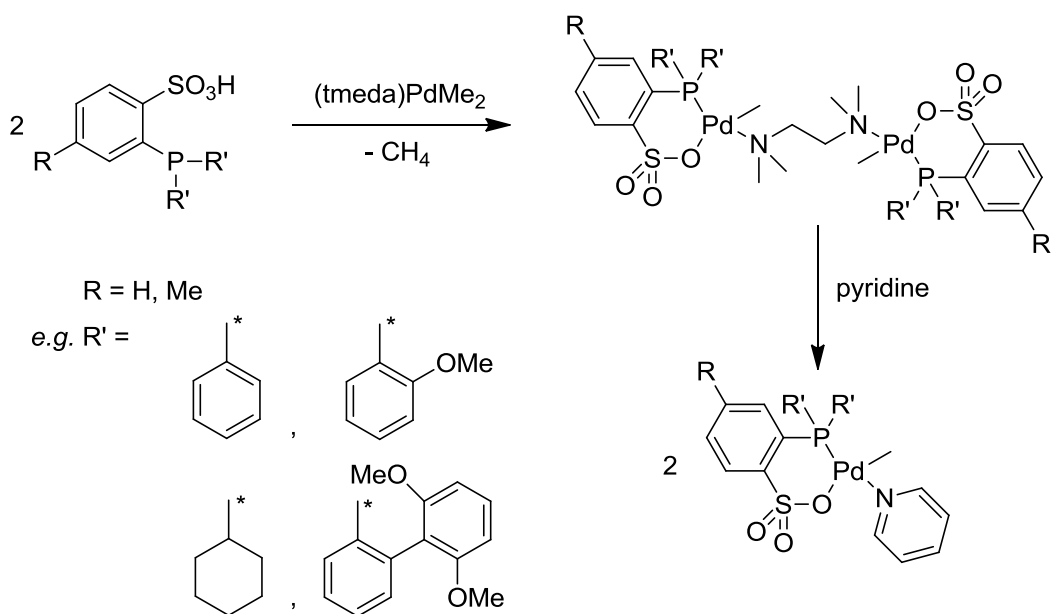
Scheme 33: *Synthesis of neutral pyridine stabilised phosphine sulphonate-based Pd(II) polymerisation catalysts* via *a dimeric tmeda-bridged intermediate.*

6.3. Synthesis of the methoxy substituted [{κ^2-(P,O)-*o*-TPPMS(OMe)}PdMe(pyridine)] as reference catalyst

For extended analytical investigation and as reference catalyst the synthesis of [{κ^2-(P,O)-*o*-TPPMS(OMe)}PdMe(pyridine)] **4** was performed according to the described literature procedure.[50] The phosphine sulphonate ligand **7** was synthesised from benzene sulphonic acid, PCl$_3$ and 2-bromo-anisole *via* the "one pot reaction" described above (Section 6.2). After crystallisation from chloroform the zwitterionic form of the ligand was obtained in low yield (20.6%). Reaction of **7** with (tmeda)PdMe$_2$ and subsequent addition of pyridine gives **4** in good yield (89.4%) (Scheme 34). For comparison with other related complexes characterisation of **7** by ^{31}P NMR spectroscopy shows a broad doublet with a characteristic high H-P coupling constant (doublet, δ$_P$ = 10.4 ppm, ^1J (P,H) = 591.2 Hz) and a single peak (singlet, δ$_P$ = 22.3 ppm) for the respective neutral phosphine sulphonate catalyst **4**.

6. Substitution Effects in Phosphine Sulphonate Catalysts
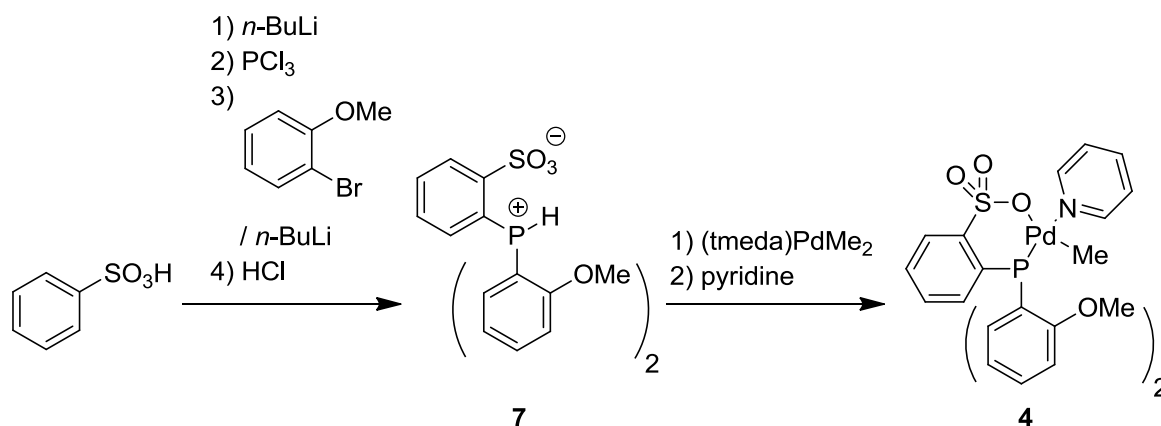
Scheme 34: *Synthesis of the phosphine sulphonate ligand 7 and the reference catalyst 4.*

Detailed analysis of **4** by multinuclear 1D and 2D NMR spectroscopy confirms the structure of the obtained neutral single component catalyst. During the depicted reaction (Scheme 34) first the formation of **7** and later its conversion to **4** can be monitored by the chemical shifts of peaks observed by ^{31}P NMR spectroscopy. Particular attention was paid to the examination of 2D spectra, especially the interpretation of the NOESY NMR spectrum for the determination of the complex structure in solution. In general NOESY NMR spectra can provide information about the alignment of functional groups in solution from observed cross peaks. These signals origin from the nOe (nuclear Overhauser effect), which describes the inter space relaxation of two NMR signals if the corresponding protons are in close contact. As this effect is strongly dependant on the distance d between two protons (~ $1/d^6$), relations with d between 2 and maximal 5 Å, respective to each other, can be observed. Sample preparation is important, as the nOe is strongly dependant on the concentration of a sample and the presence of paramagnetic components (such as oxygen), which both lead to faster relaxation and therefore decrease the nOe. Furthermore the intensity of the nOe is dependent on the molecular structure as well as the molecular weight of the substance. As the investigated molecules in this work show molecular weights between 600 and 800 g·mol^{-1} NOESY NMR spectra are appropriate for these cases. For larger molecules around 2000 g·mol^{-1} ROESY NMR spectra would be the suitable alternative.[100]

For interpretation of H-H distances *via* NOESY NMR the observed signals are compared to an internal reference signal with known H-H distance. Equation 2 shows the general formula for the intensity of a NOESY NMR signal and its dependence on the H-H distance. The calibration constant C can be determined by the reference relation, which gives Equation 3. In the present case the H-H distance of the *ortho* and *meta* pyridine H-atoms is an ideally

suitable reference signal for distance approximation in phosphine sulphonate-based palladium catalysts with coordinated pyridine. Comparison of different reported molecular structures shows only minor variation from the obtained reference distance (2.3 Å), as expected.[46, 80] Also it has to be noted, that for investigation of dynamic processes the distance determination *via* observed NOESY NMR crosspeaks will give an average value. Due to the dependence of the nOe on $1/d^6$ short distances are weighted more than long ones which means that no arithmetic average values are observed.

Equation 2:

$$I_{ij} = \frac{C}{d_{ij}^6}$$

with: C = calibration constant

       I_{ij} = integral value of nOe signal *ij*

Equation 3:

$$d_{ij} = \sqrt[6]{\frac{I_{no}}{I_{ij}}} \cdot d_{no}$$

with: I_{no} = integral value of nOe signal *no* (reference signal)

       I_{ij} = integral value of nOe signal *ij* (x)

       d_{no} = reference distance *no* (r)

       d_{ij} = determined distance *ij* (x)

Figure 30 shows the structure of **4** with assigned and labelled H-H relations which could be observed in the corresponding NOESY NMR spectrum (Figure 31). The pyridine H-H-distance (2.31 Å) was taken from the reported molecular structure[80] and compared to values determined in this work (Section 6.6) as well as literature reference data for related complexes[46]. However several possible error sources have to be considered for these approximations. The determined H-H distances for the relations **A-D** are listed in Table 6 and show good agreement of the solution- and solid state-structure of **4**.

6. Substitution Effects in Phosphine Sulphonate Catalysts

i) Integration errors

Due to minor errors in phase- and baseline-correction the integrals of observed NOESY NMR crosspeaks differ slightly in f1 and f2 direction. Therefore only average values from f1 and f2 are compared to H-H distances determined from the molecular structure.

ii) Dynamic processes

Dynamic processes for non-rigid structural fragments as well as a possible rotation of substituents have to be considered. These processes will lead to considerable deviations of the solution structure, as well as of determined bond lengths, from the refined molecular structure. However, in the present structures, functionalities with a high degree of freedom such as the OMe groups can be identified relatively easily.

iii) Proton positions in molecular structures

Positions of protons in molecular structures are normally calculated *via* a riding model which might lead to deviations from actual positions. However, these are considered as minor compared to dynamic processes. Furthermore the shortest H-H distances observed in the molecular structure are taken which disregard possible structural flexibility, such as a possible rotation of methyl groups in the solid state. Also Crystal packing effects have to be considered.
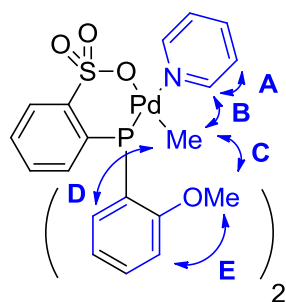
Figure 30: Labelling of observed H-H-inter space relations (blue) for **4**, as observed in the corresponding NOESY NMR spectrum, Figure 31.

Previous analysis of **4** and related complexes by ^{1}H NMR spectroscopy show the presence of an dynamic process with two possible alignments of the aryl groups due to the bent κ^2-(P,O) chelate at the sulphur position. At room temperature these compounds show fast

inversion of the κ^2-(P,O) chelate and variable temperature NMR experiments show a splitting of the OMe resonance at lower temperatures.[41] The molecular structure of **4** was reported by *Sen et al.*[80] and shows a non-equal alignment of the methoxylated aryl substituents which was also reported for related compounds[41].
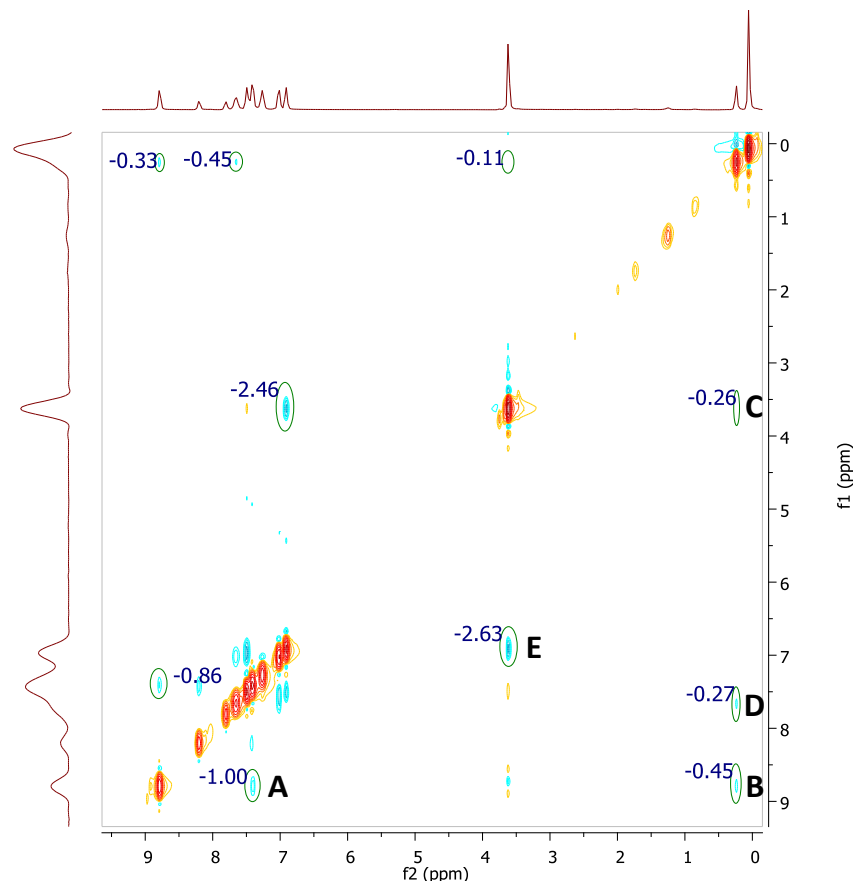
Figure 31: *NOESY NMR spectrum of complex **4** (500MHz, CDCl₃). Crosspeaks originating from H-H relations relevant for the interpretation of the ligand alignment in solution are integrated and labelled as assigned in Figure 30.*

Table 6: *Determined H-H distances for NOESY relations shown in Figure 30 and Figure 31.*

relation[1]	I_x (f1)[2]	I_x (f2)[2]	d_x (nOe, f1) / Å[3]	d_x (nOe, f2) / Å[3]	d_x (average) / Å[4]	d_x (mol. struc.) / Å[5]
A	0.86	1.00	reference	reference	**reference**	**2.3**
B	0.33	0.45	2.7	2.6	**2.7**	**2.6**
C	0.11	0.26	3.3	2.9	**3.1**	**3.7**
D	0.45	0.27	2.6	2.8	**2.7**	**2.8**
E	2.46	2.63	1.9	2.0	**2.0**	**2.2**

[1]nOe relation as defined in Figure 41, [2]nOe integral in f1 and f2 direction, [3]distance x for f1 and f2, [4]average distance from f1 and f2, [5]determined from the molecular structure[80].

Interpretation of the NOESY spectrum now shows that these two conformations are also present in solution. Both signals for spatial H-H relations of the palladium methyl group with the OMe functionality **C** as well as the *o*-H atom of the methoxylated aryl groups **D** can be observed. Here the weak H-H relation **C** indicates a relatively long distance (3.1 Å) of the OMe group to the Pd-Me group. Furthermore **D** shows the second interaction, from the *ortho*-hydrogen atom to the Pd-Me group, of the functionalised aryl groups with a slightly shorter distance of 2.7 Å. As the ^{1}H NMR spectrum shows only one signal for both methoxy functionalities at room temperature, this observation confirms a dynamic equilibrium with one OMe-functionality aligned towards the Pd-Me group and the other directed away. Both distances correlate well to the observed H-H distances from the molecular structure if the rotational freedom of the methoxy group is considered. In addition the H-H relation **B** shows a distance of 2.7 Å between the pyridine proton *ortho* to nitrogen and the Pd-Me group. Furthermore, the last and most pronounced resonance **E** shows close contact of the OMe groups to the adjacent H-atoms on the aromatic substituents with H-H distances of 2.0 Å. Again these last H-H distances correlate well to the molecular structure which allows the conclusion that the solid state structure of **4** resembles the solution structure with good approximation.

6.4. Thioether substituted phosphine sulphonate ligands
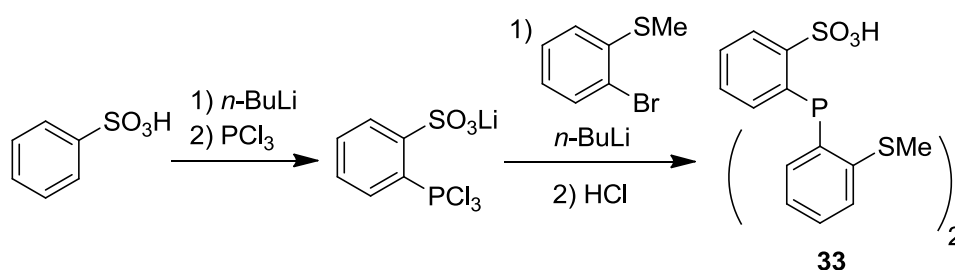
Scheme 35: *Synthesis of the thioether-functionalised phosphine sulphonic acid ligand 33.*

Following the investigations on the molecular structure of **4** in solution the phosphine sulphonate structure was altered by exchange of the methoxy functionality with a methyl thioether group to investigate possible interactions with the metal centre. Such a thioether substitution *ortho* to phosphorus is noteworthy as numerous available reports in the literature show the coordinating potential of sulphur in this position. These observations were confirmed for a considerable amount of transition metal based-phosphine complexes. Corresponding *o*-SMe-functionalised phosphines are usually P{(*o*-SMe-Ph)$_n$Ph$_m$} (n+m = 3)

6. Substitution Effects in Phosphine Sulphonate Catalysts

in combination to metals such as Ni, Pt, Pd, Cr, Mo, W. Thus the coordinating ability, or at least the occurrence of significant metal-sulphur interactions of phosphines with methyl thioether functionalities, can be acknowledged as established.[101] Due to their strong interaction with metal centres introduction of *o*-SMe functionalities to the aryl substituents at phosphorus in phosphine sulphonate palladium-based polymerisation catalysts is an ideally suitable modification, to evaluate the influence of functionalities at this position on the polymerisation reaction. Specific attention is directed to possible influences of metal-ligand interactions on the *cis-trans* isomerisation which is essential for chain growth and chain termination. Such effects could possibly assist, or hinder, this required process.

Successful introduction of the methyl thioether functionality into novel phosphine sulphonate ligands could be achieved in the synthesis of **33** from PCl$_3$, 2-bromo-thioanisole and benzenesulphonic acid (Scheme 35). The general reaction procedure is a combination of the common protocol for synthesis of phosphine sulphonates and phosphines with *o*-SMe substituents respective to phosphorus.[102] However during reaction work-up specific attention was directed to prevent formation and exposition to potentially hazardous thio-functionalised phosphorus products. This precaution is important to rule out potential rearrangement reactions which might lead to alkylated P(III)-esters. Members of this category are often hazardous pesticides and in some cases extremely toxic nerve gases. Therefore during isolation of **33** all volatiles were removed under reduced pressure and the residual solid was extracted with pentane prior to acidification. The obtained solid was dissolved in a water/methylene chloride mixture and acidified with aqueous HCl. Isolation of the organic phase and careful removal of volatiles under reduced pressure was followed by washing with pentane providing a solid dark yellow crude product mixture. Repeated washing with degassed water and dry THF, diethyl ether and pentane gave a yellow powder.

Analysis of this product by multinuclear NMR spectroscopy in combination with high resolution ESI MS spectrometry shows successful synthesis of the ligand **33**. The broadened lineshape of observed peaks, both in ^{1}H and ^{31}P NMR spectra, indicates presence of a dynamic process on the NMR experiment timescale. Quantitative analysis of the signals for phosphorus containing species shows 96.1% purity of **33** (respective to the total phosphorus content observed by ^{31}P NMR spectroscopy). The broad singlet peak with a relatively low high field shift (δ_P = -8.4 ppm) observed in the proton coupled ^{31}P NMR spectrum confirms presence of **33** as the free phosphine sulphonic acid. This stands in contrast to the zwitterionic methoxylated analogue **7** which shows a broad doublet with a characteristic H-P coupling

constant (doublet, δ_P = 10.4 ppm, ^1J (P,H) = 591.2 Hz). In general this indicates a lower basicity of **33** compared to **7**. The exchange process mentioned above prevents analysis of the ^{13}C NMR spectra due to the occurrence of several sets of NMR signals. Interpretation of the ^{1}H NMR spectrum shows presence of **33** in addition to solvent impurities (THF). Furthermore a second SMe-containing species with approximately 20 mol% is present, either as an additional conformation of **33** or a non-phosphorus containing side product impurity. Multinuclear NMR spectroscopic analysis is supported by successful identification of **33** in high resolution ESI MS spectra, a combination which unambiguously confirms the successful synthesis of **33**. The compound was employed as received in the subsequent complex formation reaction.
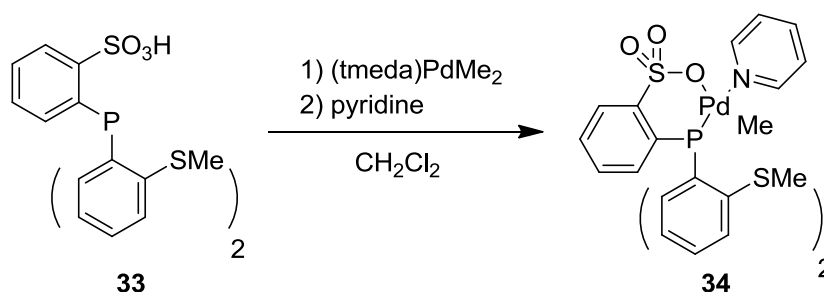
Scheme 36: *Synthesis of the thioether-functionalised neutral phosphine sulphonate-based Pd(II) catalyst **34**.*

Following the convenient synthetic route to pyridine stabilised neutral [{κ^2-(P,O)phosphine sulphonate}PdMe(pyridine)] catalysts mentioned above (Section 6.2) **34** was successfully isolated from the reaction of **33** with (tmeda)PdMe$_2$ and pyridine.[50] As expected evolution of methane was observed upon addition of (tmeda)PdMe$_2$ to a solution of **33**. However, as the tmeda-stabilised intermediate shows good solubility in methylene chloride solution, an excess of pyridine was added to the reaction and the complex **34** could be precipitated from the solution by addition of diethyl ether. Reprecipitation from methylene chloride/diethyl ether allowed isolation of the catalyst in low yield (28.8%) after filtration and drying *in vacuo*.

Again detailed analysis of **34** by multinuclear NMR spectroscopy clearly shows the presence of a dynamic process at room temperature which is not resolved on the NMR timescale. In both, the ^{1}H and ^{31}P NMR spectra the lineshape of observed peaks is extremely broadened while residual solvent peaks remain sharp and well resolved. However, integration of the ^{1}H NMR spectrum together with the single peak for phosphorus in the ^{31}P NMR

6. Substitution Effects in Phosphine Sulphonate Catalysts

spectrum [δ_P = 34.5 ppm (br s); free ligand: -8.31 ppm (br s)] and two dimensional NMR spectroscopy confirms the presence of the neutral catalyst, which is also supported by elemental analysis. Presumably as a consequence of this dynamic process crystallisation of **34** for determination of the molecular structure was not successful. Multinuclear variable temperature NMR spectroscopic experiments were carried out to investigate the behaviour of **34** at higher temperatures in solution as well as the influence on the dynamic process. Figure 32 and Figure 33 show a comparison of the ^{1}H and ^{31}P NMR spectra, respectively, in C$_2$D$_2$Cl$_4$ solution from 20 °C to 120 °C followed again by cooling to 20 °C.
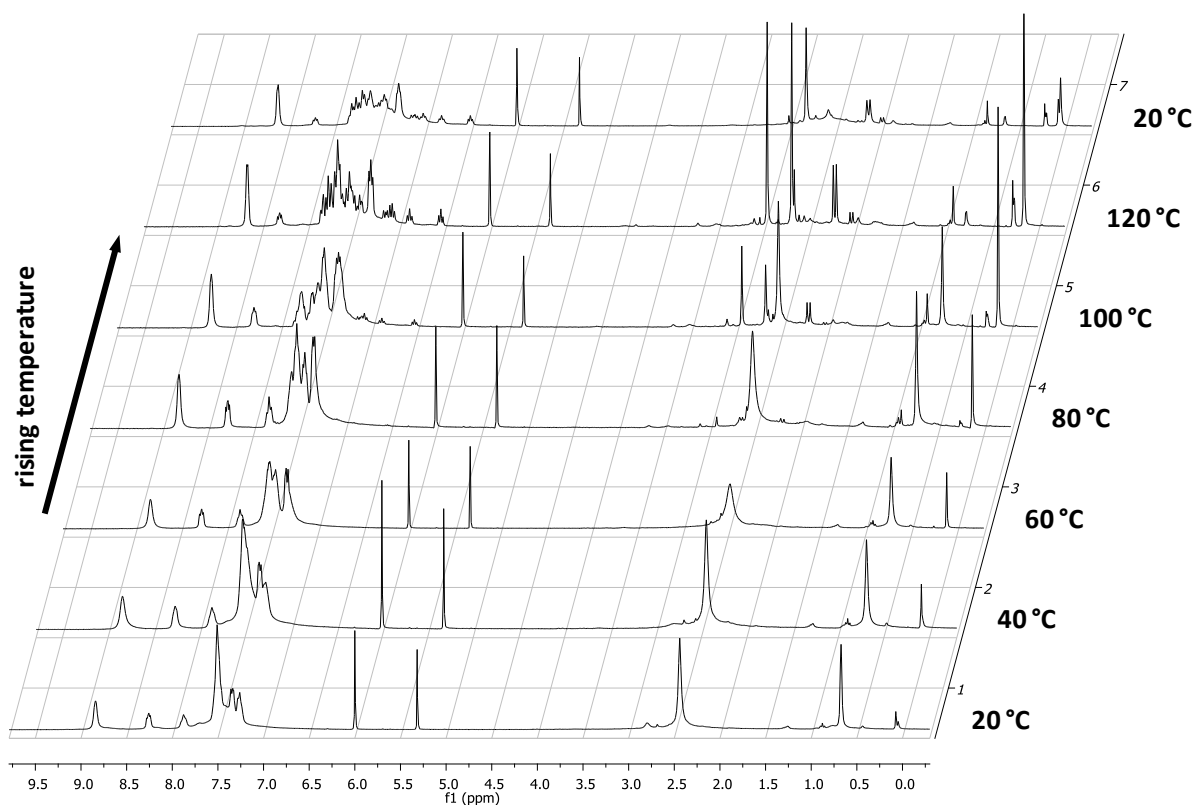
Figure 32: *^{1}H NMR spectra stack plot obtained for **34** at varying temperatures from 20-120 °C and 20 °C after cooling (300 MHz, C$_2$D$_2$Cl$_4$).*

97
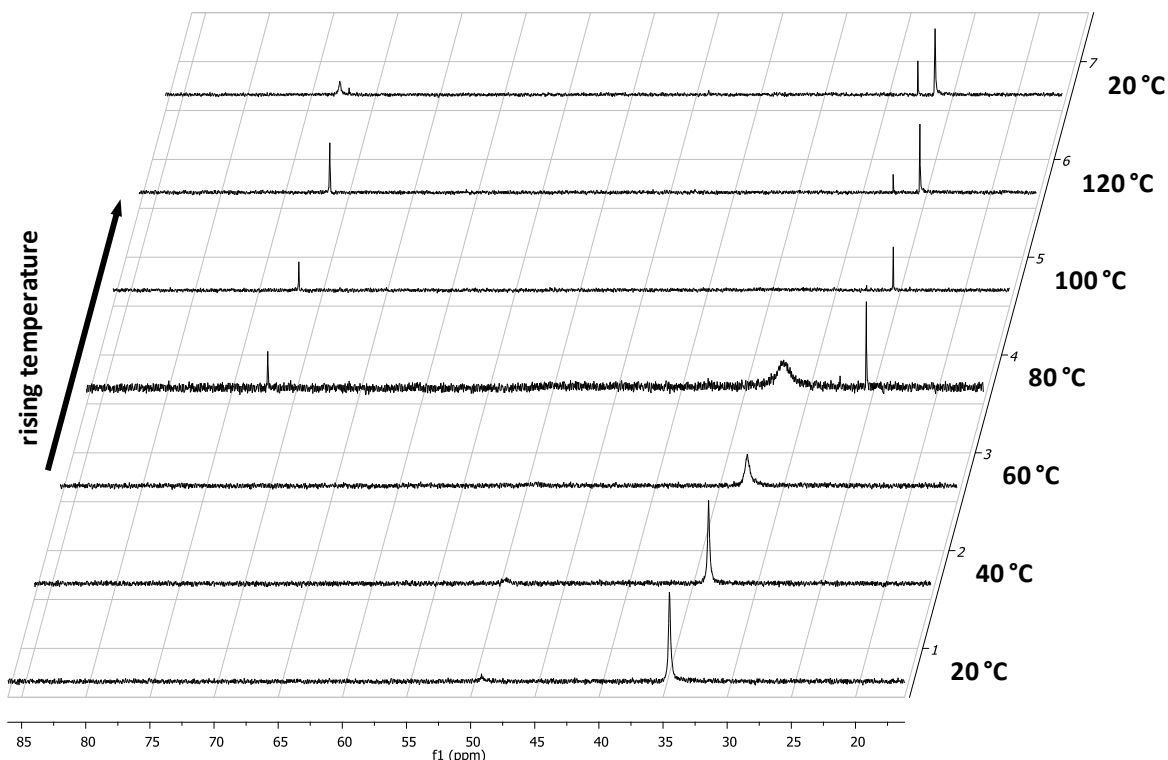
Figure 33: *^{31}P NMR spectra stack plot obtained for **34** at varying temperatures from 20-120 °C and 20 °C after cooling (300 MHz, C$_2$D$_2$Cl$_4$).*

In the depicted variable temperature ^{1}H NMR spectroscopic measurements the aromatic- as well as the SMe region both show formation of new species with increasing temperature due to decomposition of **34**. This was also confirmed by the parallel variable temperature ^{31}P NMR spectroscopic study where the singlet for **34** is significantly broadened and decomposition could be observed at 80 °C showing the relatively low temperature stability of **34** in absence of olefins. Unfortunately the phosphorus-containing decomposition products could not be identified. Furthermore the variable temperature ^{31}P NMR experiment indicates that the dynamic process is favoured at higher temperatures, as expected and a modification of the spectroscopic parameters such as increased relaxation time did not lead to significant changes in the NMR spectra.

Additionally **34** was investigated by two dimensional NMR spectroscopy to determine possible spatial H-H interactions in the NOESY spectrum of the compound in solution. Here it could be shown that **34** shows significant difference in comparison to **4** (Section 6.3). Unfortunately the quality of the NOESY spectrum is reduced due to the peak broadening. However, several crosspeaks for spatial H-H interactions could be identified. Figure 34 shows the labeling of observed intramolecular H-H interactions. In difference to the related complex

6. Substitution Effects in Phosphine Sulphonate Catalysts

4 only the pyridine-methyl group interaction **C** (2.31 Å) and the SMe-aryl proton interaction **B** (2.40 Å) are observable next to the reference signal **A**.
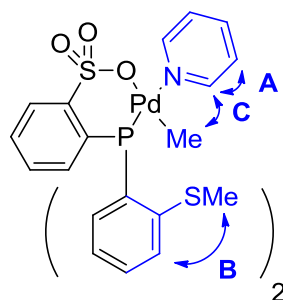
Figure 34: *Structure of **34** and labeling (blue) of observed intramolecular H-H interactions (compare* Scheme 35*)*

These obtained values show a slight elongation of the distance from the SMe group to the adjacent hydrogen atom (relation **B**, 2.3 Å) in **34** compared to **4** (relation **E**, 2.0 Å), a finding which is expected, due to the increased size of the sulphur atom. The slightly reduced Me-pyridine H-H relation **C** indicates either a modified coordination environment at palladium or, most likely, a more planar alignment of the pyridine ligand in respect to the pyridine-Pd-Me coordination. Nevertheless the determined bond lengths are in good accordance to related structures, which justifies the interpretation of the corresponding NOESY spectrum without the molecular structure of **34** for comparison. Furthermore the missing proton relations for **34** in comparison to **4** indicate no significant interaction of the palladium-methyl group with *i)* the SMe functionality and *ii)* the hydrogen atom in position 6 of the thioether-functionalised aryl substituents at phosphorus. The latter shows that an alignment in which the thioether functionalities are pointing away from the metal centre is unlikely.

In general these NMR spectroscopic experiments, in comparison to literature reports for other *o*-SMe functionalised phosphine complexes, indicate an interaction of the sulphur with the palladium metal centre. Unfortunately, as the molecular structure for this compound could not be obtained, this assumption cannot be unambiguously confirmed.
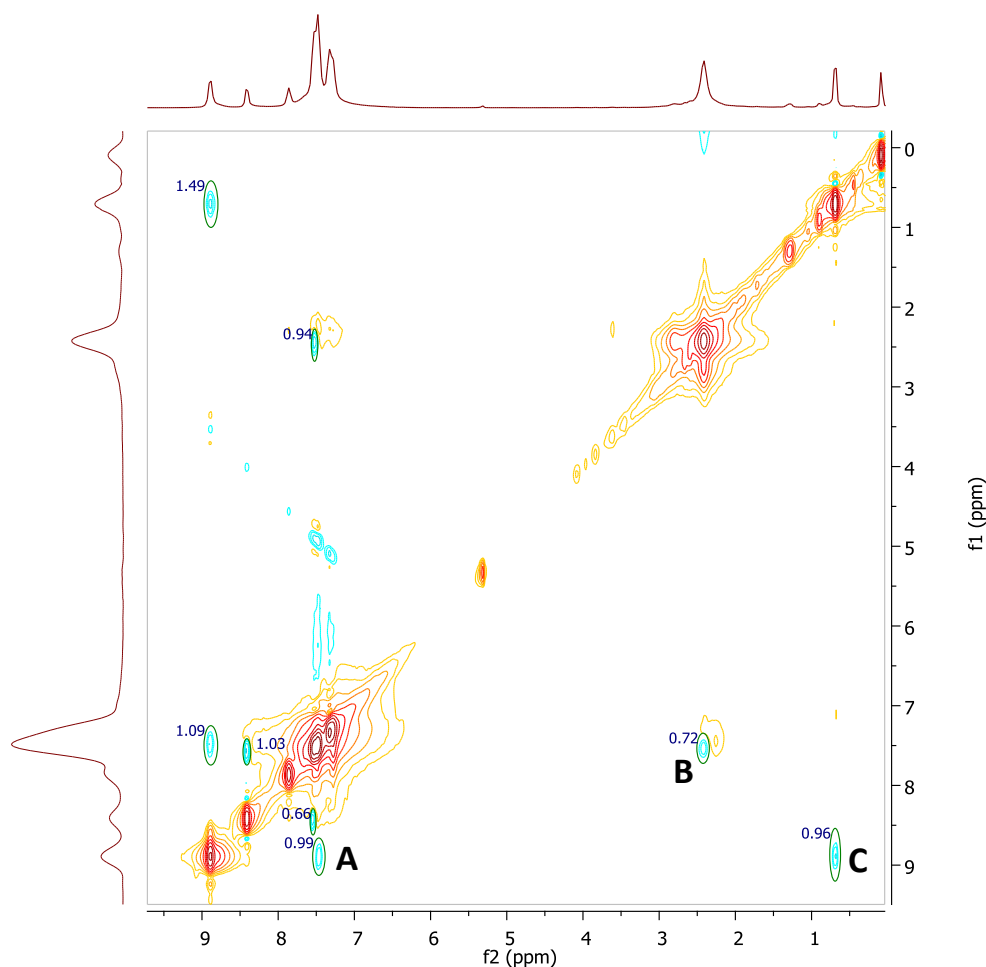
*Figure 35: NOESY spectrum for **34** (500 MHz, CDCl₃). Observed spatial proton correlations labeled as shown in* Figure 34*, due to the a dynamic process on the NMR timescale the observed peaks are broadened. The determined H-H bond lengths are listed in* Table 7.

Table 7: *Determined H-H distances from the observed NOESY interactions (*Figure 35*) for **34***.

relation[1]	I_x (f1)[2]	I_x (f2)[2]	d_x (nOe, f1) / $Å^3$	d_x (nOe, f2) / $Å^3$	d_x (average) / $Å^4$	d_x (mol. struc.) / Å
A	0.99	1.09	reference	reference	**reference**	**2.3[5]**
B	0.96	1.09	2.3	2.3	**2.3**	**n.d.**
C	0.72	0.4	2.4	2.4	**2.4**	**n.d.**

[1]nOe relation as defined in Figure 41, [2]nOe integral in f1 and f2 direction, [3]distance x for f1 and f2, [4]average distance from f1 and f2, [5]reference value from related compounds, n.d. = not determined.

6.5. Regioselective lithiation of methoxylated naphthalene derivatives

For a detailed investigation of the substitution effect not only the exchange of functional groups is important (Section 6.1). Also the alteration of the ligand substitution pattern is interesting to evaluate possible interactions of functional groups with the coordination environment. Therefore the possibilities for a change of the location of the methoxy group on the phosphine sulphonate ligand backbone were investigated. A regioselective substitution of methoxylated naphthalene derivatives was found to be an ideally suitable concept as, depending on the position of the methoxy group and the reaction conditions, regioselective functionalisation is possible. For example literature reports describe the selective lithiation of 1-[103] or 2[104]-methoxynaphthalene *via* halogen-metal exchange reactions or aromatic lithiation reactions (Scheme 37). However in the lithiation of 2-methoxy naphthalene a reaction equilibrium has been observed which leads to both 1- and 3-metallation.[104] Such interchanges are problematic, as complete regioselectivity during lithiation is required to prevent formation of non-symmetrically substituted phosphine sulphonate ligands. For this reason the lithiation of 2-methoxy naphthalene was not employed for synthesis of phosphine sulphonate ligands.

To achieve high conversions in the lithiation reaction halogen-metal exchange reactions are generally favoured, as quantitative lithiation of the aryl species can be achieved at short reaction times. A suitable example is the selective lithiation of 2-bromo-1-methoxy naphthalene in the 2-position with *n*-BuLi. Alternative to this lithiation type the isolation and purification of lithiated naphthalene intermediates is also appropriate. Direct lithiation of 1-methoxy naphthalene in 8-position with *t*-BuLi is a suitable example. Detailed literature reports on this reaction note a strong dependence on the reaction conditions, especially the solvent and the nature of the lithiating agent.[103a] Thus either the 8- or 2-lithiated species can be obtained either selectively or in mixtures with varying ratios. An equilibrium between these species has been also noted which can increase the ratio of the thermodynamically favoured 8-lithio-1-methoxy naphthalene. This interesting compound can be selectively obtained by reaction with *t*-BuLi and facile purification of the solid Li salt.

6. Substitution Effects in Phosphine Sulphonate Catalysts
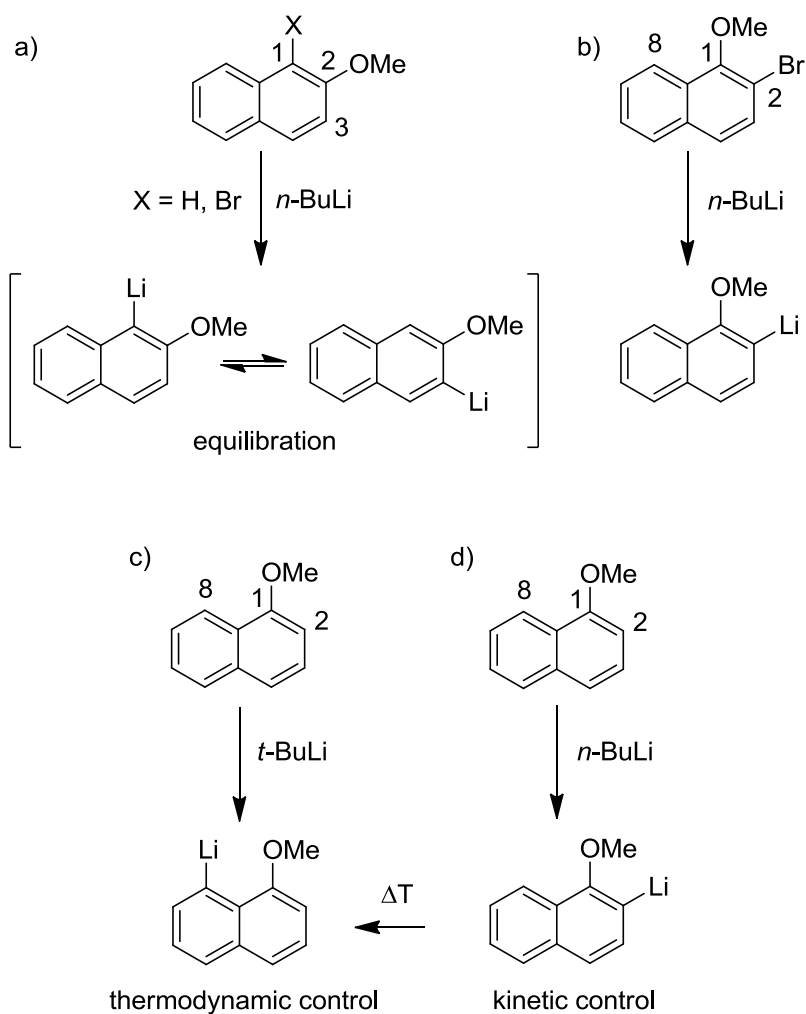
Scheme 37: *Regioselectivity and equilibration reactions in the lithiation of 1- and 2-methoxynaphthalene.*

6.6. Synthesis of neutral methoxylated naphthalene-based [{κ²-(P,O)-phosphine sulphonate}PdMe(pyridine)] catalysts from phosphine sulphonate ligands.

6.6.1. Synthesis and characterisation of phosphine sulphonate ligands based on methoxylated naphthalenes

As explained above the controlled lithiation of 1-methoxylated naphthalene derivatives (Section 6.5) was exploited for the synthesis of defined phosphine sulphonate ligands. This was followed by subsequent reaction to the corresponding neutral [{κ²-(P,O)phosphine

6. Substitution Effects in Phosphine Sulphonate Catalysts

sulphonate}PdMe(pyridine)] catalysts (Section 6.6.2), in order to investigate the effect of the methoxy group location on ethene homopolymerisation reactions (Section 6.7).

i) *Synthesis of a phosphine sulphonate* via *2-lithiation of 1-methoxy naphthalene*
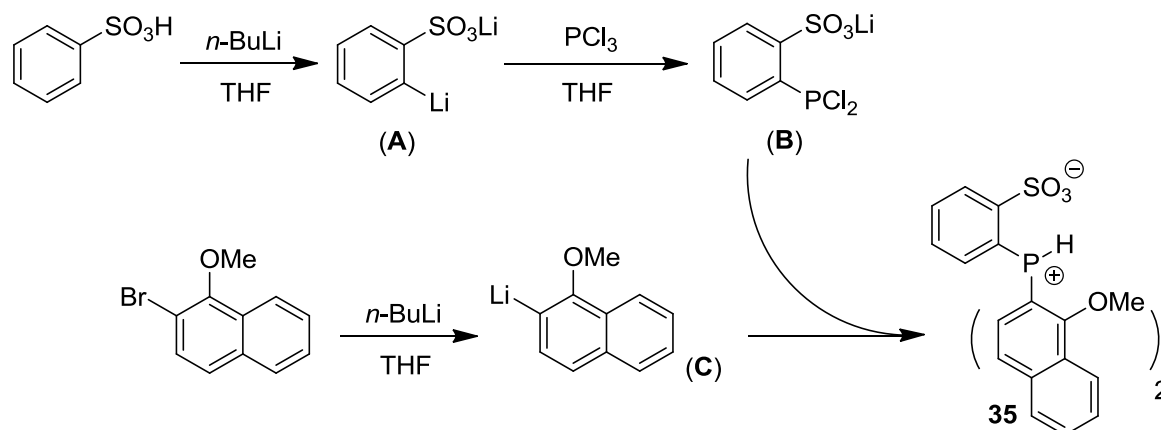
Scheme 38: *Synthesis of the phosphine sulphonate ligand* **35** via *selective lithiation of 2-bromo-1-methoxy naphthalene in 2-position.*

Synthesis of **35** was performed following the general synthetic procedure (Scheme 32) for phosphine sulphonate ligands. The lithiated aryl component (**C**) was prepared *via* halogen-metal exchange in 2-bromo-1-methoxy naphthalene. This reactant was treated at -78 °C in THF with *n*-BuLi for 45 min which gave a green solution. Subsequent reaction with the pre-formed dichlorophosphine species, formed *in situ* from lithiated benzenesulphonic acid and PCl₃, gives the phosphine sulphonate ligand **35**. Termination of the reaction with water is followed by the removal of volatiles and subsequent extraction of the solid residue with a methylene chloride/water mixture after acidification with aqueous HCl. The organic phase was dried over MgSO₄ followed by removal of the solvent *in vacuo*, giving a yellow crude product which was washed with THF, diethyl ether and pentane. Subsequent attempts to crystallise **35** were not successful. Therefore the obtained compound was analysed by multinuclear NMR spectroscopy as received.

Proton coupled and decoupled ^{31}P NMR spectra in combination to high resolution ESI MS spectrometry clearly show the presence of a phosphine sulphonate, most likely **35**, in the zwitterionic form as observed from the characteristic ^{1}J (P-H) coupling constant (for reference purposes: δ_P = -25.7 ppm, ^{1}J (P-H) = 568.1 Hz). However, this phosphine is only present with 73.1% of the total observed phosphorus content in addition to non-identified phosphorus

6. Substitution Effects in Phosphine Sulphonate Catalysts

containing species. The exact substitution pattern of the naphthalene substituents could not be determined due to impurities which prevent unambiguous assignment of the ^{1}H NMR spectrum. However the high resolution ESI MS spectrum confirms the presence of a phosphine sulphonate ligand with two methoxylated naphthalene substituents. As **35** could not be purified by crystallisation the compound was used as received for the subsequent complex formation reaction, with the intent to purify the resulting complex by crystallisation for detailed analysis.

ii) Phosphine sulphonate synthesis via *8-lithiation of 1-methoxy naphthalene*
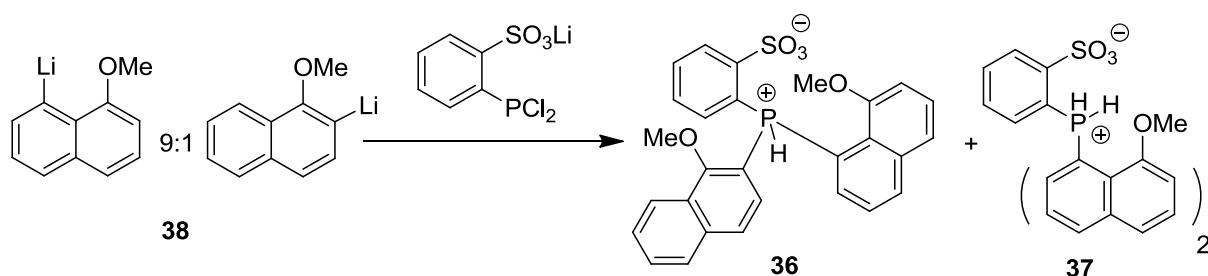
Scheme 39: *Ligand synthesis based on **38** leading to a mixture of phosphine sulphonates **36** and **37**.*

Analogous to the previous synthesis of **35** the related constitutional isomer **37** was obtained from the pre-formed 8-lithiated 1-methoxynaphthalene salt **38** (Scheme 39). As reported in the literature, lithiation of 1-methoxy-naphthalene with *t*-BuLi at room temperature predominantly leads to lithiation in 8-position. Due to the low solubility of this Li salt in pentane **38** was successfully isolated by filtration and could be purified by repeated washing with pentane (obtained mixture of 90.1 mol% 8-Li species **38** and 9.9 mol% 2-Li species). The literature-reported quantitative 8-lithiation was not obtained, attributed to a variation of the employed solvent (pentane instead of cyclohexane) as this has a large impact on the reaction selectivity.[103a]

Synthesis of the phosphine sulphonic acid based on **38** (Section 6.2) predominantly leads to formation of **37** in addition to a second species. This is the non-symmetrically substituted phosphine sulphonate **36** with methoxy groups in 1- and 8-position respective to phosphorus. For high selectivity towards **37** the controlled addition of **38** at low temperatures seems to be advantageous. The highest achieved content with 80.2 mol% **37** (determined by ^{31}P NMR spectroscopy) could be obtained by addition of a suspension of **38** in pentane at -78 °C to the

6. Substitution Effects in Phosphine Sulphonate Catalysts

solution of the pre-formed dichlorophosphine species at -78 °C. Hereby a brown suspension was obtained which was slowly solubilised with stirring at -78 °C. Afterwards the mixture was slowly warmed to room temperature and the reaction was allowed to continue for 16 h. Reaction work-up, as described above for **35**, leads to an off-white powder with from which the isolation of **37** was successful in low yields (27.6%) by crystallisation from chloroform. Subsequent analysis of **37** was performed by multinuclear and two dimensional NMR spectroscopy, high resolution ESI MS spectrometry and elemental analysis.

Analysis of the crude product mixture by ^{31}P NMR spectroscopy shows the presence of two phosphine sulphonate species, as stated above, in their zwitterionic form ($\delta_{P, 36}$ = +20.5 ppm, ^{1}J (H-P) = 663.2 Hz and $\delta_{P, 37}$ = +16.5 ppm, ^{1}J (H-P) = 674.3 Hz). Through successful isolation and subsequent complexation as well as detailed structural analysis the latter could be confirmed as **37**. The other minor species is assumed to be the chiral non-symmetrically substituted phosphine sulphonate **36**. Comparison to **35** (δ_P = -25.7 ppm, ^{1}J (P-H) = 568.1 Hz) shows an unexpected strong low field shift of phosphorus especially for **36** in the corresponding ^{31}P NMR spectra.

As reported by *Tolman*[15b] the chemical shift of phosphorus is dependent on different factors *i)* the SPS angle for the substituted phosphine, *ii)* changes of the electronegativity from the substituents and *iii)* resulting changes for the *s*-character of the phosphine lone pair. These observations also show that the basicity of a phosphine is increased by introduction of electron donating substituents. Furthermore steric restraints leading to an increased SPS angle for the substituents on phosphorus can increase the basicity of phosphines. In both cases the *s*-character of the phosphorus lone pair is increased which can often be recognised from a downfield shift in the corresponding ^{31}P NMR spectra. In general the phosphine basicity has to be considered as a complex interaction of steric and electronic effects, and for example the introduction of substituents in *ortho*-position to phosphorus introduce a strong high field shift due to steric reasons.[105] Reports show that instead of the chemical shift, the coupling constants for phosphines with hetero atoms such as ^{77}Se or ^{1}H represent a more suitable concept for the comparison of phosphine basicity. In many cases linear correlations of the substituent electro negativity or the phosphine basicity to the value of the coupling constants are described. *Tolman*[15b] describes a decreasing ^{1}J (P-H) coupling constant for protonated phosphines with increasing basicity.

With respect to ligands **35-37** it can be reasoned, that the observed upfield shift of **36** in the corresponding ^{31}P NMR spectrum is a result of steric effects from the substituent pattern

6. Substitution Effects in Phosphine Sulphonate Catalysts

(δ_P = -25.7 (**35**), +20.5 (**36**), +16.5 (**37**) ppm). Direct comparison of the ^1J (H-P) coupling constants for these zwitterionic phosphines shows a decreasing basicity in the row **35**, **36** to **37** as expected due to the altered substitution pattern and reduced electron donating ability of methoxy groups in 8-position of the naphthalene substituents (^1J (H-P) = 568.1 (**35**), 663.2 (**36**) 674.3 (**37**) Hz). However, it has to be noted that the structure of **35** and **36**, with the exact location of the methoxy functionalities, could not be unambiguously determined.

As stated above, the novel phosphine sulphonate ligand **37** could be isolated by crystallisation from chloroform and its structure was analysed by a combination of NMR spectroscopy, elemental analysis and high resolution ESI MS spectrometry. This unambiguously confirmed the structure of this ligand as shown in Scheme 39. Detailed analysis by ^{1}H NMR spectroscopy clearly shows presence of two non-equivalent methoxylated functionalised naphthalene substituents. This has been recognised from the distinct 0.67 ppm shift of the separated signals for the non-equivalent methoxy groups as well as from the complex signal pattern observed in the aromatic region. Therefore this behaviour was attributed to a chiral conformation of the zwitterionic structure in solution. Investigation of the ligand structure by two dimensional NMR spectroscopy confirmed the location of both methoxy groups in 8-position respective to phosphorus. Also the four distinguishable spin systems of the naphthalene substituents, with three proton signals each, could be identified. Additionally the spin system of the sulphonated phenyl substituent with four proton signals was observed. All peaks were assigned by careful interpretation of the 2D COSY, NOESY, TOCSY, HMBC and HSQC spectra. The non-equivalent configuration is attributed to two distinct arrangements of the naphthalene substituents in relation to the protonated phosphorus. Therefore rotation has to be hindered due to the steric bulk of the ligands. Figure 36 and Figure 37 show the labelled structure of **37** together with the ^{1}H NMR, COSY and TOCSY NMR spectra which were employed for the complete characterisation of all observed peaks.
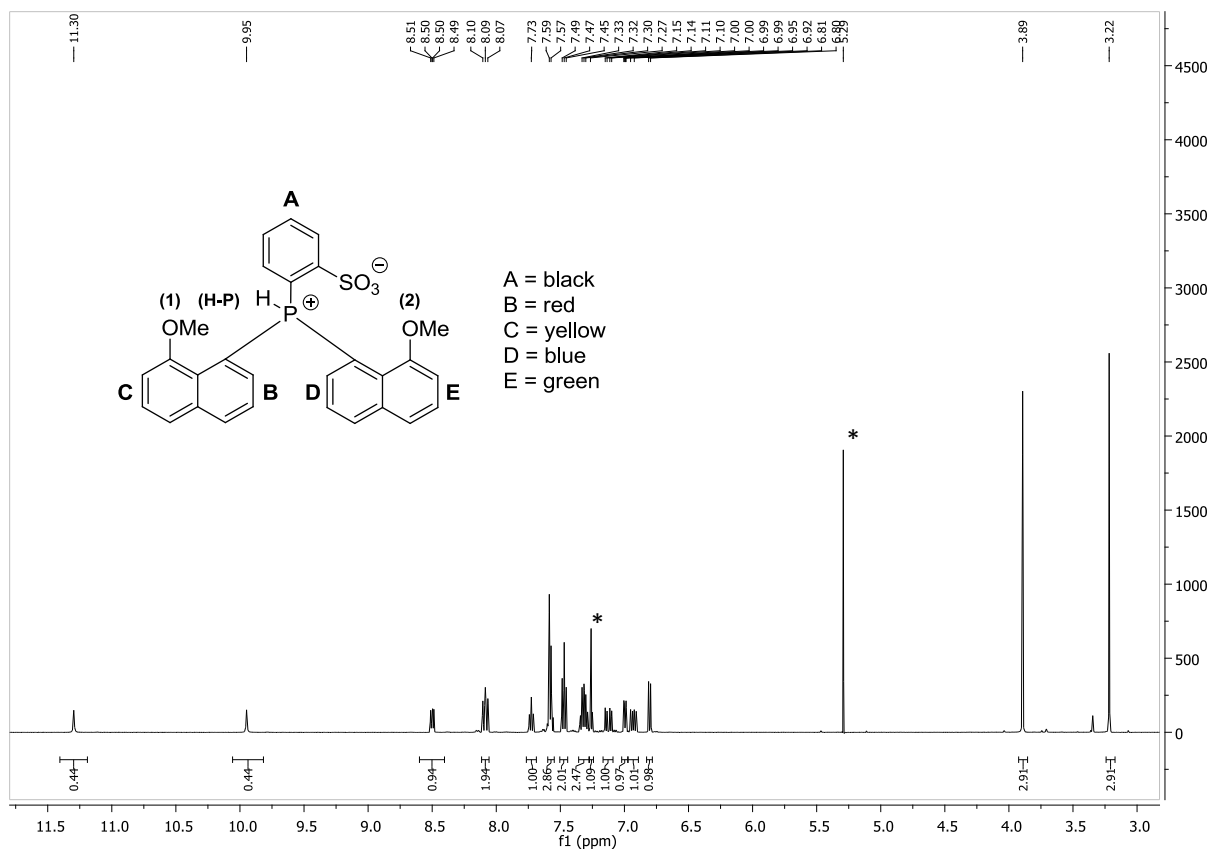
Figure 36: *¹H NMR spectrum and structure of phosphine sulphonate* **37**. *Colour labelling detailed for identification and assignment of spin systems and proton signals by the COSY and TOCSY NMR spectra displayed in* Figure 37.
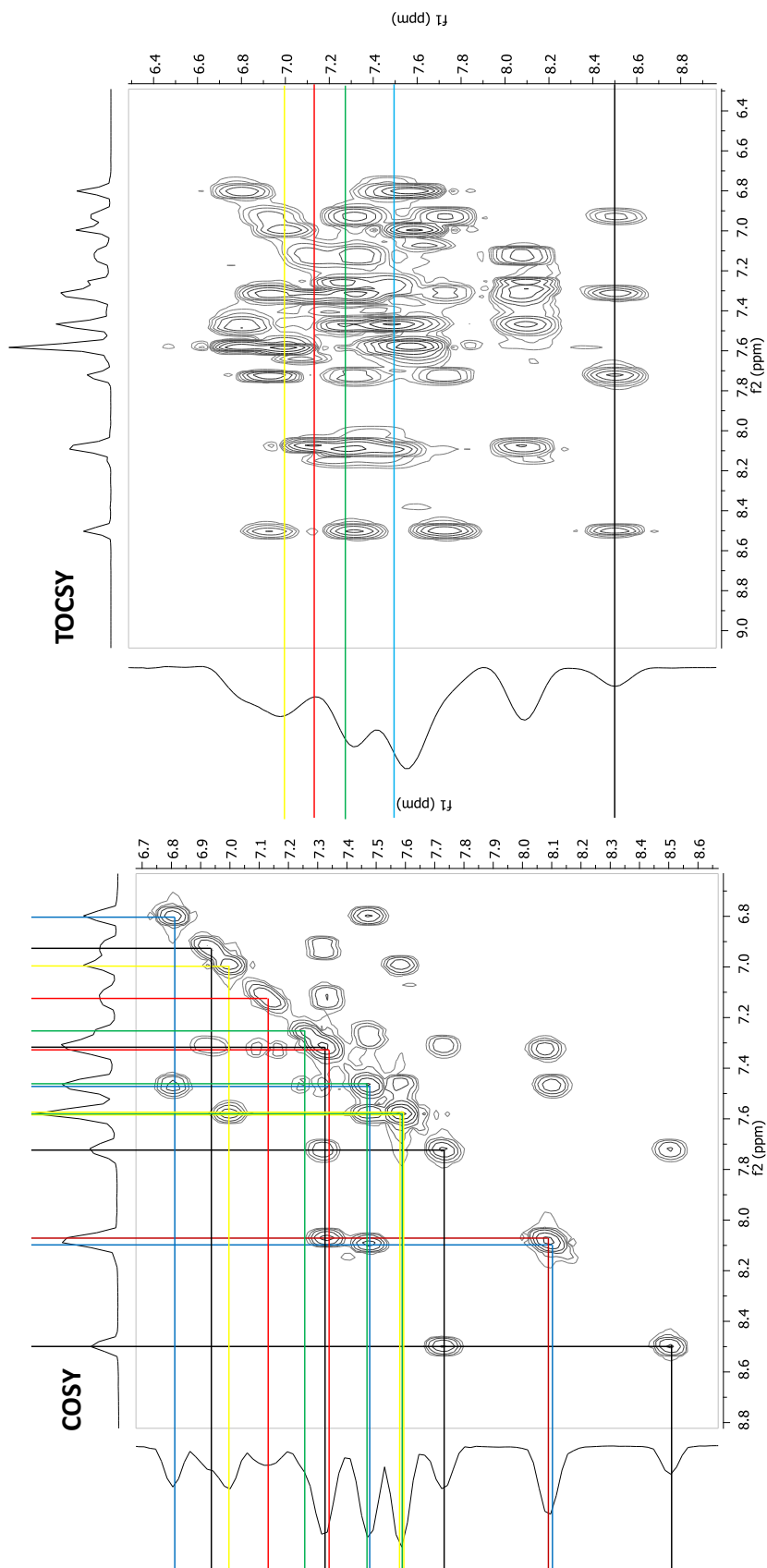
Figure 37: *Schematic assignment of spin systems and peaks for **37** by COSY and TOCSY NMR spectroscopy, labelling and ligand structure given in* Figure 36.

6. Substitution Effects in Phosphine Sulphonate Catalysts

6.6.2. Synthesis and characterisation of neutral [{κ²-(P,O)-phosphine sulphonate}PdMe(pyridine)] complexes with methoxylated naphthalene substituents

Formation of [{κ²-(P,O)-phosphine sulphonate}PdMe(pyridine)] complexes with the synthesised zwitterionic phosphine sulphonate salts **35** and **37** (Section 6.6.1) were performed following the procedure detailed above (Section 6.2 and Scheme 33). Subsequent analysis of the reactions of these ligands with (tmeda)PdMe₂ and pyridine indicates successful formation of the catalysts **39** and **40**, respectively. However, crystallisation of **39** was not achieved and this compound is therefore disregarded for polymerisation reactions.

Synthesis of **40** was performed by reaction of **37** with (tmeda)PdMe₂ and pyridine. Precipitation of the complex from methylene chloride solution by addition of pentane followed by crystallisation of the isolated off-white powder from chloroform/pentane mixtures affords **40** in moderate yields (52.5%) (Scheme 40).
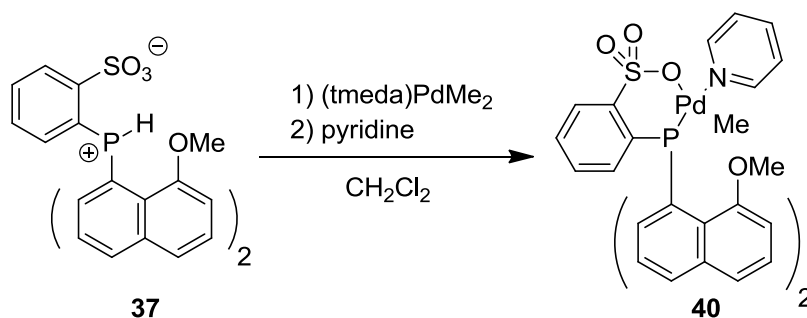
Scheme 40: *Synthesis of the neutral phosphine sulphonate catalyst **40**.*

The novel neutral phosphine sulphonate complex **40** could be successfully characterised by multinuclear 1D and 2D NMR spectroscopy, elemental analysis and X-ray diffraction. Coordination of the ligand to Pd(II) can be observed from the single phosphorus signal in the ^{31}P NMR spectrum of **40** and the coordination shift in comparison to the parent ligand **37** ($\delta_{P,37}$ = +16.5 ppm, $\delta_{P,40}$ = +47.0 ppm). Furthermore the relatively broad peak indicates the presence of a dynamic process on the NMR timescale, probably due to a wagging of the ligand substituents. Similar to the parent ligand **37** the corresponding complex **40** shows a chiral conformation in the solid state as well as in solution. For instance the well resolved ^{1}H NMR spectrum shows the spectroscopic difference of both naphthalene substituents in solution. In consequence of these different alignments for the naphthalene substituents, the

corresponding peaks in the ^{1}H as well as the ^{13}C NMR spectra are split and shifted respective to each other. By assistance of 2D NMR spectroscopy (COSY, TOCSY, NOESY, HMBC, HSQC) all proton signals as well as the primary and tertiary carbon atoms could be definitely assigned to the ligand structure. However, due to overlapping peaks not all quaternary carbon signals could be identified and assigned in the ^{13}C NMR spectrum. The COSY and TOCSY NMR spectra are shown in Figure 39, together with the ^{1}H NMR spectrum with the assignment and labelling of the observed spin systems in Figure 38. Nevertheless the qualitative analysis is supported by elemental analysis which shows presence of **40** in addition to minor amounts of CHCl$_3$ (CHCl$_3$ observed by ^{1}H NMR spectroscopy) and the molecular structure determined by X-Ray diffraction (Figure 42).
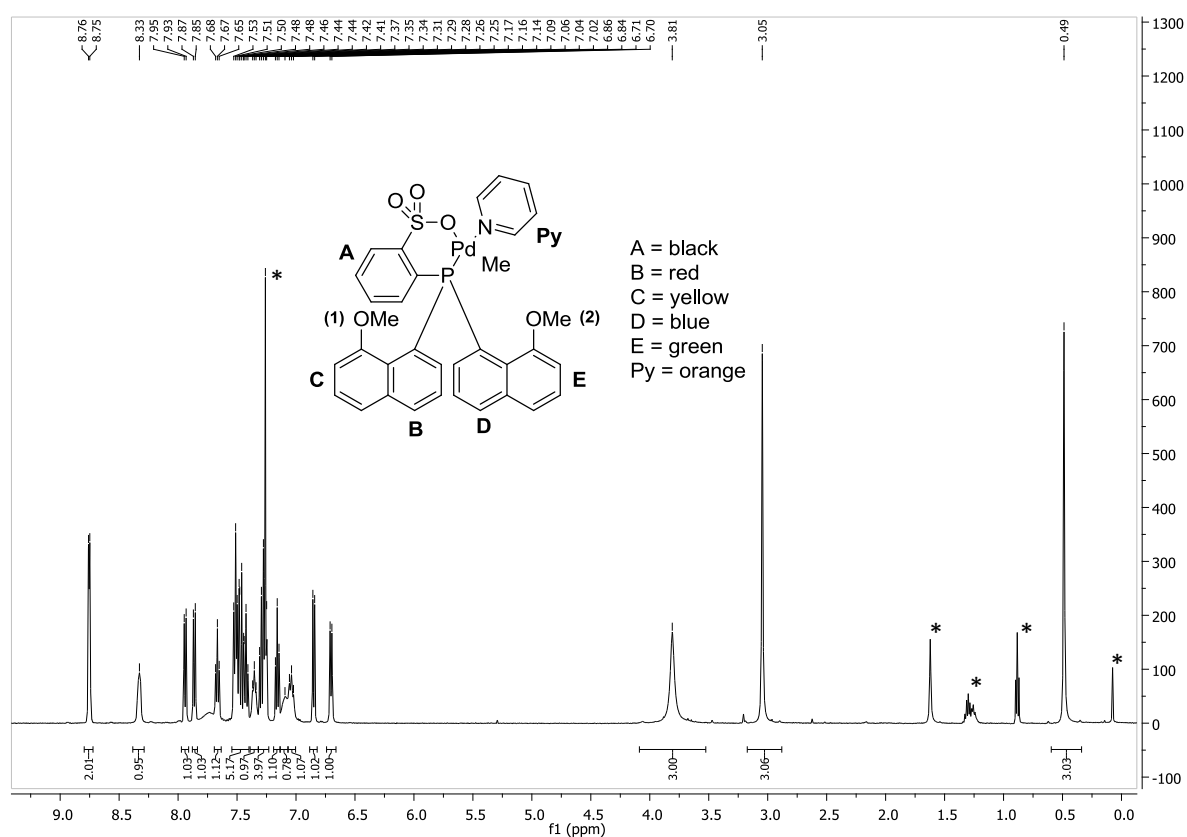
Figure 38: *^{1}H NMR spectrum and structure of the neutral phosphine sulphonate catalyst **40**. Colour labelling detailed for identification and assignment of spin systems and proton signals by COSY and TOCSY NMR (*Figure 39*), the NOESY NMR spectrum of **40** is displayed in Figure 40.*
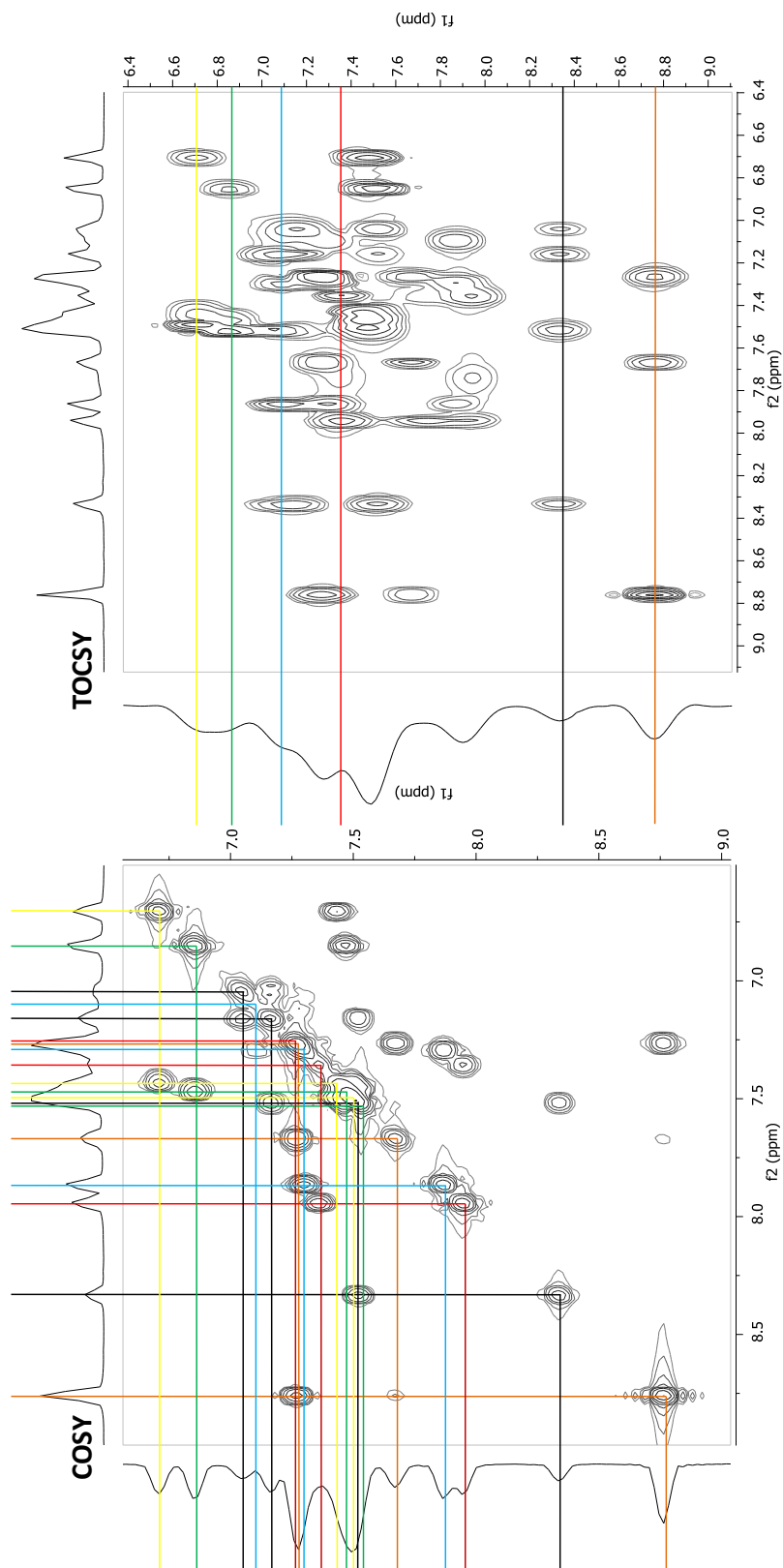
Figure 39: *Schematic assigntion of spin systems and peaks for **40** by COSY and TOCSY NMR spectroscopy, labelling displayed in* Figure 38.
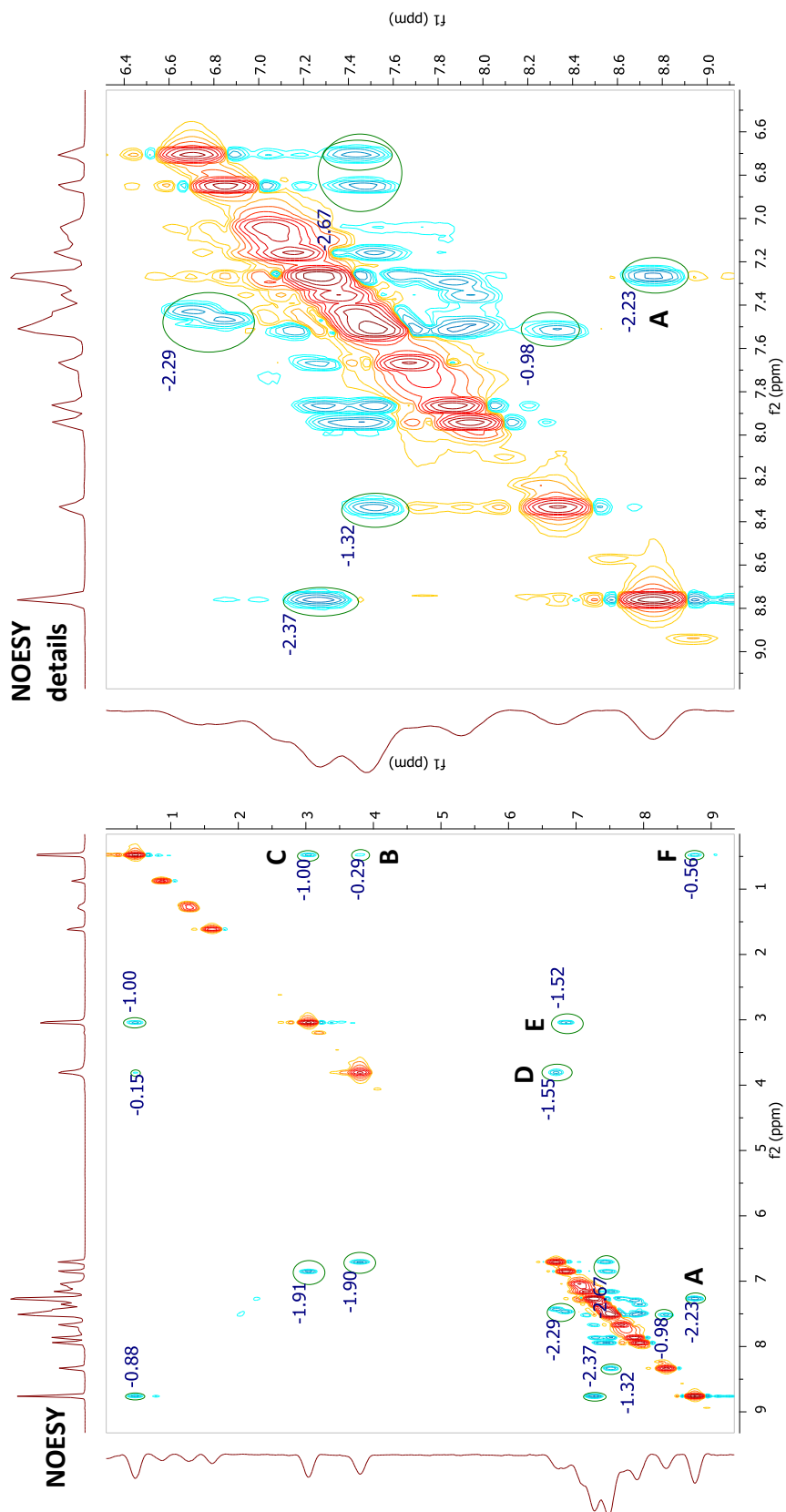
Figure 40: *NOESY spectrum of complex **40** together with the expansion of the aromatic region. The assignment of the NOESY crosspeaks is displayed in* Figure 41.

6. Substitution Effects in Phosphine Sulphonate Catalysts

Due to observation of several relevant crosspeaks in the NOESY NMR spectrum of **40**, which could be assigned to spatial interactions of groups in the complex coordination environment with the ligand, the solution structure of this compound was analysed (Section 6.3). The spatial interaction of the pyridine *ortho*- and *meta*-hydrogen atoms was employed as the reference signal for the distance determination in solution *via* integration of NOESY NMR crosspeaks. This reference value was obtained from the molecular structure of **40** (Figure 42) compared to literature references (Section 6.3).

Figure 40 shows the NOESY NMR spectrum of **40** together with the enlarged aromatic region. Assignment of the observed spatial H-H relations is displayed in Figure 41, in comparison to Figure 40. Distance determination for inter space H-H relations was carried out by Equation 3 (Section 6.3). Table 8 lists the aproximated proton distances compared to distances determined from the molecular structure of **40**.
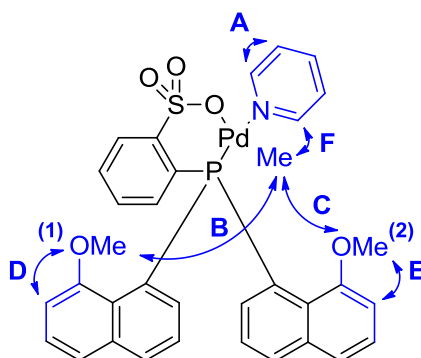
Figure 41: *Labelling (blue) of the nOe relations for assignment of the crosspeaks observed in the NOESY spectrum of 40 displayed in* Figure 40.

Table 8: Comparison of the solution proton distances determined by the NOESY signals for different H-H relations with values obtained from the molecular structure of **40**.

relation x[1]	V_x (f1)[2]	V_x (f2)[2]	d_x (nOe, f1) / Å[3]	d_x (nOe, f2) / Å[3]	d_x (average) / Å[4]	d_x (mol. struc.) / Å[5]
A	2.37	2.23	reference	reference	reference	2.31
B	0.15	0.29	3.7	3.2	3.4	2.4
C	1.00	1.00	2.7	2.6	2.7	2.3
D	1.90	1.55	2.4	2.5	2.4	2.3
E	1.91	1.52	2.4	2.5	2.4	3.0
F	0.88	0.56	2.7	2.9	2.8	2.5

[1]nOe relation as defined in Figure 41, [2]nOe integral in f1 and f2 direction, [3]distance d_x for f1 and f2 direction, [4]average distance from f1 and f2, [5]determined from the molecular structure.

6. Substitution Effects in Phosphine Sulphonate Catalysts

The determined H-H distances for the complex **40** in solution show relatively close contact of the methoxylated naphthalene substituents with ligands at the palladium coordination centre of the complex. No interactions of a proton *ortho* to phosphorus on the naphthalene substituents can be observed with either the Pd-Me or the pyridine protons. In contrast to complex **4** this shows a relatively constrained structure of **40** in solution where both methoxy functionalities are directed towards palladium. This assignment is based on the H-H relations **B** and **C** of the OMe functionalities with the Pd-Me group. The OMe(1) functionality, which shows a slightly broadened peak indicating some flexibility, is slightly further (d_B = 3.4 Å) away from the Pd-Me group compared to the OMe(2) functionality with (d_C = 2.7 Å). The latter also shows a sharp signal which indicates stabilisation from the Pd-centre, reducing wagging motions of the OMe(2)-functionality and corresponding naphthalene substituent in solution. Relations **D** and **E** were employed to assign the methoxy functionalities to their corresponding naphthalene systems in the structural analysis of the phosphine sulphonate ligands by NMR spectroscopy. Finally the H-H interaction **F** represents the distance of the Pd-Me group from the pyridine H-atoms. With 2.8 Å this value is slightly larger than the values for **4** (2.7 Å) and **34** (2.4 Å) and is attributed to a more twisted configuration of the pyridine ligand in the near square planar coordination environment at palladium as seen in Figure 42.

Single crystals of **40**, suitable for the determination of the molecular structure by X-Ray diffraction, were obtained from chloroform/pentane mixtures. Figure 42 shows the preliminary ORTEP plot of the molecular structure of **40**. The obtained H-H distances (Table 8) are compared to the corresponding values from analysis of the solution structure which clearly confirms a resemblance of the present solution- and the solid state-structures of **40**. Comparison also explains the observed broadened NMR signal for the OMe(1) functionality. This, as well as the longer Pd-OMe(1) distance obtained from the molecular structure, indicate an increased dynamic behaviour of this group which results in a waging motion in solution. In contrast the signal for the OMe(2) group is a sharp singlet which confirms a relatively fixed position with respect to the palladium centre. Analysis of the molecular structure shows, that the close contact of the OMe(2) group to the palladium atom and to the Pd-methyl group leads to a significant distortion of the corresponding naphthalene substituent. This behaviour can be either explained by the steric hindrance from the large naphthalene substituents or a Pd-O interaction which forces the ligand substituents in a relatively

constrained conformation. Especially the space filling model for the molecular structures of **4** and **40** indicate a more pronounced Pd-O interaction for complex **40**. In general, the slightly increased deviations of the H-H distances in solution from the solid state are attributed to the observed steric hindrance which favours a slight distortion of the molecule from the solid state structure in solution. Free rotation of the functionalised naphthalene substituents is hindered for complex **40**. Despite the steric bulk of the phosphine sulphonate ligand near the palladium centre the axial positions show an unexpected accessibility of the metal atom. The resulting effect of the complex structure on the ethene homopolymerisation reaction is detailed in Section 6.7.
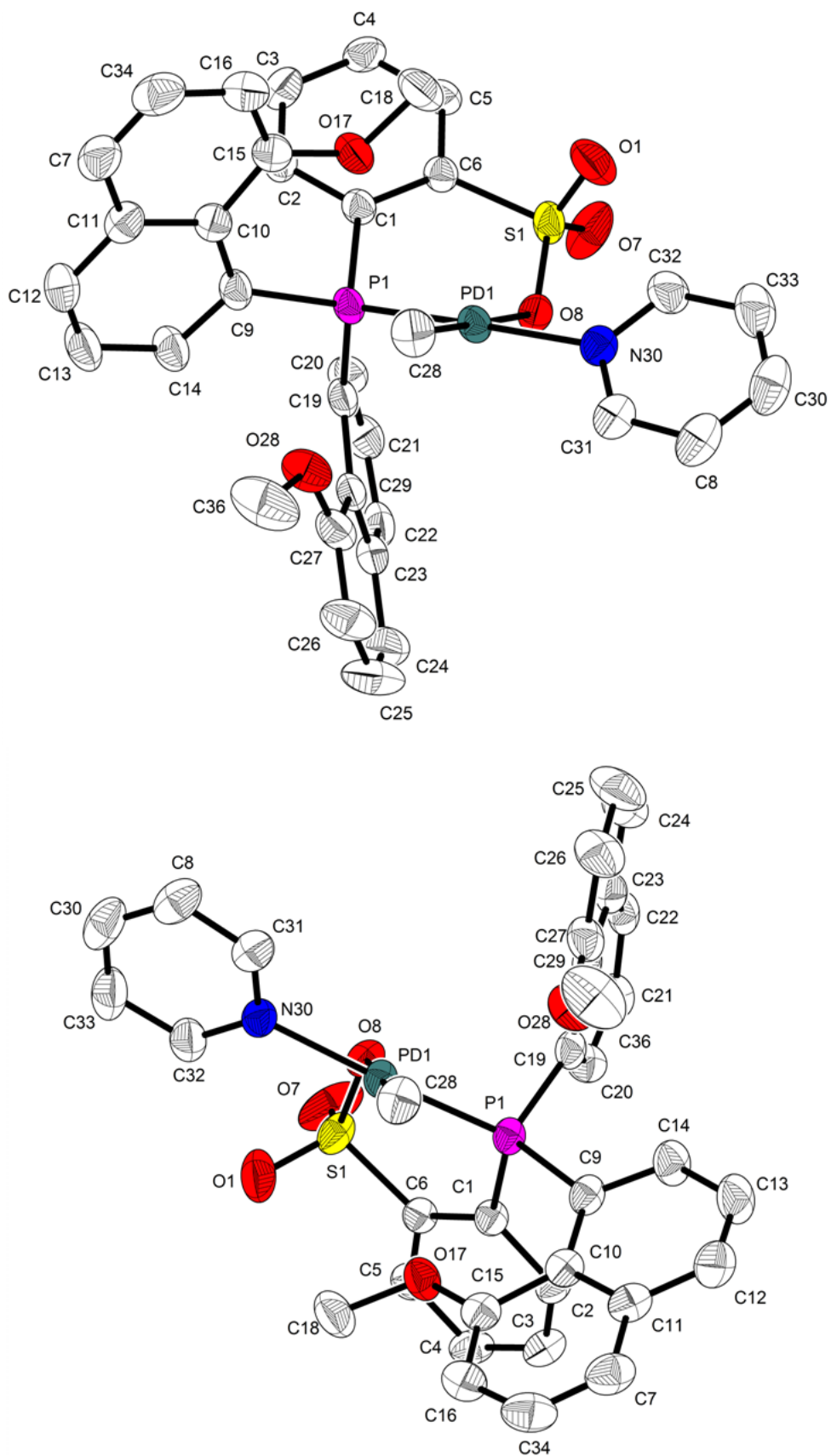
Figure 42: *Preliminary ORTEP plot of the molecular structure of **40**, the displacement ellipsoids are at the 50% probability level. Two view directions shown.*

6. Substitution Effects in Phosphine Sulphonate Catalysts
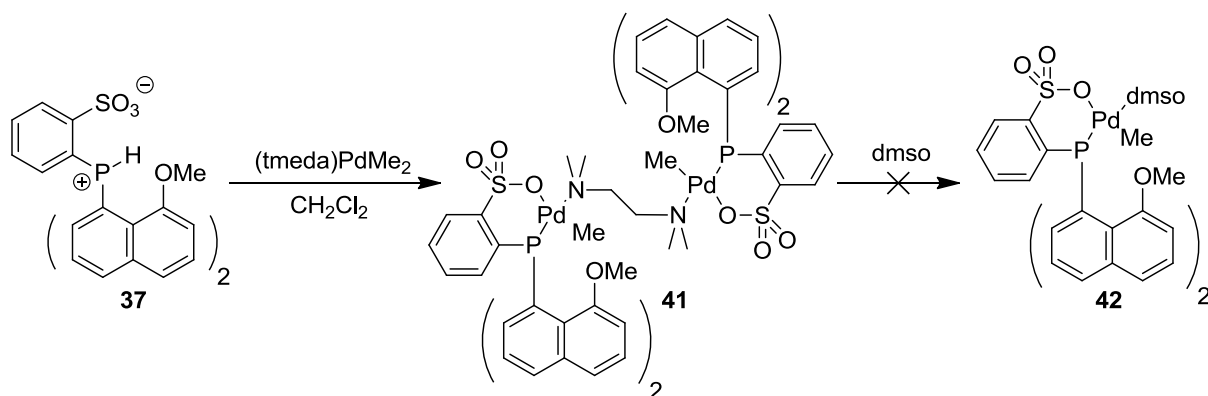
Scheme 41: *Attempted synthesis of the dmso stabilised complex 42 leading to the dimeric tmeda-bridged 41*.

Due to the reported observation that replacement of the stabilising pyridine base with the weaker coordinating dmso ligand can increase the polymerisation activity of catalyst **4**,[48] a similar reaction was also tested with the novel phosphine sulphonate **37**. In the test reaction the ligand **37** was reacted with (tmeda)PdMe$_2$ in methylene chloride solution, followed by addition of dmso (excess). After precipitation of a reaction product by addition of diethyl ether and recrystallisation of the off-white solid from chloroform/pentane the dimeric complex **41** instead of the dmso adduct **42** was observed (Scheme 41). **41** demonstrates limited solubility in chloroform which prevents analysis by ^{13}C NMR spectroscopy. ^{1}H and ^{31}P NMR spectroscopy of the compound is supported by elemental analysis and determination of the molecular structure by X-ray diffraction. However due to the relatively low polymerisation activity (Section 6.7) of **40**, compared to **4**, repeated attempts to introduce dmso as the stabilising ligand were not performed. Single crystals for determination of the molecular structure of **41** (Figure 43) could be obtained from chloroform/pentane solution.
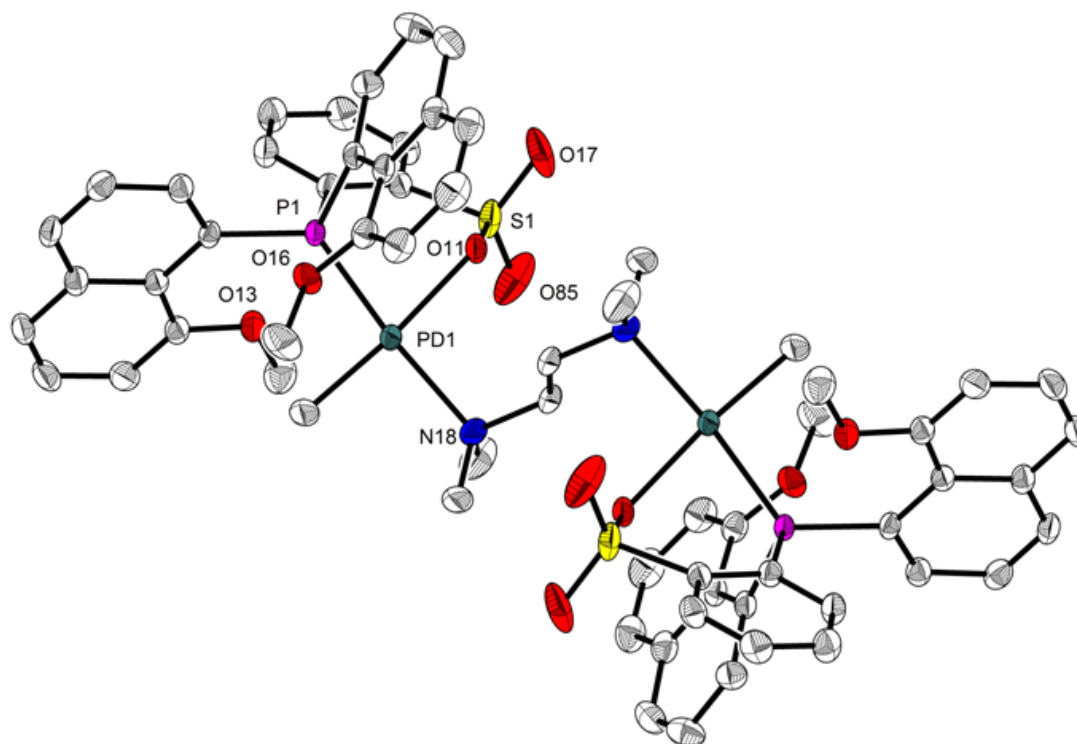
Figure 43: *Preliminary ORTEP plot of the molecular structure of **41**, the displacement ellipsoids are at the 50% probability level.*

6.7. Ethene homopolymerisation as test reaction for the determination of substitution effects on the catalyst structure/activity relation

The previously described novel neutral pyridine-stabilised [{κ^2-(P,O)-phosphine sulphonate}PdMe(pyridine)] complexes **34** and **40** were tested in ethene homopolymerisation reactions under varying conditions. Comparison with literature known reference catalysts such as **4** (Figure 44) or **6** (Figure 7, Section 3.2.2) could provide further insights into the structure/activity relation of neutral pyridine-stabilised phosphine sulphonate-based Pd(II) catalysts. An additional test reaction was performed for the tmeda-bridged dimeric neutral complex **41** (Scheme 41). As these catalysts are single component catalysts no further activation is required. Obtained PE samples were characterised by high temperature NMR spectroscopy, GPC and DSC for the determination of the polymer architecture and properties and the identification of general trends which can be assigned to the complex structure. Table 9 lists the obtained results for ethene homopolymerisation reactions with catalysts **4**, **34**, **40** and **41**.

118

6. Substitution Effects in Phosphine Sulphonate Catalysts
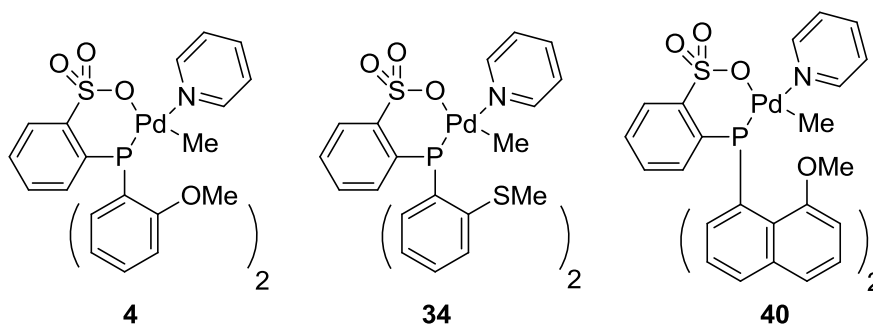
Figure 44: *Overview of neutral pyridine coordinated phosphine sulphonate-based Pd(II) complexes compared in ethene olefin polymerisation reactions.*

i) Investigation of methoxylated naphthalene-based phosphine sulphonate catalysts in ethene homopolymerisation

Data from the performed polymerisation reactions with the methoxylated naphthalene-based catalyst **40** (Table 9, Entries 1-8) show a relatively low polymerisation activity in comparison to **4** and literature reports on related catalysts. This is combined with an unexpected reduction of the PE molecular weights leading to a M_w of approximately 1000 g·mol^{-1}. As this is on the lower detection limit of the GPC instrument, the low molecular weights were also confirmed by high temperature NMR spectroscopy. Additionally these NMR spectroscopic experiments were employed for the examination of the PE microstructure. ^{1}H NMR spectroscopy shows a complete internalisation of the olefinic species, created by chain termination *via β*-hydride elimination and subsequent olefin exchange, for experiments performed up to 80 °C. Increase of the polymerisation temperature to 100 °C leads to a change of the catalyst behaviour, as indicated from a decreased degree of olefin internalisation and formation of a second medium molecular weight PE fraction (Table 9, Entries 3-4).

In general, high degrees of internal olefins (~70 %) have been previously reported, but only presence of 1- to 3-olefins could be observed, which are formed by a chain walking mechanism.[41] In the present case, for PE formation with catalyst **40**, the observed polymer microstructure is significantly different. A majority of +3-olefins can be determined by ^{13}C NMR spectroscopy (Figure 45) and, as no internal branches were observed by ^{1}H NMR spectroscopy a completely linear PE backbone is present.[41] The ethene pressure has apparently no significant influence on the observed molecular weight and the degree of olefin internalisation (Table 9, Entries 2, 5-6) at the applied conditions.

119

6. Substitution Effects in Phosphine Sulphonate Catalysts

Table 9: *Comparison of the ethene homopolymerisation reactions with the neutral phosphine sulphonate-based Pd(II) catalysts 4, 34, 40 and 41.*

Entry[1]	cat.	$n_{Cat.}$ (μmol)	T (°C)	p (bar)	t (h)	yield (g)	Activity[2]	M_w[3]	PDI[3]	T_m (°C)[6]	M_n (NMR)[8]	% int.[9]
1	**40**	10	50	5	2	0.28	2.8	1.8	2.2	117[7]	1.29	100
2	**40**	10	80	5	2	0.64	6.4	0.8	1.6	105[7]	0.79	100
3	**40**	10	100	5	2	0.65	6.5	0.6[4]	1.5	111[7]	0.97	94.3
4	**40**	10	100	10	2	0.88	4.4	0.7[4]	1.7	115[7]	1.00	85.5
5	**40**	10	80	10	2	2.33	12	0.9	2.2	109[7]	1.00	100
6	**40**	10	80	20	2	2.49	6.2	0.9	2.0	110[7]	0.95	100
7	**40**	10	80	5	4	4.09	21	0.9	1.8	107[7]	0.95	100
8	**40**	10	80	5	16	4.48	5.6	0.8	1.8	105[7]	0.98	90.4
9	**41**	5	80	5	2	0.78	7.8	1.7	3.6	106[7]	1.03	100
10	**34**	10	50	20	20	0.07	0.02	700[5]	6.3[5]	133	n.d.	n.d.
11	**34**	10	80	20	20	0.10	0.03	450[5]	3.9[5]	135	n.d.	n.d.
12	**4**	10	50	20	2	0.70	1.8	33	1.7	131	n.d.	n.d.
13	**4**	5	100	5	2	1.64	33	13	1.9	127	n.d.	n.d.

[1]200 mL stainless steel reactor, 30 mL toluene; [2]in $kg_{polymer} \cdot g_{palladium}^{-1} \cdot bar_{ethene}^{-1} \cdot h^{-1}$; [3]determined by GPC, RI; [4]bimodal distribution observed with minor amounts of higher molecular weight fractions, Entries 3 and 4: $56 \cdot 10^3$ and $79 \cdot 10^3$, respectively; [5]determined by GPC, multi detection; [6]determined by DSC, 2nd heating cycle; [7]broad undistinguished melting area; [8]determined by ^{1}H NMR spectroscopy at 120 °C in $C_2D_2Cl_4$, no branching observed; n.d. = not determined.
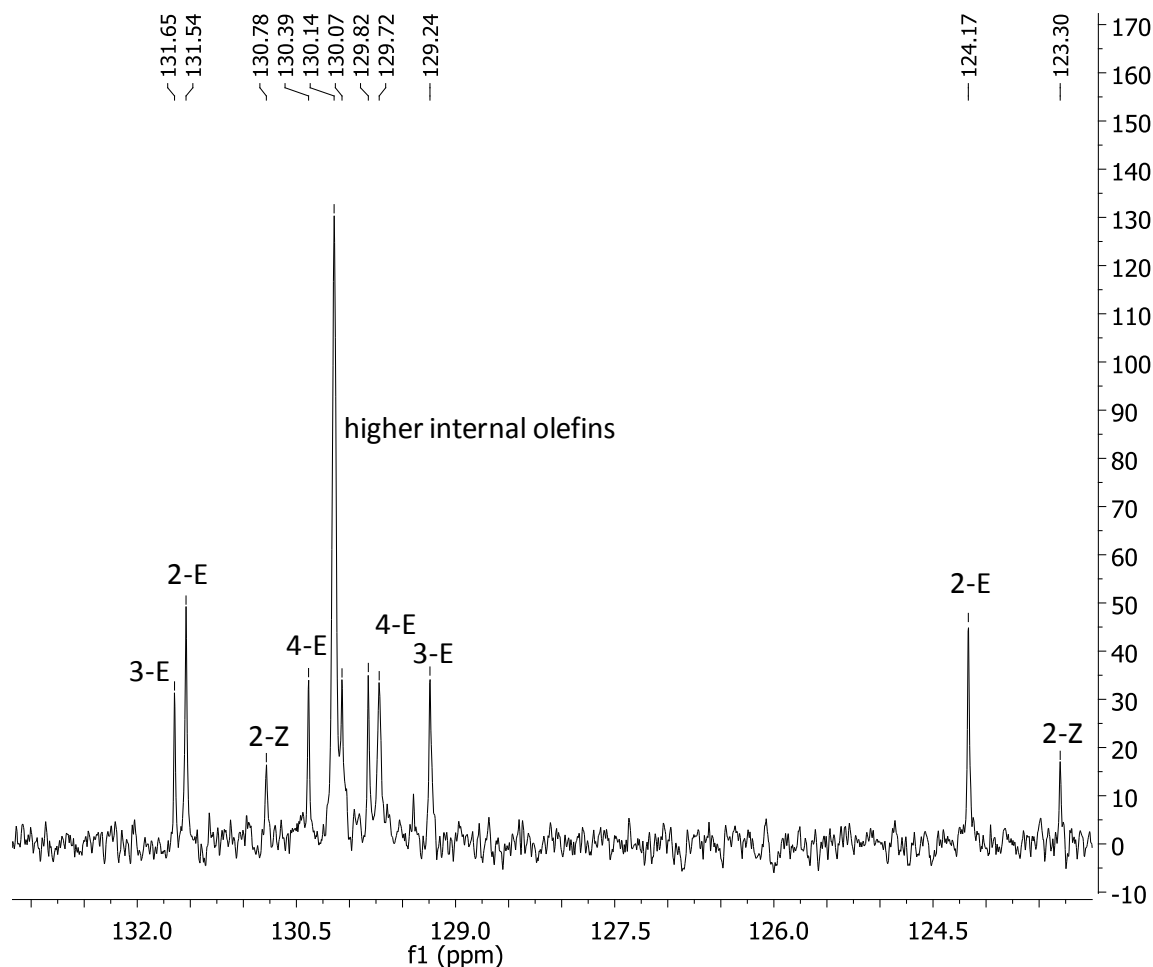
Figure 45 *Olefinic region of the low molecular weight PE sample from* Table 9, Entry 2.

In general these experiments show a significantly increased chain walking, which means a series of *β*-hydride elimination, reorientation of the formed olefin and reinsertion steps, with the present catalyst **40**. Hereby the high linearity of the polymer chain, a characteristic feature of the phosphine sulphonate Pd(II) catalyst system, is retained. This is unusual in comparison with other late transition metal-based catalyst systems, such as for example the *α*-diimine Pd(II) complexes and was previously attributed to energetic differences of the corresponding transition states.[35] The present observations confirm the clearly disfavoured migratory insertion reaction of secondary alkyl groups within this system. Due to the complete linearity of obtained PE the pronounced chain walking leads to a series of intermediates which trap the polymer chain in a non reactive state until chain walking reaches one polymer chain end and reduces the apparent polymerisation activity. Chain termination occurs by olefin exchange towards ethene and leads to low molecular weight, an observation which is in line with the proposed associative olefin exchange for phosphine sulphonate-based Pd(II) catalysts.[45, 106]

6. Substitution Effects in Phosphine Sulphonate Catalysts

A test experiment for the κ-(N,N')-tmeda-bridged bimetallic complex **41** shows a similar behaviour albeit the slightly increased molecular weights are attributed to the different coordination behaviour of the tmeda base.

Based on these observations the molecular structure of **40**, in comparison to **4** and **6**, was examined for the interpretation of these results, especially of the high degree of chain walking. The major observed difference for these complexes is the significantly decreased steric protection of the axial positions at the palladium centre of **40**. Furthermore the ligand substituents show a relatively rigid conformation which results in an opened coordination sphere facilitating the arrangement of the growing polymer chain. In comparison, the molecular structure of **4** shows protection of one axial position from the aryl functionality by the close contact of the proton in 6-position of one aryl substituent at phosphorus to the Pd centre (Section 6.1 and 6.3).[80] Even more pronounced is the protection of the axial positions in the related complex **6** which produces high molecular weight PE at high catalyst activities. A very recent report on a phosphine sulphonate-Ni(II) system related to **6** shows that protection of one axial position of the metal centre is required to significantly increase the obtained PE molecular weights.[107] Especially the space filling model of the molecular structure shows the accessibility of the axial positions in complex **40**. Thus in comparison with other reported molecular structures of phosphine sulphonate-based catalysts the environment of complex **40** provides more space for the polymer chain alignment and orientation which clearly favours chain walking. With respect to this consideration occurrence of mainly 1- to 3-olefins, for catalysts related to **4**, can be interpreted as the result of a steric hindrance which does not allow formation of internal +3-olefinic species. Therefore chain walking in **4** seems to be restricted to a small area of the polymer chain.

Additional investigations on the PE formation with catalyst **4**, which were reported recently by *Claverie et al.*[45], show that, due to the strongly coordinating pyridine base, the concentration of ethene coordinated species under reaction conditions is low. Furthermore, coordination of ethene has a high probability for a migratory insertion event (~ 30%) which shows that the pyridine replacement by ethylene is a major rate limiting step.

Especially in context of the present results, highlighting the important role of chain walking with catalyst **40**, the formation of internalised olefin intermediates which are not available for chain growth has to be considered as a general limitation for the phosphine sulphonate system. The pronounced steric hindrance of catalyst **6** with a resulting high catalyst activity and the formation of high molecular weight PE might support this assumption

due to a even more hindered chain walking which does not lead to the formation of apparently dormant internal olefinic species.[46] Unfortunately the polymer microstructure for the obtained PE with 4[46] as well as the low molecular weight PE obtained (molecular weight ~ 3-10·10³ g·mol⁻¹) with related catalysts[47] is not described in the literature for comparison validating these assumptions.

ii) Investigation of thioether-functionalised phosphine sulphonate-based catalysts in the

ethene homopolymerisation reaction

In contrast the methyl thioether-functionalised catalyst **34** displays only minimal polymerisation activity even at long reaction times and high ethene pressures. However, this is combined with a significant increase of the obtained PE molecular weight (Table 9, Entries 10-11) in comparison to a reference experiment with the catalyst **4** (Table 9, Entry 12). It was also observed that an increase of the polymerisation temperature leads to decreased obtained molecular weights by facilitated chain termination. Due to the established decomposition reaction at higher temperatures (at least in absence of olefins) the polymerisation reaction was performed at temperatures which do not exceed 80 °C.

With respect to the general consensus on the phosphine sulphonate-based Pd(II) polymerisation mechanism (Section 3.2.2) these observations for **34** are attributed to changes for the relevant transition states in comparison to **4**. As chain growth and chain termination require similar intermediate states for the essential *cis-trans* isomerisation[35], increased transition state energies would affect their relative ratio as well as their rate. Thus the introduction of methyl thioether functionalities apparently decreases the overall *cis-trans* isomerisation rate. Therefore the polymerisation activity is significantly reduced and formation of linear high molecular weight PE is promoted. As an origin for the observed catalyst behaviour the proposed Pd-S interactions (Section 6.4) have to be considered. However, this could not be directly observed an is based on the interpretation of performed experiments

6. Substitution Effects in Phosphine Sulphonate Catalysts

7. Summary

Olefin co- or homo-polymerisation reactions *via* a coordination-insertion type mechanism in presence of polar-functionalised olefins are highly attractive as the catalyst structure can permit significant control over the reaction. These possible influences concern not only the polymerisation activity but also the olefin insertion regio- or stereo-selectivity. Therefore catalyst design can provide an excellent means to customise polymer properties. However, introduction of functional groups *via* a coordination-insertion type polymerisation mechanism is highly challenging due to the reaction of Lewis basic functional groups of the olefins with the Lewis acidic metal centres. Strong or even irreversible coordination can either hamper or prevent catalyst activity, respectively. Here neutral late transition metal-based polymerisation catalysts, specifically the phosphine sulphonate-based Pd(II) catalyst system, show exceptional functional group tolerance in copolymerisation reactions of ethene and polar-functionalised olefins due to their lower Lewis basicity.
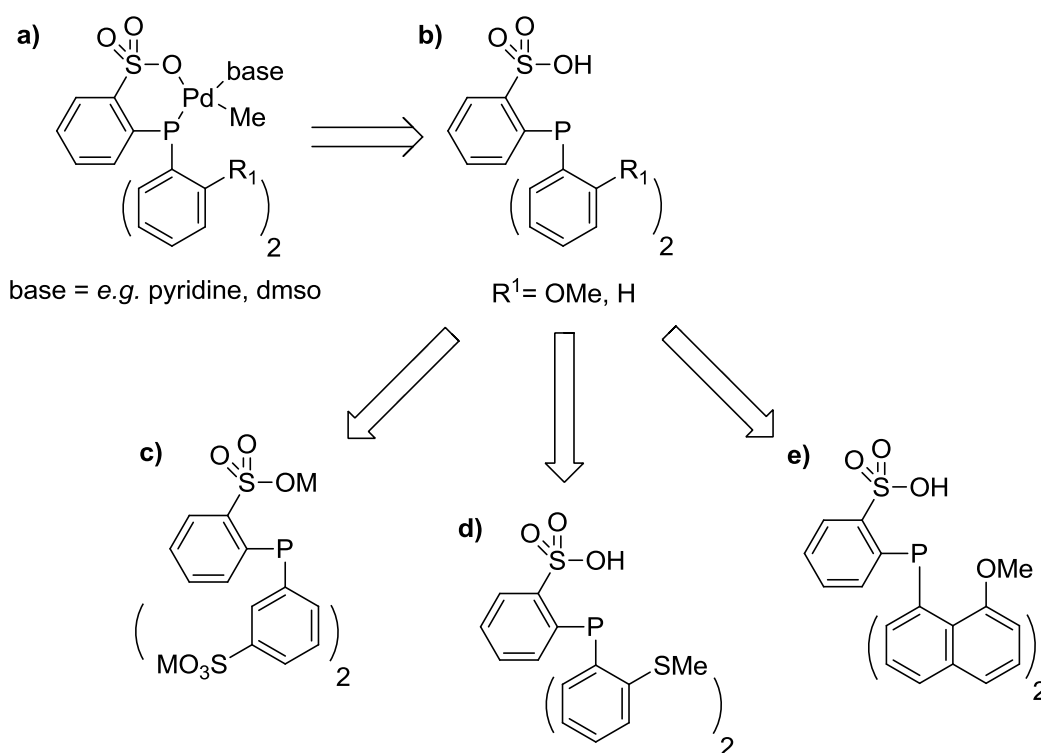
Figure 46: *Schematic depiction of the a) [{κ-(P,O)-phosphine sulphonate}PdMe(base)] catalyst system and presentation of performed modifications for the b) phosphine sulphonic acid ligand system: c) Introduction of anionic functionalities by sulphonation; investigation of functional group modification d) introduction of a methyl thioether functionality, e) position change of the OMe group on a naphthalene substituent.*

7. Summary

The scope of the present work was the investigation of the phosphine sulphonate-based Pd(II) catalyst system and the examination of possible concepts for *i)* optimisation of the functional group incorporation as well as *ii)* the enhancement of the catalyst activity in the polymerisation reactions. Ligand design was applied to investigate the catalyst structure-activity relationship to address these fundamental problems. Figure 46 shows the employed approaches for structural modification of the general phosphine sulphonate ligand system. Both the introduction of anionic functionalities as well as the investigation of possible metal ligand interactions *via* functional groups were analysed regarding their influence on the catalyst structure and polymerisation reactions.
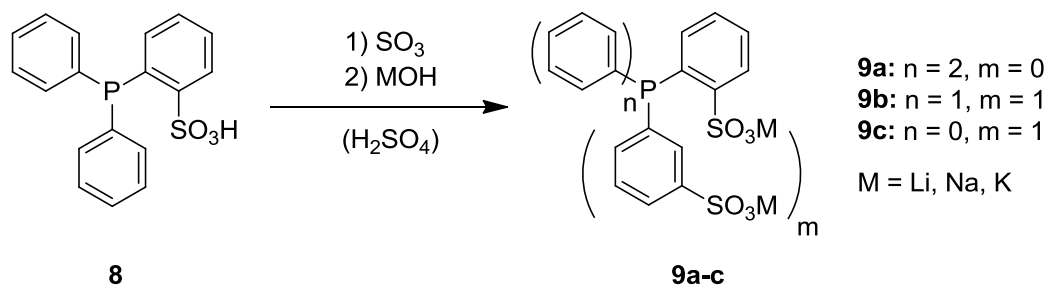
Scheme 42: *Synthesis of hydrophilic non-symmetrically sulphonated phosphine salts with chelating potential.*

Introduction of anionic charges in the coordination environment of the metal centre is a promising concept for optimisation of the functional group tolerance of transition metal-based polymerisation catalysts. Several literature reports propose this as a suitable means to enhance π-coordination of functionalised olefins due to an electrostatic repulsion of the functional group from the anionic functionality. Therefore, this could lead to a weakening of the catalyst poisoning σ-coordination to the metal centre. Based on this concept a new synthetic route towards anionically charged phosphine sulphonate catalysts was developed involving the direct sulphonation of **8** which leads to novel non-symmetrically sulphonated phosphine salts **9b-c** (Scheme 42). Conditions of the sulphonation reaction were optimised to gain insight into the detailed reaction mechanism, to control product selectivity and to facilitate the isolation of reaction components. For subsequent complexation of these ligands phase transfer reactions were investigated to ensure compatibility of the hydrophilic sulphonated phosphines with non-protic polar solvents and organometallic palladium precursors.

7. Summary
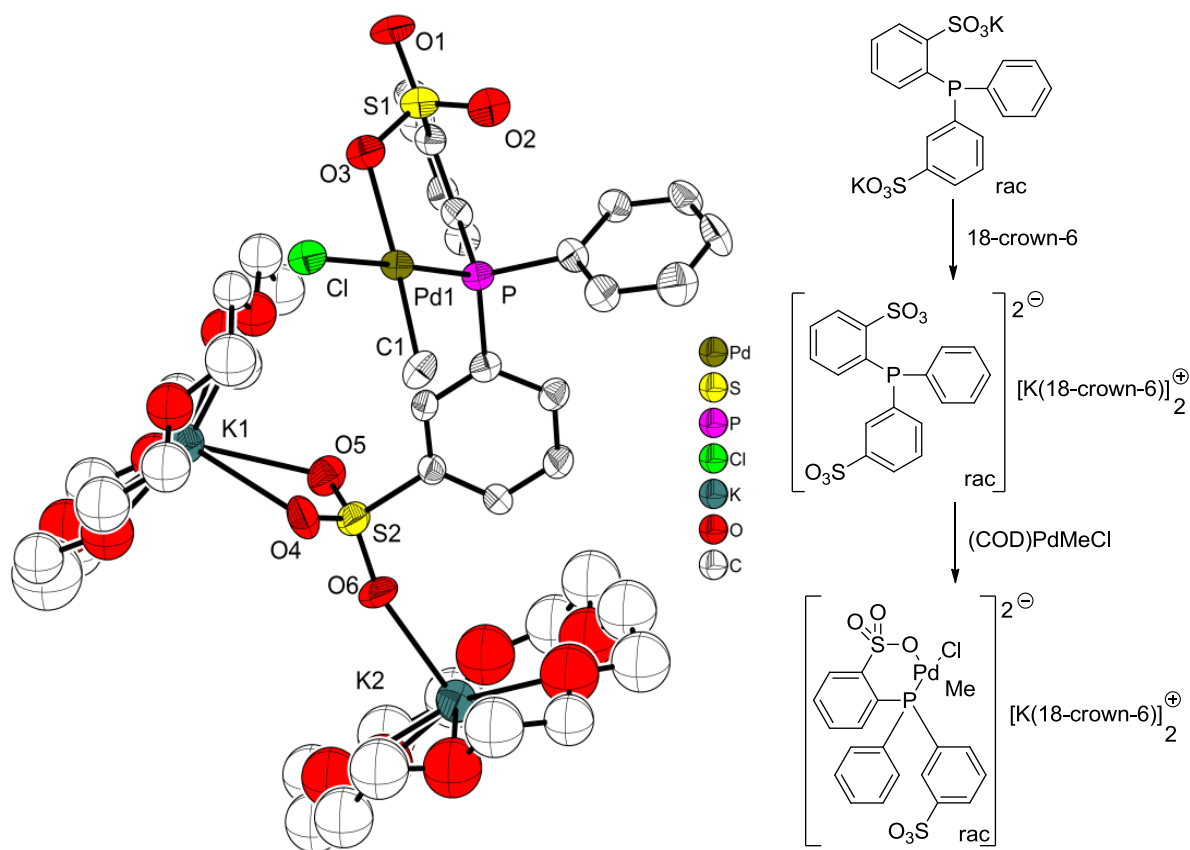
Figure 47: *Synthesis and molecular structure of the novel dianionic [K(18-crown-6)]₂[{κ-(P,O)*-rac-o,m-*TPPDS}PdMeCl] pre-catalyst for olefin polymerisation reactions.*

Crown ether complexation proved to be an ideal method to obtain a novel dianionic catalyst precursor suitable for polymerisation reactions after activation by chloride abstraction with silver salts (Figure 47). [K(18-crown-6)]₂[{κ-(P,O)-*rac-o,m*-TPPDS}PdMeCl] was thoroughly characterised and tested in homo- and co-polymerisation reactions of ethene and polar-functionalised olefin comonomers. It was observed that aggregation of the catalyst in solution leads to the formation of bimodal homo- and co-polymer molecular weight distributions. Anticipated increased incorporation of functionalised olefins in the obtained copolymers could not be observed.

Furthermore the catalyst structure was studied with respect to possible interactions of functional groups from the ligand with the metal centre, as evaluation of recent literature reports led to the question if such effects could determine the catalyst activity. Therefore the most common phosphine sulphonate ligand (Figure 46, b) was successfully modified by

127

7. Summary

exchange of the OMe functionality with a SMe group (Figure 46, d) as well as by a position change of the OMe group on a naphthalene substituent at phosphorus (Figure 46, e). Starting from these ligands subsequent formation of neutral [{κ-(P,O)-phosphine sulphonate}PdMe(pyridine)] complexes was performed and the resulting compounds were analysed regarding their structure in solution and solid state, including a comparison with literature reference complexes (*e.g.* Figure 48).
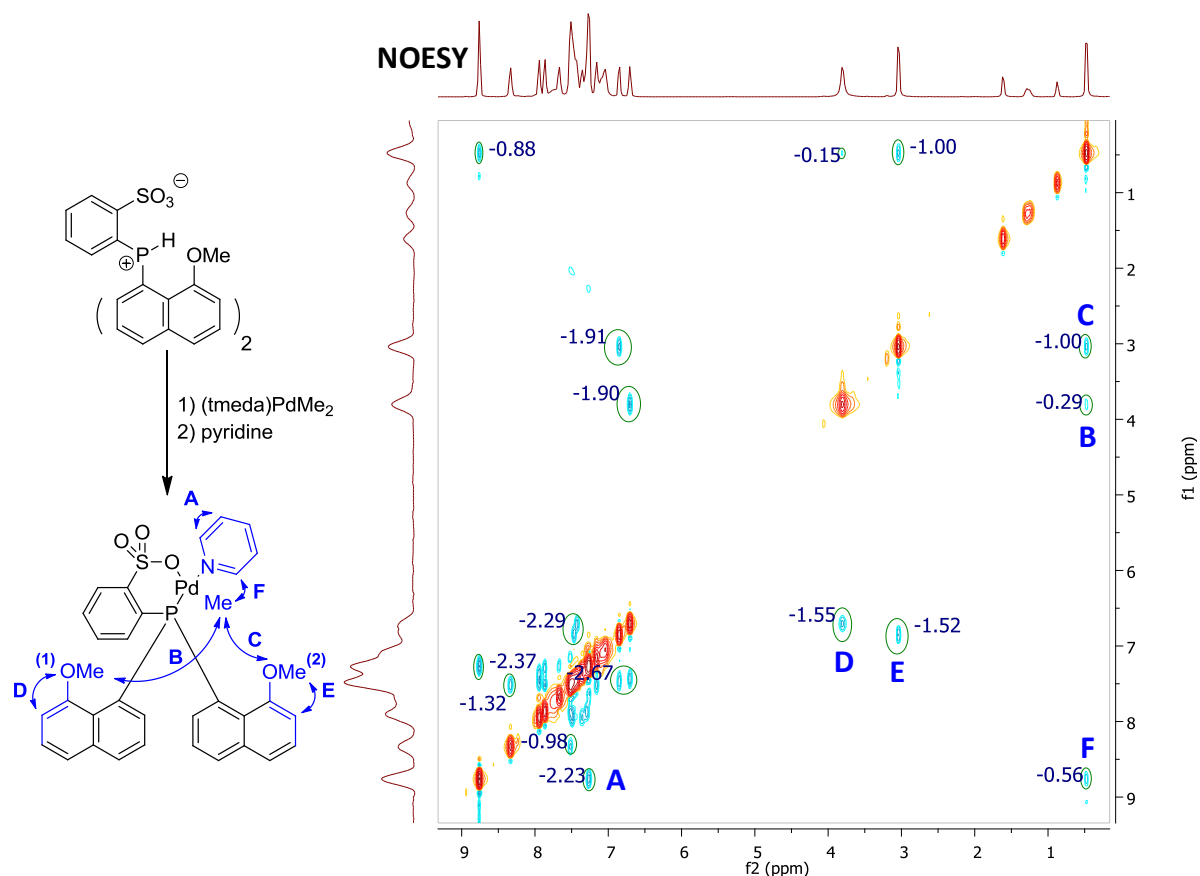
Figure 48: *Synthesis of a novel polymerisation catalyst with methoxylated naphthalene substituents at phosphorus and depiction of the NOESY spectrum (500 MHz, CDCl₃) employed for the investigation of the catalyst solution structure. Assigned spatial proton interactions labelled in blue.*

The obtained new single component catalysts were investigated for ethene homopolymerisation reactions. In comparison to published literature data it could be shown that both examined modifications lead to drastic changes in the polymerisation behaviour of the corresponding catalysts. For instance the introduction of the SMe functionality which is

7. Summary

attributed to S-Pd interactions, apparently increases the transition state energies of a *cis-trans* isomerisation reaction. This was reported as an essential requirement for chain growth and chain termination. As a result this change leads to an increase of the obtained PE molecular weight combined with extremely low catalyst activities. In contrast the alteration of the OMe location with respect to the metal centre by the introduction of a 8-methoxylated naphthalene substituents at phosphorus leads to formation of low molecular weight PE. Here the chiral and relatively rigid catalyst structure with an opened coordination environment at palladium seems to favour a chain walking mechanism *via* a series of β-hydride elimination reaction, reorientation and reinsertion steps. Due to the observation that the catalyst produces only linear PE the polymer chain is trapped in a series of resting states until chain growth can continue when chain walking reaches a terminal position. In consequence the polymerisation rate is reduced and facilitated olefin exchange leads to low molecular weight PE with internal olefinic functionalities (Figure 49).
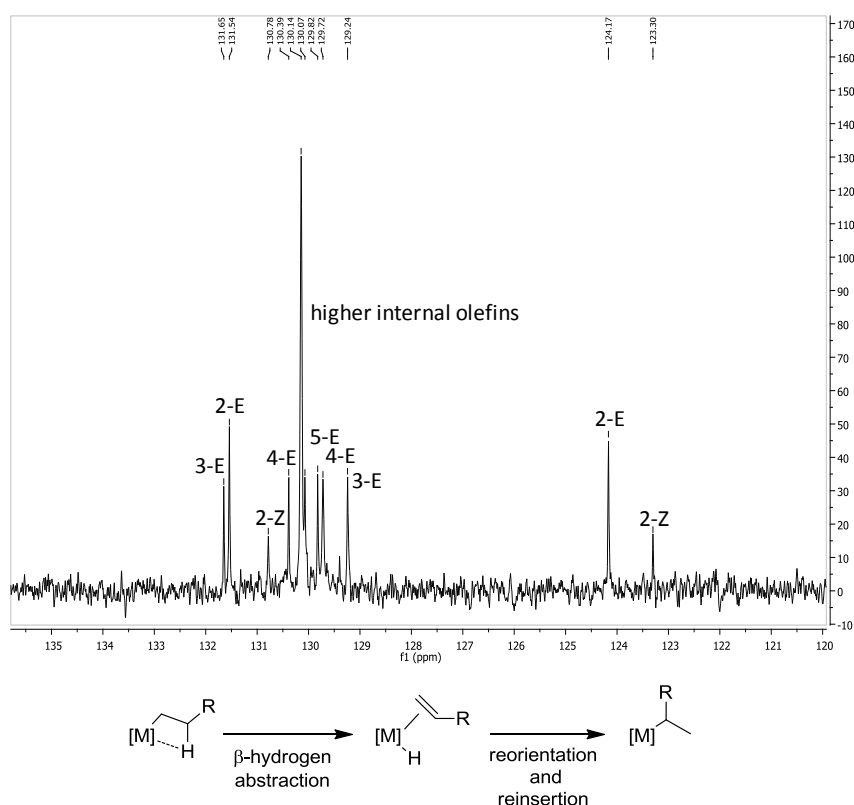
Figure 49: *Olefinic region of the ^{13}C NMR spectrum (75 MHz, $C_2D_2Cl_4$, 120 °C) of a low molecular weight PE sample showing complete internalisation of the olefinic end group (2-olefins and higher) and mechanism of the chain walking process.*

7. Summary

8. Zusammenfassung

Olefin Homo- und Co-Polymerisationen in Gegenwart von polar-funktionalisierten Olefinen die nach einem Koordinations-Insertions-Mechanismus ablaufen sind attraktive Reaktionen, da die Struktur der eingesetzten Katalysatoren gute Möglichkeiten zur Reaktionskontrolle bietet. Diese Einflussmöglichkeiten betreffen neben der Katalysatoraktivität auch die Olefin Insertions Regio- und Stereoselektivität. Aus diesem Grund ist das Katalysator Design eine hervorragende Möglichkeit Polymere und ihre Eigenschaften zu kontrollieren. Allerdings stellt die Einführung von funktionellen Gruppen über Koordinations-Insertions-Polymerisationen ein großes Problem dar. Aufgrund von koordinativen Wechselwirkungen kann eine starke reversible, oder sogar irreversible, Koordination dieser Funktionalitäten an das Metallzentrum die Katalysator Aktivität beeinträchtigen oder unterbinden. Neutrale Katalysatoren mit späten Übergangsmetallen, insbesondere das Phosphan-Sulfonat Pd(II) System, zeigen in Copolymerisationsreaktionen von Olefinen aufgrund der verminderten Lewis Azidität eine außergewöhnliche Toleranz gegenüber funktionellen Gruppen
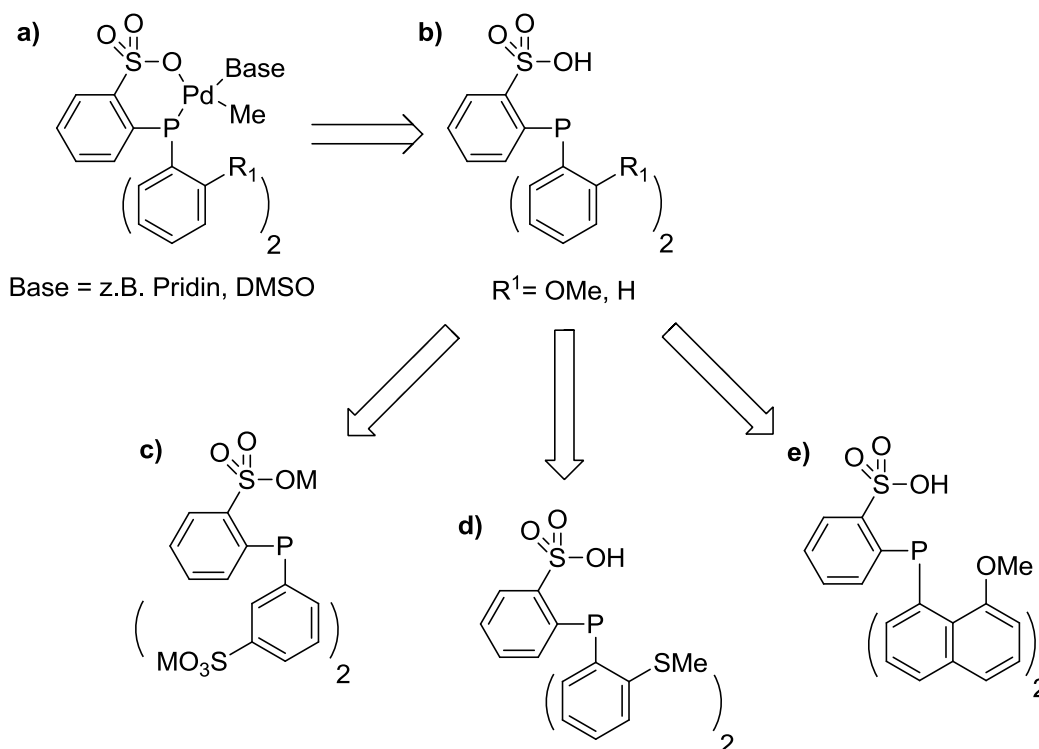
Abbildung 1: *a) Katalysatorstruktur des [{κ-(P,O)-Phosphan-Sulfonat}PdMe(Base)] Systems und Übersicht über hier durchgeführte Liganden-Modifikationen: b) Ausgangssystem, c) Einführung anionischer Funktionalitäten; Untersuchung des Einflusses funktioneller Gruppen: d)Methyl Thioether, e) Positionsänderung der OMe Funktionalität.*

8. Zusammenfassung

Die vorliegende Arbeit umfasst die Untersuchung des Phosphan-Sulfonat Pd(II) Katalysator Systems im Hinblick auf mögliche Konzepte zur *i)* Optimierung des Einbaus funktionalisierter Olefine in Copolymerisations Reaktionen mit Ethen und *ii)* die Verbesserung der Katalysator Aktivität. Die in Abbildung 1 gezeigten Ansätze des Liganden Designs wurden zur Beurteilung der Struktur-Aktivitäts-Beziehung entwickelt um diese fundamentalen Probleme zu untersuchen. Hierbei wurden die Effekte von einer Einführung anionischer Funktionalitäten sowie von möglicherweise auftretenden Metall-Ligand Wechselwirkungen im Hinblick auf die Katalysatorstruktur und Polymerisationsreaktionen analysiert (Abbildung 1).
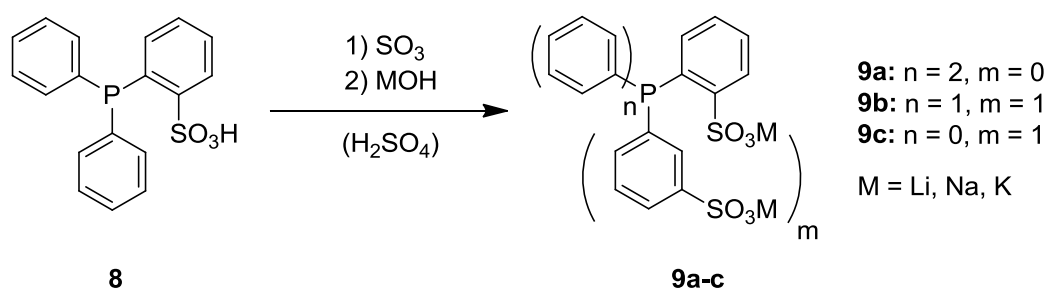
Abbildung 2: *Synthese hydrophiler nichtsymmetrisch sulfonierter Phosphan Salze.*

Die Einführung anionischer Gruppen in die Koordinationsumgebung des Katalysatorzentrums ist ein vielversprechendes Konzept um die Toleranz später Übergangmetall-basierter Polymerisationskatalysatoren gegenüber polar funktionalisierten Olefinen zu verbessern. Mehrere Arbeiten schlagen dieses Konzept als eine Möglichkeiten vor die π-Koordination dieser Olefine an den Katalysator zu erleichtern. Die durch anionische Funktionalitäten erzeugte elektrostatische Abstoßung der funktionellen Gruppen soll eine σ-Koordination der funktionellen Gruppe zum Metallzentrum schwächen und somit eine Beeinträchtigung des Katalysators reduzieren. Nach diesem Konzept wurden ausgehend von der direkten Sulfonierung von **8** neue, nicht symmetrisch sulfonierte, Phosphansalze **9b-c** entwickelt (Abbildung 2). Die Bedingungen der Sulfonierung wurden detailliert betrachtet um Einblick in den Mechanismus der Reaktion und die Produktselektivität zu erlangen, sowie die Isolierung der Produkte zu optimieren. Um eine nachfolgende Komplexierung dieser Liganden zu ermöglichen wurden Phasen-Transfer Reaktionen untersucht um eine Kompatibilität der hydrophilen Phosphane mit nicht-protischen polaren Lösemitteln und organometallischen Palladium Verbindungen zu gewährleisten (Abbildung 3).
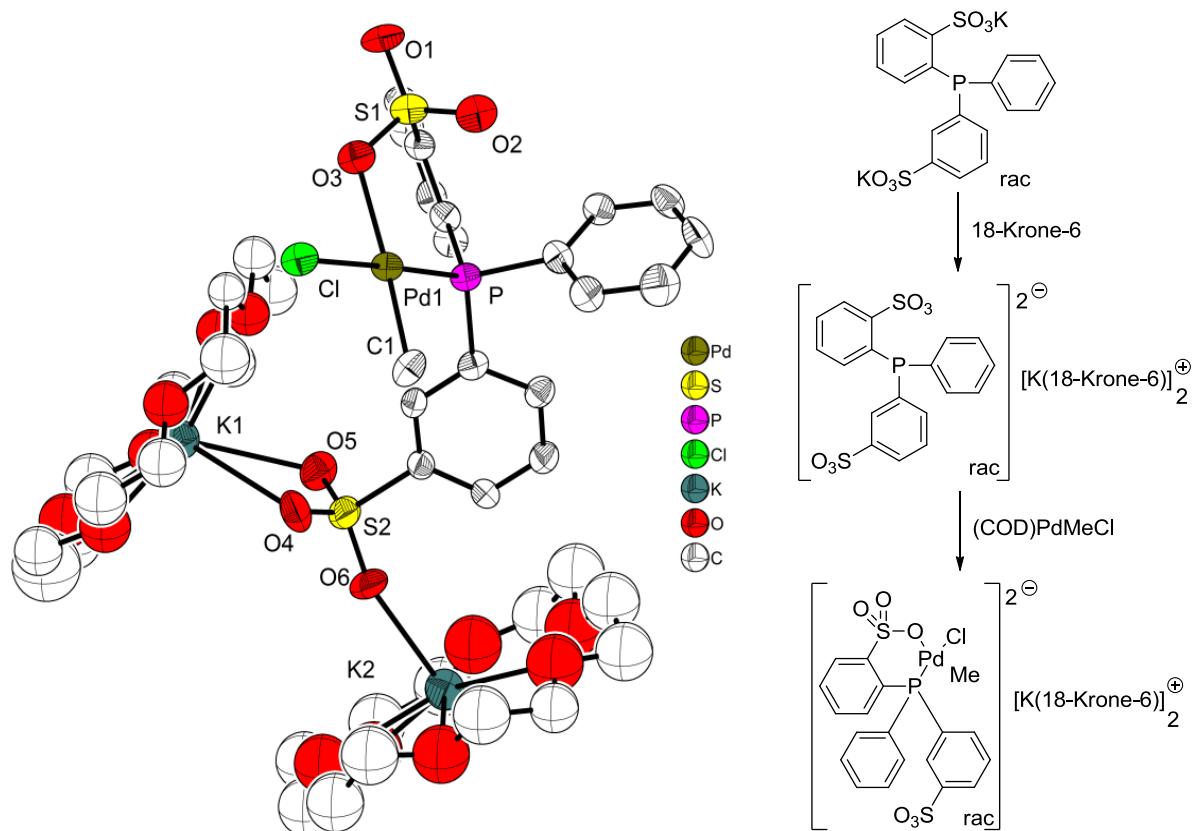
Abbildung 3: *Synthese und Molekülstruktur des dianionischen [K(18-crown-6)]₂[{κ-(P,O)*-rac-o,m*-TPPDS}PdMeCl] Präkatalysators für Olefin Polymerisationsreaktionen.*

Die Komplexierung von Kalium mit Kronenethern hat sich als ideale Methode für die Isolierung eines neuen dianionischen Pd(II) Komplexes erwiesen (Abbildung 3). [K(18-crown-6)]₂[{κ-(P,O)-*rac-o,m*-TPPDS}PdMeCl] zeigt nach Chloridabstaktion mit Silbersalzen Aktivität als Polymerisationskatalysator und wurde ausführlich in Homo- und Co-Polymerisationsreaktionen von Ethen mit Funktionalisierten Olefinen getestet. Es konnte gezeigt werden das eine Aggregation des Katalysators in Lösung zu bimodalen Molekulargewichtsverteilungen führen kann. Die erwartete Verbesserung des Einbauverhaltens von funktionalisierten Olefinen konnte nicht bestätigt werden.

Zusätzlich wurde die Katalysatorstruktur im Hinblick auf mögliche Interaktionen von funktionellen Gruppen der Liganden mit dem Metallzentrum untersucht, nachdem Vergleiche mit Literatursystemen diese Fragestellung aufgeworfen haben. Hierfür wurde das bekannte Standardsystem (Abbildung 1) erfolgreich modifiziert. Dies erfolgte durch einen Austausch der Methoxy Gruppen gegen Methyl-Thioether Funktionalitäten sowie die Einführung von

8. Zusammenfassung

Naphtyl Substituenten zur Veränderung der OMe Position in Bezug auf das Katalysatorzentrum. Ausgehend von diesen Liganden wurden neutrale [{κ-(P,O)-Phosphan-Sulphonat}PdMe(Pyridin)] Komplexe synthetisiert, ihre Struktur in Lösung und im Festkörper analysiert und mit literaturbekannten Referenzkomplexen verglichen.
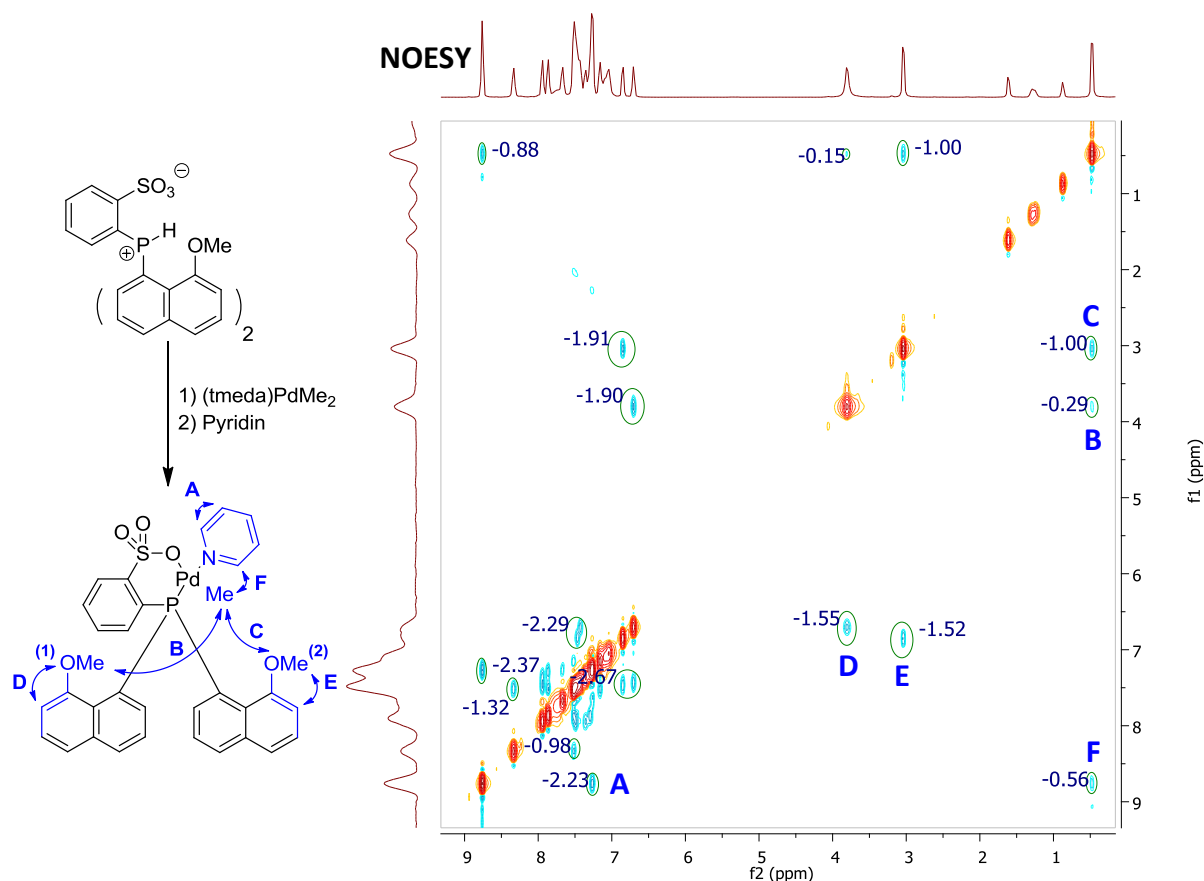
Abbildung 4: *Synthese eines Polymerisationskatalysators mit methoxylierten Naphthyl-Substituenten und eine Abbildung des NOESY Spektrums (500 MHz, CDCl₃) welches zur Untersuchung der Katalysatorstruktur in Lösung verwendet wurde. Beobachtete räumliche Protonenwechselwirkungen sind blau markiert.*

Die erhaltenen direkt aktiven neutralen Polymerisationskatalysatoren wurden in der Ethen Homopolymerisation untersucht. Im Vergleich zu literaturbekannten Referenzsystemen konnte gezeigt werden, dass die beschriebenen Veränderungen deutliche Auswirkungen auf das Polymerisationsverhalten der Katalysatoren haben. So konnte für die Einführung der SMe Gruppe, wahrscheinlich aufgrund von S-Pd Wechselwirkungen, eine erschwerte *cis-trans*-Isomerisierung beobachtet werden, welche ein essentieller Schritt für Kettenwachstum und Kettenabbruch ist. Hierdurch kommt es zu einem Anstieg des Molekulargewichtes von dem

8. Zusammenfassung

erhaltenen PE bei gleichzeitig sehr niedrigen Katalysatoraktivitäten. Im Gegensatz dazu führt eine Veränderung der Position der Methoxy Funktionalität, bezogen auf das Metallzentrum, durch Einführung von 8-methoxylierten Naphthylsubstituenten am Liganden zu einer Bildung von niedermolekularem PE. Die beobachtete chirale und relativ steife Katalysatorstruktur mit einer offenen Koordinationsumgebung am Palladium scheint eine Wanderung des Katalysators entlang der Polymerkette zu begünstigen. Dies geschieht über eine Serie von β-Hydrid-Eliminierungs-, Reorientierungs- und Reinserions-Schritte. Da dieser Katalysator ausschließlich lineares PE bildet wird die Polymerkette in einer Serie von Zwischenzuständen gefangen bis die Wanderung ein Kettenende erreicht und die Polymerisation fortgesetzt werden kann. Aus diesem Grund wird die beobachtete Polymerisationsaktivität im Vergleich zu anderen Systemen verringert und kurzkettiges PE mit ausschließlich internen olefinischen Gruppen gebildet (Abbildung 5).
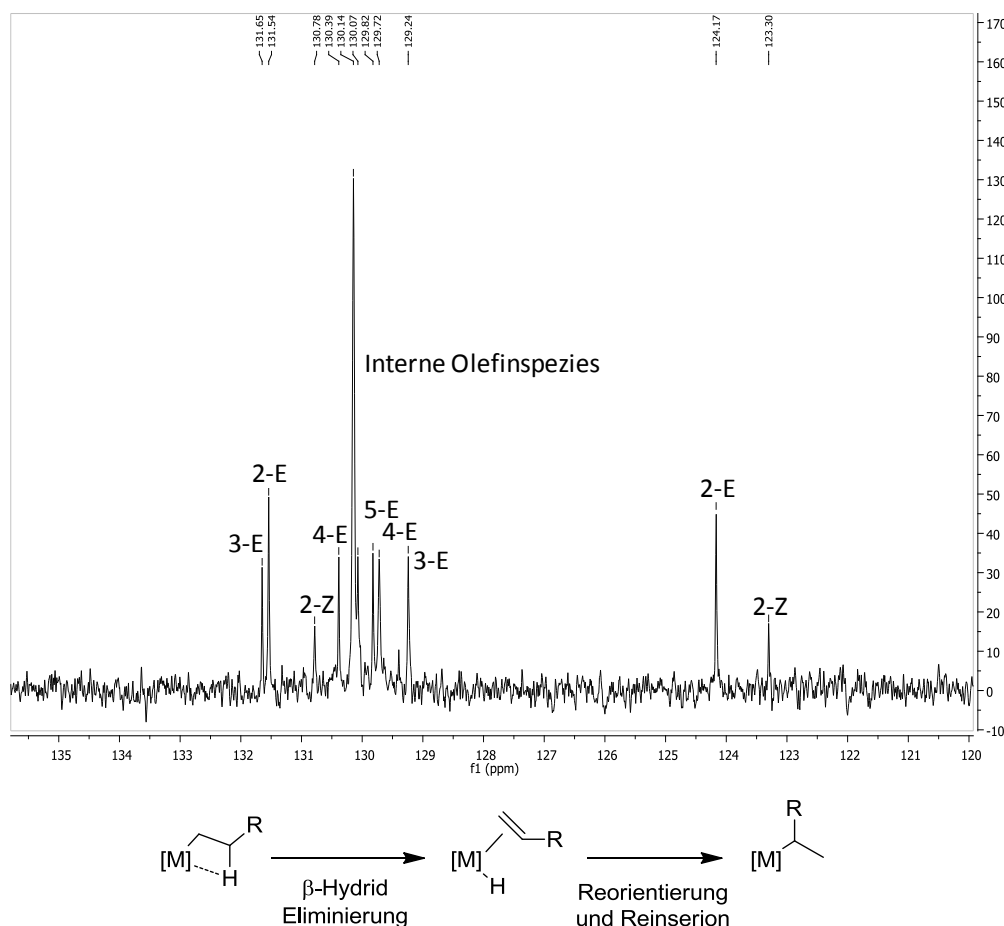
Abbildung 5: *Olefinischer Bereich des ^{13}C NMR Spektrums (75 MHz, $C_2D_2Cl_4$, 120 °C) einer niedermolekularen PE Probe welche eine komplette Internalisierung der Olefin Funktionalität zeigt, sowie Schema des Kettenwanderungsmechanismus.*

8. Zusammenfassung

9. Experimental Part

9.1. General Information

All reactions were routinely carried out under argon using standard Schlenk techniques or in a glovebox unless described otherwise. Chemicals were obtained from Sigma Aldrich, Acros Organics or ABCR and used as received without further purification unless stated otherwise. Dry solvents were obtained from a MBraun MB-SPS-800 solvent purification system and all other solvents were degassed prior to use. Benzenesulphonic acid was dried by azeotropic distillation with toluene and 18-crown-6 was sublimed *in vacuo* before use. (COD)PdMeCl[108] and (tmeda)PdMe$_2$[109] were prepared by slightly modified literature procedures. All palladium compounds were stored under exclusion of light at -20 °C in a glovebox fridge. Solution NMR spectra were collected at room temperature using a Bruker ARX300 or AV500 spectrometer. High temperature solution NMR spectra were recorded at 100 to 130 °C in C$_2$D$_2$Cl$_4$ on a Bruker ARX300 spectrometer. ^{1}H and ^{13}C NMR spectra are referenced to the residual solvent peak of SiMe$_4$ or in case of ^{31}P NMR spectra to 85% phosphorus acid as external standard, values given as ppm. Polymer samples were filtered at 160 °C before GPC on a Polymer Laboratories PL-GPC 220 high temperature chromatograph, equipped with two Olexis 300·7.5 mm columns and triple detection by a differential refractive index detector, a PL-BV 400 HT Viscometer and a Precision Detectors Model 2040 Light Scattering Detector (15°, 90°). The solvent was 1,2,4-trichlorobenzene (BHT stabilised) at 160 °C, with a PE standard. DSC was measured on a TA Instruments DSC Q2000 calorimeter at a heating/cooling rate of 10 K/min. Elemental analyses were performed by the micro analytical laboratory of the department of Inorganic Chemistry at Technische Universität München. Due to the presence of residual solvent molecules the elemental analyses of phosphine sulphonate salts show significant deviation from calculated values. Therefore phosphine sulfonates, which were used for synthesis of Pd(II) complexes employed in polymerisation reactions, were also analysed by high resolution ESI-MS spectrometry, performed with a Bruker micrOTOF-Q, calibrated against sodium formiate 5mmol/L with 0.2% (v/v) formic acid in a water/isopropanol 1/1 mixture. The elemental analyses were corrected according to the residual solvent peaks observed in the NMR spectra. ESI MS spectra were recorded on a Varian LC-MS 500 spectrometer. Isotope Pattern Calculator v4.0 was employed for the calculation of mass spectra and simulation of isotope patterns.

9. Experimental Part

9.2. Synthesis of Materials

9.2.1.   2-(Diphenylphosphine)benzenesulphonic acid (*o*-TPPMS), 8
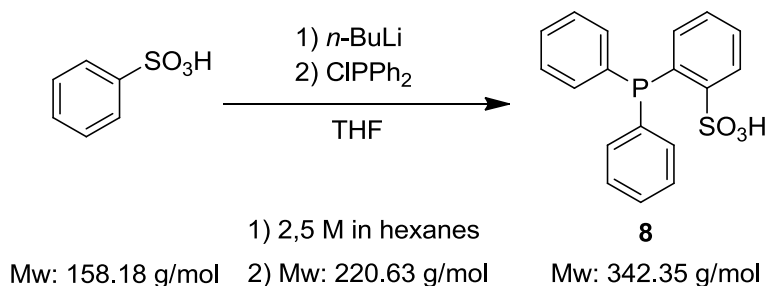
Scheme 43: *Synthesis of 2-(diphenylphosphine)benzenesulphonic acid **8**.*

Benzenesulphonic acid (14.6 g, 92.3 mmol, 1 eq) was dissolved in tetrahydrofuran (400 mL) and the solution was stirred at -78 °C followed by drop-wise addition of *n*-BuLi (73.6 mL, 2.5 M, 184.0 mmol, 2 eq.) over the course of one hour. The resulting dark red solution was allowed to warm to room temperature and stirred over night, causing the precipitation of a colourless solid. After cooling to -78 °C a solution of chlorodiphenylphosphine (16.5 mL, ρ = 1.2 g · cm^{-3}, 19.8 g, 89.7 mmol, 1 eq.) in tetrahydrofuran (150 mL) was added drop-wise under vigorous agitation. Again the reaction mixture was allowed to warm to room temperature and stirred overnight. Termination of the reaction was carried out by careful addition of water (150 mL) followed by addition of diethyl ether (500 mL), extraction and separation of the aqueous layer which was reduced to 50 mL under reduced pressure. Acidified by addition of aqueous HCl (1 M) causes the precipitation of a colourless solid, which was isolated by filtration and subsequent repeated washing with water and pentane. Drying of **8** at 100 °C *in vacuo* provides (26.0 g, 76.0 mmol, 85%) the compound as a colourless powder.

^{1}H NMR (300 MHz, CDCl$_3$) δ 8.37 (dd, *J* = 7.5, 4.9 Hz, 1H), 7.85 – 7.54 (m, 11H), 7.49 (td, *J* = 7.5, 2.1 Hz, 1H), 7.29 – 7.19 (m, 1H).

^{13}C{^{1}H} NMR (75 MHz, CDCl$_3$) δ 152.7 (d, *J* = 8.8 Hz), 135.4 (d, *J* = 2.9 Hz), 134.6 (s), 134.6 (s), 134.4 (s), 133.9 (d, *J* = 11.2 Hz), 130.1 (d, *J* = 13.4 Hz), 129.4 (d, *J* = 9.1 Hz), 118.8 (d, *J* = 89.0 Hz), 113.4 (d, *J* = 95.0 Hz).

^{31}P NMR (121 MHz, CDCl$_3$) δ +4.4 (s).

^{31}P{^{1}H} NMR (121 MHz, CDCl$_3$) δ +δ 4.4 (s).

9. Experimental Part

High-res. ESI-MS (neg., MeCN): $m/z = 341.0408$ (M-H$^+$).

Calculated for $C_{18}H_{14}PSO_3$: $m/z = 341.0407$ (M$^-$).

EA Found: C 62.98, H 4.47, S 9.30.

Calculated for $C_{18}H_{15}PSO_3$:   C 63.15, H 4.41, S 9.32.

9.2.2. 2-(Diphenylphosphine)benzenesulphonate, potassium salt, [K][o-TPPMS], 9a(K)
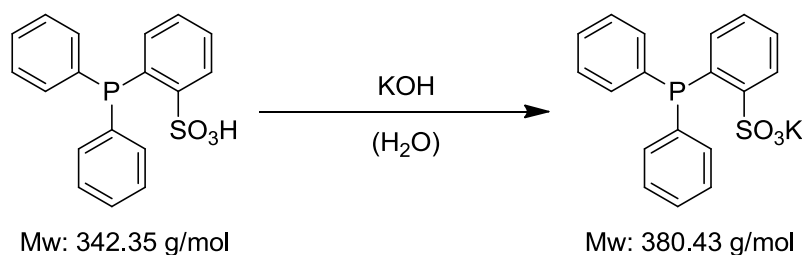
Scheme 44: *Synthesis of 2-(diphenylphosphine)benzenesulphonate potassium salt **9a(K)**.*

8 (3.42 g, 10.0 mmol, 1 eq.) was suspended in water (15 mL) and aqueous KOH (0.56 mL, 0.1 g/mL, 0.56 g, 1 eq.) was added, immediately leading to a clear solution. The solvent was removed *in vacuo* and **9a(K)** (2.90 g, 7.62 mmol, 76.%) was obtained after recrystallisation from methanol and drying *in vacuo*.

Analysis:
^{1}H NMR (300 MHz, D$_2$O) δ 7.94 (dd, $J = 7.8$, 3.9 Hz, 1H), 7.34 (d, $J = 7.3$ Hz, 1H), 7.09 (t, $J = 7.6$ Hz, 1H), 6.99 – 6.83 (m, 10H), 6.56 (t, $J = 7.5$ Hz, 1H).
^{31}P{^{1}H} NMR (121 MHz, D$_2$O) δ -10.7.

ESI-MS (neg., H$_2$O): $m/z = 340.9$ (M-K$^+$).

Calculated for $C_{18}H_{14}PSO_3$: $m/z = 341.0$ (M$^-$).

EA Found: C 55.79, H 4.00, S 7.91.

Calculated for $C_{18}H_{14}KO_3PS$:   C 56.83, H 3.71, S 8.43.

Calculated for $C_{18}H_{14}KO_3PS \times 0.5$ MeOH: C 56.05, H 4.07, S 8.09.

9. Experimental Part

9.2.3. General Procedure for the sulphonation of *o*-TPPMS 8
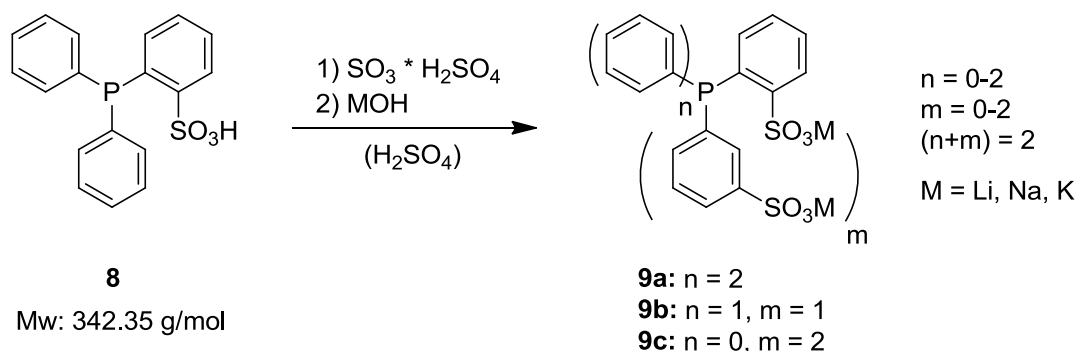
Scheme 45: *General scheme for the sulphonation of 8 and generation of phosphine sulphonate salts 9a-c.*

A Schlenk flask was charged with the desired amount of concentrated sulphuric acid (95-97%). After cooling to 0 °C aliquots of **8** were added repeatedly and upon complete dissolution, the required amount of fuming sulphuric acid with the appropriate content of SO_3 was added drop wise under vigorous agitation, whilst maintaining cooling of the reaction to prevent temperature increases exceeding 40 °C. Subsequently the reaction mixture was heated to 30 °C and stirred for the desired reaction time. Termination of the reaction was carried out by careful drop-wise addition of water at 0 °C. The reaction mixture was diluted by addition of water (twofold). Neutralisation was carried out by addition of the desired aqueous alkali metal solution (5 M, NaOH or KOH) and the pH was adjusted to *ca*. pH 9 with diluted aqueous sulphuric acid and the appropriate alkali metal solution. Majority of the water was removed *in vacuo* and the remaining brown solid was extracted by refluxing with MeOH. Filtration of the hot solution and subsequent complete removal of volatiles *in vacuo* provides the pale brown crude product mixture as a fine powder. For the isolation of specific reaction components this mixture was redissolved in hot anhydrous methanol and the desired product was obtained by crystallisation or fractional precipitation. Detailed isolation procedures are provided in the following sections for the main reaction products (Scheme 46).

9. Experimental Part
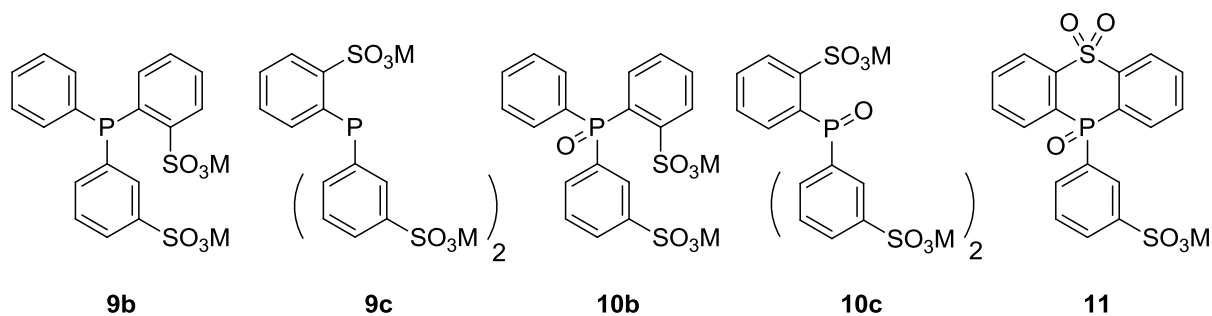
Scheme 46: *Overview of observed reaction products in the sulphonation of 8; from left to right:* rac-o,m-*TPPDS* **9b**, o,m,m-*TPPTS* **9c**, rac-o,m-*TPPDSO* **10b**, o,m,m-*TPPTSO* **10c**, Sulphone **11**.

9.2.4.   Synthesis of [K]₂[*rac-o,m*-TPPDS] 9b(K)

9b(K)
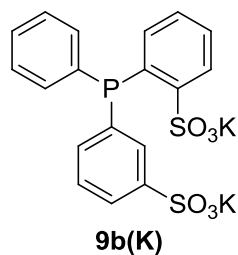
Mw: 498.59 g/mol

Figure 50: *Structure of rac-o,m-TPPDS potassium salt* **9b(K)**.

Synthesis of the racemic **9b(K)** was performed from **8** (10.0 g, 29.2 mmol) dissolved in concentrated sulphuric acid (10 mL, 95-97%) followed by sulphonation after addition of fuming sulphuric acid (13 mL, 65% (w/w) SO₃) over the course of 20 h. The crude product mixture was obtained after neutralisation with an aqueous KOH solution (5 M) as described above (**9b(K)** content: 75.3% of total phosphorus content determined by ³¹P NMR spectroscopy). After dissolution in hot, anhydrous MeOH and filtration **9b(K)** was obtained by fractional precipitation upon cooling to -25 °C (9.43 g, 90.0% of total phosphorus content) as the hydrate.

Details: Reaction time 20 h, n(SO₃):n(phosphine) 6:1, SO₃: 28% (w/w), H₂SO₄: 55% (w/w).
¹H NMR (500 MHz, D₂O) δ 8.06 (m, 1H), 7.82 (m, 1H), 7.70 (m, 1H), 7.51 (m, 1H), 7.41 (m, 2H), 7.37 – 7.29 (m, 3H), 7.26 (m, 3H), 7.04 (m, 1H).

9. Experimental Part

$^{13}C\{^1H\}$ NMR (75 MHz, D$_2$O) δ 148.2 (d, J (C-P) = 26.2 Hz), 143.7 (d, J (C-P) = 6.4 Hz), 139.6 (d, J (C-P) = 12.8 Hz), 137.1 (d, J (C-P) = 10.3 Hz), 137.0 (d, J (C-P) = 7.9 Hz), 136.9 (s), 134.7 (s), 134.5 (d, J (C-P) = 21.8 Hz), 134.4 (s), 132.3 (s), 131.0 (s), 130.8 (s), 130.7 (s), 130.2 (s), 130.2 (d, J (C-P) = 5.9 Hz), 129.8 (d, J (C-P) = 7.0 Hz), 128.3 (d, J (C-P) = 4.7 Hz), 126.7 (s).

$^{31}P\{^1H\}$ NMR (121 MHz, D$_2$O) δ -10.5.

High-res. ESI-MS (neg., H$_2$O):   m/z = 458.9561 (M-K$^+$).

Calculated for C$_{18}$H$_{13}$KO$_6$PS$_2$:   m/z = 458.9528 (M$^-$).

EA Found: C 42.32, H 2.79, S 11.34.

Calculated for C$_{18}$H$_{13}$K$_2$O$_6$PS$_2$:   C 43.36, H 2.63, S 12.86.

9.2.5.   Synthesis of [Na]$_3$[o,m,m-TPPTS] 9c(Na)
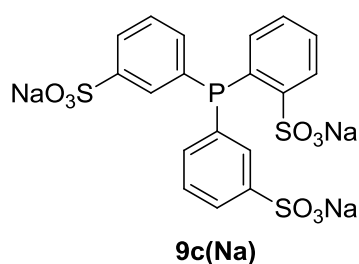
9c(Na)

Mw: 568.42 g/mol

Figure 51: *Structure of the* o,m,m-*TPPTS sodium salt* *9c(Na)*.

Synthesis of **9c(Na)** was performed from **8** (5.00 g, 14.6 mmol) dissolved in concentrated sulphuric acid (10 mL, 95-97%) followed by sulphonation after addition of fuming sulphuric acid (13 mL, 65% (w/w) SO$_3$) over the course of 20 h. 9.67 g of the crude product mixture were obtained after neutralisation with an aqueous NaOH solution (5 M) as described above (**9c(Na)** content:78.1% of total phosphorus content, determined by ^{31}P NMR spectroscopy). **11** as by-product was separated from the reaction mixture by crystallisation from hot methanol at 5 °C. Subsequent precipitation with ethanol provided **9c(Na)** (5.35 g, 84.0% of total phosphorus content, determined by ^{31}P NMR spectroscopy) as the hydrate.

Details: Reaction time: 18 h, n(SO$_3$):n(phosphine) 12:1, SO$_3$: 30% (w/w), H$_2$SO$_4$: 60% (w/w).
^{1}H NMR (500 MHz, D$_2$O) δ 8.09 (m, 1H), 7.89 – 7.85 (m, 2H), 7.73 – 7.69 (m, 2H), 7.61 (m, 1H), 7.55 (m, 2H), 7.49 – 7.42 (m, 3H), 7.14 (m, 1H).

9. Experimental Part

$^{13}C\{^1H\}$ NMR (75 MHz, D_2O) δ 148.1 (d, *J (C-P)* = 26.5 Hz), 143.7 (d, *J (C-P)* = 6.4 Hz), 138.8 (d, *J (C-P)* = 13.0 Hz), 137.3 (d, *J (C-P)* = 19.2 Hz), 137.1 (d, *J (C-P)* = 1.3 Hz), 133.7 (d, *J (C-P)* = 21.7 Hz), 132.5 (s), 131.0 (d, *J (C-P)* = 2.6 Hz), 130.8 (s), 130.3 (d, *J (C-P)* = 6.2 Hz), 128.3 (d, *J (C-P)* = 4.9 Hz), 127.0 (s).

$^{31}P\{^1H\}$ NMR (121 MHz, D_2O) δ -10.3 (s).

High-res. ESI-MS (neg., H_2O):	m/z = 544.9198 (M-Na$^+$).
Calculated for $C_{18}H_{12}Na_2O_9PS_3$:	m/z = 544.9176 (M$^-$).
EA Found:	C 35.54, H 2.46, S 13.19.
Calculated for $C_{18}H_{12}Na_3O_9PS_3$:	C 38.03, H 2.13, S 16.92.

9.2.6. Synthesis of the 10-(3-Sulphonatophenyl)-10*H*-9-thia-10-phospha-anthracene-9,9,10-trioxide, sodium salt 11

11
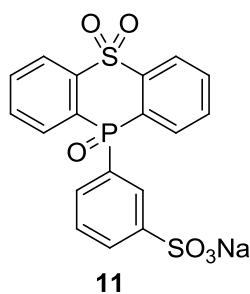
Mw: 442.38 g/mol

Figure 52: *Structure of the 10-(3-sulphonatophenyl)-10*H*-9-thia-10-phospha-anthracene-9,9,10-trioxide sodium salt* **11**.

Synthesis of **11** was performed from **8** (5.00 g, 14.6 mmol) dissolved in concentrated sulphuric acid (7 mL, 95-97%) followed by sulphonation after addition of fuming sulphuric acid (33 mL, 65% SO_3 (w/w)) over the course of 40 h. The crude product mixture was obtained after neutralisation with an aqueous NaOH solution (5 M) as described above. Subsequent dissolution in hot anhydrous MeOH and filtration allow crystallisation of **11** upon cooling to -5 °C. After drying *in vacuo* **11** was obtained in colourless needles as the hydrate (2.15 g).

Details: Reaction time: 40 h. n(SO_3):n(Phosphine) 35:1, SO_3: 49% (w/w), H_2SO_4: 45% (w/w).

^{1}H NMR (500 MHz, D$_2$O) δ 8.17 (m, 2H), 8.05 – 8.01 (m, 2H), 7.98 (m, 2H), 7.91 (m, 2H), 7.76 (m, 2H), 7.67 (m, 2H), 7.57 – 7.48 (m, 2H).

^{13}C{^{1}H} NMR (75 MHz, D$_2$O) δ 144.7 (d, *J (C-P)* = 13.6 Hz), 141.3 (d, *J (C-P)* = 7.6 Hz), 135.3 (s), 135.2 (d, *J (C-P)* = 11.5 Hz), 134.8 (d, *J (C-P)* = 11.9 Hz), 134.0 (d, *J (C-P)* = 4.9 Hz), 132.2 (d, *J (C-P)* = 113.7 Hz), 131.5 (s), 130.9 (d, *J (C-P)* = 13.5 Hz), 129.1 (d, *J (C-P)* = 12.8 Hz), 128.9 (d, *J (C-P)* = 102.0 Hz), 126.3 (d, *J (C-P)* = 7.5 Hz).

^{31}P{^{1}H} NMR (121 MHz, D$_2$O) δ +8.9 (s).

High-res. ESI-MS (neg., H$_2$O):	m/z = 418.9831 (M-Na$^+$).
Calculated for C$_{18}$H$_{12}$O$_6$PS$_2$:	m/z = 418.9813.
Found:	C 47.34, H 3.38, S 13.56, P 6.30, Na 5.20.
Calculated for C$_{18}$H$_{12}$O$_6$NaPS$_2$:	C 48.87, H 2.73, S 14.50, P 7.00, Na 5.20.

9.2.7. ^{31}P NMR spectroscopic kinetic investigation of the sulphonation reaction

i) Investigation of the reaction leading to the isolation of 9c.

Analogous to the reaction procedure in Section 9.2.5 **8** (2.00 g, 5.84 mmol) was dissolved in concentrated sulphuric acid (4 mL) at 0 °C. A reference sample was taken as explained below. Fuming sulphuric acid (5 mL, 65% (w/w) SO$_3$) was added drop wise at 0 °C over the course of 15 min followed by sulphonation after stirring at 30 ° for 10 h. Small aliquots were taken repeatedly at defined time intervals. After termination of these samples, by addition of deuterated ice cooled aqueous NaOH (5 M), ^{31}P NMR spectroscopy was performed for determination of the reaction progress. Conversion of the present phosphorus-containing species namely the phosphines **9a-c**, phosphine oxides and **11** was plotted against the reaction time (compare Figure 16, Section 5.3.3).

ii) Investigation of the reaction to the isolation of 9b.

Analogue the procedure detailed in Section 9.2.4, the kinetic investigation for the sulphonation of **8** (2 g, 5.84 mmol) dissolved in concentrated sulphuric acid (4 mL) by addition of fuming sulphuric acid (3 mL, 65% SO$_3$ (w/w)) was carried out and analysed as described in 9.2.7, i) (compare Figure 17, Section 5.3.3).

9. Experimental Part

9.2.8. Synthesis of 2-[bis-(2-methoxyphenyl)phosphine]benzenesulphonic acid [*o*-TPPMS(OMe)] 7
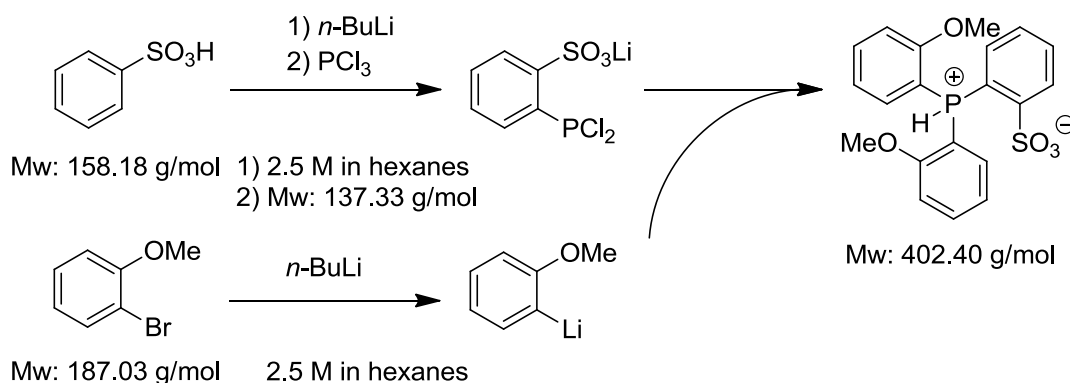
Scheme 47: *Synthesis of 2-[bis-(2-methoxyphenyl)phosphine]benzenesulphonic acid, o-TPPMS(OMe) 7.*

Benzenesulphonic acid (9.44 g, 59.7 mmol, 1 eq.) was dissolved in tetrahydrofuran (200 mL) (Flask **A**) and cooled to -78 °C, followed by slow addition of *n*-BuLi in hexanes (47.8 mL, 2.5 M, 119.5 mmol, 2 eq.). The resulting dark red solution was stirred overnight at room temperature. In a second flask (Flask **B**) PCl₃ (5.2 mL, ρ = 1.57 g · cm⁻³, 8.16 g, 59.4 mmol, 1 eq.) was dissolved in tetrahydrofuran (300 mL) at -78 °C and stirred for 15 min. The contents of Flask **A** were transferred by cannula to Flask **B** under vigorous agitation, yielding a pale yellow solution. Parallel, in a third flask (Flask **C**) 1-bromanisole (22.2 g, ρ = 1.50 g · cm⁻³, 14.8 mL, 119 mmol, 1 eq.) was dissolved in tetrahydrofuran (250 mL). At -78 °C *n*-BuLi (47.6 mL, 2.5 M, 119 mmol) was slowly added to Flask **C** and the reaction mixture was stirred for 3.5 h at -78 °C. Finally the content of Flask **C** was transferred by cannulla to Flask **B** at -78 °C, the reaction was allowed to warm to room temperature and was stirred for three days. Termination of the reaction was carried out by slow addition of water. For isolation of the product water and diethyl ether (200 mL and 400 mL, respectively) were added to the reaction, the aqueous phase was separated and subsequently reduced to 50 mL. Acidification with aqueous HCl (1 M) causes precipitation of a white precipitate which was isolated by filtration, redissolved in chloroform and crystallised by addition of diethyl ether at -25 °C. **7** was obtained as a fine colourless solid (4.93 g, 12.3 mmol, 21%).

¹H NMR (300 MHz, CDCl₃) δ 8.29 (dd, *J* = 7.4, 5.2 Hz, 1H), 7.74 – 7.56 (m, 3H), 7.38 (t, *J* = 7.0 Hz, 1H), 7.15 – 6.86 (m, 7H), 3.70 (s, 6H).

$^{13}C\{^1H\}$ NMR (75 MHz, CDCl$_3$) δ 161.3 (d, *J* = 2.2 Hz), 152.4 (d, *J* = 9.2 Hz), 136.8 (s), 134.7 (s), 134.6 (d, *J* = 7.8 Hz), 133.5 (d, *J* = 11.7 Hz), 129.6 (d, *J* = 13.1 Hz), 129.4 (s), 122.0 (d, *J* = 13.2 Hz), 112.9 (d, *J* = 100.0 Hz), 112.0 (d, *J* = 6.1 Hz), 106.4 (d, *J* = 95.9 Hz), 56.5 (s).

^{31}P NMR$\{^1H\}$ (121 MHz, CDCl$_3$) δ -10.4.

^{31}P NMR (121 MHz, CDCl$_3$) δ -10.4 (d, ^1J (P-H) = 593.6 Hz).

High-res. ESI-MS (neg., MeCN):   m/z = 401.0642 (M-H$^+$).

Calculated for C$_{20}$H$_{18}$O$_5$PS: m/z = 401.0618 (M$^-$).

EA Found: C 47.38, H 3.90, S 5.65.

Calculated for C$_{20}$H$_{19}$O$_5$PS: C 59.70, H 4.76, S 7.97.

Calculated for C$_{20}$H$_{19}$O$_5$PS × 1.1 CHCl$_3$:   C 47.38, H 3.86, S 5.95.

9.2.9.   Synthesis of the [K][*o*-TPPMS(OMe)] salt
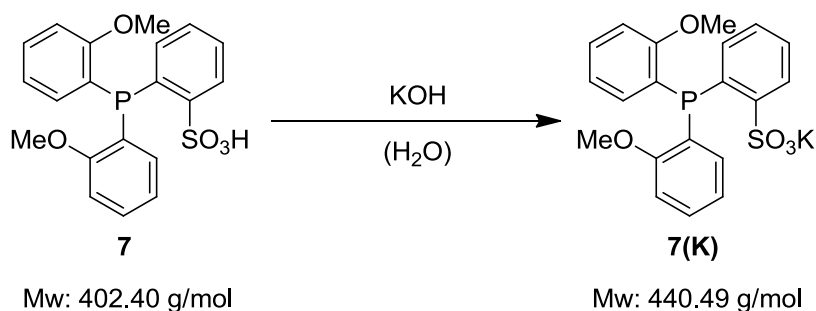
Scheme 48: *Synthesis of the* o-*TPPMS(OMe) potassium salt.*

7 (2.41 g, 6.00 mmol, 1 eq) was suspended in water (40 mL) and aqueous KOH (0.45 mL, 0.1 g/mL, 2 eq.) was added and the solvent was subsequently removed from the soapy mixture under reduced pressure. The residue was dissolved in anhydrous methanol and the obtained solution was filtered followed by crystallisation at -25 °C. After filtration and drying *in vacuo* the *o*-TPPMS(OMe) potassium salt was obtained as a white powder (981 mg) as the hydrate with residual inorganic impurities.

^1H NMR (300 MHz, DMSO) δ 7.70 (ddd, *J* = 7.7, 4.1, 1.2 Hz, 1H), 7.15 – 7.03 (m, 3H), 6.96 (td, *J* = 7.4, 1.3 Hz, 1H), 6.81 – 6.70 (m, 2H), 6.64 – 6.47 (m, 3H), 6.21 (ddd, *J* = 7.4, 3.3, 1.6 Hz, 2H), 3.41 (s, 6H).

^{13}C{^{1}H} NMR (75 MHz, DMSO) δ 160.6 (d, J = 16.8 Hz), 152.3 (d, J = 27.4 Hz), 134.2 (d, J = 1.6 Hz), 133.9 (d, J = 25.0 Hz), 133.4 (s), 129.5 (s), 128.4 (s), 127.9 (s), 127.3 (d, J = 4.5 Hz), 127.1 (d, J = 19.4 Hz), 120.6 (s), 110.50 (s), 55.5 (d, J = 1.2 Hz).

^{31}P{^{1}H} NMR (121 MHz, DMSO) δ -29.3.

EA Found: C 44.12, H 3.70, S 5.82.

Calculated for $C_{20}H_{19}O_5PSK$:   C 54.53, H 4.12, S 7.28.

9.2.10. Synthesis of [K]$_3$[*o,m,m*-TPPTS(OMe)] 12(K)

7
Mw: 402.40 g/mol

12(K)
Mw: 676.80 g/mol
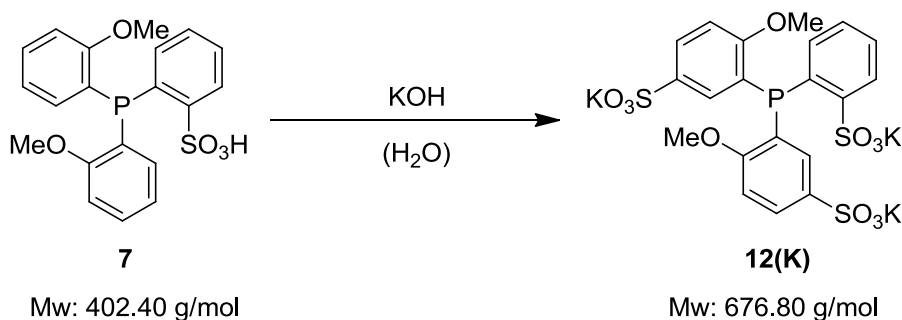
Scheme 49: *Synthesis of o,m,m-TPPTS(OMe) as the potassium salt **12(K)**.*

A flask was charged with fuming sulphuric acid (10 mL, 20% (w/w) SO$_3$), cooled to 0 °C and **7** (2.50 g, 6.21 mmol) was dissolved in small portions until a brown solution was obtained. The reaction was stirred for 3 h at room temperature, terminated by careful addition of water at 0 °C and adjustment of the pH to 9-10 with an aqueous KOH solution (5 M). The majority of the water was removed *in vacuo* and the residue was extracted with refluxing methanol. After filtration of the hot solution and complete removal of volatiles *in vacuo* the crude product mixture was obtained as a brown powder. **12(K)** was isolated by extraction of the crude product with hot anhydrous methanol, filtration and crystallisation at -25 °C. A second crystal crop was obtained by reducing the volume of the mother solution and repeated crystallisation at -25 °C. The beige product (2.90 g, 4.28 mmol, 85.5% of total phosphorus content) was obtained as the hydrate.

The sodium salt of this compound can be obtained by a similar workup procedure of the sulphonation reaction with aqueous NaOH. Due to the increased solubility of **12(Na)** in MeOH the product is obtained by fractional precipitation with diethyl ether.

^{1}H NMR (500 MHz, D$_2$O) δ 8.11 – 8.06 (m, 1H), 7.87 (dd, *J* = 8.5, 1.7 Hz, 2H), 7.59 (t, *J* = 7.7 Hz, 1H), 7.44 (t, *J* = 7.6 Hz, 1H), 7.19 – 7.15 (m, 2H), 7.12 (dd, *J* = 6.8, 3.8 Hz, 1H), 7.03 (s, 1H), 3.79 (s, 6H).

^{13}C{^{1}H} NMR (75 MHz, D$_2$O) δ 163.4 (d, *J* = 16.0 Hz), 148.1 (d, *J* = 27.6 Hz), 136.5 (s), 136.0 (s), 132.8 (d, *J* = 19.7 Hz), 132.3 (s), 131.50 (s), 130.9 (s), 129.2 (s), 128.1 (d, *J* = 5.0 Hz), 125.7 (d, *J* = 14.6 Hz), 111.8 (s), 111.80 (s), 56.8 (s).

^{31}P{^{1}H} NMR (121 MHz, D$_2$O) δ -29.5 (1.00).

High-res. ESI-MS (pos., H$_2$O):	m/z = 638.9028 (M-K$^+$+2H$^+$).
Calculated for C$_{20}$H$_{16}$PS$_3$O$_{11}$K$_2$:	m/z = 638.9023 (M-K$^+$+2H$^+$).
EA Found:	C 32.29, H 3.02, S 13.29.
Calculated for C$_{20}$H$_{16}$PS$_3$O$_{11}$K$_3$:	C 35.49, H 2.38, S 14.21.

9.2.11. Synthesis of [NBu$_4$]$_2$[*rac-o,m*-TPPDS] 14b
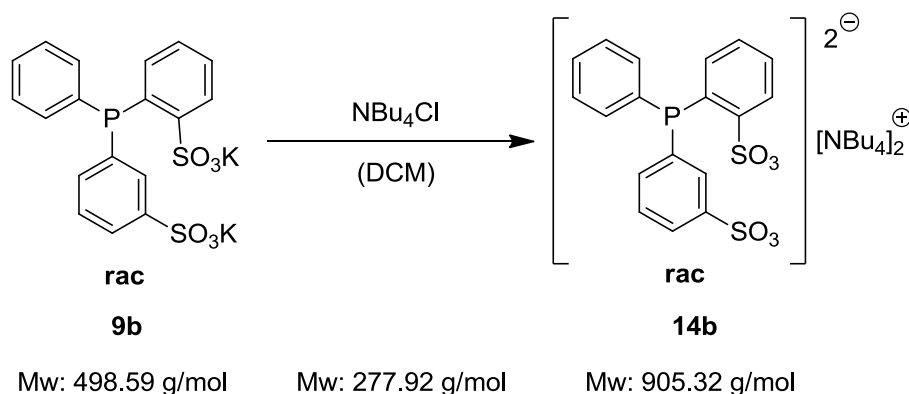
Scheme 50: *Synthesis of the [NBu$_4$]$_2$[rac-o,m-TPPDS] salt **14b**.*

The potassium salt of *rac-o,m*-TPPDS (670 mg, 1.34 mmol, 1 eq.) and NBu$_4$Cl (744 mg, 2.68 mmol, 2 eq.) were dissolved in water (20 mL) and the reaction was stirred for 15 min followed by addition of methylene chloride (20 mL). Extraction by vigorous agitation for 4 h was followed by separation of the organic phase and reextraction of the aqueous phase with methylene chloride (10 mL). The combined organic phases were reextracted with water (20 mL) and the volatiles were removed *in vacuo*. **14b** was obtained as a colourless powder (985 mg, 1.09 mmol, 81%).

9. Experimental Part

^{1}H NMR (300 MHz, CD$_2$Cl$_2$) δ 8.05 (dd, J = 7.1, 3.6 Hz, 1H), 7.67 (t, J = 8.3 Hz, 2H), 7.32 – 6.98 (m, 10H), 3.10 (dd, J = 21.4, 12.8 Hz, 16H), 1.62 – 1.44 (m, 16H), 1.40 – 1.18 (m, 16H), 0.92 (t, J = 7.3 Hz, 24H).

^{31}P{^{1}H} NMR (121 MHz, CD$_2$Cl$_2$) δ -9.7.

EA Found: C 64.16, H 9.47, S 6.40, N 3.13.

Calculated for C$_{50}$H$_{85}$N$_2$O$_6$PS$_2$:   C 66.33, H 9.46, S 7.08, N 3.09.

The compound could not be purified by crystallisation or chromatographically.

9.2.12. Synthesis of [NBu$_4$]$_3$[*o,m,m*-TPPTS] 14c
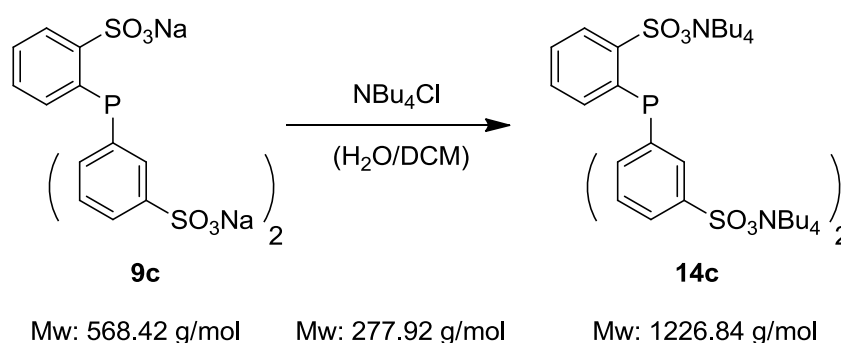
Scheme 51: *Synthesis of* o,m,m-*TPPTS as the NBu$_4$ salt* **14c**.

9c which was thoroughly dried at 100 °C *in vacuo* (991 mg, 1.74 mmol, 1 eq.) and NBu$_4$Cl (1.50 g, 5.40 mmol, 3.1 eq.) were dissolved in water (20 mL). The reaction mixture was stirred overnight, followed by addition of methylene chloride (20 mL). After extraction and separation of the organic phase, washing with lwater (20 mL) and removal of volatiles *in vacuo*, **14c** (1.45 g, 1.18 mmol, 68%) was obtained a colourless powder.

^{1}H NMR (300 MHz, CD$_2$Cl$_2$) δ 8.04 (ddd, J = 7.6, 4.0, 1.4 Hz, 1H), 7.74 – 7.66 (m, 3H), 7.33 – 7.02 (m, 8H), 3.22 – 2.93 (m, 24H), 1.64 – 1.42 (m, 24H), 1.38 – 1.19 (m, 24H), 0.91 (t, J = 7.3 Hz, 36H).

^{13}C{^{1}H} NMR (75 MHz, CD$_2$Cl$_2$) δ 153.5 (d, J = 27.5 Hz), 148.40(d, J = 6.9 Hz), 140.0 (d, J = 18.2 Hz), 136.2 (s), 134.6 (d, J = 25.7 Hz), 134.4 (d, J = 16.6 Hz), 131.1 (d, J = 26.1 Hz), 128.7 (d, J = 32.7 Hz), 127.9 (d, J = 4.9 Hz), 126.3 (s), 59.1 (s), 24.31 (s), 20.0 (s), 13.9 (s).

^{31}P{^{1}H} NMR (121 MHz, CD$_2$Cl$_2$) δ -9.7.

EA Found: C 63.13, H 9.77, S 6.93, N 3.26.

Calculated for C$_{66}$H$_{120}$N$_3$O$_9$PS$_3$:   C 64.61, H 9.86, S 7.84, N 3.43.

The compound could not be purified by crystallisation or chromatographically.

9.2.13.   Synthesis of [NBu$_4$]$_3$[*o,m,m*-TPPTS(OMe)] 15
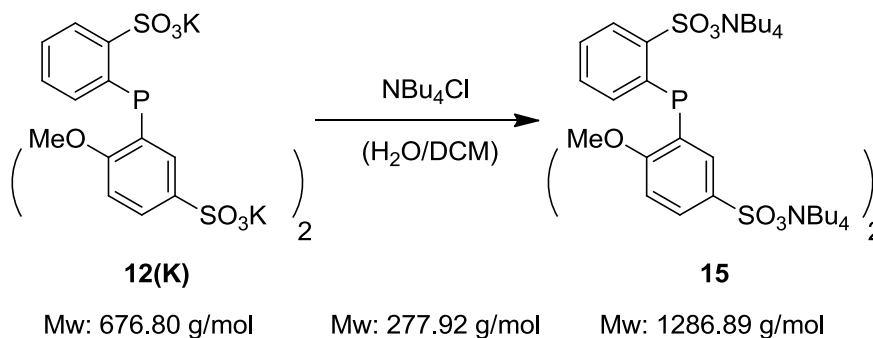
Scheme 52: *Synthesis of the [NBu$_4$]$_3$[o,m,m-TPPTS(OMe)] salt* **15**.

12(K) (0.50 g, 0.74 mmol, 1 eq.) and NBu$_4$Cl (0.62 g, 2.23 mmol, 3 eq.) were dissolved in water (15 mL). Methylene chloride (15 mL) was added and the reaction was vigorously stirred for 2 h to extract the desired ammonium salt. After separation of the organic phase the volatiles were removed *in vacuo* and **15** was obtained as a fine colourless powder (577 mg, increasing phosphine oxide concentration over time, 1,25 equivalents of excess NBu$_4$Cl determined by NMR spectroscopy).

^{1}H NMR (300 MHz, CD$_2$Cl$_2$) δ 8.05 – 7.83 (m, 4H), 7.43 – 7.31 (m, 1H), 7.25 – 7.14 (m, 2H), 6.91 – 6.79 (m, 1H), 3.64 (s, 6H), 3.33 – 3.09 (m, 35H), 1.72 – 1.50 (m, 35H), 1.45 – 1.23 (m, 37H), 0.94 (t, *J* = 7.3 Hz, 54H), 0.37 (s, 1H), 0.31 (d, *J* = 3.4 Hz, 1H).

^{31}P{^{1}H} NMR (121 MHz, CD$_2$Cl$_2$) δ 18.7 (s).

EA Found: C 61.72, H 10.24, S 6.21, N 3.59.

Calculated for C$_{68}$H$_{124}$N$_3$O$_{11}$PS$_3$:   C 63.47, H 9.71, S 7.47, N 3.27.

15 could not be purified by crystallisation or chromatographically and shows rapid oxidation in solution. Therefore ^{13}C NMR spectroscopy was not performed.

9. Experimental Part

9.2.14. Synthesis of [K(18-crown-6][*o*-TPPMS] 16a

Scheme 53: *Synthesis of the [K(18-crown-6)][o-TPPMS] salt **16a**.*

9a(K) (2.44 g, 6.41 mmol, 1 eq.) and freshly sublimed 18-crown-6 (1.69 g, 6.41 mmol, 1 eq.) were suspended in 35 mL methylene chloride and stirred over night. After filtration through a Whatman filter and evaporation of the solvent **16b** was obtained as a white powder (4.26 g, 6.35 mmol, 1.1 eq. coordinated 18-crown-6, 99%) with 87.7% purity as determined by ^{31}P NMR spectroscopy.

^{1}H NMR (300 MHz, CD$_2$Cl$_2$) δ 8.11 (m, 1H), 7.42 – 7.15 (m, 12H), 7.04 (m, 1H), 3.56 (s, 27H).

^{13}C{^{1}H} NMR (75 MHz, CD$_2$Cl$_2$) δ 152.7 (d, *J (C-P)* = 27.1 Hz), 139.9 (d, *J (C-P)* = 14.5 Hz), 135.9 (d, *J (C-P)* = 2.4 Hz), 135.0 (d, *J (C-P)* = 23.2 Hz), 134.2 (s), 133.9 (s), 129.4 (s), 128.9 (s), 128.5 (d, *J* = 6.1 Hz), 128.3 (s), 128.0 (d, *J (C-P)* = 5.1 Hz), 70.5 (s).

^{31}P{^{1}H} NMR (121 MHz, CD$_2$Cl$_2$) δ -9.0 (s).

EA Found: C 54.55, H 6.02, S 4.45.

Calculated for C$_{30}$H$_{38}$KO$_9$PS: C 55.89, H 5.94, S 4.97.

The compound could not be purified by crystallisation or chromatographically.

9. Experimental Part

9.2.15. Synthesis of [K(18-crown-6)]₂[*rac-o,m*-TPPDS] 16b
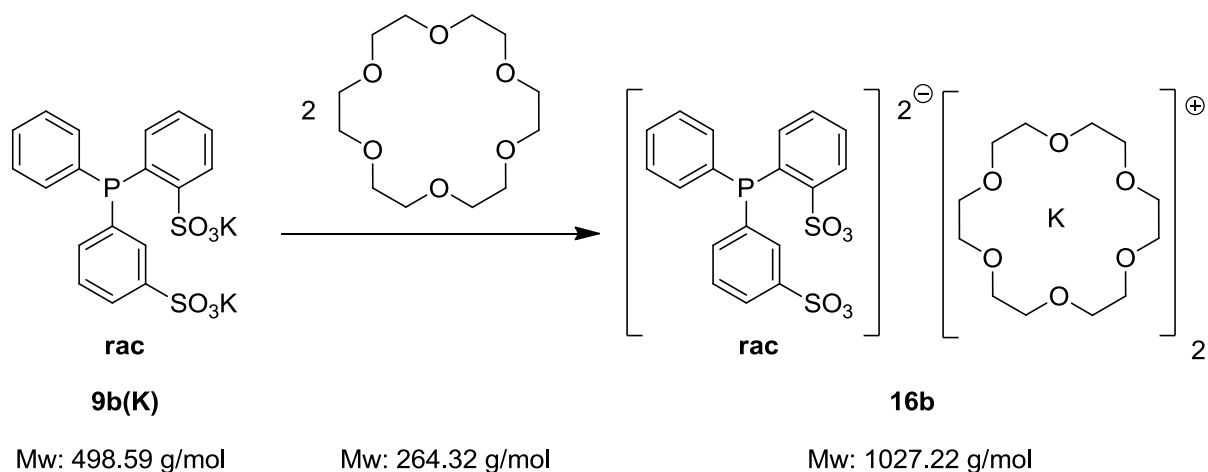
Scheme 54: *Synthesis of the [K(18-crown-6)]₂[rac-o,m-TPPDS] salt **16b**.*

9b(K) was dried at 120 °C *in vacuo* and weighed (1.50 g, 3.01 mmol, 1 eq.). Sublimed 18-crown-6 (1.59 g, 6.02 mmol, 2 eq.) was added in a glovebox to the potassium salt of the phosphine. The mixture was suspended in methylene chloride (50 mL) and stirred overnight. After filtration through a Whatman filter, the volatiles were removed from the solution and **16b** was obtained as a colourless powder (2.89 g, 2.55 mmol, 0.4 eq. additional coordinated 18-crown-6, $Mw_{corrected}$= 1132.95 g·mol^{-1}, 85%).

^{1}H NMR (300 MHz, CD₂Cl₂) δ 8.09 (m, 1H), 7.95 (m, 1H), 7.76 (m, 1H), 7.35 − 7.15 (m, 8H), 7.10 − 7.03 (m, 2H), 3.53 (s, 57H).

^{13}C{^{1}H} NMR (75 MHz, CD₂Cl₂) δ 152.8 (d, ^1J *(C-P)* = 27.3 Hz), 147.7 (d, ^3J *(C-P)* = 7.9 Hz), 139.9 (d, *J (C-P)* = 14.2 Hz), 139.5 (d, *J (C-P)* = 16.7 Hz), 136.1 (d, *J (C-P)* = 2.5 Hz), 135.0 (d, *J (C-P)* = 23.5 Hz), 134.6 (d, *J (C-P)* = 11.7 Hz), 134.0 (d, *J (C-P)* = 19.4 Hz), 131.7 (d, *J (C-P)* = 29.2 Hz), 129.4 (s), 128.8 (s), 128.4 (d, *J (C-P)* = 6.1 Hz), 128.2 (s), 128.1 (d, *J (C-P)* = 3.6 Hz), 128.0 (d, *J (C-P)* = 6.1 Hz), 126.4 (s), 70.4 (s).

^{31}P{^{1}H} NMR (121 MHz, CD₂Cl₂) δ -9.3 (s).

EA Found: C 48.14, H 6.21, S 5.02.

Calculated for C₄₂H₆₁K₂O₁₈PS₂: C 49.11, H 5.99, S 6.24.

The compound could not be purified by crystallisation or chromatographically.

9.2.16. Synthesis of [Na(15-crown-5)]₃[*o,m,m*-TPPTS] 16c
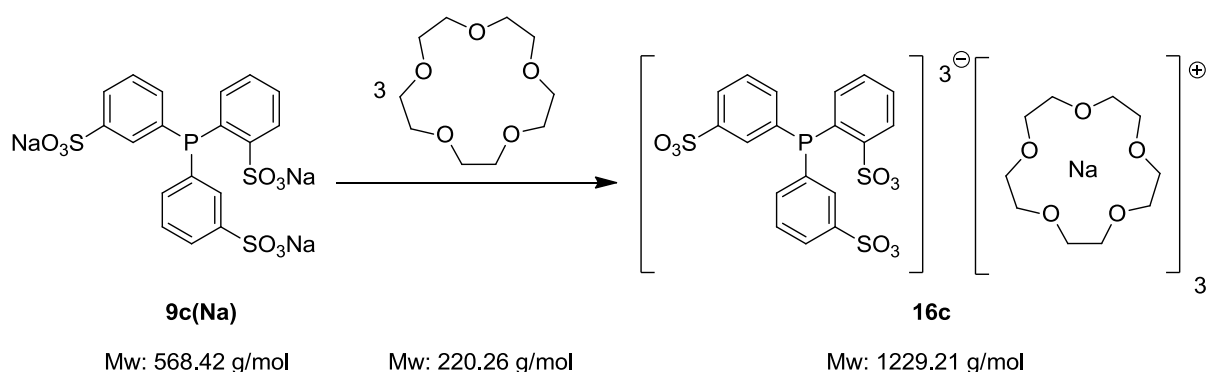
Scheme 55: Synthesis of the [Na(15-crown-5)]₃[o,m,m-TPPTS] salt **16c**.

9c(Na) was dried at 120 °C *in vacuo* and weighed (483 mg, 0.850 mmol). 15-crown-5 (0.7 mL, ρ = 1.11 g/mL, 0.779 mg, 3.54 mmol) was added together with methylene chloride (20 mL) and the suspension was stirred overnight. The reaction was extracted with water (20 mL) and the organic phase was separated followed by the removal of volatiles *in vacuo*. **16c** was obtained as a colourless powder (535 mg, 3.25 additionally coordinated 15-crown-5 units, $Mw_{corrected}$ 1945 g·mol⁻¹, 0.275 mmol, 32%) in 87.3% purity as determined by ³¹P NMR spectroscopy.

¹H NMR (300 MHz, CD₂Cl₂) δ 8.06 (ddd, *J* = 7.5, 4.0, 1.4 Hz, 1H), 7.99 (dt, *J* = 8.8, 1.4 Hz, 2H), 7.77 – 7.72 (m, 2H), 7.35 – 7.29 (m, 1H), 7.24 (dd, *J* = 10.4, 4.5 Hz, 3H), 7.09 (ddd, *J* = 7.6, 3.3, 1.2 Hz, 1H), 7.00 (ddt, *J* = 7.6, 5.0, 1.4 Hz, 2H), 3.58 (s, 140H).
³¹P{¹H} NMR (121 MHz, CD₂Cl₂) δ -10.20 (s).

EA Found: C 49.27, H 6.91, S 4.52.

Calculated for C₄₈H₇₂Na₃O₂₄PS₃: C 46.90, H 5.90, S 7.83.

The compound could not be purified by crystallisation or chromatographically.

9. Experimental Part

9.2.17. Synthesis of [K(18-crown-6)]₃[*o,m,m*-TPPMS(OMe)] 17

12(K)   **17**

Mw: 676.80 g/mol   Mw: 264.32 g/mol   Mw: 1469.74 g/mol
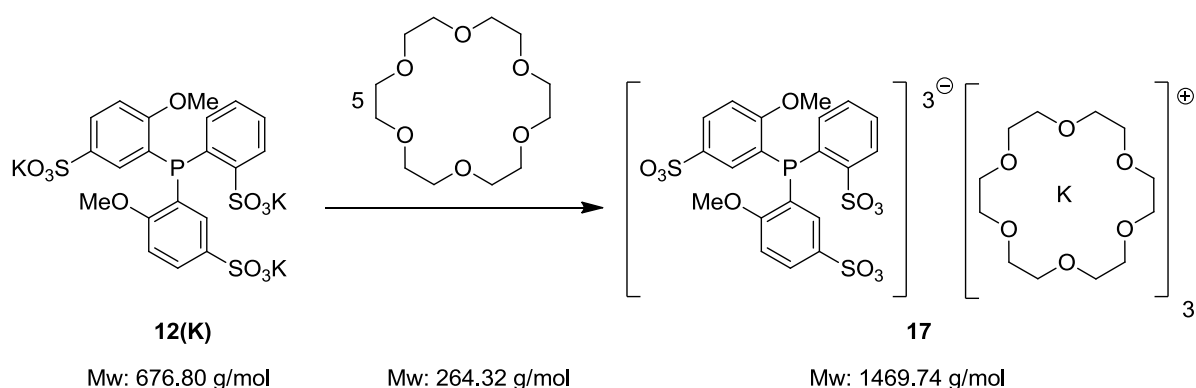
Scheme 56: *Synthesis of the [K(18-crown-6)]₃[o,m,m-TPPTS(OMe)] salt 17.*

12(K), dried at 100 °C *in vacuo* (0.502 g, 0.742 mmol, 1 eq.) and freshly sublimed 18-crown-6 (0.590 g, 2.23 mmol, 3 eq.) were suspended in methylene chloride (20 mL) and the reaction was stirred overnight. After filtration through a Whatman filter and removal of volatiles from the solution *in vacuo* **17** (1.12 g, 0.75 additionally coordinated 18-crown-6 units, $Mw_{corrected}$= 1668 g·mol⁻¹, 69.2% phosphine content, determined by ³¹P NMR spectroscopy) was obtained as a colourless powder. Oxidation was observed in solution (rapid) and solid state with prolonged standing (slow).

¹H NMR (300 MHz, CD₂Cl₂) δ 8.13 (d, *J* = 8.7 Hz, 1H), 8.02 (dd, *J* = 7.5, 4.2 Hz, 1H), 7.68 – 7.62 (m, 2H), 7.23 – 7.19 (m, 2H), 7.07 – 7.01 (m, 2H), 6.70 (dd, *J* = 8.5, 4.0 Hz, 2H), 3.83 – 3.27 (m, 115H). (Oxide peaks disregarded and 18-crown-6 peak reduced accordingly)

³¹P{¹H} NMR (121 MHz, CD₂Cl₂) δ 35.0 (s, 44%), -21.5 (s, 100%).

EA Found: C 43.68, H 6.27, S 5.70.

Calculated for C₅₆H₈₈K₃O₂₉PS₃: C 45.76, H 6.03, S 6.55.

The compound could not be purified by crystallisation or chromatographically. Due to the oxidation reaction ¹³C NMR analysis was not performed.

9. Experimental Part

9.2.18. Synthesis of (COD)PdCl$_2$
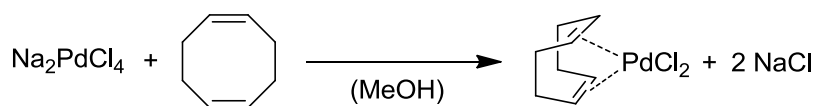
Mw: 294.21 g/mol; 108.18 g/mol   Mw: 285.51 g/mol

Scheme 57: *Synthesis of (COD)PdCl$_2$*

Na$_2$PdCl$_4$ (6.06 g, 20.6 mmol, 1 eq.) was dissolved in methanol (350 mL). 1,5-Cyclooctadiene (8 mL, ρ = 0.882 g/mL, 7.06 g, 65.3 mmol, 3.2 eq.) was added to the solution, immediately causing the precipitation of a bright yellow solid. The reaction mixture was stirred for 2 h and the product was isolated by filtration, subsequent washing with water, MeOH and hexane (twice each) and recrystallisation from refluxing glacial acetic acid (750 mL). (COD)PdCl$_2$ was received as orange needles (4.32 g, 15.1 mmol, 73%) after drying *in vacuo*.

^{1}H NMR (300 MHz, CDCl$_3$) δ 6.32 (s, 4H), 2.92 (d, *J* = 11.6 Hz, 4H), 2.71 – 2.39 (m, 4H).
^{13}C{^{1}H} NMR (75 MHz, CDCl$_3$) δ 116.8, 31.1.

EA Found:	C 33.67, H 4.28, Cl 24.83.
Calculated for C$_8$H$_{12}$Cl$_2$Pd:	C 33.65, H 4.24, Cl 24.84.

9.2.19. Synthesis of (COD)PdMeCl
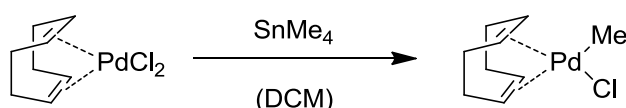
Mw: 285,51 g/mol   Mw: 265,09 g/mol

Scheme 58: *Synthesis of (COD)PdMeCl.*

(COD)PdCl$_2$ (4.32 g, 15.1 mmol, 1 eq.) was suspended in methylene chloride (60 mL) and SnMe$_4$ (2.3 mL, ρ = 1.29 g/mL, 2.97 g, 16.6 mmol, 1.1 eq.) was added under exclusion of light followed by stirring of the reaction for 2 days. The solvent was evaporated without external heating to prevent the decomposition of the product and the residue was suspended again in methylene chloride (50 mL) followed by addition of one equivalent of SnMe$_4$. After stirring overnight a colourless solution with minor amounts of palladium black was obtained,

indicating full conversion. The solution was filtered through Celite to remove the Pd(0), and the volatiles were removed *in vacuo* without external cooling and the colourless residue was thoroughly washed with diethyl ether and pentane (each three times, 20 mL) to remove organo-tin residues. The colourless light and temperature sensitive product (3.99 g, 15,1 mmol, quantitative yield) was stored at -20 °C in a glovebox fridge and showed to be stable for several months.

^{1}H NMR (300 MHz, CDCl$_3$) δ 5.96 – 5.80 (m, 2H), 5.21 – 5.00 (m, 2H), 2.71 – 2.32 (m, 8H), 1.15 (s, 3H).

^{13}C{^{1}H} NMR (75 MHz, CDCl$_3$) δ 124.0, 101.0, 31.1, 27.8, 12.5.

EA found   C 40.63, H 5.76.

Calculated for C$_9$H$_{15}$ClPd: C 40.78, H 5.70.

9.2.20. Synthesis of [K(18-crown-6)][(*o*-TPPMS)PdMeCl] 19
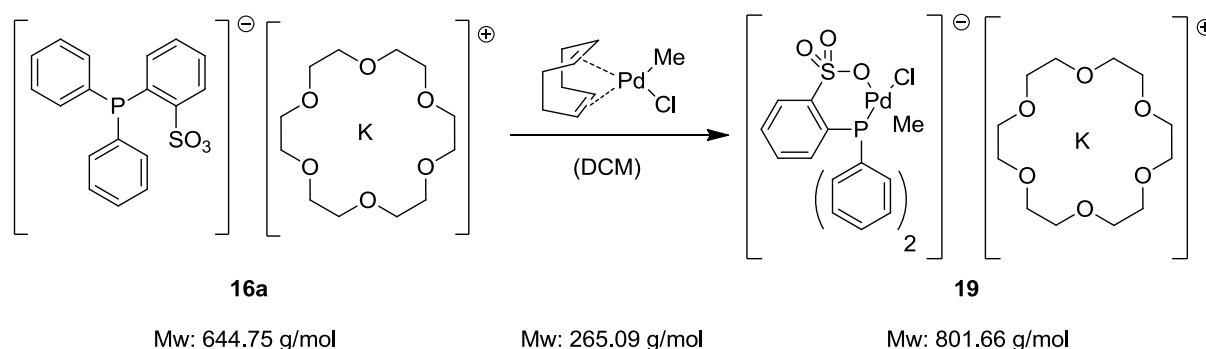
Scheme 59: *Synthesis of [K(18-crown-6)][(o-TPPMS)PdMeCl] 19.*

16a (1.29 g, 2.00 mmol, 1 eq.) and (COD)PdMeCl (530 mg, 2.00 mmol, 1 eq.) were dissolved in methylene chloride (20 mL) and the reaction mixture was stirred overnight under exclusion of light. Subsequently the volatiles were removed at reduced pressure, the solid residue was washed twice with pentane (10 mL each) and the obtained complex **19** was recrystallised from DCM/pentane at 4 °C. After filtration the product was obtained as a white powder (1.17 g, 1.46 mmol, 73%).

^{1}H NMR (300 MHz, CD$_2$Cl$_2$) δ 8.00 (m, 1H), 7.55 – 7.18 (m, 12H), 6.91 (m, 1H), 3.47 (s, 24H), 0.44 (d, ^3J *(H-P)* = 3.4 Hz, 3H).

^{13}C{^{1}H} NMR (75 MHz, CD$_2$Cl$_2$) δ 150.1 (d, *J (C-P)* = 14.0 Hz), 135.3 (d, *J (C-P)* = 1.4 Hz), 134.9 (d, *J (C-P)* = 12.5 Hz), 131.6 (d, *J (C-P)* = 52.5 Hz), 130.9 (d, *J (C-P)* = 2.4 Hz), 130.8 (d, *J (C-P)* = 2.1 Hz), 130.4 (d, *J (C-P)* = 41.0 Hz), 130.0 (d, *J (C-P)* = 6.3 Hz), 128.8 (d, *J (C-P)* = 11.0 Hz), 128.3 (d, *J (C-P)* = 7.5 Hz), 70.5 (s), -2.5 (s).

^{31}P NMR (121 MHz, CD$_2$Cl$_2$) δ +26.6.

EA Found: C 46.13, H 5.12, S 3.60.

Calculated for C$_{31}$H$_{41}$KO$_9$PPdClS: C 46.44, H 5.15, S 4.00.

Calculated for C$_{31}$H$_{41}$KO$_9$PPdClS × 0.1 DCM: C 46.11, H 5.13, S 3.96.

9.2.21. Synthesis of [K(18-crown-6)]$_2$[(*rac-o,m*-TPPDS)PdMeCl] 20
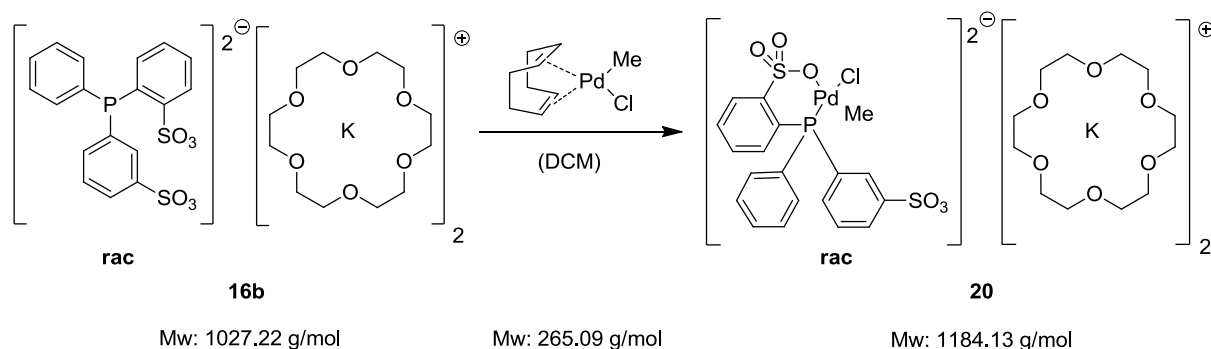
Scheme 60: *Synthesis of [K(18-crown-6)]$_2$[(rac-o,m-TPPDS)PdMeCl] 20.*

16b (1.72 g, Mw$_{corrected}$ = 1132.95 g·mol^{-1}, 1.52 mmol, 1 eq.) and (COD)PdMeCl (398 mg, 1.50 mmol, 1 eq.) were dissolved in methylene chloride (15 mL) and the reaction mixture was stirred over night under exclusion of light. The volatiles were removed at reduced pressure and the solid residue washed twice with pentane (10 mL each). Complex **20** was recrystallised twice from methylene chloride/pentane and obtained after filtration as a white powder (1.42 g, 1.20 mmol, 80%).

^{1}H NMR (500 MHz, CD$_2$Cl$_2$) δ 8.07 (m, 1H), 8.03 (m, 1H), 7.94 (m, 1H), 7.64 (m, 2H), 7.46 (m, 2H), 7.36 (m, 5H), 7.06 (m, 1H), 3.54 (s, 48H), 0.53 (d, ^{3}*J (H-P)* = 3.2 Hz, 3H).

^{13}C{^{1}H} NMR (75 MHz, CD$_2$Cl$_2$) δ 150.1 (d, *J (C-P)* = 14.0 Hz), 148.4 (d, *J (C-P)* = 10.5 Hz), 135.6 (d, *J (C-P)* = 1.5 Hz), 135.5 (s), 135.4 (d, *J (C-P)* = 11.9 Hz), 135.4 – 135.2 (m), 132.0 – 131.5 (m), 131.3 (d, *J (C-P)* = 13.4 Hz), 131.3 – 130.8 (m), 131.0 (d, *J (C-P)* = 2.6

Hz), 130.8 (d, *J (C-P)* = 2.1 Hz), 130.7 − 129.8 (m), 130.2 (d, *J (C-P)* = 6.4 Hz), 129.0 − 128.9 (m), 128.9 − 128.8 (m), 128.4 − 128.3 (m), 128.2 (d, *J (C-P)* = 3.6 Hz).

$^{31}P\{^{1}H\}$ NMR (121 MHz, CD_2Cl_2) δ +27.4.

EA Found:	C 42.55, H 5.61, S 5.14
Calculated for $C_{43}H_{64}K_2O_{18}PPdS_2$:	C 43.62, H 5.45, S 5.42.
Calculated for $C_{43}H_{64}K_2O_{18}PPdS_2 \times 0.5$ DCM:	C 42.59, H 5.34, S 5.23.

9.2.22. Synthesis of [K(18-crown-6)]₃[{*o,m,m*-TPPTS(OMe)}PdMeCl] 22
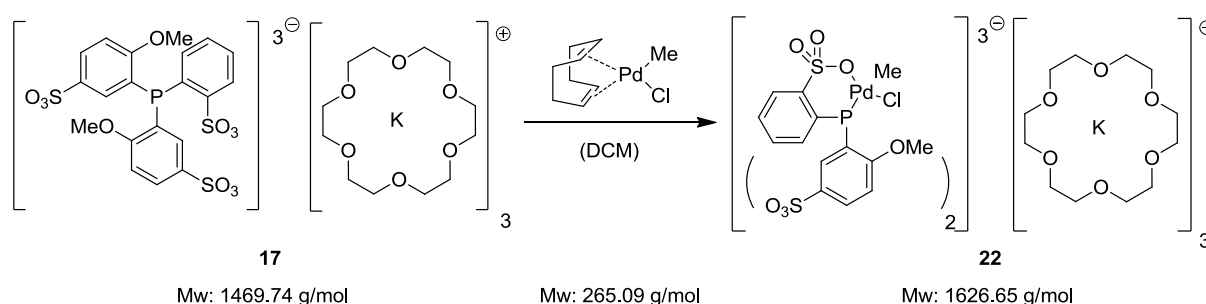
Scheme 61: *Synthesis of [K(18-crown-6)]₃[{o,m,m-TPPTS(OMe)}PdMeCl] 22*.

The mixture of **17** contaminated with the corresponding phosphine oxide (0.982 g, 69.2% purity of the phosphine as observed by ^{31}P NMR spectroscopy, 0.680 g Phosphine **17**, 1.5 additional equivalents of coordinated 18-crown-6, Mw$_{corrected}$ = 1866 g·mol^{-1}, 0.364 mmol, 1 eq.) and (COD)PdMeCl (0.106 g, 0.400 mmol, 1.1 eq) were dissolved in methylene chloride (10 mL) and the reaction mixture was stirred overnight under exclusion of light. Subsequently the solvent was removed at reduced pressure without external heating to prevent decomposition of the formed complex and the residue was washed with pentane. The colourless solid was precipitated twice from methylene chloride (10 mL each) by addition of pentane (20 mL each). The solution was decanted, the remaining oil dried *in vacuo* and **22** was obtained as a colourless powder (0.474 g, 63.7% content of **22** as observed by ^{31}P NMR spectroscopy, 1.3 additionally coordinated 18-crown-6 units).

^{1}H NMR (300 MHz, CD_2Cl_2) δ 8.24 − 8.15 (m, 2H), 7.99 − 7.89 (m, 2H), 7.76 − 7.64 (m, 1H), 7.38 − 7.14 (m, 4H), 7.07 (dd, *J* = 8.4, 5.7 Hz, 1H), 6.87 (dd, *J* = 8.4, 4.0 Hz, 2H), 3.66 (s, 6H), 3.56 (s, 128H), 0.24 (d, *J* = 3.7 Hz, 3H).

$^{31}P\{^1H\}$ NMR (121 MHz, CD$_2$Cl$_2$) δ +21.3 (s).

| EA Found: | C 41.06, H 5.85, S 5.47. |
| Calculated for C$_{57}$H$_{91}$O$_{29}$ PS$_3$PdClK$_3$: | C 42.09, H 5.64, S 5.91. |

The compound could not be purified by crystallisation or chromatographically. The free phosphine **17** shows rapid oxidation in solution oxidation.

9.2.23. Synthesis of [NBu$_4$]$_2$[(*rac-o,m*-TPPDS)PdMeCl] 23
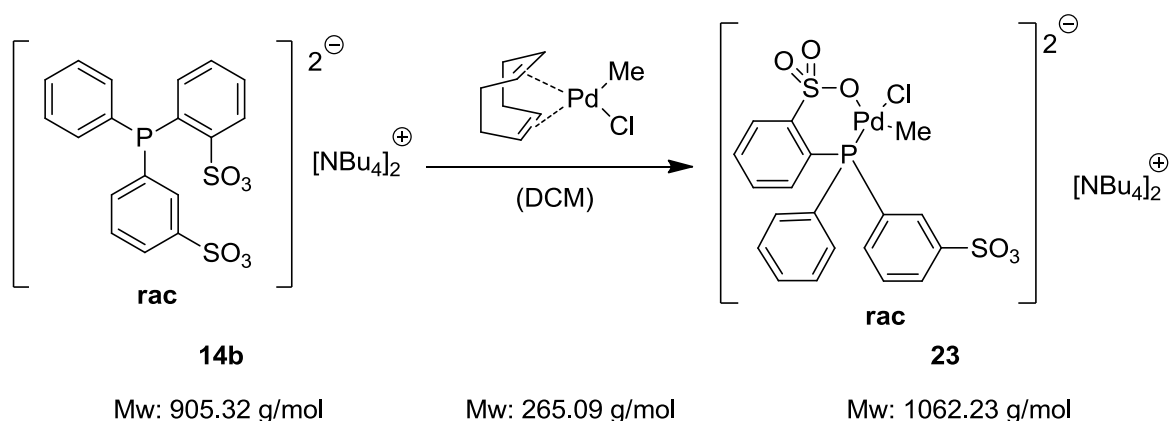
Scheme 62: *Synthesis of [NBu$_4$]$_2$[(rac-o,m-TPPDS)PdMeCl]* **23**.

14b (409 mg, 0.45 mmol) and (COD)PdMeCl (120 mg, 0.45 mmol) were dissolved in methylene chloride (10 mL) and the reaction mixture was stirred overnight under exclusion of light. The volatiles were removed *in vacuo* without heating (vide supra), the crude product was washed with pentane and precipitated from in methylene chloride solution (10 mL) by addition of pentane (20 mL). After decanting of the solution the oily residue was dried *in vacuo* providing **23** as a colourless solid (375 mg, contaminated by residual COD).

^{1}H NMR (300 MHz, CD$_2$Cl$_2$) δ 8.08 – 8.00 (m, 1H), 7.94 – 7.81 (m, 2H), 7.59 (dt, J = 17.3, 6.8 Hz, 2H), 7.53 – 7.28 (m, 8H), 7.05 (t, J = 8.3 Hz, 1H), 3.18 (dd, J = 21.2, 12.6 Hz, 16H), 1.61 (dt, J = 15.8, 7.8 Hz, 16H), 1.45 – 1.24 (m, 16H), 0.94 (t, J = 7.3 Hz, 24H), 0.48 (d, J = 3.4 Hz, 3H).

$^{31}P\{^1H\}$ NMR (121 MHz, CD$_2$Cl$_2$) δ +26.7 (s).

EA Found:	C 59.54, H 8.54, S 5.22, N 2.54.
Calculated for C$_{51}$H$_{88}$O$_6$N$_2$S$_2$PPdCl:	C 57.67, H 8.35, S 6.04, N 2.64.
Calculated for C$_{51}$H$_{88}$O$_6$N$_2$S$_2$PPdCl × 0.5 COD:	C 59.18, H 8.49, S 5.51, N 2.51.

9. Experimental Part

9.2.24. Synthesis of [NBu₄]₃[(*o,m,m*-TPPTS)PdMeCl] 24
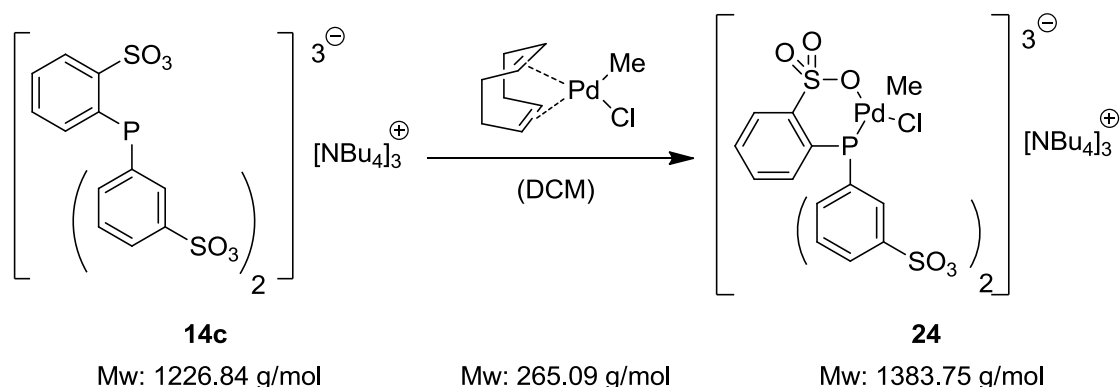
Scheme 63: *Synthesis of [NBu₄]₃[(o,m,m-TPPTS)PdMeCl] 24*.

14c (1.02 g, 0.830 mmol, 1 eq.) and (COD)PdMeCl (0.220 g, 0.830 mmol, 1 eq.) were added to a Schlenk tube in a glovebox. Methylene chloride (30 mL) was added and the reaction mixture was stirred over night under exclusion of light. The volatiles were removed *in vacuo* without external heating to prevent decomposition of the formed complex. **24** was washed twice with pentane and the fine colourless powder was dried *in vacuo* (1.09 g, 0.786 mmol, 95%, two similar coordinated phosphine species ratio 84.0:16.0%, compare Section 5.6).

^{1}H NMR (300 MHz, CD₂Cl₂) δ 7.97 (ddd, J = 7.6, 4.1, 1.3 Hz, 1H), 7.89 – 7.77 (m, 3H), 7.44 – 7.22 (m, 7H), 7.01 – 6.91 (m, 1H), 3.09 (dd, J = 21.4, 12.9 Hz, 24H), 1.53 (dq, J = 11.8, 7.7 Hz, 24H), 1.33 – 1.15 (m, 25H), 0.84 (q, J = 7.0 Hz, 37H), 0.46 (d, J = 3.4 Hz, 2H), 0.49 – 0.38 (m, 2.45H), 0.40 (d, J = 3.3 Hz, 0.55H).

^{31}P{^{1}H} NMR (121 MHz, CD₂Cl₂) δ +27.0 (s, large), +26.6 (s, small).

EA Found: C 58.00, H 9.04, S 5.74, N 2.90.

Calculated for C₆₇H₁₂₃O₉N₃S₃PPdCl: C 58.15, H 8.96, S 6.95, N 3.04.

The compound could not be purified by crystallisation or chromatographically.

9. Experimental Part

9.2.25.   Synthesis of [NBu$_4$]$_3$[{*o,m,m*-TPPTS(OMe)}PdMeCl] 25
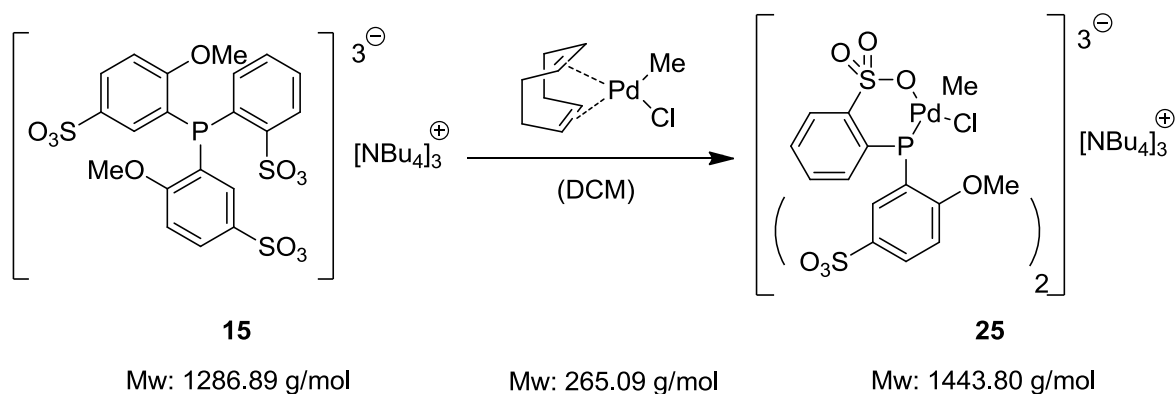
Scheme 64: *Synthesis of [NBu$_4$]$_3$[(o,m,m-TPPTS(OMe)PdMeCl)] 25*.

15 (431 mg, 0.34 mmol, impurities disregarded) and (COD)PdMeCl (89.6 mg, 0.34 mmol, 1 eq.) were dissolved in methylene chloride (10 mL) and the reaction mixture was stirred overnight under exclusion of light. The volatiles were removed *in vacuo* without external heating to prevent decomposition of the formed complex. Subsequently the crude product was washed with pentane, the obtained powder redissolved in methylene chloride (10 mL) and precipitated by addition of pentane (20 mL). After decanting the solvent the obtained oily residue was dried *in vacuo*, providing **25** as a colourless solid (329 mg, two similar coordinated phosphine species ratio 88.5/11.5%, low oxide content, 0.25 eq NBu$_4$ containing impurities).

^{1}H NMR (300 MHz, CD$_2$Cl$_2$) δ 8.05 – 7.83 (m, 4H), 7.43 – 7.31 (m, 1H), 7.25 – 7.14 (m, 2H), 6.91 – 6.79 (m, 1H), 3.64 (s, 6H), 3.33 – 3.09 (m, 35H), 1.72 – 1.50 (m, 35H), 1.45 – 1.23 (m, 37H), 0.94 (t, *J* = 7.3 Hz, 54H), 0.37 (s, 0.45H), 0.31 (d, *J* = 3.4 Hz, 2.55H).

^{31}P{^{1}H} NMR (121 MHz, CD$_2$Cl$_2$) δ +18.7 (s, large), +17.3 (s, small).

EA Found: C 56.79, H 9.11, S 5.39, N 3.50.

Calculated for C$_{69}$H$_{127}$N$_3$O$_{11}$S$_3$PPdCl: C 57.40, H 8.87, S 6.66, N 2.91.

The compound could not be purified by crystallisation or chromatographically.

9.2.26. Investigation on the COD insertion on anionic phosphine sulphonate-based Pd(II) complexes
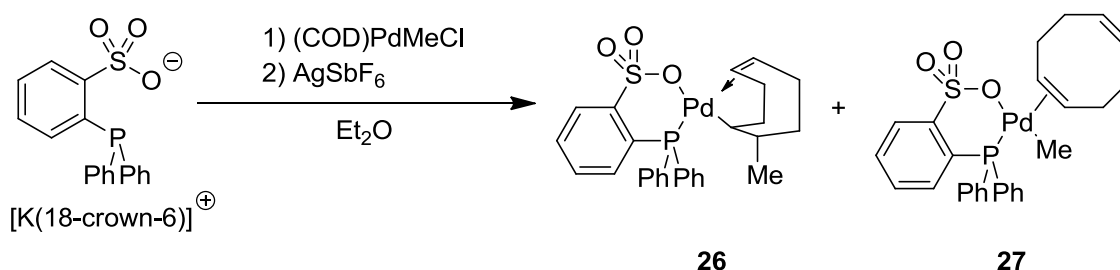
Scheme 65: *Insertion of COD into the Pd-Me bond after chloride abstraction without presence of a stabilizing base.*

[K(18-crown-6)][*o*-TPPMS] (190 mg, 0.29 mmol, 1 eq.) and (COD)PdMeCl (78.1 mg, 0.29 mmol, 1 eq.) were weighed in a glovebox and dissolved in methylene chloride (5 mL). After addition of 0.1 mL diethyl ether for stabilisation of reaction intermediates, AgSbF₆ (111,4 mg, 0.32 mmol, 1.1 eq.) was added causing immediate precipitation of AgCl. The reaction mixture was stirred overnight at 30 °C under exclusion of light. After filtration the volatiles were removed from the filtrate at reduced pressure and the obtained colourless solid was washed with pentane (2 · 10 mL). The product contains a mixture of **26** and **27** as observed from multinuclear and multidimensional NMR spectroscopy (Section 5.6). Fractional crystallisation of the compounds was not successful.

Characteristic signals:

26: ^{1}H NMR (300 MHz, CD$_2$Cl$_2$) δ 0.29 (d, ^1J (H-H) = 7.0 Hz, 3H).

^{31}P{^{1}H} NMR (121 MHz, CD$_2$Cl$_2$) δ +14.5 (s, sharp).

27: ^{31}P{^{1}H} NMR (121 MHz, CD$_2$Cl$_2$) δ +31.1 (broad).

9. Experimental Part

9.2.27. Chloride abstraction and pyridine stabilisation based on the anionic phosphine sulphonate-based Pd(II) complexes 19 and 20

19: Ar = Ph
20: Ar = [K(18-crown-6)]-3-SO$_3$Ph

28: Ar = Ph
29: Ar = [K(18-crown-6)]-3-SO$_3$Ph

19: Mw: 801.66 g/mol   1) Mw: 343.62 g/mol   **28**: Mw: 541.90 g/mol
20: Mw: 1184.13 g/mol   2) Mw: 79.10 g/mol   **29**: Mw: 924.36 g/mol
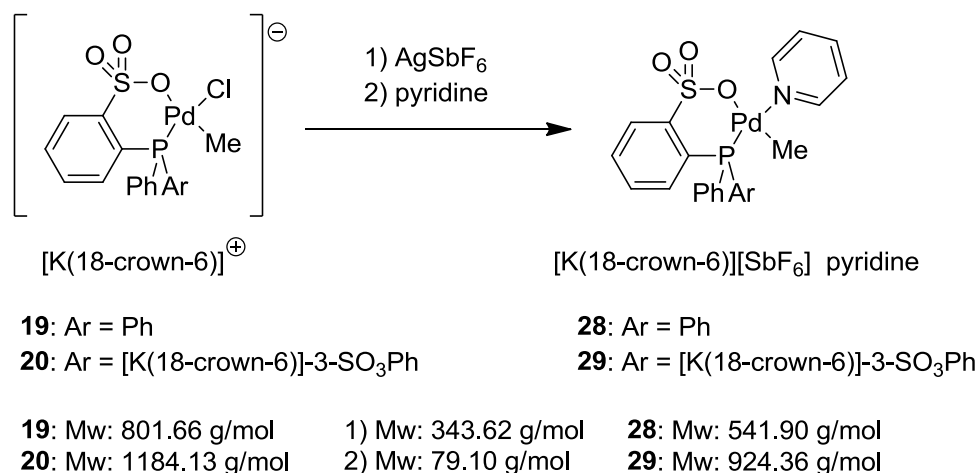
Scheme 66: *Synthesis of the pyridine-stabilised phosphine sulphonate complexes 28 and 29.*

Synthesis of **28**:

19 (389 mg, 0.49 mmol, 1 eq.) and AgSbF$_6$ (183 mg, 0.53 mmol, 1.1 eq.) were weighed in a glove box, dissolved in methylene chloride (10 mL) and the reaction was stirred for 30 min. Subsequently pyridine (0.1 mL. excess) was added and the reaction was continued by stirring overnight in absence of light. After filtration the volatiles were removed from the filtrate *in vacuo* and the obtained solid was washed with pentane (10 mL). **28** (411 mg) was obtained with 1.5 eq. coordinated pyridine in addition to [K(18-crown6)]SbF$_6$. Fractional crystallisation was not successful and unambiguous assignment of all NMR signals was not achieved.

Characteristic signals:

^{1}H NMR (300 MHz, CD$_2$Cl$_2$) δ 0.52 (d, ^3J (H-P) = 2.5 Hz, 3H).

^{31}P NMR{^{1}H} (121 MHz, CD$_2$Cl$_2$) δ +28.8 (s).

Synthesis of **29**:

For exact procedure see above, **20** (307 mg, 0.26 mmol, 1 eq.), AgSbF$_6$ (98.0 mg, 0.29 mmol, 1.1 eq.), pyridine (0.1 mL, excess), **29** (357 mg, 2.5 eq. coordinated pyridine in addition to [K(18-crown6)]SbF$_6$. Fractional crystallisation was not successful.

Characteristic signals:

^{1}H NMR (300 MHz, CD$_2$Cl$_2$) δ 0.45 (d, ^3J (H-P) = 2.7 Hz, 3H).

^{31}P NMR{^{1}H} (121 MHz, CD$_2$Cl$_2$) δ +29.1 (s).

9. Experimental Part

9.2.28. Synthesis of [bis{κ²-(P,O)-2-(bis-2-methoxyphenylphosphine)benzene-sulphonate}Pd] 30
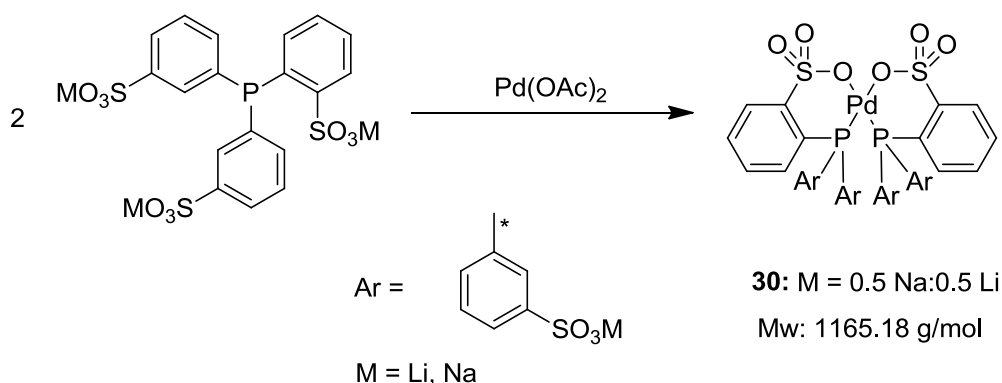
Scheme 67: *Synthesis of **30** as the Li:Na 1:1 cocrystallate.*

The hydride of **9c(M)** (40 mg) as the sodium salt with Li impurities was reacted with Pd(OAc)$_2$ (7.19 mg) in anhydrous MeOH (2 mL). Slow evaporation yielded yellow crystals of **30** suitable for determination of the molecular structure by X-ray diffraction (compare Section 5.8 and 9.4 for crystallographic data).

9.2.29. Synthesis of 2-(bis-2-thiomethylphenylphosphine)benzenesulphonic acid 33
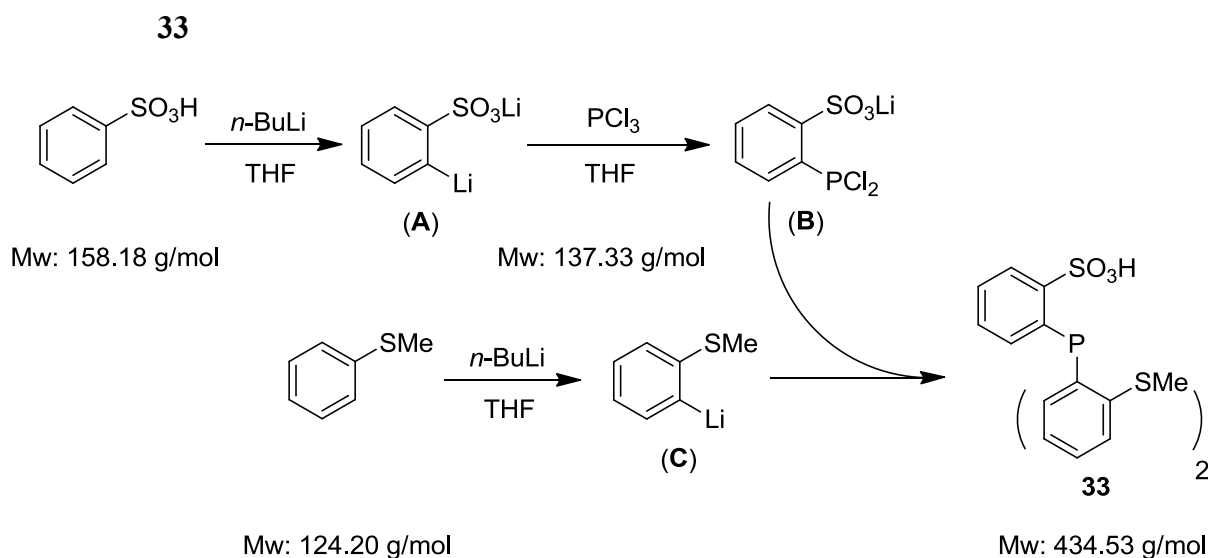
Scheme 68: *Synthesis of 2-(bis-2-thiomethylphenylphosphine)benzenesulphonic acid **33**.*

Benzenesulphonic acid (2.05 g, 13.0 mmol, 1 eq.) was dissolved in tetrahydrofurane (50 ml, Flask **A**), *n*-BuLi (13.0 ml, 26.0 mmol, 2,0 M in hexane, 2 eq.) was added at -78 °C and the

164

reaction was stirred for 3 h after warming to room temperature. PCl_3 (1.14 mL, 1.79 g, 13.0 mmol, 1 eq.) was added to a separate flask charged with tetrahydrofurane (80 mL, Flask **B**) at -78 °C and the contents of Flask **A** were slowly added *via* a dropping funnel at vigorous agitation. The obtained yellow solution was stirred for 1 h at -78 °C. Parallel a third flask charged with 2-bromo-thioanisole (5.30 g, 26.1 mmol, 2 eq.) and tetrahydrofurane (100 mL, Flask **C**) was cooled to -78 °C and *n*-BuLi (13.0 mL, 26.0 mmol, 2.0 M in hexane, 2 eq.) were added. The obtained orange solution was transferred by cannula to flask **B** and stirred 30 min at -78 °C followed by warming to room temperature. After stirring for 1 h termination of the reaction was achieved by addition of H_2O (5 mL) followed by removal of volatiles *in vacuo*. After washing with pentane (20 mL) and drying *in vacuo* the solid was dissolved in a mixture of methylene chloride (180 mL) and water (100 mL), acidified with an aqueous HCl solution (5 mL, 37%), for extraction. The aqueous phase was removed, extracted with methylene chloride (50 mL) and the combined organic phases were dried over $MgSO_4$. Subsequent removal of volatiles *in vacuo* provides an orange crude product mixture, which was washed with pentane (2·10 mL), tetrahydrofurane (3·10 mL) and Et_2O (2·10 mL). **33** was obtained as a yellow powder after drying at reduced pressure (3.49 g, 8.03 mmol, 62%) and is used as received despite a low content of residual impurities as purification by crystallisation could not be achieved.

^{1}H NMR (300 MHz, CD_2Cl_2) δ 8.34 – 8.17 (m, 1H), 7.85 – 7.59 (m, 4H), 7.46 (t, *J* = 7.1 Hz, 1H), 7.42 – 7.22 (m, 3H), 7.18 – 6.86 (m, 3H), 2.48 (s, 6H).
^{31}P{^{1}H} NMR (121 MHz, CD_2Cl_2) δ -8.4 (s, br).
^{31}P NMR (121 MHz, CD_2Cl_2) δ -8.4 (s, br).

High-res. ESI-MS (neg., MeCN):	m/z = 433.0164 (M⁻).
Calculated for $C_{20}H_{18}PS_3O_3$:	m/z = 433.0156 (M-H⁺).
Found:	C 54.37, H 4.78, S 20.02.
Calculated for $C_{20}H_{19}PS_3O_3$:	C 55.28, H 4.41, S 22.14.
Calculated for $C_{20}H_{19}PS_3O_3$ × 0.3 DCM × 0.5 THF:	C 54.34, H 4.82, S 19.56.

Due to a dynamic process on the NMR timescale the 13C NMR spectra could not be unambiguously assigned.

9. Experimental Part

9.2.30. Synthesis of [{κ²-(P,O)-2-(bis-2-thiomethylphenylphosphine)benzene-sulphonate}PdMe(pyridine)] 34
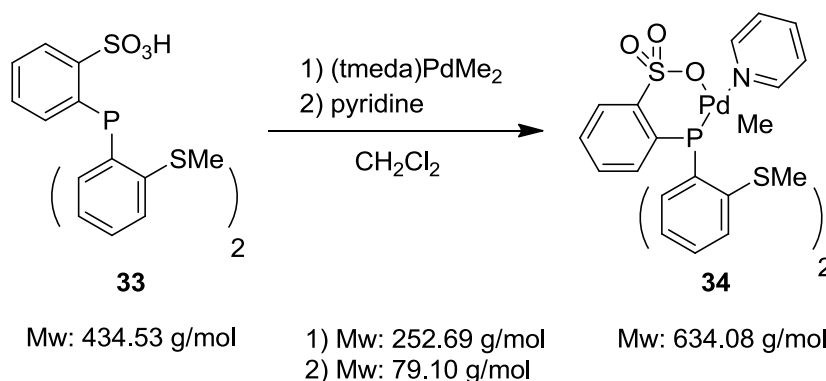
Scheme 69: *Synthesis of [{κ²-(P,O)-2-(bis-2-thiomethylphenyl-phosphine)benzene-sulphonate}PdMe(pyridine)] 34.*

The phosphine sulphonate **33** (348 mg, 0.80 mmol, 1 eq.) was dissolved in methylene chloride (10 mL) and (tmeda)PdMe$_2$ (202 mg, 0.80 mmol, 1 eq) was added. Evolution of gas was observed during formation of a yellow solution which was stirred for 30 min. Pyridine was added (0.5 mL, excess) and the solution turned orange. After stirring for 1 h at room temperature the solution was reduced to 5 mL and the complex precipitated by addition of Et$_2$O (20 mL). The liquid was removed by filtration and the obtained solid was re-precipitated from methylene chloride (10 mL)/Et$_2$O (20 mL). After filtration and removal of volatiles **7** was obtained as an off white solid (145 mg, 0.23 mmol, 29%). Crystallisation of this compound could not be achieved.

^{1}H NMR (500 MHz, CDCl$_3$) δ 8.88 (s, 1H), 8.40 (s, 1H), 7.85 (s, 1H), 7.67 – 7.08 (m, 10H), 2.42 (s, 4H), 0.69 (s, 2H).

^{31}P NMR (121 MHz, CD$_2$Cl$_2$) δ 34.5.

EA Found:	C 47.26, H 4.03, N 1.86, S 14.76.
Calculated for C$_{26}$H$_{26}$PNS$_3$O$_3$Pd:	C 49.25, H 4.13, N 2.21, S 15.17.
Calculated for C$_{26}$H$_{26}$PNS$_3$O$_3$Pd×0.3 CH$_2$Cl$_2$:	C 47.05, H 4.02, N 2.07, S 14.22.

9.2.31. Synthesis of 2-(bis-1-methoxynaphthalene-2-phosphine)benzene sulphonic acid 35
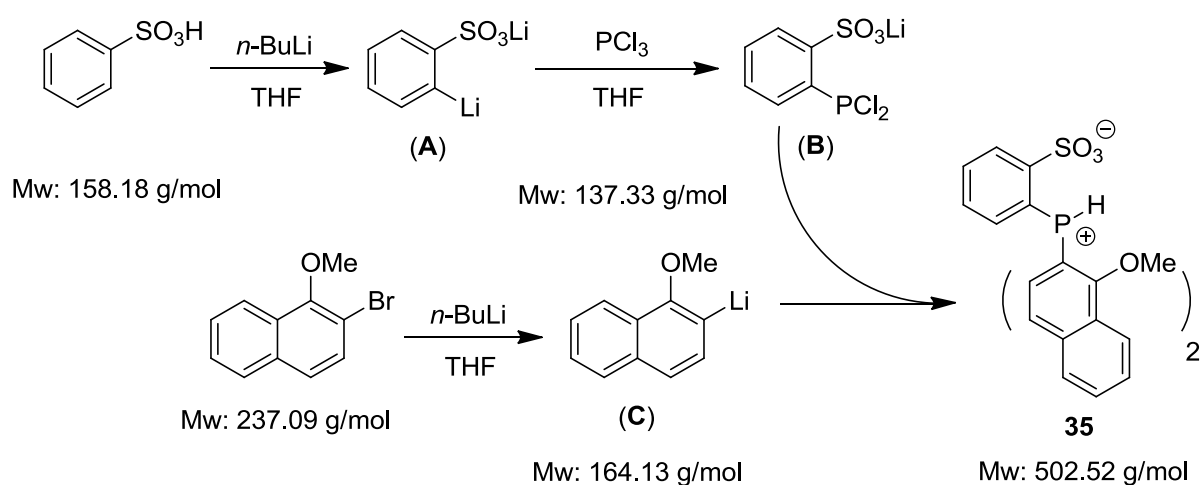
Scheme 70: *Synthesis of 2-(bis-1-methoxynaphthalene-2-phosphine)benzene sulphonic acid 35.*

Benzenesulphonic acid (1.27 g, 8.03 mmol, 1 eq.) was dissolved in tetrahydrofuran (40 ml, Flask **A**) and cooled to -78 °C followed by addition of *n*-BuLi (8.00 ml, 16.0 mmol, 2.0 M in cyclohexane, 2 eq). The obtained dark red solution was allowed to warm to room temperature over the course of 1 h and was stirred for 3 h. A solution of PCl_3 (0.70 mL, 1.10 g, ρ = 1.57 g/mL, 8.01 mmol, 1 eq.) in tetrahydrofuran (60 mL, Flask **B**) at -78 °C was prepared, the contents of Flask **A** were slowly added *via* dropping funnel upon vigorous agitation and the obtained yellow solution was stirred for 1 h. Parallel, a solution of (3.80 g, 16.0 mmol, 2 eq) 2-bromo-1-methoxy naphthalene in tetrahydrofuran (50 mL, Flask **C**) at -78 °C was prepared and *n*-BuLi (8.00 mL, 16.0 mmol, 2 M in cyclohexane, 2 eq.) was added dropwise. The obtained clear green solution was transferred by cannula to Flask **B** and stirred 30 min at -78 °C followed by warming to room temperature and stirring for 1 h. Termination of the reaction was achieved by addition of H_2O (5 mL) and removal of volatiles under reduced pressure. The obtained solid residue was dissolved in methylene chloride (150 mL) and H_2O (100 mL) and extracted after addition of aqueous HCl (5 mL, 37%). The aqueous phase was removed and reextracted with 50 mL of methylene chloride. Drying of the combined organic phases over $MgSO_4$ and removal of volatiles *in vacuo* provides the yellow crude product mixture, which was transferred into a Schlenk frit. Subsequent washing with tetrahydrofuran (3·10 mL), Et_2O (2·10 mL) and pentane (2·10 mL) provides enriched **35** as an off white

powder after drying under reduced pressure (1.67 g, 70% total phosphorus content). Crystallisation of the compound was not successful and was used as received for complexation.

Selected analytical data:

$^{31}P\{^1H\}$ NMR (121 MHz, CD_2Cl_2) δ 33.4 (2.3%), 24.0 (2.9%), -6.4 (11.8%), -20.5 (8.0%), -25.7 (100.0%), -42.3 (11.8%).

^{31}P NMR (121 MHz, CD_2Cl_2) δ -25.7 (d, ^1J (H-P) = 568.1 Hz).

High-res. ESI-MS (neg., MeCN):	m/z = 501.0931 (M⁻).
Calculated for $C_{28}H_{22}PSO_5$:	m/z = 501.0926 (M-H⁺).
EA Found:	C 64.90, H 5.02, S 5.93.
Calculated for $C_{28}H_{23}PSO_5$:	C 66.92, H 4.61, S 6.38.

9.2.32. Synthesis of [{κ²-(P,O)-2-(bis-1-methoxynaphthalene-2-phosphine)benzene sulphonate}PdMe(pyridine)] 39
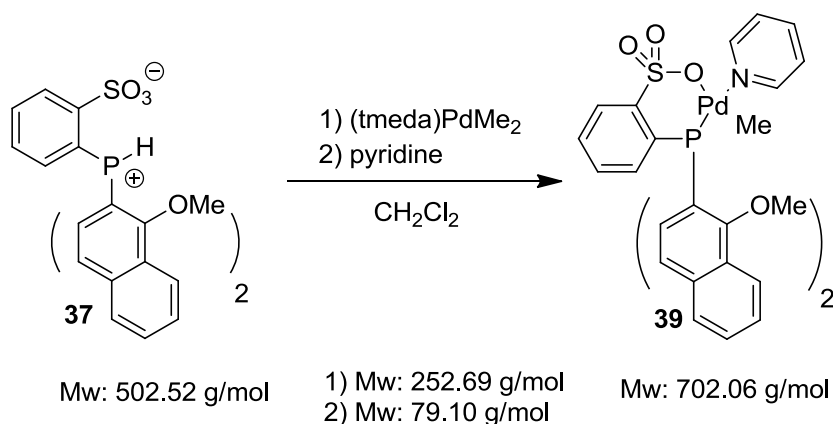
Scheme 71: *Synthesis of [{κ²-(P,O)-2-(bis-1-methoxynaphthalene-2-phosphine)benzene sulphonate}PdMe(pyridine)] 39.*

The phosphine sulphonate **35** (402 mg, 0.80 mmol, 1 eq.) was dissolved in methylene chloride (5 mL) and (tmeda)PdMe₂ (202 mg, 0.80 mmol, 1 eq) was added. Evolution of gas was observed upon formation of a yellow solution which was stirred for 1 h at room temperature followed by addition of pyridine (0.5 mL, excess) and continued stirring for 30 min. After subsequent precipitation by addition of Et₂O (15 mL) the solution was filtered off and the

obtained solid was reprecipitated from methylene chloride/Et$_2$O (15 mL and 20 mL, respectively). The solution and precipitate were analysed by NMR spectroscopy which indicates formation of **39** but purification by crystallisation was not successful.

9.2.33. Synthesis of 8-lithio-1-methoxynaphthalene 38
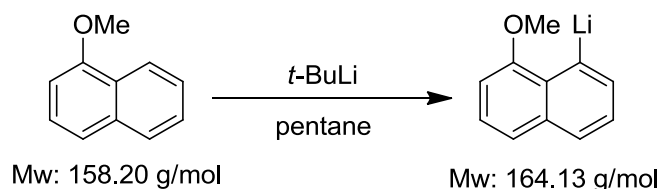
Scheme 72: *Synthesis of Synthesis of 8-lithio-1-methoxynaphthalene 38.*

1-Methoxy naphthalene (5.45 g, 5.00 mL, ρ = 1.09 g/mL, 34.5 mmol, 1 eq) was dissolved in 30 mL pentane and *t*-BuLi (20.4 mL, 1.7 M in pentane, 34.7 mmol, 1 eq) was added slowly *via* syringe at room temperature. The reaction was stirred for 36 h at room temperature which led to formation of a dark red solution and a white precipitate. After filtration the solid was washed repeatedly with pentane (4·20 mL) until the solution was colourless. **38** was obtained (4.31 g, 26.3 mmoL, 76.2%) with a 9:1 ratio of 8- to 2-lithiation, respectively (determined by ^{1}H NMR spectroscopy).

^{1}H NMR (300 MHz, d8-THF) δ 8.14 (dd, *J* = 5.9, 1.2 Hz, 1H), 7.34 (dd, *J* = 8.0, 1.2 Hz, 1H), 7.28 (d, *J* = 7.6 Hz, 1H), 7.21 – 7.09 (m, 2H), 6.71 (d, *J* = 7.1 Hz, 1H), 3.91 (s, 3H).

For this intermediary product only characterisation of the lithiation regioselectivity was carried out by ^{1}H NMR spectroscopy.

9. Experimental Part

9.2.34. Synthesis of 2-(bis-8-methoxynaphthalene-1-phosphine)benzene sulphonic acid 37
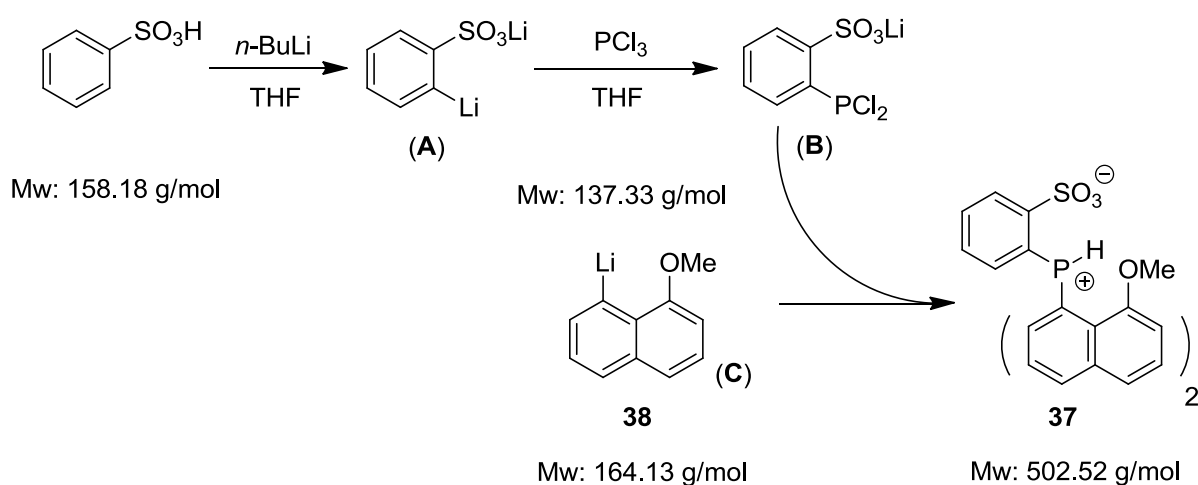
Scheme 73: *Synthesis of 2-(bis-8-methoxynaphthalene-1-phosphine)benzene sulphonic acid 37.*

Benzenesulphonic acid (2.06 g, 13.0 mmol, 1 eq.) dissolved in tetrahydrofurane (50 ml, Flask **A**), *n*-BuLi (10.4 mL, 2.5 M in hexane, 16.0 mmol, 2 eq.) was added slowly at -78 °C and the reaction was stirred for 3 h after warming to room temperature. PCl$_3$ (1.12 mL, 1.79 g, 13.0 mmol, 1 eq.) was added to a separate flask charged with tetrahydrofurane (80 mL, Flask **B**) at -78 °C followed by slow addition of the contents of Flask **A** *via* a dropping funnel at vigorous agitation and the obtained yellow solution was stirred for 1 h at -78 °C. Parallel, **8** (4.70 g, 28.7 mmol, 2.2 eq.) was suspended in pentane (100 mL, Flask **C**) at -78 °C and the contents were transferred to Flask **B** *via* a V-connection tube. The obtained brown suspension cleared slowly and was stirred for 16 h after warming to room temperature. Termination of the reaction was achieved by addition of H$_2$O (5 mL), removal of volatiles *in vacuo* and subsequent dissolution of the residue in a mixture of methylene chloride (180 mL) and water (100 mL), acidified with an aqueous HCl solution (5 mL, 37%), for extraction. The aqueous phase was removed, extracted with methylene chloride (100 mL) and the combined organic phases were dried over MgSO$_4$ followed by removal of the volatiles *in vacuo*. Afterwards the obtained residue was washed with tetrahydrofurane (6·20 mL), Et$_2$O (2·20 mL) and pentane (2·20 mL) which provides the crude product mixture after drying *in vacuo* (4.59 g, 9.13 mmol, 70.2% yield, 80.6% content of **37** determined by ^{31}P NMR spectroscopy in CDCl$_3$). Crystallisation of this crude product mixture (2 g) from hot CHCl$_3$ gave colourless needles of the pure phosphine sulphonate **37** (682 mg, 28%).

9. Experimental Part
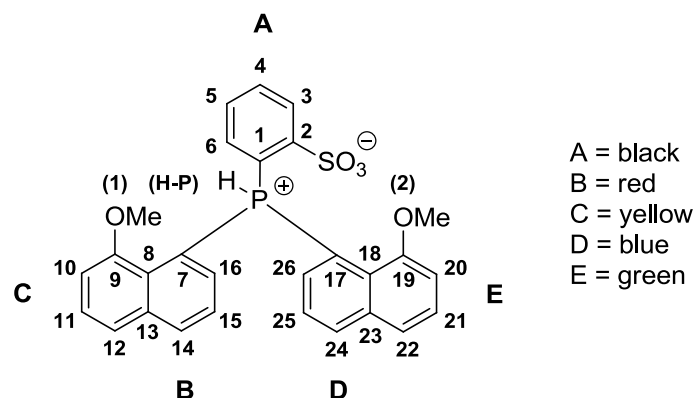
Figure 53: *Numbering scheme used for the interpretation of NMR spectra of **37**. Colour labels used as markers for the spin systems A-E in* Figure 37, Section 6.6.

^{1}H NMR (500 MHz, CDCl$_3$) δ 10.62 (d, ^1J (H-P) = 674.3 Hz, 1H, *H*-P), 8.50 (dd, ^3J (H-H) = 7.7 Hz, ^4J (H-P) = 4.8 Hz, 1H, *H3*), 8.12 – 8.05 (m, 2H, *H14, 24*), 7.73 (m, 1H, *H4*), 7.60 – 7.56 (m, 3H. *H11, 12, 22*), 7.47 (m, 2H, *H21, 25*), 7.36 – 7.28 (m, 2H, *H5, 15*), 7.26 (d, ^3J (H-H) = 7.3 Hz, 1H, *H26*), 7.12 (dd, ^3J (H-P) = 18.0 Hz, ^3J (H-H) = 7.3 Hz, 1H, *H16*), 7.00 (dd, J (H-H) = 6.7, 2.0 Hz, 1H, *H10*), 6.93 (dd, ^3J (H-P) = 14.4Hz, ^3J (H-H) = 7.7 Hz, 1H, *H6*), 6.80 (d, ^3J (H-H) = 7.7 Hz, 1H, *H20*), 3.89 (s, 3H, *OMe1*), 3.22 (s, 3H, *OMe2*).

^{31}P{^{1}H} NMR (121 MHz, CDCl$_3$) δ +16.5 (s).

^{31}P NMR (121 MHz, CDCl$_3$) δ +16.5 (ddd, ^1J (H-P) = 674.3, J (H-P) 32.2, 15.5 Hz).

^{13}C{^{1}H} NMR (75 MHz, CDCl$_3$) δ 154.9 (s, *C9*), 154.2 (s, *C19*), 151.3 (d, ^2J (C-P) = 8.2 Hz, *C2*), 136.8 (d, ^2J (C-P) = 9.2 Hz, *C26*), 135.9 (d, ^2J (C-P) = 9.1 Hz, *C16*), 135.5 (s, *C23*), 135.4 (s, *C13*), 134.5 (d, ^4J (C-P) = 3.2 Hz, *C24*), 134.3 (s, *C14*), 133.9 (d, ^4J (C-P) = 3.3 Hz, *C4*), 133.9 (d, ^2J (C-P) = 4.1 Hz, *C6*), 130.4 (d, ^3J (C-P) = 8.7 Hz, *C3*), 129.8 (d, ^3J (C-P) = 12.2 Hz, *C5*), 128.3 (s, *C11*), 127.7 (s, *C21*), 126.3 (d, ^3J (C-P) = 15.0 Hz, *C25*), 125.8 (d, ^3J (C-P) = 14.7 Hz, *C15*), 125.4 (d, ^2J (C-P) = 5.1 Hz, *C8*), 124.6 (d, ^2J (C-P) = 5.3 Hz, *C18*), 122.5 (s, *C12*), 121.8 (s, *C22*), 118.1 (d, ^1J (C-P) = 94.7 Hz, *C17*), 117.0 (d, ^1J (C-P) = 89.7 Hz, *C7*), 115.9 (d, ^1J (C-P) = 92.8 Hz, *C1*), 107.9 (s, *C10*), 107.8 (s, *C20*), 56.3 (s, *OMe1*), 55.08 (s, *OMe2*).

EA Found:	C 55.20, H 3.76, S 4.98.
Calculated for C$_{28}$H$_{23}$PSO$_5$:	C 66.92, H 4.61, S 6.38.
Calculated for C$_{28}$H$_{23}$PSO$_5$ ×1.1 CHCl$_3$:	C 55.14, H 3.83, S 5.06.
High-res. ESI-MS (neg., MeCN):	m/z = 501.0936 (M$^-$).
Calculated for C$_{28}$H$_{22}$PSO$_5$:	m/z = 501.0926 (M-H$^+$).

9.2.35. Synthesis of [{κ²-(P,O)-2-(bis-8-methoxynaphthalene-1-phosphine)benzene sulphonate}PdMe(pyridine)] 40
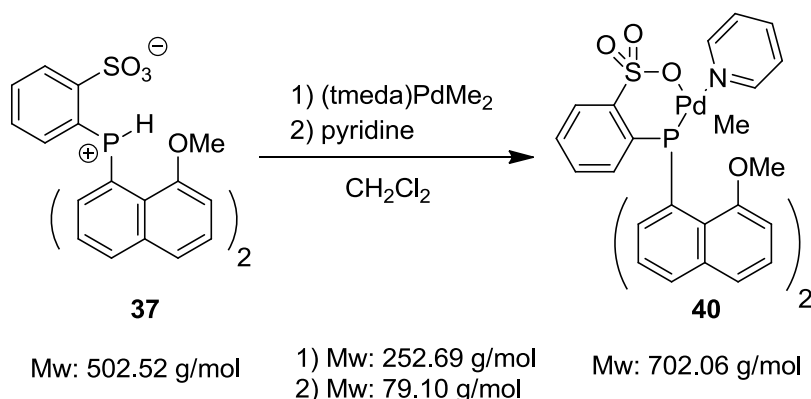
Scheme 74: *Synthesis of [{κ²-(P,O)-2-(bis-8-methoxynaphthalene-1-phosphine)benzene sulphonate}PdMe(pyridine)] 40.*

The phosphine sulphonate **37** (200 mg, 0.40 mmol, 1 eq.) was dissolved in methylene chloride (10 mL) and (tmeda)PdMe$_2$ (100 mg, 0.40 mmol, 1 eq.) was added. Evolution of gas was observed upon formation of a pale yellow solution which was stirred for 20 min followed by pyridine addition (0.25 mL, excess). After stirring the clear pale yellow solution for 1 h at room temperature the solution was reduced to 2 mL *in vacuo* and precipitated by addition of pentane (8 mL). The solution was filtered off and the obtained solid was recrystallised from chloroform (7 mL)/pentane (20 mL). 150 mg of the complex **40** (0.21 mmol, 53%) were obtained as yellow crystals.
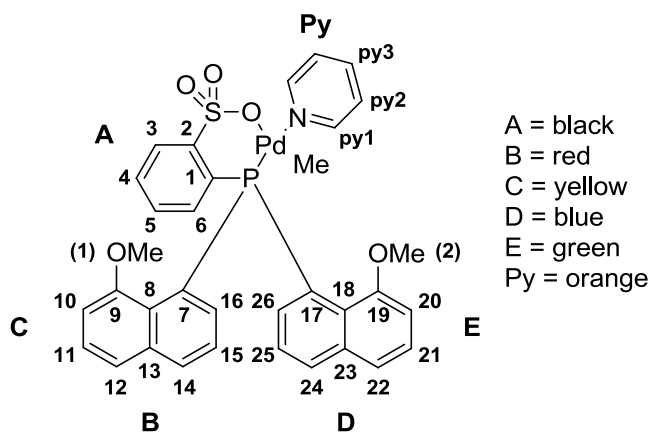
Figure 54: *Numbering scheme used for the interpretation of NMR spectra of 39. Colour labels used as markers for the spin systems A-Py in* Figure 39, Section 6.6.

^{1}H NMR (500 MHz, CDCl$_3$) δ 8.75 (d, ^{3}J (H-H) = 5.3 Hz, 2H, *Hpy1*), 8.39 – 8.28 (m, 1H, *H3*), 7.94 (d, ^{3}J (H-H) = 8.1 Hz, 1H, *H14*), 7.86 (d, ^{3}J (H-H) = 8.1 Hz, 1H, *H24*), 7.67 (t, ^{3}J (H-H) = 7.6 Hz, 1H, *Hpy3*), 7.55 – 7.39 (m, 5H, *H4, 11, 12, 21, 22*), 7.39 – 7.32 (m, 1H, *H15*), 7.32 – 7.23 (m, 4H, *Hpy2, 16, 25*), 7.16 (t, ^{3}J (H-H) = 7.6 Hz, 1H, *H5*), 7.13 – 7.07 (s, 1H, *H26*), 7.07 – 7.01 (m, 1H, *H6*), 6.85 (d, ^{3}J (H-H) = 7.6 Hz, 1H, *H20*), 6.70 (d, ^{3}J (H-H) = 7.6 Hz, 1H. *H10*), 3.71 (s, broad, 3H,), 3.05 (s, sharp, 3H, *OMe2*), 0.49 (s, 3H, *PdMe*).

^{31}P{^{1}H} NMR (121 MHz, CDCl$_3$) δ +47.0.

^{31}P NMR (121 MHz, CDCl$_3$) δ +47.0.

^{13}C{^{1}H} NMR (75 MHz, CDCl$_3$) δ 156.1 (s, *C19*), 155.8 (s, *C9*), 150.9 (s, *py1*), 137.7 (s, *py3, C16*), 136.2 (d, *J* = 7.5 Hz), 135.5 (d, *J* = 5.2 Hz, *C26*), 135.4 (d, *J* = 7.6 Hz), 133.4 (d, ^{2}J (C-P) = 1.6 Hz. *C6*), 132.0 (s), 131.8 (s, *C24*), 131.3 (s, *C14*), 130.3 (s, *C4*), 129.9 (s, broad, *C3, 5*), 127.1 (s), 126.9 (s, *C11*), 126.4 (s, *C21*), 126.0 (d, ^{3}J (C-P) = 8.5 Hz, *C25*), 125.5 (d, ^{3}J (C-P) = 10.5 Hz, *C15*), 125.1 – 124.7 (m, *py2, C16*), 122.0 (s, *C22*), 120.9 (s, *C12*), 107.1 (s, *C20*), 105.3 (s, *C10*), 56.5 (s, broad, *OMe2*), 53.7 (s, sharp, *OMe1*), -0.17 (s, *Pd-Me*). Due to a superposition of peaks most quaternary carbon atoms could not be assigned and detected.

EA Found:	C 57.15, H 4.32, N 2.11, S 4.42.
Calculated for C$_{35}$H$_{31}$NPPdSO$_5$:	C 58.17, H 4.31, N 2.00, S 4.57.
Calculated for C$_{35}$H$_{31}$NPPdSO$_5$×0.1 CHCl$_3$:	C 57.16, H 4.23, N 1.95, S 4.47.

9.2.36. Synthesis of [{κ^2-(P,O)-2-(bis-8-methoxynaphthalene-1-phosphine)benzene sulphonate}PdMe]$_2$[κ-(N, N')-tmeda] 41
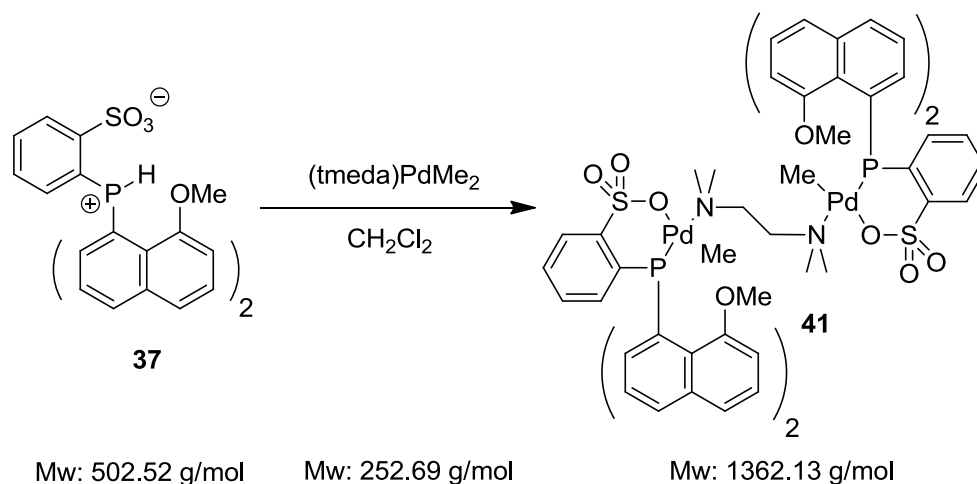
Scheme 75: *Synthesis of the dimeric complex [{κ^2-(P,O)-2-(bis-8-methoxynaphthalene-1-phosphine)benzene sulphonate}PdMe]$_2$[κ-(N, N')-tmeda].*

The phosphine sulphonate **37** (600 mg, 1.19 mmol, 1 eq.) was dissolved in methylene chloride (30 mL) and (tmeda)PdMe$_2$ (302 mg, 1.20 mmol, 1 eq.) was added. Evolution of gas was observed upon formation of a pale yellow solution which was stirred for 20 min. Dmso (2 mL) was added, the reaction stirred for 1 h followed by reduction of the solution to 20 mL and precipitation by addition of diethyl ether (20 mL). A pale yellow solid was obtained (547 mg, 0.40 mmol, 67.2%) which was recrystallised from chloroform/pentane. Despite dmso addition in a large excess, replacement of tmeda by dmso was not successful.

^{1}H NMR (300 MHz, CDCl$_3$) δ 8.24 (dd, J = 7.4, 3.7 Hz, 1H), 7.90 (d, J = 8.1 Hz, 1H), 7.79 (d, J = 8.2 Hz, 1H), 7.65 (dd, J = 14.0, 7.3 Hz, 1H), 7.53 – 7.36 (m, 5H), 7.34 – 7.19 (m, 4H), 7.09 (t, J = 7.5 Hz, 1H), 7.03 – 6.86 (m, 3H), 6.66 (d, J = 6.6 Hz, 1H), 3.68 (s, 3H), 2.98 (s, 3H), 2.17 (s, 3H), 1.55 (s, 3H), 0.16 (s, 3H).

^{31}P{^{1}H} NMR (121 MHz, CDCl$_3$) δ +47.6.

EA Found:	C 53.18, H 4.77, N 2.01, S 4.17.
Calculated for C$_{64}$H$_{66}$N$_2$P$_2$Pd$_2$S$_2$O$_{10}$:	C 56.43, H 4.88, N 2.06, S 4.71.
Calculated for C$_{64}$H$_{66}$N$_2$P$_2$Pd$_2$S$_2$O$_{10}$×0.9 CHCl$_3$:	C 53.08, H 4.59, N 1.91, S 4.37.

Limited solubility of **41** prevents characterisation by ^{13}C NMR spectroscopy

9.2.37. Synthesis of [{κ^2-(P,O)-2-[bis-(2-methoxyphenyl)phosphine]benzene sulphonate}PdMe(pyridine)] 4
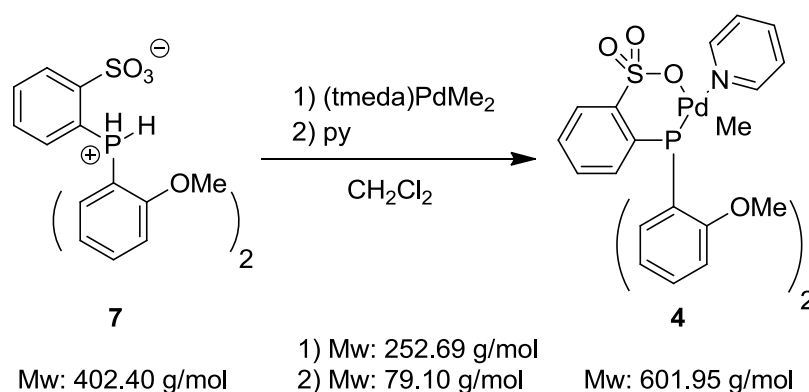
Scheme 76: *Synthesis of the neutral [{κ^2-(P,O)-2-[bis-(2-methoxyphenyl)phosphine]benzene sulphonate}PdMe(pyridine)] catalyst **4**.*

9. Experimental Part

The phosphine sulphonate **7** (404 mg, 1.00 mmol, 1 eq.) was dissolved in tetrahydrofuran (60 mL) and (tmeda)PdMe$_2$ (254 mg, 1.00 mmol, 1 eq.) was added. Evolution of gas was observed and the reaction was stirred for 20 min. Diethyl ether (40 mL) was added, the solvents were filtered off and the residue was washed with pentane (10 mL). The colourless precipitate was dissolved in methylene chloride and 1 mL of pyridine was added (1 mL, excess). After filtration the solvent was removed at reduced pressure and the residue was washed with pentane (2·10 mL). **4** was obtained as a colourless solid (538 mg, 0.89 mmol, 89.4%).

^{1}H NMR (500 MHz, CDCl$_3$) δ 8.79 (d, ^3J (H-H) = 3.9 Hz, 2H, *Hpy1*), 8.25 − 8.16 (m, 1H, *H3*), 7.81 (t, ^3J (H-H) = 7.6 Hz, 1H, *Hpy3*), 7.65 (s, 2H, *H12*), 7.49 (t, ^3J (H-H) = 7.8 Hz, 2H, *H10*), 7.47 − 7.37 (m, 3H, *Hpy2, 4*), 7.32 − 7.22 (m, 2H, *H5, 6*), 7.02 (t, ^3J (H-H) = 7.4 Hz, 2H, *H11*), 6.91 (dd, *J* = 8.2, 4.7 Hz, 2H, *H9*), 3.63 (s, 6H, *OMe*), 0.25 (s, 3H, *Pd-Me*).

^{13}C{^{1}H} NMR (75 MHz, CDCl$_3$) δ 160.6 (d, ^2J (C-P) = 2.3 Hz, *C8*), 150.5 (s, *Cpy1*), 138.1 (s, *Cpy3, 12*), 134.5 (s, *C6*), 133.3 (d, ^4J (C-P) = 1.7 Hz, *C10*), 130.1 (d, ^4J (C-P) = 2.3 Hz, *C4*), 128.4 (d, ^3J (C-P) = 7.1 Hz, *C5*), 128.1 (d, ^3J (C-P) = 8.5 Hz, *C3*), 125.0 (s, *Cpy2*), 120.8 (d, ^3J (C-P) = 11.8 Hz, *C11*), 116.5 (d, ^3J (C-P) = 57.0 Hz, *C7*), 111.4 (d, ^3J (C-P) = 4.5 Hz, *C9*), 55.4 (s, *OMe*), 0.31 (s, *Pd-Me*).

^{31}P{^{1}H} NMR (121 MHz, CDCl$_3$) δ +22.3 (s).

EA found:	C 50.51, H 4.34, N 2.40, S 4.94.
EA calculated for C$_{26}$H$_{26}$NO$_5$PPdS:	C 51.88, H 4.35, N 2.33, S 5.33
EA calculated for C$_{26}$H$_{26}$NO$_5$PPdS×0,25 CH$_2$Cl$_2$:	C 50.59, H 4.30, N 2.25, S 5.15

9.3. General Procedures for Homo- and Co-polymerisation Experiments

A stainless steel autoclave (100 mL or 200 mL) was heated at 120 °C and previous to the polymerisation reaction the autoclave was evacuated whilst cooling to room temperature. After addition of the catalyst, and if necessary activator, under protective gas atmosphere the solvent, and comonomer if necessary, were also added to the autoclave which was closed and stirred 15 min at room temperature. Ethene was introduced into the reactor which was placed in a pre-heated oil bath where the reaction mixture was stirred for the given reaction time. Termination of the reaction was carried out by cooling of the reactor at 0 °C followed by venting. The formed polymer was isolated by precipitation in methanol, filtration and drying over night at 60-80 °C in a vacuum oven. Characterisation of the obtained polymer was

carried out by high temperature NMR spectroscopy (d4-tetrachlorethane as solvent), high temperature GPC (trichlorbenzene as solvent) and DSC as necessary.

9.4. Details for the determination of molecular structures by X-ray diffractometry

Structure of [K(18-crown-6)]₂[(*rac-o,m*-TPPDS)PdMeCl] 20:

Single crystal X-ray diffraction data of crystals of compound **20** were collected at 110(2) K on a Bruker APEX II diffractometer equipped with a rotating anode FR 591 (Mo K$_\alpha$ radiation, Montel mirror optics) and a CCD detector. Crystal data: $PdPClK_2S_2C_{43}O_{18}H_{64}$, M = 1184.10, triclinic, $a = 10.4999(9)$, $b = 16.624(1)$, $c = 16.890(1)$; $\alpha = 83.955(4)$, $\beta = 78.587(4)$, $\gamma = 79.133(4)$, $V = 2831.0(5)$, space group: $P\bar{1}$, $Z = 2$, $\mu = 0.687$ mm^{-1}, 11707 reflections measured, 7210 unique (R_{int} 0.0709), final R-values: $R_1 = 0.1088$, $wR_2 = 0.2304$, all data $R_1 = 0.1469$, $wR_2 = 0.2383$.

The structure of the compound was solved using Direct Methods in SHELX[110] and refined on F^2 using Jana2006[111]. For one of the crown ether molecules a second orientation could be detected but disorder hindered a free refinement. It was therefore refined with two orientations of a rigid body with the angles (Θ, Φ, Ψ) and a translational vector along the crystallographic axes. The atomic positions of the main crown ether orientation were taken from the structure solution and were used to define the rigid body. The ratio of the two orientations refined to 0.769(6):0.231(6). The atoms of both crown ether molecules were refined isotropically and the displacement parameters of the crown ether with two positions were refined as one. All other non-hydrogen atoms were refined anisotropically. Due to heavy disorder of the solvent molecules in the voids their contribution to the structure factors were modelled using the "SQUEEZE" program in PLATON.[112] The positions of the hydrogen atoms were calculated using a riding model.

10. Literature

[1]   a) V. Busico, *Macromol. Chem. Phys.* **2007**, *208*, 26; b) E. Y.-X. Chen, T. J. Marks, *Chem. Rev.* **2000**, *100*, 1391; c) *Metal Catalysts in Olefin Polymerization* (Ed. Z. Guan), Springer, Heidelberg, **2009**.

[2]   C. Cobzaru, S. Hild, A. Boger, C. Troll, B. Rieger, *Coord. Chem. Rev.* **2006**, *250*, 189.

[3]   a) Z. Z. Jiang, M. T. Boyer, A. Sen, *J. Am. Chem. Soc.* **1995**, *117*, 7037; b) Z. Z. Jiang, A. Sen, *J. Am. Chem. Soc.* **1995**, *117*, 4455.

[4]   S. Klaus, M. W. Lehenmeier, C. E. Anderson, B. Rieger, *Coord. Chem. Rev.* **2011**, *25*, 1460.

[5]   a) Z. B. Guan, P. M. Cotts, E. F. McCord, S. J. McLain, *Science* **1999**, *283*, 2059; b) S. D. Ittel, L. K. Johnson, M. Brookhart, *Chem. Rev.* **2000**, *100*, 1169.

[6]   M. Delferro, T. J. Marks, *Chem. Rev.* **2011**, doi: 10.1021/cr1003634.

[7]   M. Zintl, B. Rieger, *Angew. Chem.-Int. Ed.* **2007**, *46*, 333.

[8]   a) A. Schoebel, M. Winkenstette, T. M. J. Anselment, B. Rieger, *Copolymerization of Alkenes and Polar Monomers by Early- and Late-Transition Metal Catalysts* (Ed. G. Coates), **2011**; b)L. S. Boffa, B. M. Novak, *Chem. Rev.* **2000**, *100*, 1479.

[9]   A. Nakamura, S. Ito, K. Nozaki, *Chem. Rev.* **2009**, *109*, 5215.

[10]   S. E. Lehman, K. B. Wagener, L. S. Baugh, S. P. Rucker, D. N. Schulz, M. Varma-Nair, E. Berluche, *Macromolecules* **2007**, *40*, 2643.

[11]   E. Y. X. Chen, *Chem. Rev.* **2009**, *109*, 5157.

[12]   a) C. Bianchini, G. Giambastiani, L. Luconi, A. Meli, *Coord. Chem. Rev.* **2010**, *254*, 431; b) S. Ito, K. Nozaki, *Chem. Rec.* **2010**, *10*, 315.

[13]   A. F. Hollemann, E. Wiberg, *Lehrbuch der Anorganischen Chemie*, 101 ed., de Gruyter, Berlin, **1995**.

[14]   Z. Freixa, P. W. N. M. van Leeuwen, *Dalton Trans.* **2003**, 1890.

[15]   a) C. A. Tolman, *J. Am. Chem. Soc.* **1970**, *92*, 2956; b) C. A. Tolman, *Chem. Rev.* **1977**, *77*, 313.

[16]   H. Clavier, S. P. Nolan, *Chem. Comm.* **2010**, *46*, 841.

[17]   A. Grabulosa, J. Granell, G. Muller, *Coord. Chem. Rev.* **2007**, *251*, 25.

[18]   a) M. Sperrle, G. Consiglio, *J. Am. Chem. Soc.* **1995**, *117*, 12130; b) K. Nozaki, N. Sato, H. Takaya, *J. Am. Chem. Soc.* **1995**, *117*, 9911; c) K. Nozaki, T. Hiyama, *J. Organomet. Chem.* **1999**, *576*, 248; d) K. Nozaki, N. Sato, Y. Tonomura, M. Yasutomi, H. Takaya, T. Hiyama, T. Matsubara, N. Koga, *J. Am. Chem. Soc.* **1997**,

10. Literature

119, 12779; e) S. Bronco, G. Consiglio, S. Dibenedetto, M. Fehr, F. Spindler, A. Togni, *Helv. Chim. Act.* **1995**, *78*, 883; f) S. Bronco, G. Consiglio, *Macromol. Chem. Phys*. **1996**, *197*, 355; g) C. Gambs, S. Chaloupka, G. Consiglio, A. Togni, *Angew. Chem.-Int. Ed.* **2000**, *39*, 2486; h) B. Sesto, G. Consiglio, *J. Am. Chem. Soc.* **2001**, *123*, 4097; i) A. Leone, G. Consiglio, *Helv. Chim. Act.* **2005**, *88*, 210; j) A. Leone, G. Consiglio, *J. Organomet. Chem.* **2006**, *691*, 4204; k) A. Leone, S. Gischig, G. Consiglio, *J. Organomet. Chem.* **2006**, *691*, 4816.

[19]   K. H. Shaughnessy, *Chem. Rev.* **2009**, *109*, 643.

[20]   W. A. Herrmann, C. W. Kohlpaintner, *Angew. Chem.-Int. Ed.* **1993**, *32*, 1524.

[21]   P. Kuhn, D. Semeril, D. Matt, M. J. Chetcuti, P. Lutz, *Dalton Trans.* **2007**, 515.

[22]   a) E. Kuntz, (Rhone-Poulenc Industries) *FR 2314910*, **1975**; b) E. Kuntz, (Rhone-Poulenc Industries) *FR 2,349,562*, **1976**.

[23]   E. Kuntz, (Rhone-Poulenc Industries) *Vol. US 4,248,802*, **1981**.

[24]   W. B. F. Brunnmueller, V. Weberndoerfer, (BASF AG) *EP0041134(a2)* **1981**.

[25]   a) B. Cornils, R. Gaertner, P. Lappe, (Ruhrchemie AG) *DE3235030A1* **1982**; b) J.-L. Sabot, (Rhone-Poulenc) *EP0104967(a1)* **1983**; c)B. Cornils, R Gaertner, P. Lappe, H. Springer, (Ruhrchemie AG) *EP0107006* **1983**.

[26]   W. A. Herrmann, J. A. Kulpe, W. Konkol, H. Bahrmann, *J. Organomet. Chem.* **1990**, *389*, 85.

[27]   C. Larpent, H. Patin, N. Thilmont, J. F. Valdor, *Synth. Comm.* **1991**, *21*, 495.

[28]   W. A. Herrmann, G. P. Albanese, R. B. Manetsberger, P. Lappe, H. Bahrmann, *Angew. Chem.-Int. Ed.* **1995**, *34*, 811.

[29]   a) O. Herd, A. Hessler, K. P. Langhans, O. Stelzer, W. S. Sheldrick, N. Weferling, *J. Organomet. Chem.* **1994**, *475*, 99; b) J. Chatt, R. B. Collins, (Ilford Limited) *GB 1,066,261*, **1964**; c) F. Bitterer, O. Herd, A. Hessler, M. Kühnel, K. Rettig, O. Stelzer, W. S. Sheldrick, S. Nagel, N. Rösch, *Inorg. Chem.* **1996**, *35*, 4103.

[30]   H. Gulyás, Á. Szöllősy, B. E. Hanson, J. Bakos, *Tetrahedron Lett.* **2002**, *43*, 2543.

[31]   S. Ahrland, J. Chatt, N. R. Davies, A. A. Williams, *Nature* **1957**, *179*, 1187.

[32]   a) B. Cornils., H. Bahrmann, W. Konkol, W. Lipps, (Ruhrchemie AG) *DE3412335A1* **1984**; b)H. Bahrmann., H. Bach, B. Cornils, W. Gick, V. Heim, W. Konkol, E. Wiebus, (Hoechst AG) *EP0302375* **1988**.

[33]   L. Lavenot, A. Roucoux, H. Patin, *J. Mol. Cat. a-Chem.* **1997**, *118*, 153.

10. Literature

[34]   *Late Transition Metal Polymerization Catalysis* (Eds. B. Rieger, L. S. Baugh, S. Kacker, S. Striegler), Wiley-VCH, **2003**.

[35]   S. Noda, A. Nakamura, T. Kochi, L. W. Chung, K. Morokuma, K. Nozaki, *J. Am. Chem. Soc.* **2009**, *131*, 14088.

[36]   Z. B. Guan, *Abstr. Am. Chem. Soc.* **2003**, *226*, U359.

[37]   L. K. Johnson, C. M. Killian, M. Brookhart, *J. Am. Chem. Soc.* **1995**, *117*, 6414.

[38]   R. E. Murray, (Union Carbide) *US 4689437*, **1987**.

[39]   a) J. A. van Doorn, E. Drent, P. W. van Leeuwen, N. Meijboom, A. B. van Oort, R. L. Wife, (Shell Int. Research) *EP0280380*, **1988**; b) E. Drent, W. Sjardijn, J. Suykerbuyk, K. Wanninger, (Montell Technology Company) *WO0006615*, **2000**.

[40]   a) E. Drent, R. van Dijk, R. van Ginkel, B. van Oort, R. I. Pugh, *Chem. Comm.* **2002**, 964; b) E. Drent, R. van Dijk, R. van Ginkel, B. van Oort, R. I. Pugh, *Chem. Comm.* **2002**, 744.

[41]   J. Vela, G. R. Lief, Z. L. Shen, R. F. Jordan, *Organometallics* **2007**, *26*, 6624.

[42]   a) A. Haras, A. Michalak, B. Rieger, T. Ziegler, *J. Am. Chem. Soc.* **2005**, *127*, 8765; b) A. Haras, G. D. W. Anderson, A. Michalak, B. Rieger, T. Ziegler, *Organometallics* **2006**, *25*, 4491; c) A. Haras, A. Michalak, B. Rieger, T. Ziegler, *Organometallics* **2006**, *25*, 946.

[43]   a) R. F. Jordan, P. K. Bradley, N. C. Baenziger, R. E. Lapointe, *J. Am. Chem. Soc.* **1990**, *112*, 1289; b) E. J. Arlman, P. Cossee, *J. Cat.* **1964**, *3*, 99; c) P. Cossee, *J. Cat.* **1964**, *3*, 80; d) M. K. Leclerc, H. H. Brintzinger, *J. Am. Chem. Soc.* **1996**, *118*, 9024.

[44]   C. M. Reisinger, R. J. Nowack, D. Volkmer, B. Rieger, *Dalton Trans.* **2007**, 272.

[45]   K. M. Skupov, J. Hobbs, P. Marella, D. Conner, S. Golisz, B. L. Goodall, J. P. Claverie, *Macromolecules* **2009**, *42*, 6953.

[46]   K. M. Skupov, P. R. Marella, M. Simard, G. P. A. Yap, N. Allen, D. Conner, B. L. Goodall, J. P. Claverie, *Macromol. Rap. Comm.* **2007**, *28*, 2033.

[47]   L. Piche, J. C. Daigle, R. Poli, J. P. Claverie, *Europ. J. Inorg. Chem.* **2010**, 4595.

[48]   D. Guironnet, P. Roesle, T. Rünzi, I. Göttker-Schnetmann, S. Mecking, *J. Am. Chem. Society* **2009**, *131*, 422.

[49]   D. Zhang, D. Guironnet, I. Gottker-Schnetmann, S. Mecking, *Organometallics* **2009**, *28*, 4072.

[50]   N. T. Allen, B. L. Godall, L. H. McIntosh III, (Rohm and Haas Company) *US 0049712(a1)*, **2007**.

10. Literature

[51]   G. Stojcevic, M. C. Baird, *Dalton Trans.* **2009**, 8864.

[52]   T. Kochi, A. Nakamura, H. Ida, K. Nozaki, *J. Am. Chem. Soc.* **2007**, *129*, 7770.

[53]   S. Stromberg, M. Svensson, K. Zetterberg, *Organometallics* **1997**, *16*, 3165.

[54]   H. von Schenck, S. Stromberg, K. Zetterberg, M. Ludwig, B. Akermark, M. Svensson, *Organometallics* **2001**, *20*, 2813.

[55]   S. Mecking, L. K. Johnson, L. Wang, M. Brookhart, *J. Am. Chem. Soc.* **1998**, *120*, 888.

[56]   E. Drent, P. H. M. Budzelaar, *Chem. Rev.* **1996**, *96*, 663.

[57]   L. K. Johnson, S. Mecking, M. Brookhart, *J. Am. Chem. Soc.* **1996**, *118*, 267.

[58]   A. K. Hearley, R. A. J. Nowack, B. Rieger, *Organometallics* **2005**, *24*, 2755.

[59]   R. J. Nowack, Dissertation, Ulm , **2008**.

[60]   T. Kochi, K. Yoshimura, K. Nozaki, *Dalton Trans.* **2006**, 25.

[61]   D. Guironnet, L. Caporaso, B. Neuwald, I. Göttker-Schnetmann, L. Cavallo, S. Mecking, *J. Am. Chem. Soc.* **2010**, *132*, 4418.

[62]   T. Rünzi, D. Fröhlich, S. Mecking, *J. Am. Chem. Soc.* **2010**, *132*, 17690.

[63]   A. Sen, S. Borkar, *J. Organomet. Chem.* **2007**, *692*, 3291.

[64]   T. Rünzi, D. Guironnet, I. Göttker-Schnetmann, S. Mecking, *J. Am. Chem. Soc.* **2010**, *132*, 16623.

[65]   a) W. Weng, Z. Shen, R. F. Jordan, *J. Am. Chem. Soc.* **2007**, *129*, 15450; b) Z. L. Shen, R. F. Jordan, *Macromolecules* **2010**, *43*, 8706.

[66]   a) K. Nozaki, S. Kusumoto, S. Noda, T. Kochi, L. W. Chung, K. Morokuma, *J. Am. Chem. Soc.* **2010**, *132*, 16030; b) T. Kochi, S. Noda, K. Yoshimura, K. Nozaki, *J. Am. Chem. Soc.* **2007**, *129*, 8948.

[67]   S. Luo, J. Vela, G. R. Lief, R. F. Jordan, *J. Am. Chem. Soc.* **2007**, *129*, 8946.

[68]   S. Ito, K. Munakata, A. Nakamura, K. Nozaki, *J. Am. Chem. Soc.* **2009**, *131*, 14606.

[69]   C. Bouilhac, T. Runzi, S. Mecking, *Macromolecules* **2010**, *43*, 3589.

[70]   K. M. Skupov, L. Piche, J. P. Claverie, *Macromolecules* **2008**, *41*, 2309.

[71]   S. Liu, S. Borkar, D. Newsham, H. Yennawar, A. Sen, *Organometallics* **2007**, *26*, 210.

[72]   S. Borkar, D. K. Newsham, A. Sen, *Organometallics* **2008**, *27*, 3331.

[73]   S. Ito, M. Kanazawa, K. Munakata, J.-i. Kuroda, Y. Okumura, K. Nozaki, *J. Am. Chem. Soc.* **2011**, doi: 10.1021/ja1092216.

[74]   a) D. V. Deubel, T. Ziegler, *Organometallics* **2002**, *21*, 1603; b) D. V. Deubel, T. Ziegler, *Organometallics* **2002**, *21*, 4432.

10. Literature

[75] F. Wu, S. R. Foley, C. T. Burns, R. F. Jordan, *J. Am. Chem. Soc.* **2005**, *127*, 1841.

[76] F. Wu, R. F. Jordan, *Organometallics* **2006**, *25*, 5631.

[77] L. F. Groux, T. Weiss, D. N. Reddy, P. A. Chase, W. E. Piers, T. Ziegler, M. Parvez, J. Benet-Buchholz, *J. Am. Chem. Soc.* **2005**, *127*, 1854.

[78] T. Kochi, S. Noda, K. Yoshimura, K. Nozaki, *J. Am. Chem. Soc.* **2007**, *129*, 8948.

[79] a) D. Pérez-Foullerat, S. Hild, A. Mücke, B. Rieger, *Macromol. Chem. Phys.* **2004**, *205*, 374; b) W. E. Huhn, F. Hollmann, S. Hild, T. Kriewall, B. Rieger, *Macromol. Mat. and Eng.* **2000**, *283*, 115.

[80] D. K. Newsham, S. Borkar, A. Sen, D. M. Conner, B. L. Goodall, *Organometallics* **2007**, *26*, 3636.

[81] L. Bettucci, C. Bianchini, C. Claver, E. J. Garcia Suarez, A. Ruiz, A. Meli, W. Oberhauser, *Dalton Trans.* **2007**, 5590.

[82] R. Luo, D. K. Newsham, A. Sen, *Organometallics* **2009**, *28*, 6994.

[83] M. J. Szabo, N. M. Galea, A. Michalak, S. Y. Yang, L. F. Groux, W. E. Piers, T. Ziegler, *Organometallics* **2005**, *24*, 2147.

[84] Z. L. Shen, R. F. Jordan, *J. Am. Chem. Soc.* **2010**, *132*, 52.

[85] W. A. Herrmann, C. W. Kohlpaintner, H. Bahrmann, W. Konkol, *J. Mol. Cat.* **1992**, *73*, 191.

[86] O. Pestovsky, A. Shuff, A. Bakac, *Organometallics* **2006**, *25*, 2894.

[87] a) B. M. Bhanage, S. S. Divekar, R. M. Deshpande, R. V. Chaudhari, *Org. Process Res. & Devel.* **2000**, *4*, 342; b) J. Jenck, D. Morel, (Rhone-Poulenc Recherches) *US 4668824*, **1987**.

[88] A. Michael, N. Weiner, *J. Am. Chem. Soc.* **1936**, *58*, 294.

[89] T. M. J. Anselment, S. I. Vagin, B. Rieger, *Dalton Trans.* **2008**, 4537.

[90] a) M. A. Thompson, E. D. Glendening, D. Feller, *J. Phys. Chem.* **1994**, *98*, 10465; b) E. D. Glendening, D. Feller, M. A. Thompson, *J. Am. Chem. Soc.* **1994**, *116*, 10657.

[91] S. Berger, S. Braun, H.-O. Kalinowski, *NMR Spektroskopie von Nichtmetallen, Vol. 3, ^{31}P-NMR Spektroskopie*, Georg Thieme Verlag Stuttgart New York, **1993**.

[92] R. J. Nowack, Dissertation, Ulm , **2008**.

[93] a) D. J. Darensbourg, C. J. Bischoff, J. H. Reibenspies, *Inorg. Chem.* **1991**, *30*, 1144; b) C. Balzarek, T. J. R. Weakley, D. R. Tyler, *Inorg. Chim. Act.* **2001**, *315*, 139; c) Z. Assefa, J. M. Forward, T. A. Grant, R. J. Staples, B. E. Hanson, A. A. Mohamed, J. P. Fackler, *Inorg. Chim. Act.* **2003**, *352*, 31; d) T. Bartik, B. Bartik, B. E. Hanson, K. H.

10. Literature

Whitmire, I. Guo, *Inorg. Chem.* **1993**, *32*, 5833; e) F. Tisato, F. Refosco, G. Bandoli, G. Pilloni, B. Corain, *Inorg. Chem.* **2001**, *40*, 1394.

[94] D. Guironnet, T. Rünzi, I. Göttker-Schnetmann, S. Mecking, *Chem. Comm.* **2008**, 4965.

[95] T. Schultz, A. Pfaltz, *Synthesis* **2005**, 1005.

[96] E. G. Kuntz, O. M. Vittori, *J. Mol. Cat a-Chem.* **1998**, *129*, 159.

[97] a) C. Amatore, E. Blart, J. P. Genet, A. Jutand, S. Lemaireaudoire, M. Savignac, *J. Org. Chem.* **1995**, *60*, 6829; b) G. Papadogianakis, J. A. Peters, L. Maat, R. A. Sheldon, *J. Chem. Soc.-Chem. Comm.* **1995**, 1105.

[98] a) J. M. Basset, D. Bouchu, G. Godard, T. Karame, E. Kuntz, F. Lefebvre, N. Legagneux, C. Lucas, D. Michelet, J. B. Tommasino, *Organometallics* **2008**, *27*, 4300; b) G. Verspui, Moiseev, II, R. A. Sheldon, *J. Organomet. Chem.* **1999**, *586*, 196; c) W. A. Herrmann, J. A. Kulpe, J. Kellner, H. Riepl,(Hoechst AG) *EU 0372313*, **1989**.

[99] a)C. Bianchini, A. Meli, W. Oberhauser, C. Claver, E. J. Garcia Suarez, *Europ. J. Inorg. Chem.* **2007**, 2702; b) C. Bianchini, A. Meli, W. Oberhauser, A. M. Segarra, C. Claver, E. J. G. Suarez, *J. Mol. Cat. a-Chem.* **2007**, *265*, 292.

[100] a) A. E. Derome, *Organic Chemistry* (Ed.: J. E. Baldwin), Pergamon Press, Oxford, **1987**; b) W. R. Croasmun, R. M. K. Carlson, *Methods for Stereochemical Analysis*, 2nd Edition ed. (Ed.: A. P. Marchand), VCH Puplishers Inc., Weinheim, **1994**.

[101] a) G. Dyer, D. W. Meek, *Inorg. Chem.* **1965**, *4*, 1398; b) S. M. Godfrey, C. A. McAuliffe, R. G. Pritchard, *J. Chemical Soc.-Dalton Trans.* **1993**, 2229; c) E. W. Abel, J. C. Dormer, D. Ellis, K. G. Orrell, V. Sik, M. B. Hursthouse, M. A. Mazid, *J. Chem. Soc.-Dalton Trans.* **1992**, 1073; d) L. Hirsivaara, M. Haukka, S. Jaaskelainen, R. H. Laitinen, E. Niskanen, T. A. Pakkanen, J. Pursiainen, *J. Organomet. Chem.* **1999**, *579*, 45; e)P. Suomalainen, R. Laitinen, S. Jaaskelainen, M. Haukka, J. T. Pursiainen, T. A. Pakkanen, *J. Mol. Cat. a-Chem.* **2002**, *179*, 93; f) E. W. Abel, D. Ellis, K. G. Orrell, V. Sik, *Polyhedron* **1991**, *10*, 1603.

[102] a) R. H. Laitinen, H. Riihimaki, M. Haukka, S. Jaaskelainen, T. A. Pakkanen, J. Pursiainen, *Europ. J. Inorg. Chem.* **1999**, 1253; b) R. H. Laitinen, V. Heikkinen, M. Haukka, A. M. P. Koskinen, J. Pursiainen, *J. Organomet. Chem.* **2000**, *598*, 235.

10. Literature

[103]   a) J. Betz, W. Bauer, *J. Am. Chem. Soc.* **2002**, *124*, 8699; b) B. M. Graybill, D. A. Shirley, *J. Org. Chem.* **1966**, *31*, 1221; c) D. A. Shirley, C. F. Cheng, *J. Organomet. Chem.* **1969**, *20*, 251.

[104]   a) J. M. Wilson, D. J. Cram, *J. Am. Chem. Soc.* **1982**, *104*, 881; b) J. M. Wilson, D. J. Cram, *J. Org. Chem.* **1984**, *49*, 4930.

[105]   S. Berger, S. Braun, H.-O. Kalinowski, *NMR Spektroskopie von Nichtmetallen, Vol. 3, ^{31}P-NMR Spektroskopie*, Georg Thieme Verlag Stuttgart New York, **1993**.

[106]   M. P. Conley, R. F. Jordan, *Angew. Chem.-Int. Ed.* **2011**, *50*, 3744.

[107]   P. Perrotin, J. S. J. McCahill, G. Wu, S. L. Scott, *Chem. Comm.* **2011**.

[108]   R. E. Rülke, J. M. Ernsting, A. L. Spek, C. J. Elsevier, P.van Leeuwen, K. Vrieze, *Inorg. Chem.* **1993**, *32*, 5769.

[109]   W. De Graaf, J. Boersma, W. J. J. Smeets, A. L. Spek, G. van Koten, *Organometallics* **1989**, *8*, 2907.

[110]   G. Sheldrick, *Act. Cryst. A* **2008**, *64*, 112.

[111]   V. Petricek, M. Dusek, L. Palatinus, Institute of Physics, Praha, Czech Republic, Prague, **2006**.

[112]   A. L. Spek, *Act. Cryst. D-Biolog. Cryst.* **2009**, *65*, 148.